INVESTIGATING DRIVERS OF ALGAL BLOOM SUCCESSION IN LAKE ERIE

A Dissertation Presented for the
Doctor of Philosophy
Degree
The University of Tennessee Knoxville

Brittany Noel Zepernick
May 2023

Copyright © 2023 by Brittany Noel Zepernick
All rights reserved.

DEDICATION

To my brilliant and fearless mentor • Steven Wilhelm,

my academic dads • George Bullerjahn, Mike McKay, Hans Paerl, & Jeff Krause,

my unwaveringly supportive parents • Nanette & Randy Zepernick,

my hard-working grandparents • Clyde, Ida Zepernick & Richard, Pauline Wilcox

my ambitious counterpart and loving husband • Joe Caniglia

my encouraging father-in-law • Dave Caniglia

my coven of cats & dogs.

ACKNOWLEDGEMENTS

I must acknowledge my undergraduate professors, Dr. R. Michael L. McKay and Dr. George S. Bullerjahn, who sparked my passion for harmful algal bloom research and encouraged me to pursue a graduate degree. I want to thank George for recommending Dr. Wilhelm as a graduate mentor and telling me to "put a star next to that one". I also wish to thank Dr. Jeffrey Krause for mentoring me as an undergraduate NSF REU student in 2016, despite the fact I had never touched a pipette prior. I thank Dr. Becca Pickering for being my first graduate student mentor and for teaching me how to use said aforementioned pipette (among other useful things). I also want to thank Dr. Hans Paerl, whose guidance, input and candor has been critical in shaping my career and successes to date. These individuals, whom I often refer to as my "academic dads", have consistently cheered me on throughout my career.

Dr. Wilhelm is responsible for the scientist I am today. He is an exceedingly gifted scientist who encourages us to push the boundaries of science, challenge ourselves, and cultivate a passion for our work. Beyond his countless accomplishments as a scientist, he is an exemplary mentor. From my first day as a graduate student in his lab, he has never failed to encourage, guide, support and inspire me. A compassionate mentor, he has repeatedly placed the needs of his students above his own, including sometimes a need for sleep as he is prone to answering our frantic science emails sent at all hours of the night. He has fostered a collaborative, supportive, inclusive laboratory family to which I am eternally grateful to be a part of. In short, all of my academic successes and accomplishments I owe to him.

The Wilhelm lab family is just that, my second family. Over the past 5 years, these individuals have seen me through exuberant successes and rattling failures. While there are too many to name them all, I specifically want to thank Robbie Martin, Lauren Krausfeldt, Lena

Pound, Eric Gann, Naomi Gilbert, Alex Truchon, Emily Chase, and Katelyn Houghton, for your inspiration, collaboration, and unwavering support throughout the years. I would not have been able to accomplish half of what I did without you, and you have made these past five years some of the best of my life. Beyond the lab family, I want to thank my cohort (Alexandra, Liz, Elise, Katie and Sean) for your love, laughter, and support. I must also thank the Knox establishments which offered us a relaxed respite and liquid encouragement.

I want to thank my grandparents and those who paved the way before me, whose shoulders I stand on today. I thank my dad's side (the Zepernick family), who for generations earned their keep farming. I thank my mom's side (the Wilcox family), who came from humble coal mining and fishing families. Notably, I thank my grandfather Richard Wilcox, who had to drop out of college and never complete his degree, but always spoke of his love for science, the sea, and "bacteriology". I thank him for embodying the act of being "confident yet humble" and encouraging me throughout this journey until he had to move on. I finished this degree not only for myself, but for you. This degree belongs to my bloodlines as much as it does to me.

I owe this degree to my family and to my parents, who have shown me what true hard work and sacrifice look like. To my mom and dad, I thank you for your relentless encouragement, love and unwavering support. I thank my father in law, Dave, for taking me on as the daughter you never had and never failing to offer fatherly wisdom, albeit usually unsolicited. To my husband Joe, this degree would not have been possible without you. The sacrifices that you've made so that I could pursue my goals are many, and you have been my biggest supporter. You have been steadfastly committed to this journey with me, riding shotgun through every high and low. I am eternally grateful for your love, support and your (sometimes annoying) willingness to challenge me. Thank you for being my counterpart in life.

ABSTRACT

Harmful Algal Blooms (HABs) are algae undergoing prolific, unregulated growth. A well-documented HAB taxa is the cyanobacterium *Microcystis* spp., which induces anthropogenic, ecological, and economic consequences due to the production of toxins and biomass. *Microcystis* spp. blooms are globally distributed in freshwater systems, with climate change and the aquatic continuum serving to further exacerbate bloom distribution, duration, and frequency. Lake Erie of the Laurentian Great Lakes experiences annual summer *Microcystis* spp. blooms which have rendered the drinking water unfit for human consumption (i.e., the Toledo Water Crisis of 2014). As a result, these events have incited a concerted effort within the field at large to elucidate the anthropogenic and ecological drivers of these detrimental summer cyanobacterial blooms. Thus, there exists an expansive amount of research concerning summer *Microcystis* spp. blooms in Lake Erie. Yet, gaps in the field exist, and there remains a need to elucidate the factors driving the ecological success of summer *Microcystis* blooms and the ecological "failures" of their competitors (*i.e.,* diatoms). In contrast, diatom blooms dominate the winter water column of Lake Erie. While these blooms are non-toxic, the dense biomass of these blooms has been found to induce massive summer hypoxia events and dead zones. Yet, despite the magnitude of these winter diatom blooms, they remain widely uncharacterized and unstudied to date. Hence, a seasonal pattern of algal bloom succession occurs within Lake Erie: toxic *Microcystis* spp. blooms dominate summer-fall, and nuisance diatom blooms dominate winter-spring. My dissertation utilizes physical assays and molecular approaches to conduct *in vitro, in situ, a*nd *in silico* experiments to investigate the factors contributing to the ecological success and succession of these respective bloom-forming classes. Hence, this work serves to assess Lake Erie algal bloom success and succession across spatial, temporal and climatic scales.

TABLE OF CONTENTS

CHAPTER I: A TALE OF TWO BLOOMS: REFINING ECOLOGICAL PARADIGMS OF LAKE ERIE ALGAL BLOOM SUCCESS AND SUCCESSION 1

PUBLICATION NOTE 2
ABSTRACT 3
ECOLOGICAL SUCCESS OF LAKE ERIE CYANOBACTERIAL BLOOMS 4
ECOLOGICAL SUCCESS OF LAKE ERIE DIATOM BLOOMS 7
SUCCESSIONAL DYNAMICS BETWEEN CYANOBACTERIAL AND DIATOM BLOOMS 8
REFINING THE TEMPERATURE PARADIGM OF ALGAL BLOOM SUCCESSION 11
REFINING NUTRIENT PARADIGMS OF ALGAL BLOOM SUCCESSION 14
PH A NOVEL PARADIGM OF ALGAL BLOOM SUCCESSION? 16
CONCLUSION - CAVEAT BIOLOGUS 19
DISSERTATION OVERVIEW 20
REFERENCES: 24

CHAPTER II: RE-ASSESSING CONSEQUENCES OF CLASSICAL LABORATORY TECHNIQUES USING *MICROCYSTIS AERUGINOSA* AS A MODEL SYSTEM 35

PUBLICATION NOTE 36
ABSTRACT 37
INTRODUCTION 38
METHODS 39
RESULTS 46
DISCUSSION 52
COMMENTS AND RECOMMENDATIONS 56
ACKNOWLEDGMENTS 57
REFERENCES: 58
APPENDIX 60

CHAPTER III: ELUCIDATING THE ROLE OF PH ON *MICROCYSTIS*-DIATOM COMPETITION DYNAMICS IN LAKE ERIE 67

PUBLICATION NOTE 68
ABSTRACT 69
INTRODUCTION 70
RESULTS 79
DISCUSSION 88
ACKNOWLEDGEMENTS 94
REFERENCES: 95
APPENDIX 99

CHAPTER IV: INVESTIGATING ELEVATED PH EFFECTS ON FRESHWATER DIATOM TRANSCRIPTION, MORPHOLOGY AND PHYSIOLOGY 120

PUBLICATION NOTE 121
ABSTRACT 122
INTRODUCTION 123
METHODS 124
RESULTS 129

Discussion 138
Conclusion 151
Acknowledgements 152
References: 153
Appendix 161
CHAPTER V: DIATOM RESPONSES TO DECREASING ICE COVER IN LAKE ERIE 173
Publication Note 174
Abstract 175
Introduction 176
Methods 178
Results 181
Acknowledgements 202
References: 203
Appendix 209
CHAPTER VI: CONCLUSIONS 243
VITA 249

LIST OF TABLES

Table 2.1. Buffering characteristics of five freshwater culture media……40
Table 3.1. Statistical analysis of *F. crotonensis* growth rates as a function of pH……...99
Table 3.2. Statistical analysis of *M. aeruginosa* growth rates as a function of pH……100
Table 3.3. Statistical analysis of *in vitro F. crotonensis* Si deposition as a function of pH……101
Table 3.4. Statistical analysis of *in situ* diatom Si deposition as a function of pH……102
Table 4.1. Statistical analysis of *F. crotonensis* FlowCAM data……...161
Table 4.2. Statistical analysis of *F. crotonensis* abundance and Chl *a* autofluorescence……...161
Table 4.3. Statistical analysis of *F. crotonensis* photopigment data……..161
Table 4.4. Statistical analysis of *F. crotonensis* PhytoPAM data……..162
Table 5.1. Metatranscriptomic libraries with respect to study variables……...218

LIST OF FIGURES

Figure 1.1. Cyanobacterial blooms in the Lake Erie summer water column (2012-2017)……6
Figure 1.2. Diatom blooms in the Lake Erie winter water column (2007-2010)……...9
Figure 2.1. Flame-induced declines in pH in control and flamed freshwater media ……...48
Figure 2.2. Net change in pH observed in each media after 10 days of aseptic flaming……...48
Figure 2.3. Total carbon in control and flamed CT freshwater media replicates…….51
Figure 2.4. Aseptic flaming effects on CT media and axenic *M. aeruginosa* cultures…….53
Figure 2.5. Effects of flaming on heterotrophic culturing media……60
Figure 2.6. Effects of environmental conditions on pH of CT media……..61
Figure 2.7. Determination of CO_2 as the primary driver of pH decline in freshwater media……62
Figure 2.8. Mitigation of pH decline due to flaming of CT media using TAPS amendments……..63
Figure 2.9. Effects of tube inversion on control and flame replicate pH decline……..…..64
Figure 2.10. Correlation between Chlorophyll *a* autofluorescence and cell density……...65
Figure 2.11. Comparison of *M. aeruginosa* biomass accumulation in CT vs. amended CT……....66
Figure 3.1. Environmental data corresponding to a 2015 Lake Erie *Microcystis* bloom…….80
Figure 3.2. *In vitro F. crotonensis* monoculture growth curves as a function of pH……....82
Figure 3.3. *In vitro F. crotonensis* co-culture growth curves……..83
Figure 3.4. Epifluorescent microscopy of *F. crotonensis* filaments labeled with PDMPO…….....85
Figure 3.5. Si deposited per F. crotonensis filament as a function of pH…….87
Figure 3.6. Si deposited per Chl a concentration in environmental diatoms as a function of pH….87
Figure 3.7. Dissolved Si profiles corresponding to a 2015 Lake Erie *Microcystis* bloom…….103
Figure 3.8. Chl *a* concentrations corresponding to a 2015 Lake Erie *Microcystis* bloom…….....104
Figure 3.9. FlowJo graph depicting a gated population of *F. crotonensis* filaments……....105
Figure 3.10. Standard curve for *in vitro F. crotonensis* Si deposition assay…….....106
Figure 3.11. Standard curve for *in situ* Lake Erie diatom Si deposition assay……...107
Figure 3.12. *In vitro M. aeruginosa* monoculture growth curves as a function of pH……...108
Figure 3.13. *In vitro M. aeruginosa* co-culture growth curves……..109
Figure 3.14. pH drift in *F. crotonensis* monocultures……...110
Figure 3.15. pH drift in *M. aeruginosa* monocultures……...111
Figure 3.16. pH drift in *F. crotonensis* and *M. aeruginosa* co-cultures…….112
Figure 3.17. Final pH of *F. crotonensis* and *M. aeruginosa* monoculture and co-cultures……113
Figure 3.18. Simple linear regressions of *M. aeruginosa* concentration and pH drift……...114
Figure 3.19. Epifluorescent microscopy of *in vitro F. crotonensis* filaments + PDMPO…….....115
Figure 3.20. Epifluorescent microscopy data of *F. crotonensis* PDMPO assay……116
Figure 3.21. Total Si deposited per *F. crotonensis* culture as a function of pH…….117
Figure 3.22. Total Si deposited per replicate of *in situ* diatoms as a function of pH…….....118
Figure 3.23. Water column profiles collected during a 2009 Lake Erie winter survey…….....119
Figure 4.1. Heat maps depicting DE genes relating to *F. crotonensis* morphology/growth…….....131
Figure 4.2. FlowCAM data of *F. crotonensis* pH assay……133
Figure 4.3. Heat maps depicting DE genes relating to *F. crotonensis* energy production…….135

Figure 4.4. Photopigment data of *F. crotonensis* pH assay……...137
Figure 4.5. PhytoPAM data of *F. crotonensis* pH assay……139
Figure 4.6. Heat map depicting DE genes relating to the *F. crotonensis* mobilome…….....140
Figure 4.7. nMDS of similarity between *F. crotonensis* pH transcriptomes…….....163
Figure 4.8. Top 50 genes contributing to *F. crotonensis* pH transcriptome dissimilarity…….....164
Figure 4.9. Volcano plots of DE *F. crotonensis* genes as a function of pH……165
Figure 4.10. Heat map depicting DE genes relating to *F. crotonensis* Carbon metabolism……...166
Figure 4.11. Flow cytometry and fluorometer data for photopigment pH assay……...167
Figure 4.12. Total Chl *a* concentrations from photopigment pH assay…….....168
Figure 4.13. Fucoxanthin and Neoxanthin concentrations from photopigment pH assay…….....169
Figure 4.14. Ratio of total carotenoids: total Chl *a* from photopigment pH assay…….170
Figure 4.15. Ratios of carotenoids: total Chl *a* from photopigment pH assay……...171
Figure 4.16. Ratio of Chl *a*: Chl c^1c^2 from photopigment pH assay……..172
Figure 5.1. Spatial and climatic variability across metatranscriptome samples……182
Figure 5.2. Characterization of the biotic community across 12 winter Lake Erie sites…..184
Figure 5.3. Relative transcript abundance of MEPT and diatom classes……...186
Figure 5.4. nMDS of 20winter-spring Lake Erie metatranscriptomic libraries (TPM)…….....187
Figure 5.5. Diatom transcript abundance patterns in response to ice cover of COG C…….....190
Figure 5.6. Diatom transcript abundance patterns in response to ice cover of COG M……191
Figure 5.7. Phylogenetic tree of fasciclin gene distribution within diatoms…….....193
Figure 5.8. Temperature/nutrient profiles across the 12 sample sites organized by season…....219
Figure 5.9. Contribution of Chl *a* >20 μM to total Chl *a* across sample sites……220
Figure 5.10. Cell abundance of MEPT across sample sites……...221
Figure 5.11. Cell abundance of centric filamentous diatoms across winter sample sites……...222
Figure 5.12. Cell abundance of small centric diatom taxa (5-20μm) across sample sites…….....223
Figure 5.13. Mean percent contribution of three centric diatoms to total diatom abundance……224
Figure 5.14. Relative transcript abundance of domains across 20 metatranscriptomes……225
Figure 5.15. Relative transcript abundance of major eukaryota groups……226
Figure 5.16. Relative transcript abundance of Mediophyceae genera……...227
Figure 5.17. Relative transcript abundance of Coscinodiscophyceae genera……228
Figure 5.18. Relative transcript abundance of Bacillariophyceae genera……229
Figure 5.19. Relative transcript abundance of Fragilariophyceae genera……230
Figure 5.20. Simple linear regression of diatom cell and transcript abundance……231
Figure 5.21. ANOSIM of whole community and diatom expression (TPM)……232
Figure 5.22. Taxonomic distributions of DE diatom genes by ice cover……...233
Figure 5.23. Taxonomic distribution of DE Mediophyceae genes of COG C……...234
Figure 5.24. Diatom transcript abundance patterns in response to ice cover of COG P……235
Figure 5.25. Taxonomic distribution of DE Mediophyceae genes of COG P……236
Figure 5.26. Diatom transcript abundance patterns in response to ice cover of COG G……237
Figure 5.27. Normalized expression (VST) of diatom rhodopsin genes DE by ice cover…….238

Figure 5.28. Distribution of DE genes by COG category comparing season and ice cover……...239
Figure 5.29. Taxonomic distribution of DE Mediophyceae genes of COG M……..240
Figure 5.30. MODIS satellite image of ice-free and turbid Lake Erie (2-12-2023)……...241
Figure 5.31. Plankton net tows from a 2007 Lake Erie winter survey……...242

LIST OF ATTACHMENTS

Appendix Sheet 4.1

Sheet 4.1A. Transcriptome mapping statistics

Sheet 4.1B. Similarity Percentage (SIMPER) analysis on pH transcriptome genes

Sheet 4.1C. DE genes organized by COG category.

Sheet 4.1D. FlowCAM statistics

Appendix Sheet 5.1-5.2

Sheet 5.1A. JGI and manuscript metatranscriptome library IDs, metadata

Sheet 5.1B. Metatranscriptome coassembly statistics

Sheet 5.1C. Metatranscritpome library mapping statistics

Sheet 5.1D. Water column parameters, metadata

Sheet 5.1E. Water column Chlorophyll *a*, metadata

Sheet 5.1F. Water column nutrients, metadata

Sheet 5.1G. Water column phytoplankton ID and enumeration, metadata

Sheet 5.1H. Relative transcript abundance of mapped reads for domains

Sheet 5.1I. Relative transcript abundance of mapped reads for Eukaryota groups

Sheet 5.1J. Relative transcript abundance of mapped reads for MEPT

Sheet 5.1K. Relative transcript abundance of mapped reads for diatoms by class

Sheet 5.1L. Relative transcript abundance of mapped reads for Mediophyceae genera

Sheet 5.1M. Relative transcript abundance of mapped reads for Coscinodiscophyceae

Sheet 5.1N. Relative transcript abundance of mapped reads for Bacillariophyceae genera

Sheet 5.1O. Relative transcript abundance of mapped reads for Fragilariophyceae genera

Sheet 5.1P. SIMPER analysis of whole community expression (TPM) as a function of ice cover (winter libraries 1-14)

Sheet 5.1Q. PRIMER Statistical results. ANOSIM Analysis of whole community expression (TPM) as a function of ice cover (winter libraries 1-14)

Sheet 5.1R. PRIMER Statistical results. SIMPER Analysis of whole community expression (TPM) as a function of season (libraries 1-20)

Sheet 5.1S. PRIMER Statistical results. ANOSIM Analysis of whole community expression (TPM) as a function of season (libraries 1-20)

Sheet 5.1T. PRIMER Statistical results. SIMPER Analysis of Bacillariophyta community expression (TPM) as a function of ice cover (winter libraries 1-14)

Sheet 5.1U. PRIMER Statistical results. ANOSIM Analysis of Bacillariophyta community expression (TPM) as a function of ice cover (winter libraries 1-14)

Sheet 5.1V. PRIMER Statistical results. SIMPER Analysis of Bacillariophyta community expression (TPM_ as a function of season (libraries 1-20)

Sheet 5.1W. PRIMER Statistical results. ANOSIM Analysis of Bacillariophyta community expression (TPM) as a function of season (libraries 1-20)

Sheet 5.1X. DESeq2 results for comparing winter diatom community expression by ice cover (L1-4 vs. L5-14)

Sheet 5.1Y. DESeq2 results for comparing diatom community expression by season (L1-14 vs. L15-20)

Sheet 5.1Z. DE genes by ice cover in winter libraries within COG C category

Sheet 5.2A. DE genes by ice cover in winter libraries within COG M category

Sheet 5.2B. DE genes by ice cover in winter libraries within COG P category

Sheet 5.2C. DE genes by ice cover in winter libraries within COG G category

Sheet 5.2D. The eighteen diatom fasciclin protein sequences from this study

Sheet e 5.2E. Fasciclins within the DE dataset and the proteins used to functionally annotate them from eggNOG

Sheet 5.2F. All diatoms found to contain fasciclins during phylogenetic search

CHAPTER I: A TALE OF TWO BLOOMS: REFINING ECOLOGICAL PARADIGMS OF LAKE ERIE ALGAL BLOOM SUCCESS AND SUCCESSION

Publication Note

This chapter contains content adapted from a peer-reviewed, published review article in *Environmental Microbiology Reports* by Brittany N. Zepernick, Steven W. Wilhelm, George S. Bullerjahn, and Hans W. Paerl and content from a manuscript in preparation by Brittany N. Zepernick and Steven W. Wilhelm to be submitted to the *Journal of Great Lakes Research*.

All authors contributed to the drafting and final version of the manuscripts.

Abstract

The popular press and most scientists view Lake Erie as a summertime monoculture of cyanobacteria propelled by anthropogenic nutrients. While cyanobacterial blooms (often dominated by *Microcystis* spp.) deserve attention, the rediscovery of large-scale winter-spring diatom blooms has challenged our precepts. Lake Erie algal blooms do not pertain to cyanobacteria alone, as diatom blooms have been historically and consistently reported in the literature spanning all four seasons. While history also tells us cyanobacterial blooms "like it hot", recent data suggests they "also like it cold": this challenges the classical paradigm that cyanobacterial and diatom bloom succession is an artefact of differing temperature optima. Recently, cyanobacterial blooms have emerged in the oligotrophic Lake Superior, further contesting paradigms (*i.e.,* that cyanobacteria are a symptom of eutrophication while diatoms are favored in meso-oligotrophic systems). In addition, the recent rediscovery of cyanobacterial bloom-induced elevated pH in the water column (*i.e.,* lake basification) highlights the pivotal role of other drivers of algal success and succession. Considering these observations, there is an acute need to re-assess the ecological successes of bloom-forming phyla within Lake Erie and the factors which constrain their succession. Here, we evaluate the historical and present status of Lake Erie algal blooms and their implicit interlinkage. We further suggest potential reassessments of classic paradigms of algal bloom succession, such as temperature and nutrient status, and propose a novel successional paradigm: pH. Given lakes are sentinels of climate change, there is a pressing need to identify how algal blooms "succeed" across seasonal water columns before climate change further alters the algal bloom cycle. Cumulatively, this work serves as a cautionary tale that Lake Erie algal blooms cannot be studied solitarily, and traditional paradigms cannot be applied sweepingly.

Ecological success of Lake Erie cyanobacterial blooms

Lake Erie (US/Canada) is a North American treasure: it provides potable water and serves as an economic fulcrum to over 30 million lake basin residents (Canada and Agency, 1995; Field et al., 1998; Buttle et al., 2004; Millerd, 2005). On a global scale, the Great Lakes cumulatively serve as the largest freshwater body on Earth containing 20% of the globe's freshwater (Ashworth, 1987; Gronewold et al., 2013; Huisman et al., 2018). Yet, Lake Erie has a long-standing problem with summer cyanobacterial blooms, with "blooms" defined as algae undergoing unregulated growth which invoke detrimental consequences due to high biomass and/or the production of toxins (Anderson et al., 2002). Cyanobacterial genera such as *Microcystis*, *Aphanizomenon* and *Dolichospermum* were initially reported in Lake Erie throughout the early 1900's as nutrient loads to Lake Erie increased (Davis, 1954; Allinger and Reavie, 2013b; Steffen et al., 2014a; Watson et al., 2016). Yet, it was not until the 1950's, when nitrogen-fixing *Dolichospermum* and *Aphanizomenon* began to form blooms, that the lake received enhanced public attention (Davis, 1954; 1964; Steffen et al., 2014a; Huisman et al., 2018). These dense blooms shifted Lake Erie's trophic status to "hypereutrophic"(Verduin, 1964; Sweeney, 1995; McKindles et al., 2020), a major impetus for the Great Lakes Water Quality Agreement (Ijc, 1989) instituted to decrease algal blooms. This solution worked for a time and Lake Erie was pronounced "rejuvenated" (Sweeney, 1995), with cyanobacterial blooms substantially decreased throughout the 1970's-1980's (Makarewicz and Bertram, 1991; Nicholls and Hopkins, 1993; Makarewicz et al., 1999; Huisman et al., 2018). Yet, cyanobacterial blooms returned in the mid-1990's (now dominated by non-nitrogen fixing *Microcystis* spp. and *Planktothrix* spp.), coinciding with the re-eutrophication of Lake Erie (Brittain et al., 2000; Conroy and Culver, 2005; Bridgeman et al., 2013; Watson et al., 2016). Since then, *Microcystis* spp. blooms have dominated the Lake Erie summer season, invoking detrimental consequences

for ecosystem and human health (Figure 1.1) (Rinta-Kanto et al., 2009; Bridgeman et al., 2013; Steffen et al., 2017) While *Microcystis* spp. blooms have proliferated throughout the western basin of Lake Erie, the water column is far from a *Microcystis* monoculture. *Planktothrix* spp. blooms have dominated the Sandusky Bay area (Rinta-Kanto and Wilhelm, 2006; McKindles et al., 2022) and blooms of *Dolichospermum* spp. and *Aphanizomenom* spp. manifest throughout the western-central basins (Wynne and Stumpf, 2015; Chaffin et al., 2019; Yancey et al., 2023).

In contrast to their summer notoriety, cyanobacteria are thought to remain largely sub-dominant throughout the winter-spring period (though this may be due to a disproportionate number of limnological surveys focused on the summer water column rather than the winter-spring). Beyond the lack of ecological studies concerning major cyanobacterial genera in the winter, we note there are populations of other cyanobacteria that are persistently abundant yet rarely receive attention. Genera such as *Synechococcus* and *Cyanobium* are but a couple examples of the many picocyanobacteria that can be abundant components of fresh waters (Wilhelm et al., 2014). These genera contribute to the water column algal biomass (Fahnenstiel and Carrick, 1992; Carrick and Schelske, 1997) and reach densities exceeding 100,000 cells $\bullet$ L^{-1} in both summer (Wilhelm et al., 2006c) and winter periods (Twiss et al., 2012). While these cells types are persistently present, they are often overlooked and rarely included in assessments of "the cyanobacteria" in lake systems: given the potential for this size fraction to make up significant components of water column chlorophyll, it is clear that their assessment needs to be included by ecosystems ecologists to fully understand system processes (Wilhelm et al., 2003). Nonetheless, the ecological success of certain cyanobacteria in the summer months has remained uncontested and well-documented within the Lake Erie literature.

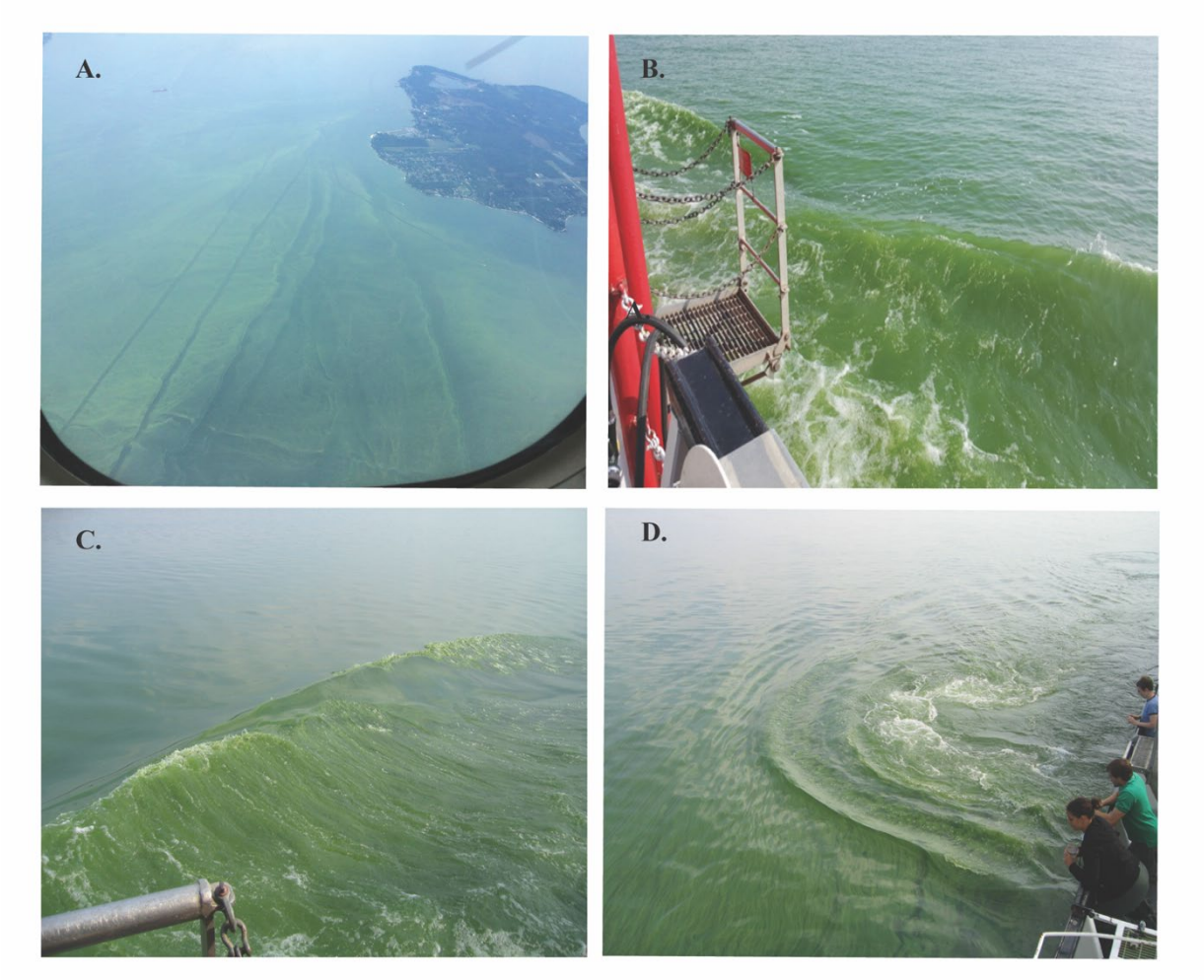


Figure 1.1: Cyanobacterial blooms (mainly comprised of *Microcystis*) in the Lake Erie summer water column (2012-2017). Pictures were taken across the western basin by Steven W. Wilhelm.

Ecological success of Lake Erie diatom blooms

One could argue diatoms lack notoriety due to the fact Lake Erie diatoms are not known to produce toxins. That said, they are not without ecological consequence, and Lake Erie has a long history of seasonally abundant diatom communities. According to the paleolimnetic record, oligotrophic diatoms (*Aulacoseira distans* and *Cocconeis disculus)* dominated the water column along with eutrophic diatoms (*Stephanodiscus, Aulacoseira granulata*, *Cyclotella bodanic*a) prior to 1850 (Stoermer et al., 1987; Stoermer et al., 1989; Stoermer et al., 1993; Stoermer et al., 1996). Cumulatively, these findings indicated Lake Erie has always contained eutrophic diatom taxa tolerant of high-nutrient conditions (Allinger and Reavie, 2013b). Subsequent nutrient loading throughout the first half of the twentieth century led to a regime shift within the diatom community, resulting in dominance by eutrophic diatom taxa such as *Fragilaria* spp. and *Stephanodiscus* spp. throughout the eutrophic western basin (Britt, 1955; Verduin, 1964; Hohn, 1969). In turn, while diatoms have been suggested to have dominated the Lake Erie summer water column for the first half of the twentieth century (Region and Davis, 1958; Nicholls et al., 1977), net diatom summer abundance declined by the 1960's (Britt, 1955; Casper, 1965). Yet, there remains a forgotten anomaly to this trend; prolific summer *Fragilaria crotonensis* blooms were reported throughout the western basin of Lake Erie throughout the late 1960's to the early 2000's, with abundances reported as high as 950,000 cells • L^{-1} (Beeton, 1965; Munawar and Munawar, 1976; Gladish and Munawar, 1980; Hartig, 1987; Munawar et al., 2008). To date, this diatom remains a prominent and metabolically active member of the Lake Erie summer water column (Saxton et al., 2012b). Indeed, in a 2019 Lake Erie study, *Fragilaria* spp. filaments were widely abundant in samples from the western basin (unpublished data associated with Zepernick et al. (2021)). Hence, this overlooked member of the planktonic community remains ecologically pertinent and present today, though the factors which constrain its ecological success are limited

to a few reports (Hartig and Wallen, 1986; Hartig, 1987; Zepernick et al., 2021; Dengg et al., 2022; Zepernick et al., 2022b). Beyond the historical summer diatom blooms, there are prominent winter-spring diatom blooms within Lake Erie (Saxton et al., 2012b; Twiss et al., 2012). Diatom blooms (comprised of *Asterionella, Synedra, Stephanodiscus*, and *Cyclotella*) were reported under Lake Erie ice in the 1930's (Chandler, 1940; Chandler, 1942; 1944; Chandler and Weeks, 1945), and remained acknowledged (Stoermer, 1975; Munawar and Munawar, 1982) yet unstudied until recently. Dense blooms of eutrophic diatoms *Aulacoseira islandica* (Coscinodiscophyceae) and *Stephanodiscus binderanus* (Mediopyceae) were rediscovered within and underneath Lake Erie ice cover by Twiss et al. (2012) (Figure 1.2). Subsequent studies determined these diatoms were metabolically active and reached Chl *a* concentrations and biovolumes that rivaled summer cyanobacterial blooms. Indeed, the large biovolumes and associated organic carbon from winter diatoms have been linked to summer hypoxia (Saxton et al., 2012b; Wilhelm et al., 2014; Reavie et al., 2016). Yet, these studies also demonstrated the winter diatom community has significantly changed since the foundational winter Chandler surveys, invoking a call to revisit comprehensive seasonal studies within the Great Lakes (Ozersky et al., 2021). Cumulatively, these studies support the critical and longstanding importance of diatom blooms in Lake Erie.

Successional dynamics between cyanobacterial and diatom blooms

As we have noted, Lake Erie literature over the last two decades has focused on summer cyanobacterial blooms, although recently this has been expanded to include winter-spring diatom blooms. Cyanobacteria and Bacillariophyta are the two most prominent Lake Erie bloom-

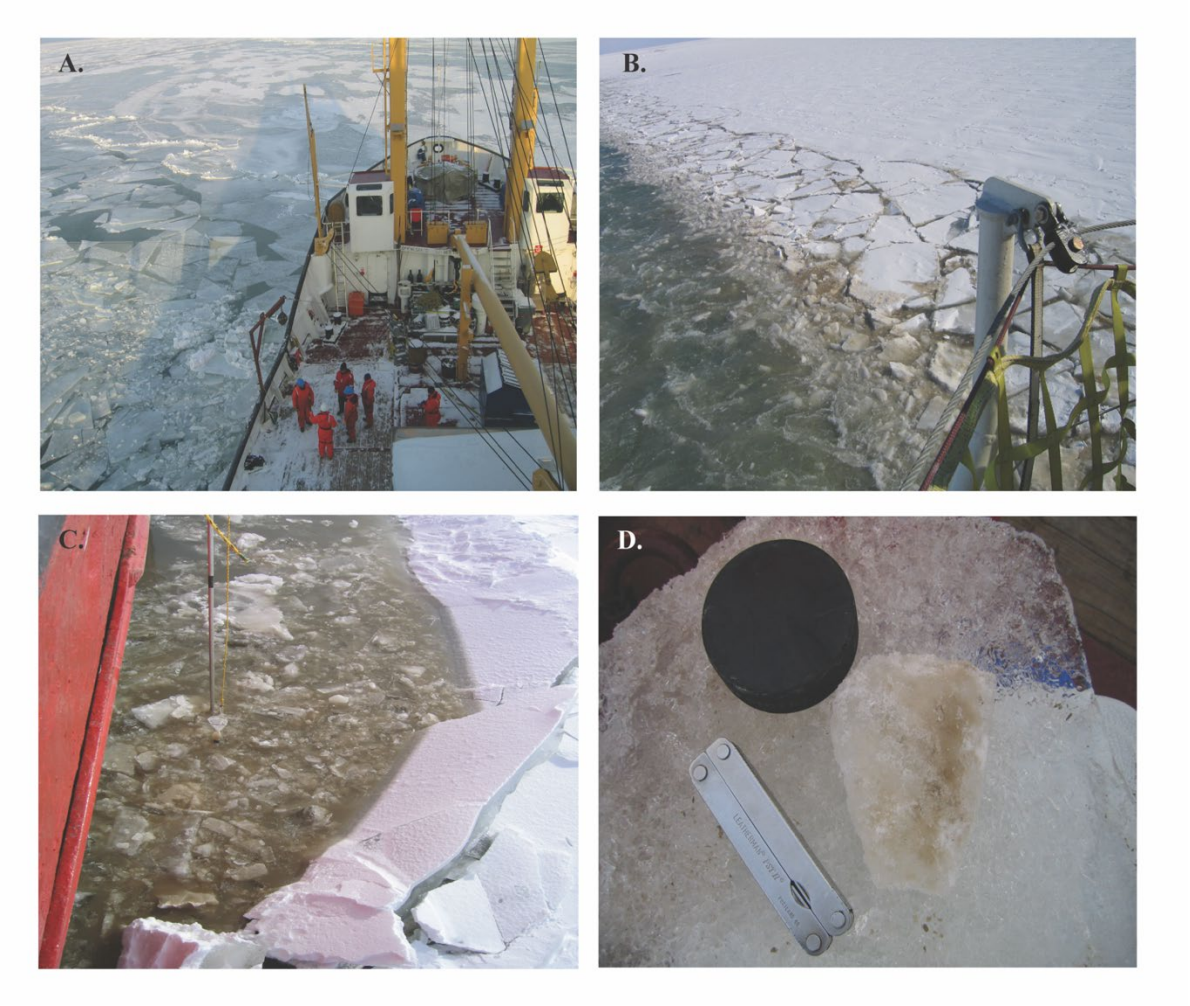


Figure 1.2: Diatom blooms (mainly comprised of *Aulacoseira islandica* and *Stephanodiscus*) in the Lake Erie winter water column (2007-2010). Pictures were taken across the western-central basin by Steven W. Wilhelm.

forming phyla which co-exist in a successional cycle: winter-spring diatom blooms are followed by summer cyanobacterial blooms, with the activity of one bloom setting the stage for the next (Wilhelm et al., 2020). Succession from one alga to another is a widely observed paradigm in itself, being reported in eutrophic freshwater systems such as Lake Tai (*Taihu*, China), Lake Victoria (Kenya), and the English Windermere South Basin amongst others (Canale and Vogel, 1974; Talling, 1976; Galat and Verdin, 1989; Krivtsov et al., 2000; Ke et al., 2008; Goldenberg and Lehman, 2012; Sitoki et al., 2012). Such studies have focused on one phylum in isolation, with relatively few studies considering both algal blooms in tandem. This is an important gap, as summer cyanobacterial and winter-spring diatom blooms are intrinsically linked (Leflaive and Ten-Hage, 2007; Niu et al., 2011; Reavie et al., 2016). Further, many studies (and models) attribute seasonal algal succession as a preference of phyla for temperature optima, relying on the classical paradigm that diatoms "like it cold" and cyanobacteria "like it hot" (Reynolds, 1997; 2006; Paerl and Huisman, 2008; Berry et al., 2017; Shatwell and Köhler, 2019). Yet, historical summer diatom blooms (Hartig, 1987) and recently addressed winter-spring cyanobacterial blooms (Reinl et al., 2023) suggest this successional trend may not be so black and white. Indeed, while there exists ample literature concerning the prevalence and causes of algal blooms in Lake Erie (Munawar and Munawar, 1976; Munawar and Heath, 2008; Allinger and Reavie, 2013b; Reavie et al., 2014; Steffen et al., 2014a; Bullerjahn et al., 2016; O'Donnell et al., 2023), there remains the need to re-visit the ecological constraints which dictate algal bloom success and succession in the face of new and shifting paradigms. Here, we refine two major paradigms (temperature and nutrients) which have been shown to constrain algal bloom succession in Lake Erie. We further propose a novel paradigm which serves to constrain algal

bloom succession: pH. Cumulatively, this work serves as a cautionary tale that Lake Erie algal blooms cannot be studied solitarily, and traditional paradigms cannot be applied sweepingly.

Refining the temperature paradigm of algal bloom succession

There exists a widely recognized temperature paradigm: *cyanobacteria are adept to warm, summer temperatures and diatoms are restricted to cold, winter temperatures*. Indeed, in the literature cyanobacteria "like it hot" (Paerl and Huisman, 2008). Prior studies demonstrated cyanobacteria achieve higher growth rates at higher temperatures (Robarts and Zohary, 1987; Reynolds, 2006; Joehnk et al., 2008; Lürling et al., 2013) and possess gas vesicles which allow them to benefit from temperature-induced stratification of the water column (Huisman et al., 2005; Paerl et al., 2006; Reynolds, 2006; Wagner and Adrian, 2009). Indeed *Microcystis* spp. peak abundances coincide with high temperatures in Lake Erie (Davis et al., 2009; Rinta-Kanto et al., 2009; Zepernick et al., 2021). While it has been previously suggested many cyanobacteria (such as *Microcystis*) "disappear" from the planktonic water column at temperatures <10°C (Reavie et al., 2016; Visser et al., 2016; Cao et al., 2022; Ming et al., 2022), emerging evidence suggests there are exceptions to this paradigm. For example Reinl et al. (2023) recently cited 37 observations of freshwater cyanobacterial "blooms" at temperatures <15° C across multiple freshwater systems. These reports suggest a need to revisit the school of thought that winter cyanobacteria are simply vegetative "overwintering" cells which are cryotolerant rather than cryophilic (Bridgeman and Penamon, 2010; Kutovaya et al., 2012; Cirés et al., 2013; Kitchens et al., 2018). In contrast, Reinl et al. (2023) found many common summer cyanobacterial bloom formers such as *Dolichospermum, Aphanizomenon, Microcystis*, *Planktothrix*, *etc*. can also grow in colder waters (Mankiewicz-Boczek et al., 2011; Babanazarova et al., 2013; Bižić-Ionescu et al., 2014; Persaud et al., 2015; Ma et al., 2016; Wejnerowski et al., 2018). Yet, while cold

tolerance in cyanobacteria is not by any means a novel concept (Dietlicher, 1974; Tang et al., 1997; Los and Murata, 1999; Vincent, 2007) it is seldomly investigated in the environment. Further, oftentimes *in vitro* studies contradict field observations. For example, *in vitro* assays demonstrated *Microcystis* elicits a cold stress response to temperature drops from 26° C to 18-19° C (Peng et al., 2018; Martin et al., 2020), which seemingly contradicts the report of a winter *Microcystis* bloom in Lake Tai (Ma et al., 2016). Further, discrepancies exist amongst *in vitro* studies investigating cold stress in *Microcystis*, with Ming et al. (2022) reporting cold temperatures of 4° C and 10° C permitted cell growth in *Microcystis* cultures in contrast to prior reports of the opposite (Peng et al., 2018; Martin et al., 2020). These incongruencies suggest a need to further elucidate cold temperature physiology of cyanobacterial bloom formers within controlled *in vitro* laboratory settings and the *in situ* environment. They also stress there may be strong degrees of variability between different strains (a phenomenon noted in the recent examination of toxin production by *Microcystis* (Hellweger et al., 2022). Surprisingly, despite Lake Erie's notoriety for cyanobacterial blooms, Reinl et al. (2023) only reported one documented instance of a cold cyanobacterial bloom within the Lake Erie water column. This study reported *Synechococcus* spp. abundances of 10^6 - 10^8 cells • L^{-1} during a 2009-2012 Lake Erie winter survey, with high abundances associated with ice-cover (Twiss et al., 2012). Yet data suggest this is not as much a bloom but instead a typical abundance for the often overlooked picoplankton (Wilhelm et al., 2006b). To this end, it may prove important to define "blooms" based on the species under discussion.

Building upon the observed winter abundances of *Synechococcus* in the winter Lake Erie water column, we observed what are considered high abundances of *Dolichospermum* (~1,800 cells • L^{-1}) during a 2020 spring survey in Lake Erie where water temperatures were ~10° C

(Bullerjahn et al., 2022; Zepernick et al., 2022a). Additionally Mckay et al. (2018) reported *Planktothrix agardhii* abundances > 1 x 10^7 • L^{-1} during early May of 2016 within the Maumee River, when water temperatures were < 15° C. Yet, beyond these studies there has been a lack of reports concerning winter/cold cyanobacterial blooms in Lake Erie. We note the absence of evidence cannot be interpreted as evidence of absence, as this may very well stem from a lack of winter surveys (Ozersky et al., 2021). Hence, there is a need to investigate the potential for psychrotolerant or psychrophilic cyanobacteria within the winter-spring Lake Erie water column and characterize cold temperature physiology in cyanobacterial bloom-forming taxa. Indeed, it may be argued these shoulder seasons could be strongly affected by projected future climates, creating a disconnect between the important biological queues of light and temperature.

There also exists the need to re-assess the paradigm that diatom blooms are constrained to cold temperatures. Shatwell et al. (2008) embodied this paradigm by stating "It is well known that cyanobacteria prefer warmer temperatures than diatoms". While temperature does constrain particular Bacillariophyta (*e.g.*, psychrophilic bloom-forming diatoms *Stephanodiscus hantzschii* and *Aulacoseira islandica* are confined to cold temperatures (Jung et al., 2009; D'souza, 2012; Saxton et al., 2012b)), there exist prominent exceptions to this paradigm which must be considered. For example, Hartig (1987) reported prolific *Fragilaria crotonensis* blooms throughout the Lake Erie summer basin. These blooms persisted throughout the latter part of the twentieth century (Beeton, 1965; Munawar and Munawar, 1976; Gladish and Munawar, 1980), and this genus remains a prominent member of the summer Lake Erie water column today (Munawar et al., 2008; Saxton et al., 2012b). Indeed, Hartig and Wallen (1986) found *in vitro F. crotonensis* cultures reached maximum growth rates at 17-23° C compared 5-11° C, and recent *in vitro* studies demonstrated *F. crotonensis* exhibits high growth rates at 26° C (Zepernick et al.,

2021; Zepernick et al., 2022b). Returning to *in situ* ecological observations, large populations of diatoms have been reported in the Nyanza Gulf and Rusinga Channel throughout the warm, dry season in Lake Victoria, Kenya which is situated directly on the Equator (Sitoki et al., 2012; Sitoki et al., 2013). Diatoms were previously reported to dominate the summer water column of Lake Constance, Germany, which reaches summer temperatures comparable to Lake Erie (Sommer and Stabel, 1983). In addition, Mancuso et al. (2021) reported diatoms were the dominant planktonic taxa throughout April-October in the Muskegon Estuary (Michigan), with summer temperatures reported at an average of ~23° C, albeit these temperatures were cooler than prior summers. Further, Stoermer (1993) reported abundances of diatoms such as *Cyclotella meneghiniana* and *Cyclotella cryptica* within the recent Lake Erie paleolimnological record, citing these diatoms have exceedingly high temperature optima conducive to the summer Lake Erie water column. Cumulatively, there is ample evidence to suggest diatoms have the potential to bloom in the warm, summer water column. Yet, Lake Erie diatoms broadly remain widely uncharacterized and unsequenced to date (Edgar et al., 2016; Zepernick et al., 2022c) ,with novel diatom species still being discovered within Lake Erie as of this year (Reavie, 2023). Thus, further research is also required regarding the potential presence of summer diatom blooms and their physiological response to warm temperatures. Broadly, this synthesis indicates the role of temperature in algal bloom success and succession requires revisiting.

Refining nutrient paradigms of algal bloom succession

There exists the widely accepted paradigm: *cyanobacteria are a symptom of eutrophication and diatoms are an indicator of meso-oligotrophic systems.* Indeed, anthropogenic nutrient loading is considered the primary driver of cyanobacterial blooms. The emergence of *Microcystis* spp. summer blooms has been attributed to the re-eutrophication of

Lake Erie (Scavia et al., 2014). Yet, the role of nitrogen and phosphorus in bloom constraint remains a topic of debate (Paerl et al., 2016; Schindler et al., 2016; Hellweger et al., 2022; Huisman et al., 2022; Stow et al., 2022; Wilhelm et al., 2022). Absent from the general discussion is the process being limited: in marine sciences "limitation" generally refers to the accumulation of biomass by phototrophs. In the present case, it appears that in Lake Erie (and other fresh waters) researchers have conflated ideas associated with both "*how much*" is there (biomass) and "*who*" is there (species composition), even though evidence suggested 20 years ago that biomass and diversity of phototrophs need to be decoupled with respect to nutrient effects (Wilhelm et al., 2003).

For example, research has indicated shifts from ammonium and nitrate to urea, which have occurred on a broad scale in North America (Paerl et al., 2016), generally promote cyanobacterial blooms (Chaffin and Bridgeman, 2014; Glibert et al., 2016; Krausfeldt et al., 2019). This phenomenon has been suggested to result from a superior ability of certain cyanobacteria to assimilate urea (relative to diatoms) as well as an ability to metabolize urea as a carbon source during periods of elevated pH (Steffen et al., 2017; Krausfeldt et al., 2019). Nonetheless, studies assert cyanobacterial blooms are constrained to eutrophic systems and exacerbated by nutrient loadings (Almanza et al., 2019). However, in the past few years this paradigm has also been called into question. The emergence of cyanobacterial blooms within oligotrophic Lake Superior was most recently suggested to "shift the high-nutrient paradigm" (Reinl et al., 2021). These blooms, comprised of *Dolichospermum,* which is typically associated with eutrophic lake conditions (Bruun, 2012), were hypothesized to be driven by temperature and precipitation rather than nutrient loading (Sterner et al., 2020). Indeed, cyanobacterial blooms have been reported in other oligotrophic freshwater systems across the Northeast U.S.

(Carey et al., 2012) and Ontario, Canada (Winter et al., 2011). Cumulatively this suggests the "high nutrient cyanobacterial paradigm" requires revisiting, and additional studies are required regarding cyanobacterial prominence and physiology in oligotrophic conditions.

In turn, there is a need to re-assess the notion that diatoms are at a disadvantage in eutrophic conditions. Throughout the decades there are various reports of diatom blooms in eutrophic freshwaters such as Lake Erie, Lake Michigan, Lake Victoria, and others (Schelske, 1975; Hartig, 1987; Middelboe et al., 1995; Sitoki et al., 2012). Most recently, *Asterionella formosa* blooms were reported in eutrophic Lake Taihu (Liu et al., 2022). In addition, numerous diatom genera serve as eutrophic ecological indicators (Kitner and Poulícková, 2003; Bellinger et al., 2006; Vilmi et al., 2015). Indeed, Stoermer (1993) indicated diatoms such as *Aulacosiera islandica, Fragilaria,* and *Stephanodiscus* serve as eutrophication indicators in the Lake Erie paleolimnological record. Further, increases in *Fragilaria crotonensis* and *Asterionella formosa* have been considered markers for when nitrogen levels have surpassed a trophic threshold in oligotrophic lakes throughout the western U.S. (Saros et al., 2005; Wolfe et al., 2006; Spaulding et al., 2015). More recently, a regime shift in the Lake Victoria diatom community was reported, with eutrophic conditions spurring a shift from endemic *Aulacosiera* species to eutrophic *Nitzschia* (Sitoki et al., 2013; Simiyu and Kurmayer, 2022). Hence, diatom prominence and physiology within eutrophic systems merits further attention within the "nutrient paradigm". In general, there exists a need to refine the role of nutrients and trophic status in algal bloom success and succession.

pH a novel paradigm of algal bloom succession?

Recent work has demonstrated diatoms are successful during periods of circumneutral pH while cyanobacteria proliferate at higher pH conditions. It is widely accepted pH constrains

phytoplankton phylogeny and physiology within the global oceans (Lomas et al., 2012; Collins et al., 2014; Das and Mangwani, 2015; Gao et al., 2019), with these works ignited by the revelation of ocean acidification (Doney et al., 2009). In contrast, there is limited literature regarding the role of pH in freshwater phytoplankton ecophysiology. This is a limnetic knowledge gap of significant importance in the face of present and future climatic changes. Looking to future climates, the Great Lakes were found to be experiencing increases in pCO_2 (and thus declines in pH) concomitantly with the global oceans (Phillips et al., 2015) due to atmospheric CO_2 accumulation with projected declines of 0.3 - 0.5 pH units by 2100. The acidification of Lake Erie has profound implications for cyanobacterial blooms: research indicates cyanobacteria are not favored by acidic conditions and prefer slightly alkaline pHs > 7.7 (Wicks and Thiel, 1990). In contrast, acidifying surface waters may benefit diatoms (Guillard and Lorenzen, 1972; Arzet et al., 1986; Hervé et al., 2012), as a body of marine literature suggests acidic conditions benefit diatoms (Wu et al., 2014; Bach and Taucher, 2019). Overall, there remains a lack of information regarding how Lake Erie algal blooms will respond to a low level, decadal increase in the acid load to the water column and this must be considered with respect to the ecological success and successional patterns of algal blooms in Lake Erie.

In contrast to atmospheric driven “lake acidification” is the biologically driven "lake basification” (Zepernick et al., 2021; Zepernick et al., 2022b; Zepernick et al., 2023). *Microcystis* blooms increase the pH of the water column as CO_2 is rapidly depleted by photosynthesis (Verspagen et al., 2014; Bullerjahn et al., 2016; Ji et al., 2020). As a result, water column pH levels can range from 9-11 during peak cyanobacterial bloom periods (Krausfeldt et al., 2019). For example, during a 2015 *Microcystis* bloom in Lake Erie the mean water column pH remained at ~9.2 for a month (Zepernick et al., 2021). Further, *Microcystis* blooms have been

documented to drive water column pH to ~10 in Lake Tai (*Taihu*, China) (Van Dam et al., 2018) and Lake Kennermermeer (The Netherlands) (Sandrini et al., 2016). During these basification events, the pH fluctuates on a diel cycle by as much as 0.5 pH units, with the highest pH levels coinciding with peak photosynthetic periods of the late afternoon as observed during a 2015 Lake Erie *Microcystis* bloom (Krausfeldt et al., 2019). Beyond episodic pH spikes, extended basification events have been observed in systems such as Lake Santa Olalla (Spain), which had a mean pH of 9.5 for 2 consecutive years due to persistent cyanobacterial blooms (Lopez-Archilla et al., 2004). Overall, this is a trend within cyanobacterial blooms which can be traced in the literature for decades (Talling, 1976; Booker and Walsby, 1981; Klemer et al., 1982; Paerl and Ustach, 1982). Yet, despite the thorough documentation of this phenomenon, few studies have directly assessed how cyanobacterial bloom-induced basification effects freshwater phytoplankton physiology.

In contrast to evidence of cyanobacterial success at high pH levels, diatoms are at a decided disadvantage. Marine diatoms are not found within the water column at pHs > 8.7, directly affecting species succession in marine environments (Hansen, 2002). Recent observations suggest this paradigm also applies to fresh waters. Alkaline pH conditions decrease growth and silica deposition within the model diatom *F. crotonensis* (*in vitro*) and environmental Lake Erie diatom communities (*in situ*). Cumulatively, observations suggest diatoms are "unsuccessful" during cyanobacterial-bloom-induced pH levels (Zepernick et al., 2021; Zepernick et al., 2022b; Zepernick et al., 2023). Further, these studies imply a pivotal role of pH in Lake Erie algal bloom succession, as prolonged basification likely suppresses diatoms throughout the summer and delays fall diatom succession (Wilhelm et al., 2020; Zepernick et al., 2021; Zepernick et al., 2022b). The recent literature lends further support for the case of a "pH

paradigm". A large-scale survey of 464 North American lakes demonstrated pH was the only variable to significantly relate to cyanobacterial biomass: with temperature, trophic status, and other factors falling short of influence (Bonilla et al., 2023). Further, Zhang (2023) demonstrated cyanobacterial-induced pH levels caused calcium carbonate precipitation and silica dissolution in a Florida subtropical lagoon. Burdick et al. (2020) reported cyanobacterial blooms in the Upper Klamath Lake (Oregon) drove the water column pH to levels of 10, which likely invokes sublethal stress on endangered Lost River and Short Nose suckers. Hence, there is a need to determine how lake basification alters the physiology of those inducing these events (cyanobacteria) and those which are also affected (diatoms and other alga). Cumulatively, the role of pH in freshwater algal bloom success and succession requires additional attention.

Conclusion - Caveat Biologus

The paradigms discussed herein undoubtedly maintain their efficacy. Yet, traditional concepts require revisiting and expansion in the face of emerging knowledge. The success of cyanobacteria such as *Microcystis* spp. has been recognized as "a complicated and confusing story" (Wilhelm et al., 2020). Undoubtedly, no one factor, or paradigm, is responsible for algal bloom success or succession at all times or in all places. In turn, no single algal bloom occurs solitarily, rather each bloom shapes the water column for the next. The observations accumulated here provide a cautionary tale that paradigms are often too liberally applied to algal blooms, which places future bloom projections and models at a significant fault. For the limnologist, a return to many ecological principles (*e.g.,* competitive exclusion theory (Hardin, 1960)) is ripe for examination in the context of fresh waters. Often the devil is in the ecological details, and this cautionary tale must be kept in mind as the field increasingly relies on models to predict bloom magnitude and severity.

Dissertation overview

The research presented in this dissertation employs *in vitro, in situ* and *in silico* approaches to investigate the drivers which constrain algal bloom success and succession in Lake Erie (US/Canada). This work primarily focuses on the often unsung and understudied diatom blooms of Lake Erie. Hence, the early Chapters of this dissertation entailed the establishment of an *in vitro* model diatom system which was subsequently used to investigate ecologically pertinent hypotheses. In turn, summer *in situ* assays and winter-spring water column samples culminate into a comprehensive snapshot of the seasonal dynamics of the Lake Erie diatom community. In total, the research delineated here assesses algal bloom success and succession across spatial, temporal and climatic gradients.

Chapter II describes the establishment of an *in vitro* pH assay developed to investigate *Microcystis* bloom-induced pH effects on freshwater diatoms. Early optimizations of the assay revealed the pH of freshwater media varied widely from the initial pH levels it was titrated to (Zepernick et al., 2020). Further investigations indicated flaming of the culture tube openings as part of aseptic technique significantly reduced the pH of freshwater culture media via the incorporation of $CO_{2\,(g)}$. Indeed, the pH pf freshwater culture media dropped by 2.0 full pH units after mimicking a 10 day growth study with daily subsampling events for cell enumeration. Further, it was discovered aseptic flaming altered *Microcystis* growth dynamics as $CO_{2\,(g)}$ serves as a carbon source for the cyanobacteria, fueling growth and variability amongst biological replicates. As a result of this work, optimizations were made to our freshwater media to ensure the pH remained constant throughout pH growth assays and aseptic flaming was markedly reduced during growth studies. In total, this work serves as a cautionary tale of the unintended consequences of classical laboratory techniques.

Following the establishment of the pH assay in Chapter II, *in vitro* pH assays were conducted using the freshwater diatom *F. crotonensis* and *Microcystis aeruginosa* to deduce to effects of pH on species success and succession in Chapter III. While the bloom induced pH of 9.2 significantly reduced F. crotonensis growth rates by ~50% compared to pH 7.7 controls, it did not significantly affect *Microcystis* growth rates (Zepernick et al., 2021). Further investigation revealed silica (Si) deposition (*i.e.,* the process of diatom cell wall formation) was significantly decreased within *in vitro F. crotonensis* cultures at pH 9.2; serving as one potential mechanism behind high pH induced declines in growth rates. Subsequent *in situ* pH assays performed within the Lake Erie water column indicated environmental communities (largely dominated by diatoms *F. crotonensis* and *Asterionella formosa*) were significantly decreased at the pH of 9.2 compared the controls. Cumulatively, this Chapter demonstrated the *Microcystis* bloom-induced pH of 9.2 decreased growth and Si deposition within the *in vitro* model diatom *F. crotonensis* and *in situ* Lake Erie diatom communities. In particular, this work suggested *Microcystis* induced pH levels likely suppress summer diatom populations and further delay diatom fall succession of the summer cyanobacterial blooms.

While Chapter III served as a preliminary investigation into the effects of pH on freshwater algal bloom taxa, it fell short of describing the intracellular mechanism behind the observed declines in diatom growth and Si deposition. To address this gap, the genome of *F. crotonensis* was sequenced (Zepernick et al., 2022b) to facilitate transcriptomic studies with the aim of generating hypotheses. Following, Chapter IV delineated results of an *in vitro* pH transcriptomic study of the model diatom *F. crotonensis.* Transcriptome-derived hypotheses were informed with *in vitro* physiological assays which revealed three central findings: 1) high pH results in smaller, rougher and "browner" *F. crotonensis* filaments, 2) high pH decreases

photosynthetic processes and increases the expression of cell cycle arrest genes in *F. crotonensis* filaments, and 3) high pH increases the expression of *F. crotonensis* transposable elements resulting in the coining of the "Genomic Roulette" hypothesis (Zepernick et al., 2022d).

In contrast to Chapters II-IV which focused on summer diatom success and succession dynamics, Chapter V pivots to the winter-spring Lake Erie diatom community which remains widely unstudied and uncharacterized to date. In efforts to address this knowledge gap, samples were throughout winter and spring 2019-202 to investigate how Lake Erie winter diatom communities respond to ice cover vs. ice-free conditions. To our knowledge, this was the first large-scale bioinformatic assessment of the winter Lake Erie community (Zepernick et al. 2022a). Transcriptomic analyses and physiochemical data indicated the winter diatom community of 2019-2020 was markedly different from prior reports of 2007-2012 (Zepernick et al., 2023 in preparation). Yet, the winter water column remained dominated by diatoms, particularly the centric filamentous diatoms *A. islandica* and *Stephanodiscus*. Despite this continued dominance, ice-free conditions reduced diatom abundance and increased heterogeneity within the diatom community. Notably, diatoms of the class Mediophyceae (polar centric) significantly increased the expression of fasciclin and photosynthesis genes within the ice-free water column, leading to the "fasciclin rafting hypothesis" which suggests diatoms may raft together into colonies to optimize their location in the ice-free turbid water column of Lake Erie. While this Chapter serves as the first large-scale bioinformatic analysis of the Lake Erie winter community, it illuminated a need for comprehensive fresh water taxonomic annotation tools and physiological assessments of the winter community.

Cumulatively, the work described above advances our knowledge of Lake Erie algal blooms and the drivers which constrain their success and succession. Further, this work

emphasizes the importance of diatoms within the Lake Erie water column while serving as a foundational basis for the establishment of a novel algal bloom successional paradigm (pH) and the emergence of a new field (lake basification).

References:

Allinger, L.E., and Reavie, E.D. (2013). The ecological history of Lake Erie as recorded by the phytoplankton community. *Journal of Great Lakes Research* 39**,** 365-382.

Almanza, V., Pedreros, P., Laughinghouse Iv, H.D., Félez, J., Parra, O., Azócar, M., and Urrutia, R. (2019). Association between trophic state, watershed use, and blooms of cyanobacteria in south-central Chile. *Limnologica* 75**,** 30-41.

Anderson, D.M., Glibert, P.M., and Burkholder, J.M. (2002). Harmful algal blooms and eutrophication: nutrient sources, composition, and consequences. *Estuaries* 25**,** 704-726.

Arzet, K., Steinberg, C., Psenner, R., and Schulz, N. (1986). Diatom distribution and diatom inferred pH in the sediment of four alpine lakes. *Hydrobiologia* 143**,** 247-254.

Ashworth, W. (1987). *The late, Great Lakes: an environmental history.* Wayne State University Press.

Babanazarova, O., Sidelev, S., and Schischeleva, S. (2013). The structure of winter phytoplankton in Lake Nero, Russia, a hypertrophic lake dominated by Planktothrix-like Cyanobacteria. *Aquatic Biosystems* 9**,** 1-11.

Bach, L.T., and Taucher, J. (2019). CO 2 effects on diatoms: a synthesis of more than a decade of ocean acidification experiments with natural communities. *Ocean Science* 15**,** 1159-1175.

Beeton, A.M. (1965). EUTROPHICATION OF THE ST. LAWRENCE GREAT LAKES 1. *Limnology and Oceanography* 10**,** 240-254.

Bellinger, B.J., Cocquyt, C., and O'reilly, C.M. (2006). Benthic diatoms as indicators of eutrophication in tropical streams. *Hydrobiologia* 573**,** 75-87.

Berry, M.A., Davis, T.W., Cory, R.M., Duhaime, M.B., Johengen, T.H., Kling, G.W., Marino, J.A., Den Uyl, P.A., Gossiaux, D., and Dick, G.J. (2017). Cyanobacterial harmful algal blooms are a biological disturbance to Western Lake Erie bacterial communities. *Environmental microbiology* 19**,** 1149-1162.

Bižić-Ionescu, M., Amann, R., and Grossart, H.-P. (2014). Massive regime shifts and high activity of heterotrophic bacteria in an ice-covered lake. *PloS one* 9**,** e113611.

Bonilla, S., Aguilera, A., Aubriot, L., Huszar, V., Almanza, V., Haakonsson, S., Izaguirre, I., O'farrell, I., Salazar, A., and Becker, V. (2023). Nutrients and not temperature are the key drivers for cyanobacterial biomass in the Americas. *Harmful Algae* 121**,** 102367.

Booker, M., and Walsby, A. (1981). Bloom formation and stratification by a planktonic blue-green alga in an experimental water column. *British phycological journal* 16**,** 411-421.

Bridgeman, T.B., Chaffin, J.D., and Filbrun, J.E. (2013). A novel method for tracking western Lake Erie Microcystis blooms, 2002–2011. *Journal of Great Lakes Research* 39**,** 83-89.

Bridgeman, T.B., and Penamon, W.A. (2010). Lyngbya wollei in western Lake Erie. *Journal of Great Lakes Research* 36**,** 167-171.

Britt, N.W. (1955). Stratification in western Lake Erie in summer of 1953: effects on the Hexagenia (Ephemeroptera) population. *Ecology* 36**,** 239-244.

Brittain, S.M., Wang, J., Babcock-Jackson, L., Carmichael, W.W., Rinehart, K.L., and Culver, D.A. (2000). Isolation and characterization of microcystins, cyclic heptapeptide hepatotoxins from a Lake Erie strain of *Microcystis aeruginosa*. *Journal of Great Lakes Research* 26**,** 241-249.

Bruun, K. (2012). Algae can function as indicators of water pollution. *Nostoca Algae Laboratory, Washington State Lake Protection Association. Available online: www. nostoca. com*.

Bullerjahn, G.S., Anderson, J.T., and Mckay, R.M. (2022). "Winter survey data from Lake Erie from 2018-2020". 3 ed. (Biological and Chemical Oceanography Data Management Office (BCO-DMO)).

Bullerjahn, G.S., Mckay, R.M., Davis, T.W., Baker, D.B., Boyer, G.L., D'anglada, L.V., Doucette, G.J., Ho, J.C., Irwin, E.G., and Kling, C.L. (2016). Global solutions to regional problems: Collecting global expertise to address the problem of harmful cyanobacterial blooms. A Lake Erie case study. *Harmful Algae* 54**,** 223-238.

Burdick, S.M., Hewitt, D.A., Martin, B.A., Schenk, L., and Rounds, S.A. (2020). Effects of harmful algal blooms and associated water-quality on endangered Lost River and shortnose suckers. *Harmful Algae* 97**,** 101847.

Buttle, J., Muir, T., and Frain, J. (2004). Economic impacts of climate change on the Canadian Great Lakes hydroelectric power producers: a supply analysis. *Canadian Water Resources Journal/Revue canadienne des ressources hydriques* 29**,** 89-110.

Canada, G.O., and Agency, U.E.P. (1995). "The Great Lakes: An environmental atlas and resource book". Great Lakes National Program Office Chicago, Illinois).

Canale, R.P., and Vogel, A.H. (1974). Effects of temperature on phytoplankton growth. *Journal of the Environmental Engineering Division* 100**,** 231-241.

Cao, H., Han, L., and Li, L. (2022). A deep learning method for cyanobacterial harmful algae blooms prediction in Taihu Lake, China. *Harmful Algae* 113**,** 102189.

Carey, C.C., Ewing, H.A., Cottingham, K.L., Weathers, K.C., Thomas, R.Q., and Haney, J.F. (2012). Occurrence and toxicity of the cyanobacterium Gloeotrichia echinulata in low-nutrient lakes in the northeastern United States. *Aquatic Ecology* 46**,** 395-409.

Carrick, H.J., and Schelske, C.L. (1997). Have we overlooked the importance of small phytoplankton in productive waters? *Limnology and Oceanography* 42**,** 1613-1621.

Casper, V.L. (1965). A phytoplankton bloom in western Lake Erie. *University of Michigan Great Lakes Res Div* 13**,** 29-35.

Chaffin, J.D., and Bridgeman, T.B. (2014). Organic and inorganic nitrogen utilization by nitrogen-stressed cyanobacteria during bloom conditions. *Journal of applied phycology* 26**,** 299-309.

Chaffin, J.D., Mishra, S., Kane, D.D., Bade, D.L., Stanislawczyk, K., Slodysko, K.N., Jones, K.W., Parker, E.M., and Fox, E.L. (2019). Cyanobacterial blooms in the central basin of Lake Erie: Potentials for cyanotoxins and environmental drivers. *Journal of Great Lakes Research* 45**,** 277-289.

Chandler, D.C. (1940). Limnological studies of western Lake Erie: I. Plankton and certain physical-chemical data of the Bass Islands region, from Septbember 1938, to November, 1939. *Ohio Journal of Science* 40**,** 291-336.

Chandler, D.C. (1942). Limnological Studies of Western Lake Erie. III, Phytoplankton and Physical-Chemical Data from November, 1939, to November 1940.

Chandler, D.C. (1944). Limnological studies of western Lake Erie IV. Relation of limnological and climatic factors to the phytoplankton of 1941. *Transactions of the American Microscopical Society* 63**,** 203-236.

Chandler, D.C., and Weeks, O.B. (1945). Limnological studies of western Lake Erie: V. Relation of limnological and meteorological conditions to the production of phytoplankton in 1942. *Ecological Monographs* 15**,** 435-457.

Cirés, S., Wörmer, L., Agha, R., and Quesada, A. (2013). Overwintering populations of Anabaena, Aphanizomenon and Microcystis as potential inocula for summer blooms. *Journal of Plankton Research* 35**,** 1254-1266.
Collins, S., Rost, B., and Rynearson, T.A. (2014). Evolutionary potential of marine phytoplankton under ocean acidification. *Evolutionary applications* 7**,** 140-155.
Conroy, J.D., and Culver, D.A. (2005). Do dreissenid mussels affect Lake Erie ecosystem stability processes? *The American midland naturalist* 153**,** 20-32.
D'souza, N.A. (2012). *Psychrophilic diatoms in ice-covered Lake Erie.* Bowling Green State University.
Das, S., and Mangwani, N. (2015). Ocean acidification and marine microorganisms: responses and consequences. *Oceanologia* 57**,** 349-361.
Davis, C.C. (1954). A Preliminary Study of the Plankton of the Cleveland Harbor Area, Ohio: II. The Distribution and Quantity of the Phytoplankton. *Ecological Monographs* 24**,** 322-347.
Davis, C.C. (1964). Evidence for the eutrophication of Lake Erie from phytoplankton records. *Limnology and Oceanography* 9**,** 275-283.
Davis, T.W., Berry, D.L., Boyer, G.L., and Gobler, C.J. (2009). The effects of temperature and nutrients on the growth and dynamics of toxic and non-toxic strains of *Microcystis* during cyanobacteria blooms. *Harmful Algae* 8**,** 715-725.
Dengg, M., Stirling, C.H., Reid, M.R., Verburg, P., Armstrong, E., Kelly, L.T., and Wood, S.A. (2022). Growth at the limits: comparing trace metal limitation of a freshwater cyanobacterium (Dolichospermum lemmermannii) and a freshwater diatom (Fragilaria crotonensis). *Scientific Reports* 12**,** 467.
Dietlicher, K. (1974). *The Water Quality of the Lakes of Zurich and" Walensee": An Essay of Description.* Zurich Waterworks.
Doney, S.C., Fabry, V.J., Feely, R.A., and Kleypas, J.A. (2009). Ocean acidification: the other CO_2 problem. *Annual Review of Marine Science* 1**,** 169-192.
Edgar, R., Morris, P., Rozmarynowycz, M., D'souza, N., Moniruzzaman, M., Bourbonniere, R., Bullerjahn, G., Phuntumart, V., Wilhelm, S., and Mckay, R. (2016). Adaptations to photoautotrophy associated with seasonal ice cover in a large lake revealed by metatranscriptome analysis of a winter diatom bloom. *Journal of Great Lakes Research* 42**,** 1007-1015.
Fahnenstiel, G.L., and Carrick, H.J. (1992). Phototrophic picoplankton in Lakes Huron and Michigan: Abundance, distribution, composition, and contribution to biomass and production. *Canadian Journal of Fisheries and Aquatic Sciences* 49**,** 379-388.
Field, C.B., Behrenfeld, M.J., Randerson, J.T., and Falkowski, P. (1998). Primary production of the biosphere: integrating terrestrial and oceanic components. *Science* 281**,** 237-240.
Galat, D.L., and Verdin, J.P. (1989). Patchiness, collapse and succession of a cyanobacterial bloom evaluated by synoptic sampling and remote sensing. *Journal of Plankton Research* 11**,** 925-948.
Gao, K., Beardall, J., Häder, D.-P., Hall-Spencer, J.M., Gao, G., and Hutchins, D.A. (2019). Effects of ocean acidification on marine photosynthetic organisms under the concurrent influences of warming, UV radiation, and deoxygenation. *Frontiers in Marine Science* 6**,** 322.

Gladish, D., and Munawar, M. (1980). The phytoplankton biomass and species composition at two stations in western Lake Erie, 1975/76. *Internationale Revue der gesamten Hydrobiologie und Hydrographie* 65**,** 691-708.

Glibert, P.M., Wilkerson, F.P., Dugdale, R.C., Raven, J.A., Dupont, C.L., Leavitt, P.R., Parker, A.E., Burkholder, J.M., and Kana, T.M. (2016). Pluses and minuses of ammonium and nitrate uptake and assimilation by phytoplankton and implications for productivity and community composition, with emphasis on nitrogen-enriched conditions. *Limnology and Oceanography* 61**,** 165-197.

Goldenberg, S.Z., and Lehman, J.T. (2012). Diatom response to the whole lake manipulation of a eutrophic urban impoundment. *Hydrobiologia* 691**,** 71-80.

Gronewold, A.D., Fortin, V., Lofgren, B., Clites, A., Stow, C.A., and Quinn, F. (2013). Coasts, water levels, and climate change: A Great Lakes perspective. *Climatic Change* 120**,** 697-711.

Guillard, R.R., and Lorenzen, C.J. (1972). Yellow-green algae with chlorophyllide C 1,2 *Journal of Phycology* 8**,** 10-14.

Hansen, P.J. (2002). Effect of high pH on the growth and survival of marine phytoplankton: implications for species succession. *Aquatic Microbial Ecology* 28**,** 279-288.

Hardin, G. (1960). The competitive exclusion principle. *Science* 131**,** 1292-1298.

Hartig, J.H. (1987). Factors contributing to development of *Fragilaria crontonensis* Kitton Pulses in Pigeon Bay waters of western Lake Erie. *Journal of Great Lakes Research* 13**,** 65-77.

Hartig, J.H., and Wallen, D.G. (1986). The influence of light and temperature on growth and photosynthesis of *Fragilaria crotonensis* Kitton. *Journal of Freshwater Ecology* 3**,** 371-382.

Hellweger, F.L., Martin, R.M., Eigemann, F., Smith, D.J., Dick, G.J., and Wilhelm, S.W. (2022). Models predict planned phosphorus load reduction will make Lake Erie more toxic. *Science* 376**,** 1001-1005.

Hervé, V., Derr, J., Douady, S., Quinet, M., Moisan, L., and Lopez, P.J. (2012). Multiparametric analyses reveal the pH-dependence of silicon biomineralization in diatoms. *PloS One* 7**,** e46722.

Hohn, M.H. (1969). *Qualitative and Quantitative Analyses of Plankton Diatoms: Bass Island Area, Lake Erie, 1938-1965, Including Synoptic Surveys of 1960-1963.* Ohio State University.

Huisman, J., Codd, G.A., Paerl, H.W., Ibelings, B.W., Verspagen, J.M., and Visser, P.M. (2018). Cyanobacterial blooms. *Nature Reviews Microbiology* 16**,** 471-483.

Huisman, J., Dittmann, E., Fastner, J., Schuurmans, J.M., Scott, J.T., Van De Waal, D.B., Visser, P.M., Welker, M., and Chorus, I. (2022). Comment on "Models predict planned phosphorus load reduction will make Lake Erie more toxic". *Science* 378**,** eadd9959.

Huisman, J., Matthijs, H., and Visser, P. (2005). Harmful Cyanobacteria Springer Aquatic Ecology Series 3. *Dordrecht, The Netheralands*.

Ijc (1989). *International Joint Commission (IJC) United States and Canada 1989. Great Lakes Water Quality Agreement of 1978.* http://www.ijc.org/agree/quality.html [Online]. [Accessed].

Ji, X., Verspagen, J.M., Van De Waal, D.B., Rost, B., and Huisman, J. (2020). Phenotypic plasticity of carbon fixation stimulates cyanobacterial blooms at elevated CO_2. *Science Advances* 6.

Joehnk, K.D., Huisman, J., Sharples, J., Sommeijer, B., Visser, P.M., and Stroom, J.M. (2008). Summer heatwaves promote blooms of harmful cyanobacteria. *Global Change Biology* 14**,** 495-512.

Jung, S.W., Kwon, O.Y., Lee, J.H., and Han, M.-S. (2009). Effects of water temperature and silicate on the winter blooming diatom Stephanodiscus hantzschii (Bacillariophyceae) growing in eutrophic conditions in the lower Han River, South Korea. *Journal of Freshwater Ecology* 24**,** 219-226.

Ke, Z., Xie, P., and Guo, L. (2008). Controlling factors of spring–summer phytoplankton succession in Lake Taihu (Meiliang Bay, China). *Hydrobiologia* 607**,** 41-49.

Kitchens, C.M., Johengen, T.H., and Davis, T.W. (2018). Establishing spatial and temporal patterns in Microcystis sediment seed stock viability and their relationship to subsequent bloom development in Western Lake Erie. *PloS one* 13**,** e0206821.

Kitner, M., and Poulícková, A. (2003). Littoral diatoms as indicators for the eutrophication of shallow lakes. *Hydrobiologia* 506**,** 519-524.

Klemer, A., Feuillade, J., and Feuillade, M. (1982). Cyanobacterial blooms: carbon and nitrogen limitation have opposite effects on the buoyancy of Oscillatoria. *Science* 215**,** 1629-1631.

Krausfeldt, L.E., Farmer, A.T., Castro Gonzalez, H., Zepernick, B.N., Campagna, S.R., and Wilhelm, S.W. (2019). Urea is both a carbon and nitrogen source for *Microcystis aeruginosa*: tracking ^{13}C incorporation at bloom pH conditions. *Frontiers in Microbiology* 10**,** 1064.

Krivtsov, V., Corliss, J., Bellinger, E., and Sigee, D. (2000). Indirect regulation rule for consecutive stages of ecological succession. *Ecological Modelling* 133**,** 73-81.

Kutovaya, O.A., Mckay, R.M.L., Beall, B.F., Wilhelm, S.W., Kane, D.D., Chaffin, J.D., Bridgeman, T.B., and Bullerjahn, G.S. (2012). Evidence against fluvial seeding of recurrent toxic blooms of Microcystis spp. in Lake Erie's western basin. *Harmful Algae* 15**,** 71-77.

Leflaive, J.P., and Ten-Hage, L. (2007). Algal and cyanobacterial secondary metabolites in freshwaters: a comparison of allelopathic compounds and toxins. *Freshwater Biology* 52**,** 199-214.

Liu, X., Li, Y., Shen, R., Jeppesen, E., Liu, Z., and Chen, F. (2022). A trophic cascade triggers blooms of Asterionella formosa in subtropical eutrophic Lake Taihu, China. *Freshwater Biology* 67**,** 1938-1948.

Lomas, M.W., Hopkinson, B.M., Ryan, J.L.D., Shi, D., Xu, Y., and Morel, F. (2012). Effect of ocean acidification on cyanobacteria in the subtropical North Atlantic. *Aquatic Microbial Ecology* 66**,** 211-222.

Lopez-Archilla, A.I., Moreira, D., López-García, P., and Guerrero, C. (2004). Phytoplankton diversity and cyanobacterial dominance in a hypereutrophic shallow lake with biologically produced alkaline pH. *Extremophiles* 8**,** 109-115.

Los, D.A., and Murata, N. (1999). Responses to cold shock in cyanobacteria. *J. Mol. Microbiol. Biotechnol* 1**,** 221-230.

Lürling, M., Eshetu, F., Faassen, E.J., Kosten, S., and Huszar, V.L. (2013). Comparison of cyanobacterial and green algal growth rates at different temperatures. *Freshwater Biology* 58**,** 552-559.

Ma, J., Qin, B., Paerl, H.W., Brookes, J.D., Hall, N.S., Shi, K., Zhou, Y., Guo, J., Li, Z., and Xu, H. (2016). The persistence of cyanobacterial *Microcystis* spp. blooms throughout winter in Lake Taihu, China. *Limnology and Oceanography* 61**,** 711-722.

Makarewicz, J.C., and Bertram, P. (1991). Evidence for the restoration of the Lake Erie ecosystem. *Bioscience* 41**,** 216-223.
Makarewicz, J.C., Lewis, T.W., and Bertram, P. (1999). Phytoplankton composition and biomass in the offshore waters of Lake Erie: pre-and post-Dreissena introduction (1983–1993). *Journal of Great Lakes Research* 25**,** 135-148.
Mancuso, J.L., Weinke, A.D., Stone, I.P., Hamsher, S.E., Villar-Argaiz, M., and Biddanda, B.A. (2021). Cold and wet: Diatoms dominate the phytoplankton community during a year of anomalous weather in a Great Lakes estuary. *Journal of Great Lakes Research* 47**,** 1305-1315.
Mankiewicz-Boczek, J., Gągała, I., Kokociński, M., Jurczak, T., and Stefaniak, K. (2011). Perennial toxigenic Planktothrix agardhii bloom in selected lakes of Western Poland. *Environmental toxicology* 26**,** 10-20.
Martin, R.M., Moniruzzaman, M., Stark, G.F., Gann, E.R., Derminio, D.S., Wei, B., Hellweger, F.L., Pinto, A., Boyer, G.L., and Wilhelm, S.W. (2020). Episodic decrease in temperature increases mcy gene transcription and cellular microcystin in continuous cultures of Microcystis aeruginosa PCC 7806. *Frontiers in Microbiology* 11**,** 601864.
Mckay, R.M.L., Tuttle, T., Reitz, L.A., Bullerjahn, G.S., Cody, W.R., Mcdowell, A.J., and Davis, T.W. (2018). Early onset of a microcystin-producing cyanobacterial bloom in an agriculturally-influenced Great Lakes tributary. *Journal of Oceanology and Limnology* 36**,** 1112-1125.
Mckindles, K., Frenken, T., Mckay, R.M.L., and Bullerjahn, G.S. (2020). Binational efforts addressing cyanobacterial harmful algal blooms in the Great Lakes. *Contaminants of the Great Lakes***,** 109-133.
Mckindles, K.M., Mckay, R.M., and Bullerjahn, G.S. (2022). Genomic comparison of Planktothrix agardhii isolates from a Lake Erie embayment. *Plos one* 17**,** e0273454.
Middelboe, M., Søndergaard, M., Letarte, Y., and Borch, N. (1995). Attached and free-living bacteria: production and polymer hydrolysis during a diatom bloom. *Microbial Ecology***,** 231-248.
Millerd, F. (2005). The economic impact of climate change on Canadian commercial navigation on the Great Lake. *Canadian Water Resources Journal* 30**,** 269-280.
Ming, H., Yan, G., Zhang, X., Pei, X., Fu, L., and Zhou, D. (2022). Harsh temperature induces Microcystis aeruginosa growth enhancement and water deterioration during vernalization. *Water Research* 223**,** 118956.
Munawar, M., and Heath, R. (2008). Checking the pulse of Lake Erie.
Munawar, M., Munawar, I., Fitzpatrick, M., Niblock, H., Bowen, K., Lorimer, J., and Heath, R. (2008). An intensive assessment of planktonic communities in the Canadian waters of Lake Erie, 1998. *Checking the pulse of Lake Erie. Aquatic Ecosystem Health and Management Society, Burlington, Ontario***,** 297-346.
Munawar, M., and Munawar, I.F. (1976). A lakewide study of phytoplankton biomass and its species composition in Lake Erie, April–December 1970. *Journal of the Fisheries Board of Canada* 33**,** 581-600.
Munawar, M.U., and Munawar, I. (1982). Phycological studies in Lakes Ontario, Erie, Huron, and Superior. *Canadian Journal of Botany* 60**,** 1837-1858.
Nicholls, K., Standen, D., Hopkins, G., and Carney, E. (1977). Declines in the near-shore phytoplankton of Lake Erie's western basin since 1971. *Journal of Great Lakes Research* 3**,** 72-78.

Nicholls, K.H., and Hopkins, G.J. (1993). Recent changes in Lake Erie (north shore) phytoplankton: cumulative impacts of phosphorus loading reductions and the zebra mussel introduction. *Journal of Great Lakes Research* 19**,** 637-647.

Niu, Y., Shen, H., Chen, J., Xie, P., Yang, X., Tao, M., Ma, Z., and Qi, M. (2011). Phytoplankton community succession shaping bacterioplankton community composition in Lake Taihu, China. *Water research* 45**,** 4169-4182.

O'donnell, D.R., Briland, R., Budnik, R.R., Ludsin, S.A., and Hood, J.M. (2023). Trends in Lake Erie phytoplankton biomass and community structure during a 20-year period of rapid environmental change. *Journal of Great Lakes Research*.

Ozersky, T., Bramburger, A.J., Elgin, A.K., Vanderploeg, H.A., Wang, J., Austin, J.A., Carrick, H.J., Chavarie, L., Depew, D.C., and Fisk, A.T. (2021). "The changing face of winter: lessons and questions from the Laurentian Great Lakes". (Journal of Geophysical Research: Biogeosciences: Wiley Online Library).

Paerl, H., Fulton, R., Graneli, E., and Turner, J. (2006). Ecology of harmful marine algae. *Ecology of harmful algae***,** 95-107.

Paerl, H.W., and Huisman, J. (2008). Blooms like it hot. *Science* 320**,** 57-58.

Paerl, H.W., Scott, J.T., Mccarthy, M.J., Newell, S.E., Gardner, W.S., Havens, K.E., Hoffman, D.K., Wilhelm, S.W., and Wurtsbaugh, W.A. (2016). It Takes Two to Tango: When and Where Dual Nutrient (N & P) Reductions Are Needed to Protect Lakes and Downstream Ecosystems. *Environmental Science & Technology* 50**,** 10805-10813.

Paerl, H.W., and Ustach, J.F. (1982). Blue-green algal scums: An explanation for their occurrence during freshwater blooms 1. *Limnology and Oceanography* 27**,** 212-217.

Peng, G., Martin, R.M., Dearth, S.P., Sun, X., Boyer, G.L., Campagna, S.R., Lin, S., and Wilhelm, S.W. (2018). Seasonally relevant cool temperatures interact with N chemistry to increase microcystins produced in lab cultures of *Microcystis aeruginosa* NIES-843. *Environmental Science & Technology* 52**,** 4127-4136.

Persaud, A.D., Paterson, A.M., Dillon, P.J., Winter, J.G., Palmer, M., and Somers, K.M. (2015). Forecasting cyanobacteria dominance in Canadian temperate lakes. *Journal of environmental management* 151**,** 343-352.

Phillips, J.C., Mckinley, G.A., Bennington, V., Bootsma, H.A., Pilcher, D.J., Sterner, R.W., and Urban, N.R. (2015). The potential for CO_2-induced acidification in freshwater: A Great Lakes case study. *Oceanography* 28**,** 136-145.

Reavie, E. (2023). Asymmetric, biraphid diatoms from the Laurentian Great Lakes. *PeerJ Aquatic Biology*.

Reavie, E.D., Barbiero, R.P., Allinger, L.E., and Warren, G.J. (2014). Phytoplankton trends in the Great Lakes, 2001–2011. *Journal of Great Lakes Research* 40**,** 618-639.

Reavie, E.D., Cai, M., Twiss, M.R., Carrick, H.J., Davis, T.W., Johengen, T.H., Gossiaux, D., Smith, D.E., Palladino, D., and Burtner, A. (2016). Winter–spring diatom production in Lake Erie is an important driver of summer hypoxia. *Journal of Great Lakes Research* 42**,** 608-618.

Region, L.E., and Davis, C.C. (1958). An Approach to Some Problems of Secondary Production in the Western. *Limnology and Oceanography* 3**,** 15-28.

Reinl, K.L., Brookes, J.D., Carey, C.C., Harris, T.D., Ibelings, B.W., Morales-Williams, A.M., De Senerpont Domis, L.N., Atkins, K.S., Isles, P.D., and Mesman, J. (2021). Cyanobacterial blooms in oligotrophic lakes: Shifting the high-nutrient paradigm. *Freshwater Biology*.

Reinl, K.L., Harris, T.D., North, R.L., Almela, P., Berger, S.A., Bizic, M., Burnet, S.H., Grossart, H.P., Ibelings, B.W., and Jakobsson, E. (2023). Blooms also like it cold. *Limnology and Oceanography Letters*.

Reynolds, C.S. (1997). Vegetation processes in the pelagic: a model for ecosystem theory.

Reynolds, C.S. (2006). *The Ecology of Phytoplankton.* Cambridge University Press.

Rinta-Kanto, J.M., Konopko, E.A., Debruyn, J.M., Bourbonniere, R.A., Boyer, G.L., and Wilhelm, S.W. (2009). Lake Erie Microcystis: relationship between microcystin production, dynamics of genotypes and environmental parameters in a large lake. *Harmful algae* 8**,** 665-673.

Rinta-Kanto, J.M., and Wilhelm, S.W. (2006). Diversity of microcystin-producing cyanobacteria in spatially isolated regions of Lake Erie. *Applied and Environmental Microbiology* 72**,** 5083-5085.

Robarts, R.D., and Zohary, T. (1987). Temperature effects on photosynthetic capacity, respiration, and growth rates of bloom-forming cyanobacteria. *New Zealand journal of marine and freshwater research* 21**,** 391-399.

Sandrini, G., Tann, R.P., Schuurmans, J.M., Van Beusekom, S.A., Matthijs, H.C., and Huisman, J. (2016). Diel variation in gene expression of the CO_2-concentrating mechanism during a harmful cyanobacterial bloom. *Frontiers in Microbiology* 7**,** 551.

Saros, J.E., Michel, T.J., Interlandi, S.J., and Wolfe, A.P. (2005). Resource requirements of Asterionella formosa and Fragilaria crotonensis in oligotrophic alpine lakes: implications for recent phytoplankton community reorganizations. *Canadian Journal of Fisheries and Aquatic Sciences* 62**,** 1681-1689.

Saxton, M.A., D'souza, N.A., Bourbonniere, R.A., Mckay, R.M.L., and Wilhelm, S.W. (2012). Seasonal Si:C ratios in Lake Erie diatoms - Evidence of an active winter diatom community. *Journal of Great Lakes Research* 38**,** 206-211.

Scavia, D., Allan, J.D., Arend, K.K., Bartell, S., Beletsky, D., Bosch, N.S., Brandt, S.B., Briland, R.D., Daloğlu, I., and Depinto, J.V. (2014). Assessing and addressing the re-eutrophication of Lake Erie: Central basin hypoxia. *Journal of Great Lakes Research* 40**,** 226-246.

Schelske, C.L. (1975). Silica and nitrate depletion as related to rate of eutrophication in Lakes Michigan, Huron, and Superior. *Coupling of land and water systems***,** 277-298.

Schindler, D.W., Carpenter, S.R., Chapra, S.C., Hecky, R.E., and Orihel, D.M. (2016). Reducing phosphorus to curb lake eutrophication is a success. *Environmental Science & Technology* 50**,** 8923-8929.

Shatwell, T., and Köhler, J. (2019). Decreased nitrogen loading controls summer cyanobacterial blooms without promoting nitrogen-fixing taxa: Long-term response of a shallow lake. *Limnology and Oceanography* 64**,** S166-S178.

Shatwell, T., Köhler, J., and Nicklisch, A. (2008). Warming promotes cold-adapted phytoplankton in temperate lakes and opens a loophole for Oscillatoriales in spring. *Global Change Biology* 14**,** 2194-2200.

Simiyu, B.M., and Kurmayer, R. (2022). Response of planktonic diatoms to eutrophication in Nyanza Gulf of Lake Victoria, Kenya. *Limnologica* 93**,** 125958.

Sitoki, L., Kofler, W., and Rott, E. (2013). Planktonic needle-shaped Nitzschia species from Lake Victoria, Africa, revisited. *Diatom research* 28**,** 165-174.

Sitoki, L., Kurmayer, R., and Rott, E. (2012). Spatial variation of phytoplankton composition, biovolume, and resulting microcystin concentrations in the Nyanza Gulf (Lake Victoria, Kenya). *Hydrobiologia* 691**,** 109-122.
Sommer, U., and Stabel, H.-H. (1983). Silicon consumption and population density changes of dominant planktonic diatoms in Lake Constance. *The Journal of Ecology***,** 119-130.
Spaulding, S.A., Otu, M.K., Wolfe, A.P., and Baron, J.S. (2015). Paleolimnological records of nitrogen deposition in shallow, high-elevation lakes of Grand Teton National Park, Wyoming, USA. *Arctic, Antarctic, and Alpine Research* 47**,** 703-717.
Steffen, M.M., Belisle, B.S., Watson, S.B., Boyer, G.L., and Wilhelm, S.W. (2014). Status, causes and controls of cyanobacterial blooms in Lake Erie. *Journal of Great Lakes Research* 40**,** 215-225.
Steffen, M.M., Davis, T.W., Mckay, R.M.L., Bullerjahn, G.S., Krausfeldt, L.E., Stough, J.M., Neitzey, M.L., Gilbert, N.E., Boyer, G.L., and Johengen, T.H. (2017). Ecophysiological examination of the Lake Erie Microcystis bloom in 2014: linkages between biology and the water supply shutdown of Toledo, OH. *Environmental Science & Technology* 51**,** 6745-6755.
Sterner, R.W., Reinl, K.L., Lafrancois, B.M., Brovold, S., and Miller, T.R. (2020). A first assessment of cyanobacterial blooms in oligotrophic Lake Superior. *Limnology and Oceanography* 65**,** 2984-2998.
Stoermer, E., Kociolek, J., Schelske, C., and Conley, D. (1987). Quantitative analysis of siliceous microfossils in the sediments of Lake Erie's central basin. *Diatom Research* 2**,** 113-134.
Stoermer, E.F. (1975). *Phytoplankton composition and abundance in Lake Ontario during IFYGL.* National Environmental Research Center.
Stoermer, E.F. (1993). Evaluating diatom succession: some pecularities of the Great Lakes case. *Journal of Paleolimnology* 8**,** 71-83.
Stoermer, E.F., Emmert, G., Julius, M.L., and Schelske, C.L. (1996). Paleolimnologic evidence of rapid recent change in Lake Erie's trophic status. *Canadian Journal of Fisheries and Aquatic Sciences* 53**,** 1451-1458.
Stoermer, E.F., Emmert, G., and Schelske, C.L. (1989). Morphological variation of Stephanodiscus niagarae Ehrenb.(Bacillariophyta) in a Lake Ontario sediment core. *Journal of Paleolimnology* 2**,** 227-236.
Stoermer, E.F., Wozin, J., and Schelske, C. (1993). Paleolimnological comparison of the Laurentian Great Lakes based on diatoms. *Limnology and oceanography* 38**,** 1311-1316.
Stow, C.A., Stumpf, R.P., Rowe, M.D., Johnson, L.T., Carrick, H.J., and Yerubandi, R. (2022). Model assumptions limit implications for nitrogen and phosphorus management. *Journal of Great Lakes Research* 48**,** 1735-1737.
Sweeney, R.A. (1995). Rejuvenation of Lake Erie. *GeoJournal* 35**,** 65-66.
Talling, J. (1976). The depletion of carbon dioxide from lake water by phytoplankton. *The Journal of Ecology***,** 79-121.
Tang, E.P., Tremblay, R., and Vincent, W.F. (1997). CYANOBACTERIAL DOMINANCE OF POLAR FRESHWATER ECOSYSTEMS: ARE HIGH-LATITUDE MAT-FORMERS ADAPTED TO LOW TEMPERATURE? 1. *Journal of Phycology* 33**,** 171-181.
Twiss, M., Mckay, R., Bourbonniere, R., Bullerjahn, G., Carrick, H., Smith, R., Winter, J., D'souza, N., Furey, P., and Lashaway, A. (2012). Diatoms abound in ice-covered Lake

Erie: An investigation of offshore winter limnology in Lake Erie over the period 2007 to 2010. *Journal of Great Lakes Research* 38**,** 18-30.
Van Dam, B.R., Tobias, C., Holbach, A., Paerl, H.W., and Zhu, G. (2018). CO_2 limited conditions favor cyanobacteria in a hypereutrophic lake: an empirical and theoretical stable isotope study. *Limnology and Oceanography* 63**,** 1643-1659.
Verduin, J. (1964). Changes in western Lake Erie during the period 1948–1962. *Verh Internat Verein Limnol***,** 639-644.
Verspagen, J.M., Van De Waal, D.B., Finke, J.F., Visser, P.M., Van Donk, E., and Huisman, J. (2014). Rising CO_2 levels will intensify phytoplankton blooms in eutrophic and hypertrophic lakes. *PloS One* 9.
Vilmi, A., Karjalainen, S.M., Landeiro, V.L., and Heino, J. (2015). Freshwater diatoms as environmental indicators: evaluating the effects of eutrophication using species morphology and biological indices. *Environmental monitoring and assessment* 187**,** 1-10.
Vincent, W.F. (2007). Cold tolerance in cyanobacteria and life in the cryosphere. *Algae and cyanobacteria in extreme environments***,** 287-301.
Visser, P.M., Verspagen, J.M., Sandrini, G., Stal, L.J., Matthijs, H.C., Davis, T.W., Paerl, H.W., and Huisman, J. (2016). How rising CO2 and global warming may stimulate harmful cyanobacterial blooms. *Harmful Algae* 54**,** 145-159.
Wagner, C., and Adrian, R. (2009). Cyanobacteria dominance: quantifying the effects of climate change. *Limnology and Oceanography* 54**,** 2460-2468.
Watson, S.B., Miller, C., Arhonditsis, G., Boyer, G.L., Carmichael, W., Charlton, M.N., Confesor, R., Depew, D.C., Höök, T.O., and Ludsin, S.A. (2016). The re-eutrophication of Lake Erie: Harmful algal blooms and hypoxia. *Harmful algae* 56**,** 44-66.
Wejnerowski, Ł., Rzymski, P., Kokociński, M., and Meriluoto, J. (2018). The structure and toxicity of winter cyanobacterial bloom in a eutrophic lake of the temperate zone. *Ecotoxicology* 27**,** 752-760.
Wicks, R.J., and Thiel, P.G. (1990). Environmental factors affecting the production of peptide toxins in floating scums of the cyanobacterium Microcystis aeruginosa in a hypertrophic African reservoir. *Environmental Science & Technology* 24**,** 1413-1418.
Wilhelm, S., Bullerjahn, G., and Rlm, M. (2020). The complicated and confusing ecology of *Microcystis* blooms. *mBio* 11**,** e00529-00520.
Wilhelm, S.W., Bullerjahn, G.S., Eldridge, M.L., Rinta-Kanto, J.M., Poorvin, L., and Bourbonniere, R.A. (2006a). Seasonal hypoxia and the genetic diversity of prokaryote populations in the central basin hypolimnion of Lake Erie: evidence for abundant cyanobacteria and photosynthesis. *Journal of Great Lakes Research* 32**,** 657-671.
Wilhelm, S.W., Carberry, M.J., Eldridge, M.L., Poorvin, L., Saxton, M.A., and Doblin, M.A. (2006b). Marine and freshwater cyanophages in a Laurentian Great Lake: evidence from infectivity assays and molecular analyses of g20 genes. *Applied and Environmental Microbiology* 72**,** 4957-4963.
Wilhelm, S.W., Debruyn, J.M., Gillor, O., Twiss, M.R., Livingston, K., Bourbonniere, R.A., Pickell, L.D., Trick, C.G., Dean, A.L., and Mckay, R.M.L. (2003). Effect of phosphorus amendments on present day plankton communitites in pelagic Lake Erie. *Aquatic Microbial Ecology* 32**,** 275-285.
Wilhelm, S.W., Hellweger, F.L., Martin, R.M., Schampera, C., Eigeman, F., Smith, D.J., and Dick, G.J. (2022). Response to "Model assumptions limit implications for nitrogent and

phosphorus management": the need to move beyond the phosphorus = biomass = toxin doctrine. *Journal of Great Lakes Research* 48.
Wilhelm, S.W., Lecleir, G.R., Bullerjahn, G.S., Mckay, R.M., Saxton, M.A., Twiss, M.R., and Bourbonniere, R.A. (2014). Seasonal changes in microbial community structure and activity imply winter production is linked to summer hypoxia in a large lake. *FEMS microbiology ecology* 87**,** 475-485.
Winter, J.G., Desellas, A.M., Fletcher, R., Heintsch, L., Morley, A., Nakamoto, L., and Utsumi, K. (2011). Algal blooms in Ontario, Canada: increases in reports since 1994. *Lake and Reservoir Management* 27**,** 107-114.
Wolfe, A.P., Cooke, C.A., and Hobbs, W.O. (2006). Are current rates of atmospheric nitrogen deposition influencing lakes in the eastern Canadian Arctic? *Arctic, Antarctic, and Alpine Research* 38**,** 465-476.
Wu, Y., Campbell, D.A., Irwin, A.J., Suggett, D.J., and Finkel, Z.V. (2014). Ocean acidification enhances the growth rate of larger diatoms. *Limnology and Oceanography* 59**,** 1027-1034.
Wynne, T.T., and Stumpf, R.P. (2015). Spatial and temporal patterns in the seasonal distribution of toxic cyanobacteria in western Lake Erie from 2002–2014. *Toxins* 7**,** 1649-1663.
Yancey, C.E., Mathiesen, O., and Dick, G.J. (2023). Transcriptionally active nitrogen fixation and biosynthesis of diverse secondary metabolites by Dolichospermum and Aphanizomenom-like Cyanobacteria in western Lake Erie Microcystis blooms. *Harmful Algae***,** 102408.
Zepernick, B.N., Denison, E.R., Chaffin, J.D., Bullerjahn, G.S., Pennacchio, C.P., Frenken, T., Peck, D.H., Anderson, J.T., Niles, D., and Zastepa, A. (2022a). Metatranscriptomic Sequencing of Winter and Spring Planktonic Communities from Lake Erie, a Laurentian Great Lake. *Microbiology Resource Announcements***,** e00351-00322.
Zepernick, B.N., Gann, E.R., Poiund, H.L., Martin, R.M., Krausfeldt, L.E., Chaffin, J.D., and Wilhelm, S.W. (2021). Elevated pH conditions associated with *Microcystis* spp. blooms decrease viability of the cultured diatom *Fragilaria crotonensis* and natural diatoms in Lake Erie. *Frontiers in Microbiology* 12**,** 598736.
Zepernick, B.N., Niknejad, D.J., Stark, G.F., Truchon, A.R., Martin, R.M., Rossignol, K.L., Paerl, H.W., and Wilhelm, S.W. (2022b). Morphological, physiological, and transcriptional responses of the freshwater diatom Fragilaria crotonensis to elevated pH conditions. *Frontiers in Microbiology* 13.
Zepernick, B.N., Truchon, A.R., Gann, E.R., and Wilhelm, S.W. (2022c). Draft Genome Sequence of the Freshwater Diatom *Fragilaria crotonensis* SAG 28.96. *Microbiology Resource Announcements***,** e00289-00222.
Zepernick, B.N., Wilhelm, S.W., Bullerjahn, G.S., and Paerl, H.W. (2023). Climate change and the aquatic continuum: A cyanobacterial comeback story. *Environmental Microbiology Reports* 15**,** 3-12.
Zhang, J.-Z. (2023). Cyanobacteria blooms induced precipitation of calcium carbonate and dissolution of silica in a subtropical lagoon, Florida Bay, USA. *Scientific Reports* 13**,** 4071.

CHAPTER II: RE-ASSESSING CONSEQUENCES OF CLASSICAL LABORATORY TECHNIQUES USING *MICROCYSTIS AERUGINOSA* AS A MODEL SYSTEM

Publication Note

This chapter is a version of a peer-reviewed, published article in *Limnology and Oceanography: Methods* 18(5) by Brittany N. Zepernick, Lauren E. Krausfeldt, and Steven W. Wilhelm.

BNZ identified initial discrepancies in media pH, and performed all media preparation, flaming assays, culture work, growth curves, and statistical analyses along with LEK. BNZ, LEK, and SWW designed the experiments. TC analyses were performed by Adrian Gonzalez at the Water Quality Core Facility at the University of Tennessee Knoxville. BNZ, LEK, and SWW contributed to manuscript editing and writing.

Abstract

Aseptic technique has historically served as a fundamental practice in microbiology, helping to maintain culture purity and integrity. This technique has been widely encouraged and employed for use with cultures of heterotrophic bacteria as well as freshwater and marine algae. Yet, recent observations have suggested these approaches may bring their own influences. We observed variations in growth amongst replicate experimental cyanobacterial cultures upon flaming of the culture tube opening during sample transfer and collection. Investigation revealed the pH of culture media had decreased from the initial pH established during media preparation. Flaming of sterile culture media alone confirmed a significant decrease, by as much as 1.7 pH units, and correlated with increased flaming events over time. We hypothesized that the causative factor was the introduction of carbon dioxide (CO_2) into the media. To test this hypothesis, qualitative and quantitative analyses were used to determine the primary driver of pH decline. We further assessed the direct effects of flaming and subsequent pH changes on *Microcystis aeruginosa* cultures, showing flame-driven pH changes and/or the introduction of CO_2 influenced experimental results. Our observations provide a cautionary tale of how classic and well-accepted approaches may have unintended consequences, suggesting new approaches may be necessary in research areas assessing pH or carbon-related effects on microbial communities.

Introduction

Aseptic technique has served as a foundational method of microbiological research for decades (Harrigan and McCance, 1966). Defined as steps to prevent contamination during manipulation of microbial cultures or sterile culture media (Madigan, 2015), aseptic technique commonly includes flame sterilization of the opening of culture vessels (Bykowski and Stevenson, 2008). Flame sterilization involves passing the opening of a culture vessel through a flame to prevent the introduction of microbial contaminants to a sample and is an approach used in a variety of laboratories, hospitals, and industrial facilities. Yet, upon review of the literature, we found a general lack of consensus within the scientific community as to the details of the method. While flaming immediately before and after sub-sampling or culture transfer is specified in a variety of publications (Andersen, 2005; Sanders, 2012; Madigan, 2015), the exact number of times required for the mouth of the vessel to pass through a flame is generally not specified. Additionally, while some argue flaming must be performed by passing the tube through the inner blue section of the flame (Bykowski and Stevenson, 2008), others instruct the tube to be passed above the flame (Coté, 1998). Further variances in flaming technique arise in the recommendation of a wait time prior to re-capping the culture post-flaming (Coté, 1998), while others recommend immediate recapping to minimize introduction of airborne contaminants (Harrigan and McCance, 1966). In fact, the primary purpose of flaming in itself is often disputed within the literature, as some sources claim it is to combust any contaminants located on the mouth of the vessel (Coté, 1998), while others indicate it is to create an upwards convection current to prevent atmospheric contaminants from entering the tube (Sanders, 2012; Madigan, 2015). These variances amongst techniques create a lapse in methodological consistency within the scientific community. Additionally, the discrepancies may be exacerbated by confounding factors that are unintentionally applied because of flaming. For example, the practice of flaming

in aseptic technique is mandated in the handling of freshwater media and phytoplankton cultures (Andersen, 2005). Yet, previous studies have demonstrated aseptic flaming may have detrimental implications on algal cultures, such as decreased growth rates and increased cell death in cyanobacterial *Prochlorococcus spp.* cultures linked to flame-generated peroxides (Morris and Zinser, 2013).

In the present study, we assessed the effects of flaming as part of aseptic technique on the pH of freshwater culture media and subsequently cyanobacterial cell growth. Effects were assessed as follows: (1) aseptic flaming on different freshwater growth media from the scientific literature, (2) aseptic flaming on the growth of *M. aeruginosa* cultures. Based on our observations, recommendations are made in the form of media modifications to effectively sterilize while eliminating the potential introduction of confounding variables.

Methods

Freshwater media selection and preparation

Four freshwater culture media commonly used for phytoplankton culturing (C, CB, CT, and CSi) were selected: recipes were taken from a publication of the *NIES-Collection Microbial Culture Collection* (Watanabe, 1997). The components and concentrations for each medium are identical except for the buffer type and concentration, allowing for direct comparisons of the specific buffers in response to flaming (Table 2.1). Briefly, the major constituents of C medium include $1.5x10^{-4}$ g/mL $Ca(NO_3)_2 \cdot 4H_2O$, $1.0x10^{-4}$ g/mL KNO_3, $5.0x10^{-5}$ g/mL $Na_2 \cdot \beta$-glycerophosphate, $4.0x10^{-5}$ g/mL $MgSO_4 \cdot 7H_2O$, and trace metals (Steffen et al., 2015a). To maintain comparability, silica was not included in CSi media used in this study. Beyond these

Table 2.1: Buffer concentration (mM), buffering pH range, and pKa for each of the five freshwater culture media used in this study (CT, C, CSi, CB, BG-11).

Media	[Buffer] / L	pH Range	pKa at 20°C
CT	1.64 mM TAPS	7.7-9.1	8.49
C	4.13 mM Tris	7.0-9.0	8.20
CSi	2.10 mM HEPES	6.8-8.2	7.55
CB	3.06 mM Bicine	7.6-9.0	8.35
BG-11	1.75mM $K_2HPO_4 \bullet 3H_20$	8.2-9.6	7.21

media, BG-11 medium (Andersen, 2005), one of the most-commonly used for cyanobacterial culture work, was also tested. We also assessed the effects of flaming on 3 heterotrophic bacterial growth media: Lysogeny broth (LB) (Bertani, 1951), Nutrient broth (Sambrook et al., 1989) and Minimal media (M9) (Miller, 1972). All media were prepared in 1 L volumes, titrated to a pH of 8.2 with 1 M NaOH and autoclaved. Samples were cooled at room temperature (20.5 °C) and gases allowed to equilibrate (for 1 day). The pH of each medium was confirmed *via* the sub-sampling a 10 mL volume and analyzed using a temperature compensating laboratory pH meter (Mettler Toledo Seven Compact^{TM} pH/Ion meter S220, fitted with a Mettler InLab Expert Pro-ISM electrode with a temperature range of up to 100ºC). The pH meter was calibrated daily using 3 pH standards (pH 4.0, 7.0, and 10.0) to yield an efficiency of 97% or higher prior to all measurements. Standard vitamin additions for freshwater media in the forms of vitamin B_{12}, thiamine HCl, and biotin were omitted from all media.

Effects of flaming on media types

Twenty-five mL of each medium were aliquoted into 50 mL sterile, acid-washed glass culture tubes (sterilized, acid-washed tubes were used in all following experiments). For each growth medium, triplicate control and flame-treated replicates were generated. The flaming technique used in this experiment was performed in accordance with protocols expected during standard lab-based sub-sampling (for cell number, *etc*.) during a typical cyanobacteria growth study. Sub-sampling consisted of the removal of a small volume of culture daily for cell enumeration, though subsampling was not performed in all of the experiments of this study to decrease risk of heterotrophic contamination. Flame replicates were inverted 3-times (normally done to ensure cell resuspension) and held at a 45° angle while passed above the blue cone of the

flame for 4 passes through the flame. After a brief pause, during which one would collect a small volume for determining cell number or inoculating cells into fresh media, the mouth of the culture tube was again passed through the flame 4-times (thus a total of 8 passes through the flame corresponds to a single sub-sampling event). The cap was then immediately replaced, and the tube inverted 3-times before it was replaced in the rack (see aseptic flaming demonstration video, https://youtu.be/Bvn6OvM8JpM). In this study, the treatment of replicates using an open flame will be denoted as "flamed". The controls in this study are subject to the same aseptic procedure as denoted above, with the exception of the presence of a flame: they have been assigned the terms "unflamed or air flamed". All samples were stored at 20.5° C and approximately 15-20 μmol photons m^{-2} s^{-1}. This mock sampling of uninoculated growth media was performed daily for 10-d. Prior to the daily flaming, pH was measured for each replicate using a pH probe, with sterilization of the probe performed prior to sampling using 70% EtOH.

Effects of buffer age on media pH

We assessed whether buffer age had any effect on the buffering capacity. Twenty-five mL volumes of CT media containing aged TAPS buffer stock (TAPS stock solution aged approximately 3.5 months and stored at 4° C) and CT media containing fresh TAPS buffer (TAPS stock solution prepared 3 days prior and stored at 4° C) were aliquoted into 50 mL glass culture tubes in triplicate manner for the control treatments. The culture tubes were air-flamed in the same manner as mentioned prior. All replicates were stored on a lab bench at ~20.5° C. The pH of replicates was monitored daily for 10-d.

Influence of gas-exchange on media pH

The potential implications of gas exchange with the atmosphere were analyzed, with 25 mL volumes of CT media aliquoted into 50 mL glass culture tubes in triplicate. The lids were closed firmly for one treatment group, while the lids were left loose for the second treatment. Replicates were stored on a lab bench at 20.5° C and 15-20 μmol photons m^{-2} s^{-1}. The pH of all replicates was monitored daily for 10-d. Efforts to explore potential mitigating-practices in reducing flaming effects on media pH were performed by abstaining from any type of inversion or simulated shaking of the media. 25 mL volumes of CT media were aliquoted in triplicate into 50 mL glass culture tubes. Control and flamed treatments were applied daily for 10-d, without inversion of the tubes or any other form of disturbance. All replicates were stored on a lab bench at 20.5° C and approximately 15-20 μmol photons m^{-2} s^{-1}.

Consequences of photo-oxidation on media pH

It has been demonstrated that light exposure causes photooxidation (and the inherent generation of reactive oxygen species, such as the weak acid HOOH) within a variety of media utilizing buffers such as HEPES, TAPS, Bicine, and TRIS (Morris and Zinser, 2013). To determine the effects of photooxidation on media pH, 25 mL volumes of CT media were aliquoted into 50 mL glass culture tubes in triplicate for air-flame treatments. All replicates were stored on a lab bench at 20.5° C and approximately 15-20 μmol photons m^{-2} s^{-1}. The "non-photooxidation" treatment replicates were wrapped in foil (kept in dark conditions) to prevent superoxide generation. The pH of all replicates was monitored daily for 10-d.

Effects of increased buffer concentration on media pH

Attempts to minimize the effects of flaming upon media pH were made by increasing the TAPS buffer concentration in CT media by 10-fold and 100-fold (the later serving as the positive control) and monitoring the effects of flaming and air-flaming upon the triplicated experimental groups. All replicates were stored on a lab bench at 20.5° C and 15-20 μmol photons m^{-2} s^{-1}. The pH of all replicates was monitored daily for 10-d.

Testing drivers of pH decline as a result of flaming

In a preliminary investigation into the potential of flame-generated CO_2 as the primary driver of pH decline, limewater ($Ca(OH)_2$ was prepared following standard protocol (Shakhashiri, 1983). Aliquots (25 mL) were dispensed in triplicate to test the effects of flaming across the following treatments: flamed 8-times, 16-times, 24-times, and 32-times. Note 8 passes through the flame corresponded to 1 sub-sampling event, or day 1 in a growth study, with 16 passes corresponding to 2 sub-samplings, or day 2 in a growth study, and so forth. Negative controls included 3 tubes which were air-flamed, and positive controls were exposed to 10 seconds of CO_2 bubbling (administered *via* exhalation into straw submerged in limewater). Qualitative assessment of turbidity due to the formation of $CaCO_3$ as an indirect proxy for CO_2 introduction was made using a spectrophotometer (Thermo Spectronic Genesys 20) at 600 nm.

Quantification of the net CO_2 (total carbon-TC) incorporated into media due to flaming was measured by the Water Quality Core Facility at the University of Tennessee Knoxville utilizing a Shimadzu Carbon/Nitrogen analyzer (TOC-L Shimadzu, detection limit of 4 μg / L according to the manufacturer's specifications). Volumes of CT media (25 mL) were aliquoted into 50 mL acid washed, sterilized tubes in triplicate per treatment. Control (unflamed), flamed

8-times, flamed 16-times, flamed 24-times, and flamed 32-times treatments were administered, then immediately analyzed for TC with technical replicates of 3 performed per sample.

Effects of flaming on freshwater cyanobacterial cultures

To determine the consequences that flaming may have on freshwater cyanobacterial cultures, axenic *Microcystis aeruginosa* NIES 843 was inoculated in triplicate into CT media at a pH of 8.2 and flamed daily for 10-d to mimic sub-sampling during growth assays. Note one mock-sampling event corresponds to 8 passes through the flame according to standard aseptic protocol performed in the video demonstration. Cultures were incubated at 26° C and approximately 55-60 μmol photons m^{-2} s^{-1} in incubators on a diel cycle (VWR low temperature diurnal illumination incubator). Chlorophyll *a* auto fluorescence (fluorescence signal units, FSU) was quantified daily as a proxy for relative biomass and cell health utilizing a fluorometer (Turner Designs TD-700), equipped with a blue mercury bulb, a #10-050R excitation filter (340 – 500 nm) and a #10-115 (680 nm) emission filter. The instrument was standardized before each use with Turner's solid standard (#7000-994). Flaming/air-flaming was performed post-FSU measurements. Final pH values were measured on day 10 after the completion of the experiment.

Effects of increased buffer concentration on freshwater cyanobacterial cultures

We assessed the effects of a 10-fold increase in the concentration of TAPS buffer in CT media on *M. aeruginosa* NIES 843 growth. Cultures were inoculated into standard TAPS-buffered CT medium as well as a 10X TAPS-buffered CT medium for comparison. Post-inoculation, the cultures were incubated at 26° C and approximately 55-60 μmol photons m^{-2} s^{-1} as mentioned previously for 10-d. FSU (Tuner Designs TD-700) and cell number (BD

FACSCalibur flow cytometer) were assessed every 2-d for additional comparison of the techniques themselves.

Statistical analyses:

Multiple T-tests corrected for multiple comparisons (Holm-Sidak method) were used to statistically assess the following: flame assays of freshwater media (Figure 2.1), *M. aeruginosa* growth rates (Figure 2.4b), flame assays of heterotrophic media (Appendix Figure 2.5), external influences on media pH (Appendix Figure 2.6), buffer concentration effects on media pH (Appendix Figure 2.8), effects of shaking on media pH (Appendix Figure 2.9), and the comparison of *M. aeruginosa* biomass accumulation in standard CT vs. 10X TAPS-buffered CT medium (Appendix Figure 2.11). One-way ANOVAs corrected for multiple comparisons (Tukey method) were used to statistically assess the following: net pH decline by buffer type (Figure 2.2), TC (mM) incorporation as a result of flaming (Figure 2.3), and limewater turbidity as an indicator for CO_2 incorporation (Appendix Figure 2.7).

Results

Effects of flaming on pH of freshwater media

After flaming the mouths of the culture tubes, a decline in pH was observed in all the freshwater media analyzed in this study compared to the controls (Figure 2.1). After 10 days, CT ($p = 0.01$) and BG-11 ($p = 0.02$) experienced the greatest decline in pH after flaming, dropping from 8.2 to average final pH values of 6.47 and 6.45, respectively (Figure 2.1d, e). TRIS ($p = 0.03$), HEPES ($p = 0.01$), and Bicine buffered- C media ($p = 0.01$) had average final pH values of 7.02, 6.86, and 6.87, respectively (Figure 2.1a, b, c). Differences between the controls and flamed replicates manifested after only 2-d of daily flame sterilization (or 16 passes through the

flame resulting from 2 standard aseptic flaming events). A comparison of net decline in pH of each media/buffer indicated there were no differences between the pH declines in CT and BG-11 ($p = 0.99$) when flamed, and neither were different from the control ($p = 0.27$) (Figure 2.2). This data confirms CT (TAPS buffer) and BG-11 (inorganic phosphate buffer) demonstrated the greatest decline in pH when flamed (1.5 - 1.7 pH units). TRIS, HEPES, and Bicine-buffered media that was flamed exhibited similar trends as in the unflamed control (Figure 2.2). The data demonstrated a consistent trend amongst the 5 freshwater media/buffers tested, in which flaming resulted in a decline in pH after just 2-d (16 passes through the flame) and continuing up to 10-d (80 passes through the flame). This trend was observed (albeit to a lesser extent) when the experiment was replicated by flaming 3 growth media used for heterotrophic bacteria culture work: LB, Nutrient broth, and M9 (Appendix Figure 2.5). In the case of the unbuffered media (LB and Nutrient broth) the declining pH trend was observed on a smaller scale, with flamed LB decreasing in pH from 8.2 to an average of 7.5 after 10-d of flaming and Nutrient broth to an average pH of 7.42 (Appendix Figure 2.5a, b). M9 media demonstrated a similar decline in pH upon flaming (Appendix Figure 2.5c). However, all time points of the M9 flamed replicates (T2-T10) were significantly different from the controls ($p < 0.01$) whereas this was not the case for LB and Nutrient broth. The data demonstrated that flame sterilization resulted in pH declines of lower magnitude in unbuffered media compared to buffered media, with freshwater media experiencing the highest decline in pH due to flaming.

Influence of external conditions on the pH of freshwater media

A pH decline was observed in the control replicates in all 5 freshwater media, though to a much lesser extent than the flamed replicates (Figure 2.2). Factors associated with

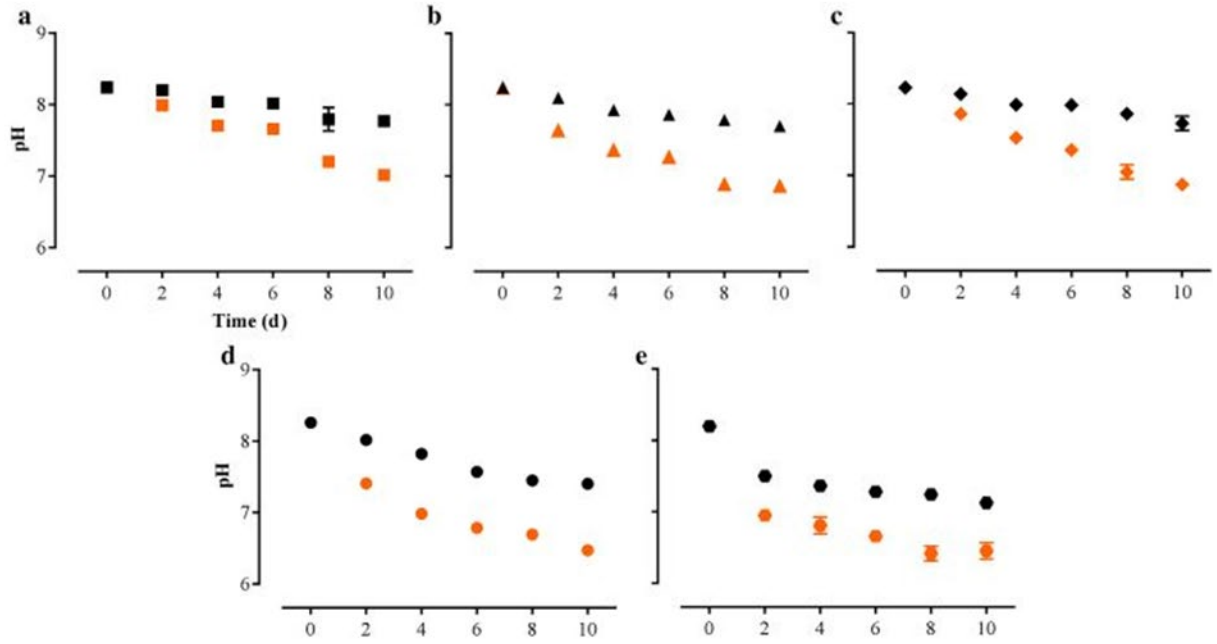


Figure 2.1: Flame-induced declines in pH in control (black) and flamed replicates (orange) of freshwater media. Data present mean ± SEM. Where not shown, error bars are within the symbol. **(a)** C media/Tris buffer (indicated by squares). **(b)** CSi/HEPES media (triangles). **(c)** CB/Bicine media (diamonds). **(d)** CT media/TAPS buffer (circles). **(e)** BG-11/inorganic phosphate buffer (hexagons).

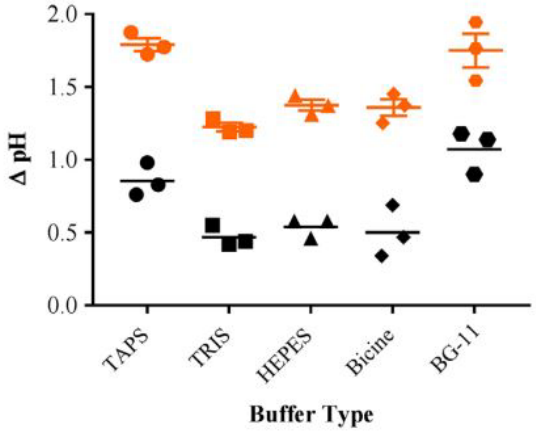


Figure 2.2: Net change in pH ($T_0 - T_{10}$ pH) observed in each media after 10 d of aseptic flaming. Net change in pH observed in the control replicates of each media indicated in black. Net change in pH of the flamed replicates for each media indicated in orange.

Analysis of carbon dioxide as driver of flame-induced pH declines

media handling and storage were analyzed to identify potential confounding variables or contributing factors to this pH decline observed in controls. Buffer age appeared to have no immediate implications corresponding to pH (Appendix Figure 2.6a). The effects of light exposure (*i.e*. photo-oxidation) on pH revealed no differences ($p = 0.99$) between CT subjected to photo-oxidation and those exposed to photo-oxidation inhibition (Appendix Figure 2.6c). Influence of gas exchange (*i.e.* tight vs. loose caps) revealed no effect on pH ($p = 0.90$) throughout the 10-d sampling (Appendix Figure 2.6b). Efforts to minimize pH decline in CT media were made by forming a CT -TAPS buffer concentration gradient. Daily flaming events over the course of 10-d revealed the largest pH declines in the control (protocol-standard concentration of TAPS), with 10-fold and 100-fold increases in TAPS resulting in more stable pH (Appendix Figure 2.8a, b). While a 10-fold increase in TAPS buffer did not result in statistical differences between the un-flamed and flamed treatments ($p = 0.07$) ($p = 0.35$), the decline in pH was observed to a lesser extent compared to the standard buffer media. Additional means of minimizing flame-induced pH decline was accomplished by abstaining from tube inversion/disturbance throughout 10-d and revealed a substantially lower net decline in pH in CT media (Appendix Figure 2.9).

Analysis of carbon dioxide as driver of flame-induced pH declines

Preliminary qualitative means for determining the absence/presence of CO_2 in flamed media were conducted utilizing a Limewater turbidity assay (Shakhashiri, 1983). After flaming, evidence of CO_2 incorporation was observed *via* the visible formation of a $Ca(CO)_3$ precipitate in the corresponding manner: negative controls or "air-flamed" replicates depicted no change in turbidity formation of precipitates, while 8, 16, and 24 passes through the flame each resulted in increased turbidity and precipitate formation, serving as a visual proxy for CO_2 introduction to

the media (Appendix Figure 2.7a). Spectrophotometric analyses further support the limewater analyses (Appendix Figure 2.7b). Although variable, as the number of passes through the flame increased, a parallel rise in turbidity and precipitate formation of $Ca(OH)_2$ occurred. Increased variability of $Ca(OH)_2$ formation amongst replicates was observed as the number of passes through the flame increased. Quantification of TC input revealed an average of 170 +/- 6.4 mM C (or 4.26 mmol C per 25mL) present in the unflamed controls, 193 +/- 3.60 mM C present in the 8 passes through the flame replicates, 196 +/- 2.0 mM C present in the 16 passes through the flame replicates, 204 +/- 3.6 mM C present in the 24 passes through the flame replicates, and 216 +/- 2.0 mM C present in the 32 passes through the flame replicates (Figure 2.3a). It was determined all flaming treatments resulted in an increase of C to the media compared to the control (p=0.002, p=0.0002, p=0.0001, p=0.000, with p values listed corresponding to tubes passed through the flame 8 to 32 times in consecutive order), and increased flaming highly correlated with the increase in TC mmol ($R^2 = 0.93$, slope = 0.06 Figure 2.3b).

Implications of flaming for freshwater cyanobacteria cultures

The *M. aeruginosa* in the CT control consistently had the lowest FSU. Replicates flamed 24-times had the highest FSU (with FSU interpreted to be indirectly indicative of cell number and biomass, while directly suggestive of cell health (Figure 2.4a). Estimates of the relationship between FSU and cell density (cells/mL) confirmed the presence of a strong and significant relationship between the two ($R^2 = 0.92$, p = 0.0001 Appendix Figure 2.10). Replicates that were flamed exhibited higher instances of culture death in comparison to the controls (death of replicates that were flamed 8-times graphed separately, Figure 2.4a). The pH of the dead replicates was considerably lower than replicates that survived, all of which remained close to

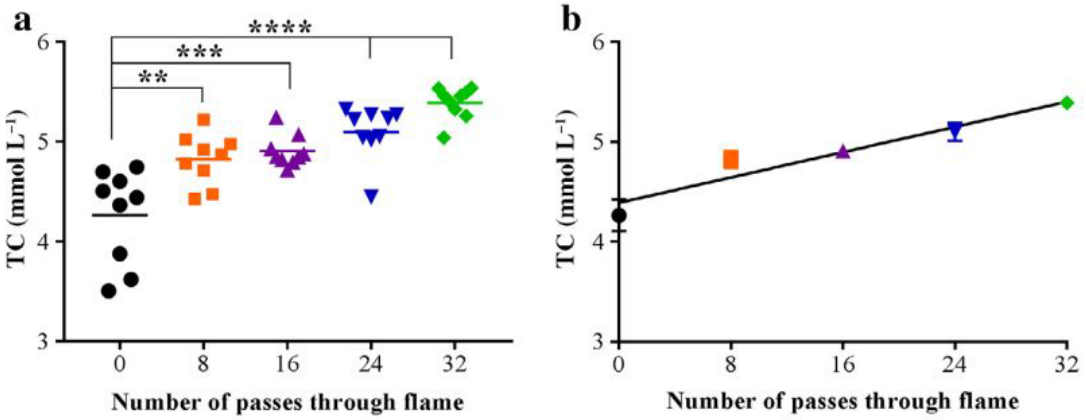


Figure 2.3: TC (mmol L^{-1}) in control and flamed CT media replicates. **(a)** Net TC (mmol L^{-1}) incorporated into CT media control and flame treatments. Eight passes through the flame indicated by orange squares, 16 passes through the flame indicated by purple triangles, 24 passes through the flame indicated by blue inverted triangles, and 32 passes through the flame indicated by green diamonds. **(b)** Linear trend of mean TC (mmol L^{-1}) introduced per flame treatment ($y = 0.06323$ [number of passes through flame] + 4.391, $R^2 = 0.93$).

the initial pH of 8.2 (Figure 2.4c). One replicate that was flamed 16-times had a correspondingly low pH, though there was no indication of death. The *M. aeruginosa* cultures that were flamed 8-times and 24-times had higher growth rates than the control ($p \geq 0.001$), with replicates flamed 16-times falling short of statistical difference ($p = 0.072$) (Figure 2.4b).

Discussion

There is little doubt of the importance of aseptic technique in microbiology and microbial ecology. In the current study, our efforts to monitor microscale changes in pH as drivers of phytoplankton community composition in lakes revealed a Heisenberg-like moment (Wheeler et al., 1983) in biology – where the process of making the measurement shapes the actual measure one is making. In short, our use of aseptic technique used during experiments examining pH effects was itself affecting pH of our culture media. These observations are critical in face of the massive number of ongoing climate change studies in aquatic systems where pH is a major variable. The data we collected suggested flaming as a part of aseptic technique had effects on 5 freshwater culture media as well as effects on the growth of the cyanobacterium *M. aeruginosa*. While flaming is a sterilization method which has been endorsed for decades (Andersen, 2005; Madigan, 2015), our results indicate media pH was altered by as much as 1.7 units *via* the introduction of CO_2, serving as a confounding variable. In contrast, the assessment of other variables including buffer age, photo-oxidation effects, and gas exchange were found to have no effect on pH. These observations effectively ruled out additional contributors to the pH decline and indicated flaming was solely responsible for the pH change. Previous studies have identified pH as a parameter of importance when culturing algae, with broad growth rate optima falling

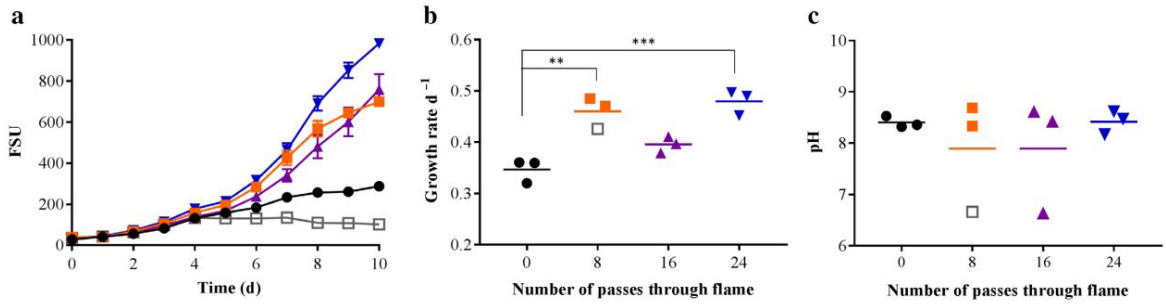


Figure 2.4: Aseptic flaming effects on CT media + axenic *M. aeruginosa*. **(a)** *M. aeruginosa* growth treated with flaming: control replicates (0 daily passes through the flame) indicated by solid black dots, 8 daily passes through the flame indicated by solid orange squares, 16 daily passes through the flame indicated by solid purple triangles, 24 daily passes through the flame indicated by solid blue inverted triangles, and dead replicates indicated in gray open symbols. **(b)** Growth rate of each replicate + mean growth rate. **(c)** pH of replicates at the completion of the experiment (after 10 daily treatments): control (0 daily passes through the flame), 8 daily passes through the flame, 16 daily passes through the flame, or 24 daily passes through the flame, respectively.

within pH values of 7 to 9, though many organisms exhibit growth outside of these ranges (Lavens and Sorgeloos, 1996; Berberoglu et al., 2008; Huang et al., 2017) . Changes in pH can effect algal cultures, with many algal species having growth optima at narrow pH ranges (Lavens and Sorgeloos, 1996; Tsaloglou, 2016). The cyanobacterium used in this study, *M. aeruginosa,* has an optimal pH for growth between 7.5 - 10 (Fang et al., 2018) with an optimal photosynthetic potential at pH > 8.0 (Bano and Siddiqui, 2004). Flaming of culture vessel openings, specifically during the process of aliquoting media for inoculation, had the capacity to drive down the pH (Figure 2.1a-e). Additionally, flaming open culture tubes post-inoculation could further decrease pH levels if CO_2 is not assimilated by the cyanobacteria. BG-11 and CT media exhibited the highest net declines in pH (Figure 2.2), which raises concern, as these are frequently utilized freshwater growth media. Random culture death in certain flamed cultures (Figure 2.4) may be due to the variability of CO_2 incorporation from flaming, as some cultures may have experienced larger-scale CO_2 inputs that resulted in marked pH decline if the CO_2 is not consumed by the culture. Previous studies have also found that up to 2 μM of HOOH may be generated as a result of flaming (Morris and Zinser, 2013). While it is recognized that mM concentrations of HOOH are needed to cause cell death (Palenik et al., 1991; Alam et al., 2001), the 2 μM of HOOH generated from flaming results in physiological changes during the upregulation of intracellular peroxidases (Price and Harrison, 1988). There may also be a role here for incomplete combustion products (although we did not investigate this).

Dissolved inorganic carbon (DIC) plays a significant role in the growth and development of phytoplankton species. CO_2 and HCO_3^- are the major chemical forms of carbon assimilated during photosynthesis (Schindler et al., 1971; Wetzel, 2001). Previous studies have indicated free CO_2 is labile and readily accessible to most algae and aquatic photoautotrophs (Wetzel, 2001).

M. aeruginosa isolates have been shown to have a high affinity for DIC which is reflective in its enzymatic low half-saturation constant, allowing it to outcompete other algal species due to its efficient carbon acquisition (Yamamoto and Nakahara, 2005).

It appeared that cultures which received CO_2 *via* flaming benefited substantially and exhibited higher growth rates in our study. This suggested C availability may have been growth limiting in CT medium when cultures were not bubbled or shaken (Figure 2.4). CO_2 is extremely soluble in aqueous solutions, demonstrating 200-times higher solubility relative to oxygen (Wetzel, 2001). H_2CO_3 is a weak acid which readily and rapidly dissociates, losing its 2 protons in a 2-step process ($pKa_1 = 6.43$, $pKa_2 = 10.43$ at 15° C) (Schindler, 1971), (Wetzel, 2001). Hence, CO_2 that is not readily taken-up by *M. aeruginosa* in its initial gaseous form readily dissolves into the media and hydrates into H_2CO_3, as demonstrated in the flaming of freshwater media alone (Figure 2.1). In addition, *M. aeruginosa's* direct uptake of flame-generated gaseous CO_2 is further supported in the consistent pH values amongst control and flamed replicates, as healthy cultures did not experience any significant declines in pH, save for 1 replicate in the flamed 16-times treatment (Figure 2.4c). Yet, when culture death did occur, the final pH was in the same range as CT media subjected to 10-d of flaming (Figure 2.1d), indicating CO_2 had dissolved into the media. Should the concentration of dissolved CO_2 become too high, H_2CO_3 formation would yield low culture pH, which would inhibit growth and development in a variety of algal species, including *M. aeruginosa* (Weisse and Stadler, 2006). Thus, while CO_2 influxes via flaming increased growth rate and biomass in carbon-limited cultures, if the CO_2 dissolution rate becomes too high, significant drops in pH will invoke detrimental effects on the culture. In total it appears likely that the availability of CO_2 coupled to pH decline shaped the inconsistency observed amongst replicates in previous experiments.

Comments and recommendations

We have demonstrated that flame sterilization of culture medium vessel openings can result in a significant decline in the pH of freshwater media due to the dissolution and hydration of CO_2. This decline in pH has several implications, as optimal pH ranges for algal photosynthesis and growth are often narrow and well-defined (Huang et al., 2018). Moreover, under current climate scenarios, research into the effects of small pH shifts is common yet could be compromised by this observation. This pH shift would also effect the bioavailability and accessibility of macro and micronutrients, including crucial trace metals within the media, many of which are associated with photosynthetic processes (Wetzel, 2001). Low pH levels that result from CO_2 introduction, coupled with HOOH generation *via* flaming and excessive trace metal bioavailability, may result in randomized spontaneous cell and culture death, as seen in our previous flamed growth assays (Figure 2.4). Flaming further effects cultures by serving as a variable yet direct source of CO_2, which is labile and thus readily accessible for uptake by *M. aeruginosa*. This CO_2 is likely consumed by *M. aeruginosa* cells, influencing cell growth rate and biomass accumulation (Figure 2.4). This mechanism is further supported by the relatively constant pH levels observed in all *M. aeruginosa* cultures (flamed and non-flamed) as after 10 days the pH remains constant (excluding the "dead" replicates who demonstrated lower pH). These CO_2 inputs may result in a higher degree of replicate variability in unshaken *M. aeruginosa* cultures in contrast to shaken cultures, as unshaken cultures in potentially C-limiting media such as CT are likely to be C-limited.

There is a need for updated aseptic alternatives to flame-induced sterilization. It is advisable to abstain from flaming when feasible, and alter flaming practices when flaming is necessary. Refraining from inverting, shaking, or otherwise disturbing the media post-flaming may decrease the dissolution of CO_2 into the media and mitigate pH decline, though this is not

always feasible. When CT media was subject to a 10-d flaming study without any inversion/shaking, it was found the pH decline was drastically diminished (Appendix Figure 2.9) and not significantly different ($p=0.30$) from the unflamed controls. Additionally, exercising caution in media selections is advised, as the commonly utilized medium (BG-11) was shown to have the highest decline in pH overall. Ten-fold increases in TAPS buffer concentration within CT media were shown to mitigate pH shifts within unflamed replicates (Appendix Figure 2.8) with no observed biological consequences (Appendix Figure 2.11). However, the approach of simply increasing buffer concentrations must be pursued with caution: *e.g.,* TRIS is toxic to cells in high concentrations and HEPES generates higher amounts of reactive oxygen species when present in higher concentrations (Morris and Zinser, 2013). Our results indicate a 10-fold TAPS increase in CT may serve as a suitable medium in future studies concerning pH (climate change research), but each specific case should be individually examined.

This study serves as a cautionary of the unintended effects of flaming of culture vessel openings upon the media and microorganisms. While flaming has served as an aseptic technique for decades, it may be time to put aside the Bunsen burner and pursue further alternatives to this classic practice.

Acknowledgments

We thank Dr. Gary LeCleir, Eric Gann, Robbie Martin, Lena Pound, Naomi Gilbert and Professor George Bullerjahn for comments. We also thank Dr. Adrian Gonzalez with the Water Quality Core Facility at the University of Tennessee Knoxville for TC analyses. This work was supported by grants from the National Science Foundation (DEB-1240870; IOS-1451528) to SWW and by funding from the NIH (1P01ES028939-01) and NSF (OCE-1840715) to the Bowling Green State University *Great Lakes Center for Fresh Waters and Human Health*.

References:

Alam, M. Z. B., M. Otaki, H. Fufami, and S. Ohgaki. 2001. Direct and indirect inactivation of *Microcystis aeruginosa* by UV radiation. Water Res. **35:** 1008-1014.

Andersen, R. A. 2005. Algal culturing techniques. Elsevier/Academic Press.

Bano, A., and P. J. Siddiqui. 2004. Characterization of five marine cyanobacterial species with respect to their pH and salinity requirements. Pakistan J. Bot. **36:** 133-144.

Berberoglu, H., L. Pilon, and A. Melis. 2008. Radiation characteristics of *Chlamydomonas reinhardtii* CC125 and its truncated chlorophyll antenna transformants *tla1*, *tlaX* and *tla1-CW*$^{+}$. Int. J. Hydrogen Energy **33:** 6467-6483.

Bertani, G. 1951. Studies on lysogenesis I.: the mode of phage liberation by lysogenic *Escherichia coli1*. J. Bacteriol. **62:** 293.

Bykowski, T., and B. Stevenson. 2008. Aseptic technique. Curr. Prot. Microbiol. **11:** A. 4D. 1-11.

Coté, R. J. 1998. Aseptic technique for cell culture. Curr. Prot. Microbiol. 1.3.1 - 1.3.10.

Fang, F., Y. Gao, L. Gan, X. He, and L. Yang. 2018. Effects of different initial pH and irradiance levels on cyanobacterial colonies from Lake Taihu, China. J. Appl. Phycol. **30:** 1777-1793.

Ferreira, C. M., I. S. Pinto, E. V. Soares, and H. M. Soares. 2015. (Un) suitability of the use of pH buffers in biological, biochemical and environmental studies and their interaction with metal ions–a review. RSC Advances **5:** 30989-31003.

Harrigan, W., and M. E. McCance. 1966. Laboratory methods in microbiology. Academic Press. London and New York. 374 pp.

Huang, J. and others 2018. New perspectives on CO_2, temperature, and light effects on BVOC emissions using online measurements by PTR-MS and cavity ring-down spectroscopy. Environ. Sci. Technol. **52:** 13811-13823.

Huang, J. and others 2017. Influence of pH on heavy metal speciation and removal from wastewater using micellar-enhanced ultrafiltration. Chemosphere **173:** 199-206.

Lavens, P; Sorgeloos, P. (eds.) Manual on the production and use of live food for aquaculture FAO Fisheries Technical Paper. No. 361. Rome, FAO. 1996. 295 pp.

Madigan, M. T., J. M. Martinko, K. S. Bender, D. H. Buckley, D.A. Stahl, and T. Brock. 2015. *Brock Biology of Microorganisms*. Fourteenth edition. ed. Pearson.

Miller, J. 1972. *Experiments in molecular biology*. Cold Spring Harbor Laboratory, Cold Spring Harbor, NY.

Morris, J., and E. R. Zinser. 2013. Continuous hydrogen peroxide production by organic buffers in phytoplankton culture media. J. Phycol. **49:** 1223-1228.

Palenik, B., N. M. Price, and F. M. Morel. 1991. Potential effects of UV-B on the chemical environment of marine organisms: a review. Environ. Pollution **70:** 117-130.

Price, N. M., and P. J. Harrison. 1988. Specific selenium-containing macromolecules in the marine diatom *Thalassiosira pseudonana*. Plant Physiol. **86:** 192-199.

Sambrook, J., E. Fritsch, and T. Maniatis. 1989. *Molecular cloning.* Cold Spring Harbor Laboratory Press. 1659 pp.

Sanders, E. R. 2012. Aseptic laboratory techniques: volume transfers with serological pipettes and micropipettors. J Vis. Exp. e2754.

Schindler, D. 1971. A hypothesis to explain differences and similarities among lakes in the Experimental Lakes Area, northwestern Ontario. Jour. Fish. Res. Bd. Canada **28:** 295-301.

Schindler, D. W., F. Armstrong, S. Holmgren, and G. Brunskill. 1971. Eutrophication of Lake 227, experimental lakes area, northwestern Ontario, by addition of phosphate and nitrate. Jour. Fish. Res. Bd. Canada 28: 1763-1782.

Steffen, M. M., B. S. Belisle, S. B. Watson, R. A. Bourbonniere, G. L. Boyer, and S. W. Wilhelm. 2015. Metatranscriptomic evidence for co-occurring top-down and bottom-up controls on toxic cyanobacterial communities. Appl. Environ. Microbiol. **81:** 3268-3275.

Talling, J. 2010. pH, the CO_2 system and freshwater science. Freshwater Rev. **3:** 133-147.

Tsaloglou, M.-N. 2016. Microalgae. Caister Academic Press, Cambridge, MA. 152 pp.

Watanabe, M. M., M. Kawachi, M. Kiroki and F. Kasai 2000. *NIES - Collection. List of Strains, Sixteh Edition 2000. Microalgae and Protozoa.* Microbial Culture Collections, National Institute for Environmental Studies, Tsukuba, Japan, 159 pp.

Weisse, T., and P. Stadler. 2006. Effect of pH on growth, cell volume, and production of freshwater ciliates, and implications for their distribution. Limnology and Oceanography **51:** 1708-1715.

Weitz, J. S. and others 2015. A multitrophic model to quantify the effects of marine viruses on microbial food webs and ecosystem processes. ISME J. **9:** 1352-1364.

Wetzel, R. G. 2001. Limnology: lake and river ecosystems. gulf professional publishing.

Wheeler, J. A., H. Zurek, J. A. Wheeler, and H. Zurek. 1983. p. 62-84. Quantum Theory and Measurement. Princeton University Press.

Yamamoto, Y., and H. Nakahara. 2005. Competitive dominance of the cyanobacterium *Microcystis aeruginosa* in nutrient-rich culture conditions with special reference to dissolved inorganic carbon uptake. Phycological Research **53:** 201-208.

Appendix

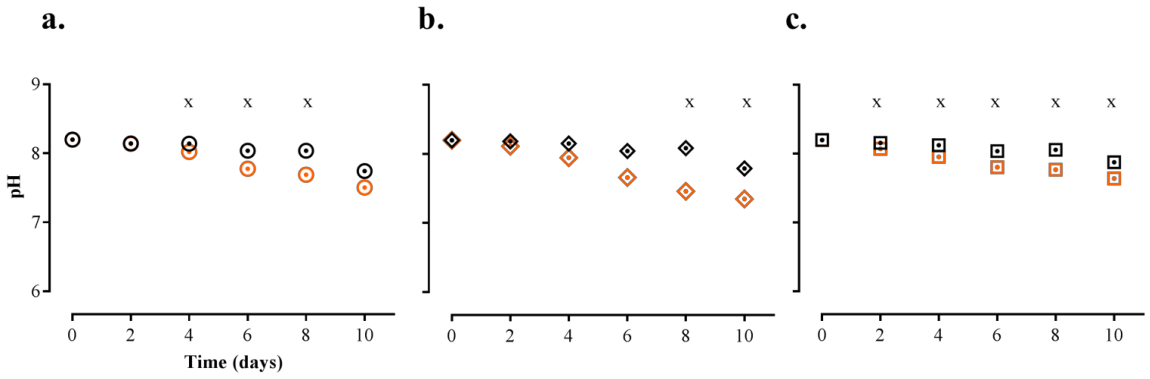


Figure 2.5 Effects of flaming on heterotrophic media. **A.)** Effects on pH of LB medium, control indicated by black circles, flaming indicated by orange circles. **B.)** Effects on pH of Nutrient broth, control replicates indicated by black diamonds, flamed replicates indicated by orange diamonds. **C.)** Effects on pH of M9, control replicates indicated by black squares, flamed replicates indicated by orange squares. Treatments that demonstrate statistical difference denoted as an x ($p < 0.01$).

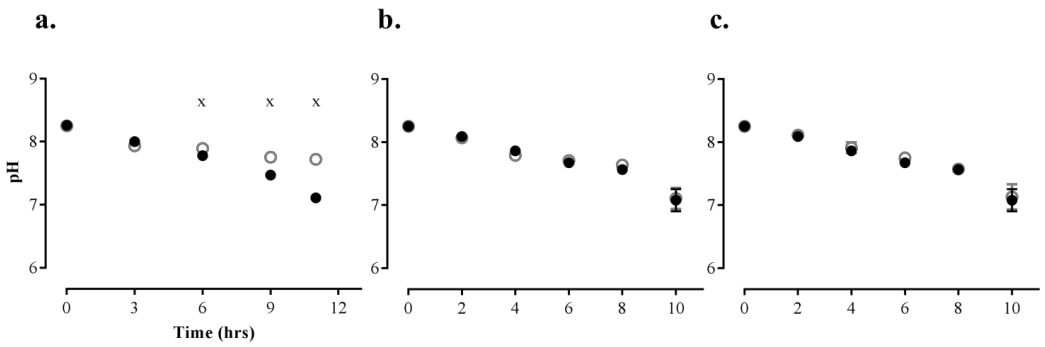


Figure 2.6 Effects of environmental conditions on pH of CT media. **A.)** Effects of buffer age on pH, aged buffer indicated by solid black circles, new buffer indicated by open grey circles **B.)** Effects of gas exchange on pH, closed caps indicated by solid black circles, loosened caps indicated by open grey circles **C.)** Effects of photooxidation on pH, light-exposed samples indicated with solid black circles, dark-treatment samples indicated with open grey circles. Where not visible, error bars are within symbols. Treatments that demonstrate statistical difference denoted as an x ($p < 0.01$).

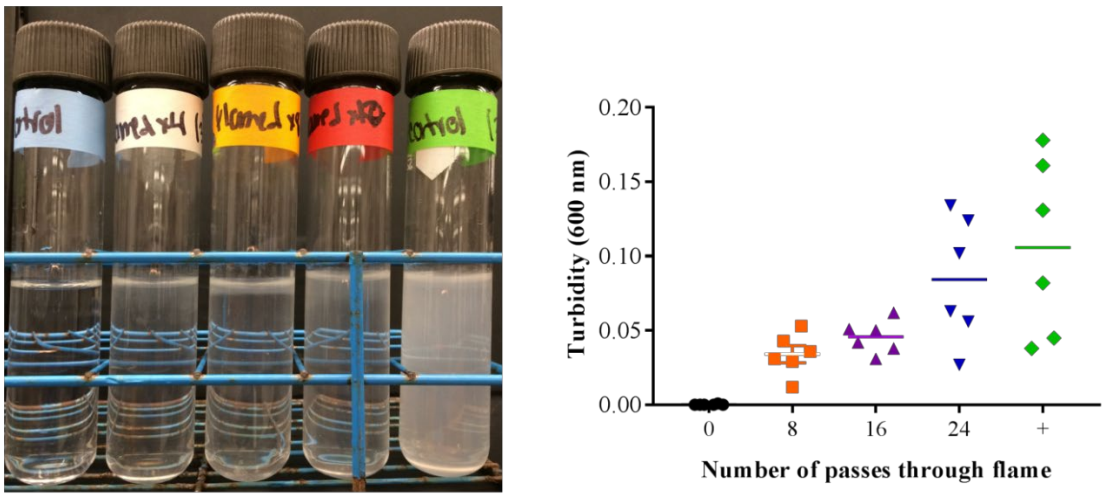


Figure 2.7 Determination of CO_2 as the primary driver of pH decline in freshwater media. **A.)** Limewater turbidity assay demonstrating increased turbidity with increased flaming. Treatments from left to right: control, flamed x8, flamed x16, flamed x24, and positive control (+). **B.)** Turbidity (600 nm) of $CaCO_3$ precipitation as indirect proxy for CO_2 incorporation.

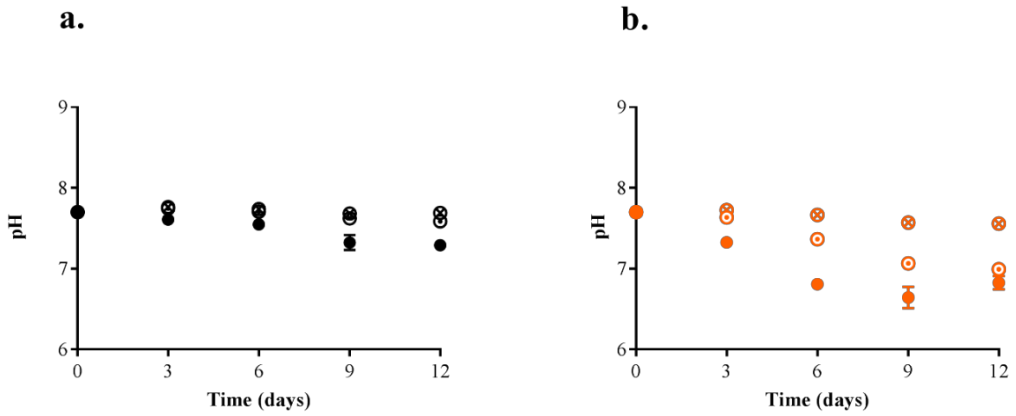


Figure 2.8 Mitigation of pH decline due to flaming of CT medium with TAPS ent. **A.)** Effects of increased buffer concentration on pH in control (standard TAPS concentration, indicated by solid black circles), TAPSx10 (open dotted circles), and TAPSx100 (open crossed circles) **B.)** Effects of increased buffer concentration on pH in flamed replicates. Standard TAPS concentration indicated by solid orange circles, TAPSx10 indicated by open dotted circles, TAPSx100 indicated by open crossed circles.

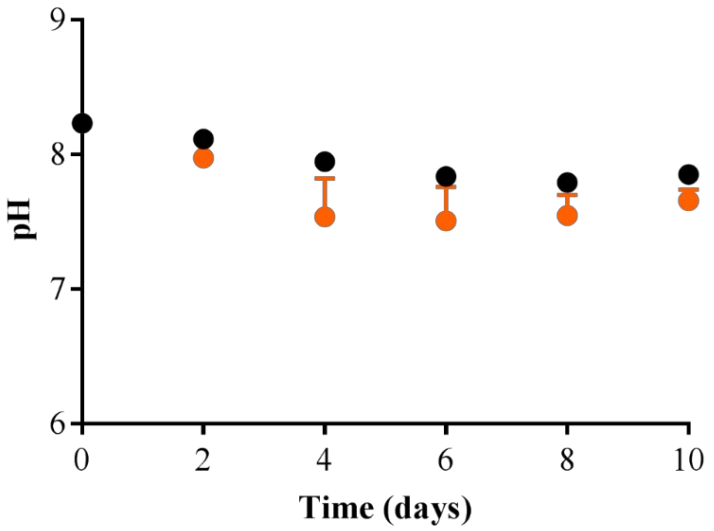


Figure 2.9 Effects of tube inversion (shaking) on control and flame replicate pH decline. Data for non-inverted CT medium control replicates indicated by solid black circles, with non-inverted flamed CT medium replicates indicated by solid orange circles.

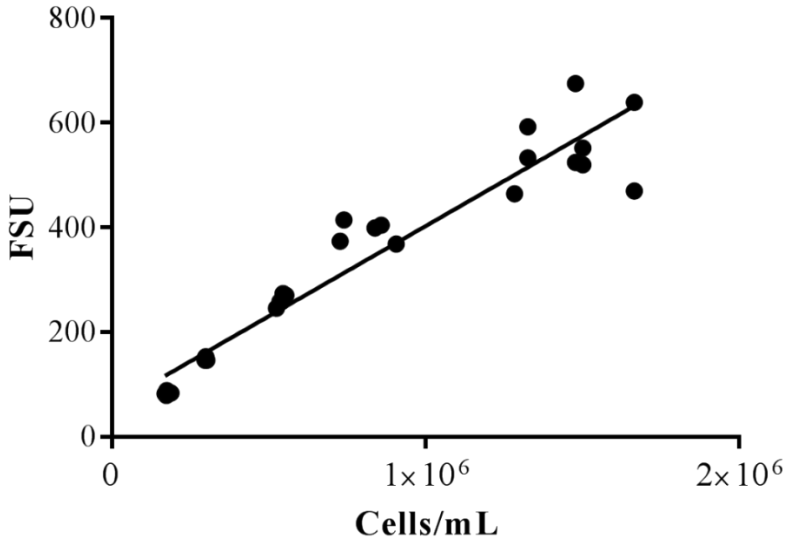


Figure 2.10 Correlation between chlorophyll *a* auto fluorescence (FSU) and cell density (cells/mL) from samples collected during *M. aeruginosa* growth curve in standard CT media (closed black circles). The data indicate a strong and significant relationship ($R^2 = 0.92$, $p = 0.0001$) suggesting fluorescence is a good predictor of cell density.

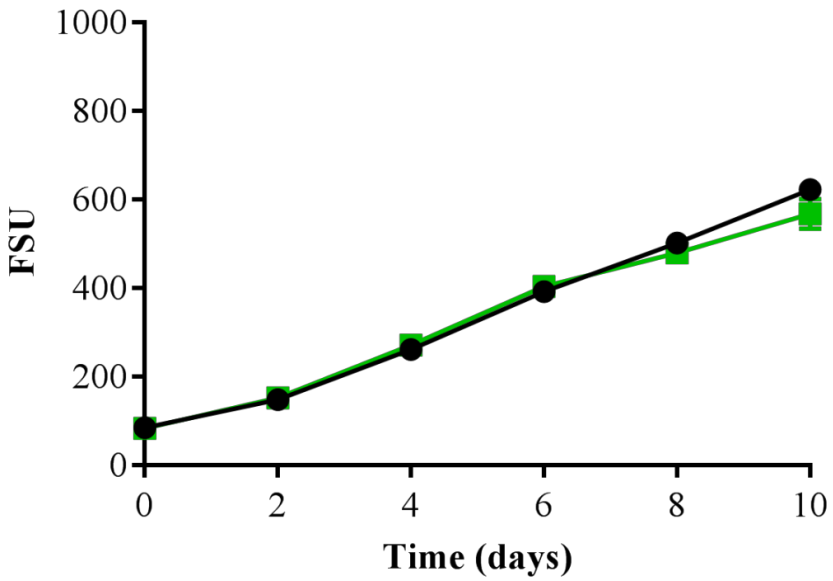


Figure 2.11 Comparison of *M. aeruginosa* biomass accumulation when grown in CT medium with standard TAPS concentration (black circles), and CT media with a ten-fold increase in TAPS concentration (green squares).

CHAPTER III: ELUCIDATING THE ROLE OF PH ON *MICROCYSTIS*-DIATOM COMPETITION DYNAMICS IN LAKE ERIE

Publication Note

This chapter is a version of a peer-reviewed, published article in *Frontiers in Microbiology* 12(2021):598736 by Brittany N. Zepernick, Eric R. Gann, Robbie M. Martin, Helena L. Pound, Lauren E. Krausfeldt, Justin D. Chaffin, and Steven W. Wilhelm.

BNZ and SWW designed these experiments. BNZ and LEK performed preliminary culture optimizations and experimental planning. *In vitro* co-culture assays and *in vitro* silica deposition assays conducted by BNZ. Epifluorescence microscopy performed by ERG and BNZ. *In situ* Lake Erie silica deposition assays conducted by BNZ, HLP and RMM with logistical support from JDC. JDC performed data collection and analyses corresponding to the 2015 *M. aeruginosa* bloom in Figure 1. Statistical analyses performed by BNZ. All authors contributed to the drafting of the manuscript.

Abstract

Cyanobacterial Harmful Algal Blooms (CyanoHABs*)* commonly increase water column pH to alkaline levels ≥ 9.2, and to as high as 11. This elevated pH has been suggested to confer a competitive advantage to cyanobacteria such as *Microcystis aeruginosa*. Yet, there is limited information regarding the restrictive effects bloom-induced pH levels may impose on this cyanobacterium's competitors. Due to the pH-dependency of biosilicification processes, diatoms (which seasonally both precede and proceed *Microcystis* blooms in many fresh waters), may be unable to synthesize frustules at these pH levels. We assessed the effects of pH on the ecologically relevant diatom *Fragilaria crotonensis in vitro*, and on a Lake Erie diatom community *in situ*. *In vitro* assays revealed *F. crotonensis* monocultures exhibited lower growth rates and abundances when cultivated at a starting pH of 9.2 in comparison to pH 7.7. The suppressed growth trends in *F. crotonensis* were exacerbated when co-cultured with *M. aeruginosa* at pH conditions and cell densities that simulated a cyanobacteria bloom. Estimates demonstrated a significant decrease in silica (Si) deposition at alkaline pH in both *in vitro F. crotonensis* cultures and *in situ* Lake Erie diatom assemblages, after as little as 48 h of alkaline pH-exposure. These observations indicate elevated pH negatively affected growth rate and diatom silica deposition; in total providing a competitive disadvantage for diatoms. Our observations demonstrate pH likely plays a significant role in bloom succession, creating a potential to prolong summer *Microcystis* blooms and constrain diatom fall resurgence.

Introduction

Toxin-producing cyanobacteria of the genus *Microcystis* have inundated fresh waters in recent decades (Steffen et al., 2014a). Blooms have detrimental ecological and economic effects due to the production of secondary metabolites and the formation of extensive biomass that, upon bloom termination, can drive anoxia (Anderson, 2009). To this end, there is a crucial need to determine the factors responsible for the ecological success of *Microcystis*.

The mechanisms by which *Microcystis* displaces other phytoplankton in fresh waters, including Lake Erie (USA/Canada), Lake Okeechobee (USA) and Lake Taihu (China) remain unclear, but are likely multifaceted. In these lakes, a seasonal pattern of phytoplankton taxa succession has emerged. Non-toxic diatoms and other algae dominate throughout fall, winter, and spring, only to be displaced by *Microcystis* blooms mid-summer into fall (Ke et al., 2008; Reavie et al., 2014). This successional trend has been evidenced in Erie's paleolimnological record, which traces the emergence of eutrophication back to the 1930's (Allinger and Reavie, 2013a). Monitoring efforts of a 2015 *Microcystis* bloom in Lake Erie's western basin further confirmed this succession, demonstrating diatoms dominated the early summer period prior to their succession by cyanobacteria in mid-summer (Figure 3.1a).

Several factors contribute to the ecological success of *Microcystis*. Summer dominance in Lake Erie's western basin has been attributed to nutrient loading (Michalak et al., 2013; Paerl et al., 2016), predation (Vanderploeg et al., 2001; Steffen et al., 2015b), and temperature (Andersson et al., 1994; Peng et al., 2018). Likewise, spring diatom decline has been linked to silica limitation and temperature intolerance (Twiss et al., 2012; Reavie et al., 2016). While these factors each contribute to *Microcystis* growth during cyanobacterial bloom years, non-cyanobacterial bloom years have demonstrated that diatoms, such as the temperature tolerant *Fragilaria crotonensis,* can persist and even dominate the summer water column in Lake Erie

(Hartig and Wallen, 1986; Saxton et al., 2012a; Reavie et al., 2014). Indeed, *F. crotonensis* summer blooms were a frequent occurrence in the western basin of Lake Erie throughout the 1960-1980's during lake remediation efforts (Hartig, 1987). Furthermore, monitoring data from the 2015 Lake Erie *Microcystis* bloom indicates dissolved silica concentrations, though lowest during the peak diatom bloom, were non-limiting during *Microcystis* succession (Appendix Figure 3.7). These observations suggest there are additional and multiple factors contributing to *Microcystis* succession of spring-summer diatoms (Wilhelm et al., 2020) Amongst these factors playing a potential role in succession dynamics is pH. For example, during the 2015 *M. aeruginosa* bloom monitoring efforts, a sharp rise in water column pH was found to co-occur with cyanobacterial bloom formation (Figure 3.1a, b). While pH can have multiple effects on cellular physiology and biogeochemistry, in the present study, we investigated the response of one physiological aspect of diatoms – silicification - to the shifts in pH that occur during *Microcystis* blooms.

Microcystis blooms increase water column pH above 9.2 as CO_2 is consumed during photosynthesis (Verspagen et al., 2014; Bullerjahn et al., 2016; Krausfeldt et al., 2019). This alkaline pH is considered advantageous to cyanobacteria (Wilson et al., 2010; Shruthi and Rajashekhar, 2014), due to their unique carbon concentrating mechanisms (CCMs) which confer a competitive advantage during growth at low CO_2 / high pH conditions (Shapiro, 1990; Raven, 2010; Sandrini et al., 2016). Yet freshwater and marine diatoms have been shown to possess a competitive array of CCMs themselves which optimize CO_2 and HCO_3^- acquisition (Clement et al., 2017). While this may allow diatoms to evade pH-induced carbon-limitation, elevated pH has been shown to decrease carbon uptake, growth rate and metabolic processes in various marine diatoms (Raven, 1981; Taraldsvik and Myklestad, 2000). While these effects of pH on diatom

carbon acquisition have been well characterized, pH-induced effects on other metabolic processes have been widely unstudied to date, particularly in freshwater diatoms.

One metabolic process that serves as a distinctive metric for diatom viability is deposition. Diatoms possess siliceous cell walls (*i.e.,* frustules) which may pose a unique disadvantage in alkaline bloom conditions. Silica deposition relies on the uptake of dissolved silica (dSi) in the form of silicic acid ($Si[OH]_4$) to synthesize biogenic silica (bSi) frustules (Vrieling et al., 1999; Otzen, 2012; Hildebrand et al., 2018). In marine and estuarine systems, diatom viability has been strongly correlated to pH, with studies demonstrating marine diatoms are unable to survive at pH > 8.7 due to silica solubility dynamics and the inhibition of biosilicification (Hansen, 2002; Hervé et al., 2012). Yet, to our knowledge, the effect of pH in freshwater diatom Si deposition remains unassessed.

In this study, we combined lab and field-based experiments to assess the effect of pH on diatom growth rate and silica deposition. As part of this effort, we assessed the effect of pH on *F. crotonensis* growth rate in monoculture and ecologically relevant co-cultures with *M. aeruginosa*. Effects of pH on silica deposition were assessed using a fluorescent dye (PDMPO) which intercalates into newly formed frustules. Laboratory and field-based results indicate pH conditions consistent with *M. aeruginosa* blooms (*i.e.,* pH $\geq$ 9.2) decreased diatom growth rate, abundance, and silica deposition. In total the pH shift reduces diatom viability and the ability to compete for valuable niche-space with cyanobacteria.

Methods

Assessing successional trends of a 2015 Lake Erie Microcystis bloom

A temporal dataset collected at the Ohio State Stone Laboratory was used to preliminarily evaluate the dynamics of cyanobacteria, diatoms, and pH during the summer of 2015, which was the largest *M. aeruginosa* bloom observed to date (Davis et al., 2019). Water column pH was recorded every 30 min *via* a Yellow Spring Instruments 6600v2 multiprobe sonde suspended at 1 m depth from a buoy located between South Bass and Gibraltar Islands (N 41.66°, W 82.92°). Water samples for phytoplankton community composition were collected next to the buoy several times a week. Diatom-specific and cyanobacteria-specific Chl *a* concentrations were recorded *via* a bbe Moldaenke FluoroProbe (Beutler et al., 2002). Total chlorophyll *a* concentrations corresponding to the sampling period have been provided (Appendix Figure 3.8), with the complete details of this dataset found in the original publication (Chaffin et al., 2018).

Effect of pH on growth in F. crotonensis and M. aeruginosa monocultures

To assess the effects of this environmentally observed pH on diatom and cyanobacteria growth, *in vitro* monoalgal experiments were performed using 2 model taxa. *F. crotonensis* SAG 28.96 (acquired from the *Culture Collection of Algae at the University of Göttingen*, Germany) and *M. aeruginosa* NIES 843 (acquired from the *National Institute for Environmental Studies*, Japan) were maintained in batch cultures using CT medium (Wilhelm, 2017) at respective optimal pH levels of pH 7.7 (Guillard and Lorenzen, 1972; Hervé et al., 2012) and 8.2 (Watanabe et al., 2000; Krausfeldt et al., 2019). To initiate *in vitro* monoculture experiments, *F. crotonensis* and *M. aeruginosa* cultures were filter-concentrated respectively using a 2.0-µm and 1.0-µm nominal pore-size 47-mm diameter polycarbonate filter and inoculated into sterile 250

mL filter-vented, baffled polycarbonate flasks (Corning) at a starting concentration of ~700 cells/mL. Monocultures were maintained in 125 mL CT medium (Steffen et al., 2015b) containing a non-limiting concentration of silicic acid (176 µM $Na_2SiO_3 \cdot 9H_2O$)(Hervé et al., 2012) and adjusted to an initial pH of 7.7 (optimal pH for diatom growth) or 9.2 (pH observed during *Microcystis* blooms). pH conditions in the lab study were maintained by adding TAPS buffer as described previously (Zepernick et al., 2020). Cultures were monitored for 30 d at 26° C, with orbital shaking at 70 rpm, and a light intensity of approximately 55-60 µmol photons m^{-2} s^{-1} on a 12:12 light: dark photoperiod cycle.

Abundances were measured every two days *via* flow cytometry (BD FACSCalibur). Populations of each species were gated and counted based on forward scatter (FSC), a proxy for size, and chlorophyll *a* fluorescence (FL3) using FlowJo™ software (Becton, Dickinson and Company). Due to the filamentous nature of *F. crotonensis*, direct estimates of individual cell abundance are challenging (Bramburger et al., 2017). In this study, *F. crotonensis* abundances are estimated based on filaments/mL, which form a tight cluster (Appendix Figure 3.9). Exponential growth rates (μ) were calculated as the slope of log -scaled data and were reported in filaments/mL for *F. crotonensis*, and cells/mL for *M. aeruginosa*. Specifically, log-scaled growth data for each replicate were fitted with a linear regression to select time points to be used for μ calculations. Time points demonstrating the logarithmic growth phase with a linear regression R2 value of ≥ 0.95 (i.e., the most linear data points) were subsequently used to calculate average growth rate). Culture pH was checked every 10-d using a sterilized pH probe (Mettler Toledo Seven Compact ™ pH/Ion meter S220 fitted with a Mettler InLab Expert Pro-ISM electrode with a temperature range and correction of up to 100°C). Growth experiments

were performed in biological triplicate. We note all results will be referred to in this study based on the initial pH condition of the treatment.

Effect of pH on growth in F. crotonensis and M. aeruginosa co-cultures

To evaluate the effects of ecologically relevant pH conditions on diatom growth, *in vitro* co-culture assays were performed. Concurrent with the monoculture assays, co-cultures of *F. crotonensis* SAG 28.96 and *M. aeruginosa* NIES 843 were inoculated. To initiate *in vitro* co-culture experiments, *M. aeruginosa* and *F. crotonensis* batch cultures were filter-concentrated and inoculated into the same experimental media and initial pH levels as previously described. Taxa were inoculated at 3 ratios (reported as *F. crotonensis: M. aeruginosa)* based on the succession patterns observed (Figure 3.1)*:* 10:1 ratio simulating a spring diatom bloom, 1:1 ratio simulating the onset of the summer *M. aeruginosa* bloom, and a 1:10 ratio simulating the peak *M. aeruginosa* bloom. All co-cultures were inoculated at net starting concentrations of ~7,000 cells/mL. Hereafter, co-culture treatments will be referred to by the *F. crotonensis: M. aeruginosa* ratio. Co-cultures were subjected to the same incubation conditions and procedures as described above. All experiments were performed in biological triplicate.

Effect of pH on in vitro F. crotonensis silica deposition

To determine the effect of pH on silica deposition *in vitro,* batch cultures of *F. crotonensis* SAG 28.96 were inoculated with the fluorescent dye PDMPO [2-(4-pyridyl) -5-((4-(2-dimethylaminoethylaminocarbamoyl) methoxy) phenyl) oxazole] (Lysosensor DND 160 Yellow/Blue; Invitrogen, Carlsbad, CA). Diatom cultures were acclimated to pH conditions of 7.7 and 9.2 for a 6-d period (*i.e.,* approximately 2 doubling times). Acclimated cultures were

filter-concentrated using a 2.0-µm nominal pore-size 47-mm diameter polycarbonate filter and inoculated in acid-clean, sterilized 50 mL glass culture tubes containing 25 mL of CT medium with 176 µM $Na_2SiO_3 \cdot 9H_2O$. Tubes were inoculated at an initial concentration of ~1500 filaments/mL. PDMPO was added at a final concentration of 0.125 µM (Leblanc and Hutchins, 2005). Cultures were incubated at 26° C and approximately 55-60 µmol photons m^{-2} s^{-1} on a 12:12 light: dark photoperiod cycle for 48 h. Abundances were determined *via* flow cytometry as described above.

Si deposition was assessed using microscopic and fluorometric approaches that detect freshly incorporated PDMPO. Bulk Si deposition into individual cells was assessed *via* epifluorescence microscopy. After 48 h, 2 mL of each culture was filtered onto 0.2-µm nominal pore-size 25 mm diameter black polycarbonate filters (Millipore), mounted onto glass slides, treated with anti-fade (Suttle and Fuhrman, 2010), and a coverslip applied prior to storage (-80° C). *F. crotonensis* killed controls (0.5% glutaraldehyde-fixed) were performed according to previous studies (Saxton et al., 2012a) to assess abiotic incorporation. Slides were viewed on a Leica DM5500 (Wetzlar, Germany) epifluorescence microscope equipped with a Hamamatsu ORCA-ER camera (Sewickley PA) according to previous methods (Saxton et al., 2012a). A "Texas red" filter cube set (λ_{ex} = 520-600nm; λ_{em} = 570-720 nm) was used to view chlorophyll *a* autofluorescence, and a "DAPI filter" cube set (λ_{ex} = 340-380 nm; λ_{em} > 425 nm) to view PDMPO fluorescence, indicative of Si deposition during the experimental period. Quantitative assessment of epifluorescence microscopy data was achieved by randomized scoring of 100 *F. crotonensis* filaments per pH treatment: analyses included chlorophyll *a* fluorescing cells per filament, PDMPO fluorescing cells per filament, and the proportion of filaments demonstrating ≥ one PDMPO fluorescing cells. Total Si deposition was quantitatively measured

fluorometrically after HCl-Milli Q lysis to remove unincorporated PDMPO from the silica deposition vesicle (SDV), followed by frustule digestion with hot-NaOH (Saxton et al., 2012a; Zepernick et al., 2019). After 48 h of growth, 20 mL of culture was collected on a 0.2-µm nominal pore-size 47-mm diameter polycarbonate filter and subjected to HCl-Milli Q lysis. Filters were flash frozen and stored at -80° C until hot NaOH digestion. After frustule digestion, samples were cooled in an ice bath and neutralized using 1M HCl. PDMPO fluorescence was quantitatively determined using a Turner Designs TD-700 fluorometer fitted with a specialized filter set (λ_{ex} = 360-380nm: λ_{em} = 522-542 nm, Andover Corporation, Salem, NH). A PDMPO standard curve was generated using PDMPO and NaOH-HCl matrix (Appendix Figure 3.10), with the PDMPO concentration converted to Si using a conversion factor of 3230:1 for Si: PDMPO (mol: mol) (Saxton et al. 2012). Total silica deposited into frustules after 48 h (µmol) was normalized to final abundance(filaments/mL). PDMPO experiments were performed with 5 biological replicates.

Effect of pH on in situ Lake Erie diatom community silica deposition

To evaluate the effects of pH on silica deposition in natural populations, we queried diatom-enriched communities from Lake Erie with PDMPO under varying pH conditions. Samples were collected in late July of 2019 from the western basin of Lake Erie near the Ohio State University Stone Laboratory on South Bass Island (N 41.69; W -82.79). Water column physiochemistry (temperature = 25.3° C; dissolved oxygen = 7.60 mg/L; pH = 8.63; turbidity = 1.46 NTFU; chlorophyll *a* = 0.13 µg/L) was recorded prior to sampling using an EXO multiparameter sonde (YSI xylem ^{TM}). Experiments were initiated by enriching for diatoms using a 64-µm mesh phytoplankton net, which was lowered to a depth of ~7 m. Equal volumes

of concentrated seston were diluted with lake water and inoculated into acid washed, rinsed 500 mL polycarbonate bottles. Lake water was buffered using TRIS (4.13 mM final concentration) in accordance with the protocol for freshwater "C medium" (Watanabe et al., 2000). The experiment consisted of three pH treatments: 7.7, 9.2, and an *in situ* pH control for the sample collection site (pH 8.6). To achieve these pH conditions, samples were incrementally titrated using 1 M HCl or NaOH. PDMPO dye was added at a final concentration of 0.125 μM (Leblanc and Hutchins, 2005), and bottles were placed into an *in situ* mesh incubation chamber for 48 h.

Sample pH and chlorophyll *a* concentration were determined at the initiation (T_0) and termination (T_f; 48 h) of the incubation. pH was assessed *via* immediate readings of 15 mL subsamples using a pH probe (Mettler Toledo Seven Compact ^{TM} pH/Ion meter S220, fitted with a Mettler InLab Expert Pro-ISM electrode with a temperature range of up to 100° C). Chlorophyll *a* concentration was determined from filtration of 100 mL onto 0.2-μm nominal pore-size 47-mm diameter polycarbonate filters. Samples were extracted in 90% acetone for 24 hrs at 4° C and assessed on a Turner Designs 10-AU Field Fluorometer (Welschmeyer, 1994). To measure silica deposition, samples were collected by filtering 100 mL of sample onto 0.2-μm nominal pore-size 47-mm diameter polycarbonate filters, followed by the HCl-Milli Q lysis method as described above. Samples were flash frozen in liquid N_2 and stored at -80° C until further processing. Quantitative Si deposition analyses were performed using hot-NaOH frustule digestion, fluorometry, and subsequent calculations using a fresh standard curve (Appendix Figure 3.11) (Zepernick et al., 2019). Total silica deposited per bottle after 48 h (μmol) was normalized to chlorophyll *a* concentration (μg/L) (Saxton et al., 2012a). Field experiments were performed with 4 biological replicates.

Statistical analyses

Statistical comparisons were made using unpaired two-tailed t-tests, ordinary one-way ANOVAs, or ordinary two-way ANOVAs, depending on experimental design. One-way and two-way ANOVA post-hoc multiple comparisons were adjusted using Tukey's HSD**.** While *F. crotonenis* and *M. aeruginosa* monoculture and co-culture growth rates are presented separately in this text, all experiments were performed concurrently in the same conditions, and thus have been statistically analyzed using ordinary two-way ANOVAs to compare both pH and abundance (Appendix Tables 3.1 and 3.2). All analyses were performed using GraphPad's Prism software (Version 8). For this study, we consider a p value < 0.05 to be significant but have reported all values so the reader may decide (Appendix Tables 3.1, 3.2, 3.3 and 3.4).

Results

Role of pH in 2015 Lake Erie bloom succession trends

Monitoring data from a 2015 *M. aeruginosa*-dominated bloom demonstrated that total chl *a* concentration across the season varied from ~ 1-3 µg/L in June to ~20-120 µg/L in July and August (Chaffin et al. 2018; Appendix Figure 3.8). The pre-cyanobacterial bloom period (June through early July) was dominated by diatoms which form ~50%-80% of the total chl *a* concentration, whereas cyanobacteria were less than 10% (Figure 3.1a). The mean daily pH during the corresponding diatom bloom period was between 8.08 and 8.56 (Figure 3.1b). Conversely, during the cyanobacterial bloom period cyanobacteria dominate, forming ~56% - 84% of the chl *a* concentration, whereas diatoms were less than 7% and frequently not detected (Figure 3.1a). The mean daily pH during the *Microcystis* bloom peaked at ~9.27 and remained higher than 9 throughout most of August (Figure 3.1b).

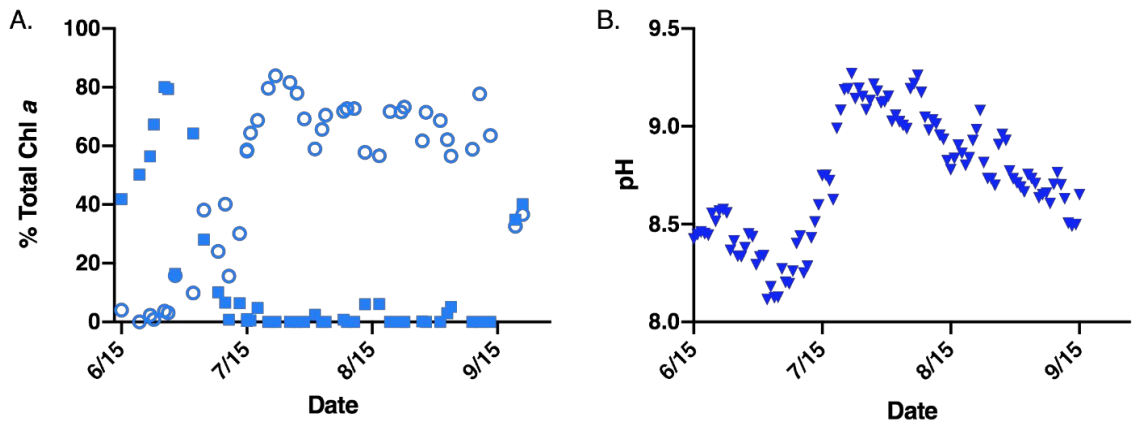


Figure 3.1 Environmental data corresponding to a 2015 Lake Erie *M. aeruginosa* bloom. (A) Relative abundance (reported as percentage of total chlorophyll *a)* of diatoms (blue squares) and cyanobacteria (blue circles) within the Lake Erie water column. (B) Average daily pH of the Lake Erie water column (closed blue circles).

Alkaline pH decreases growth rate of F. crotonensis monocultures

Monoculture experiments demonstrated *F. crotonensis* growth was suppressed at high pH. *F. crotonensis* cultures inoculated at pH 9.2 attained lower abundances throughout the 30-d experiment compared to their pH 7.7 counterparts (Figure 3.2a). *F. crotonensis* mean growth rate at pH 7.7 was $\mu = 0.34$, with pH 9.2 monocultures exhibiting a significantly lower mean growth rate of $\mu = 0.22$ (p= 0.0002) (Figure 3.2b). Overall, *F. crotonensis* monocultures inoculated at pH 9.2 had a 1.5-fold lower mean growth rate compared to its pH 7.7 equivalents.

Effects of pH on *M. aeruginosa* monoculture were less pronounced. *M. aeruginosa* reached higher cell abundances at pH 7.7 compared to pH 9.2 equivalents (Appendix Figure 3.12a). Yet, *M. aeruginosa* growth rates were unaffected by pH overall (p= 0.503) (Appendix Figure 3.12b).

M. aeruginosa modulates the effect of pH on F. crotonensis in co-culture

F. crotonensis reached higher abundances at pH 9.2 than pH 7.7 when co-cultured with non-dominant *M. aeruginosa* concentrations of 10:1 and 1:1 (Figure 3.3a, c). Additionally, *F. crotonensis* growth rates at the designated pH treatments were not significantly different in the 10:1 ratio (p= 0.999) and 1:1 ratio (p= 0.206). (Figure 3.3b, d). Conversely, at the dominant *M. aeruginosa* co-culture ratio of 1:10, *F. crotonensis* growth was substantially suppressed at pH 9.2 (Figure 3.3e). *F. crotonensis* mean growth rate at pH 7.7 in the 1:10 co-culture was $\mu = 0.35$, with pH 9.2 co-cultures exhibiting a significantly lower mean growth rate of $\mu = 0.23$ (p= 0.0002) (Figure 3.3f). Overall, at the 10:1 ratio and pH 9.2, *F. crotonensis* has a 1.5 times lower mean growth rate compared to its pH 7.7 equivalents. As in the monocultures, the effects of pH on *M. aeruginosa* growth in the co-culture replicates were less pronounced. *M. aeruginosa*

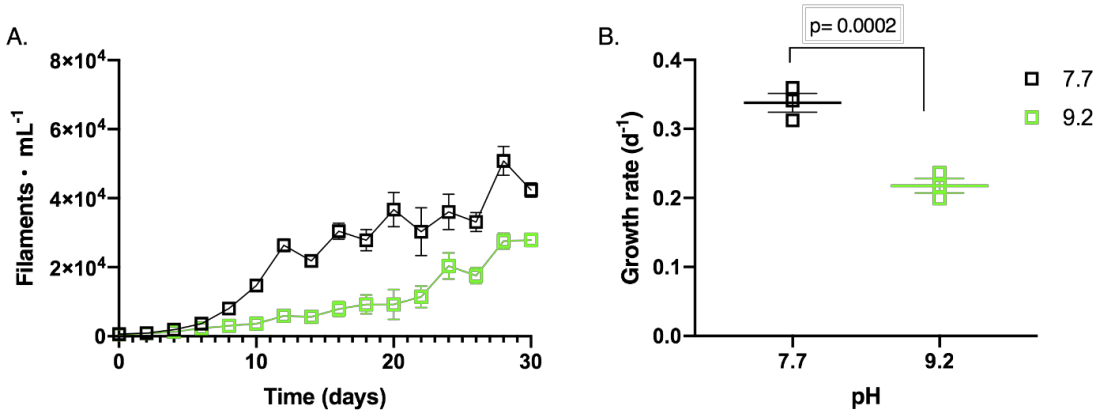


Figure 3.2 (A) *In vitro F. crotonensis* monoculture growth curves at pH 7.7 (black squares) and pH 9.2 (green squares). (B) *F. crotonensis* growth rate at pH 7.7 (black squares) and pH 9.2 (green squares). Statistically significant differences between pH treatments are denoted by p values generated by Two-way ANOVAs. Standard error of the mean reported by error bars.

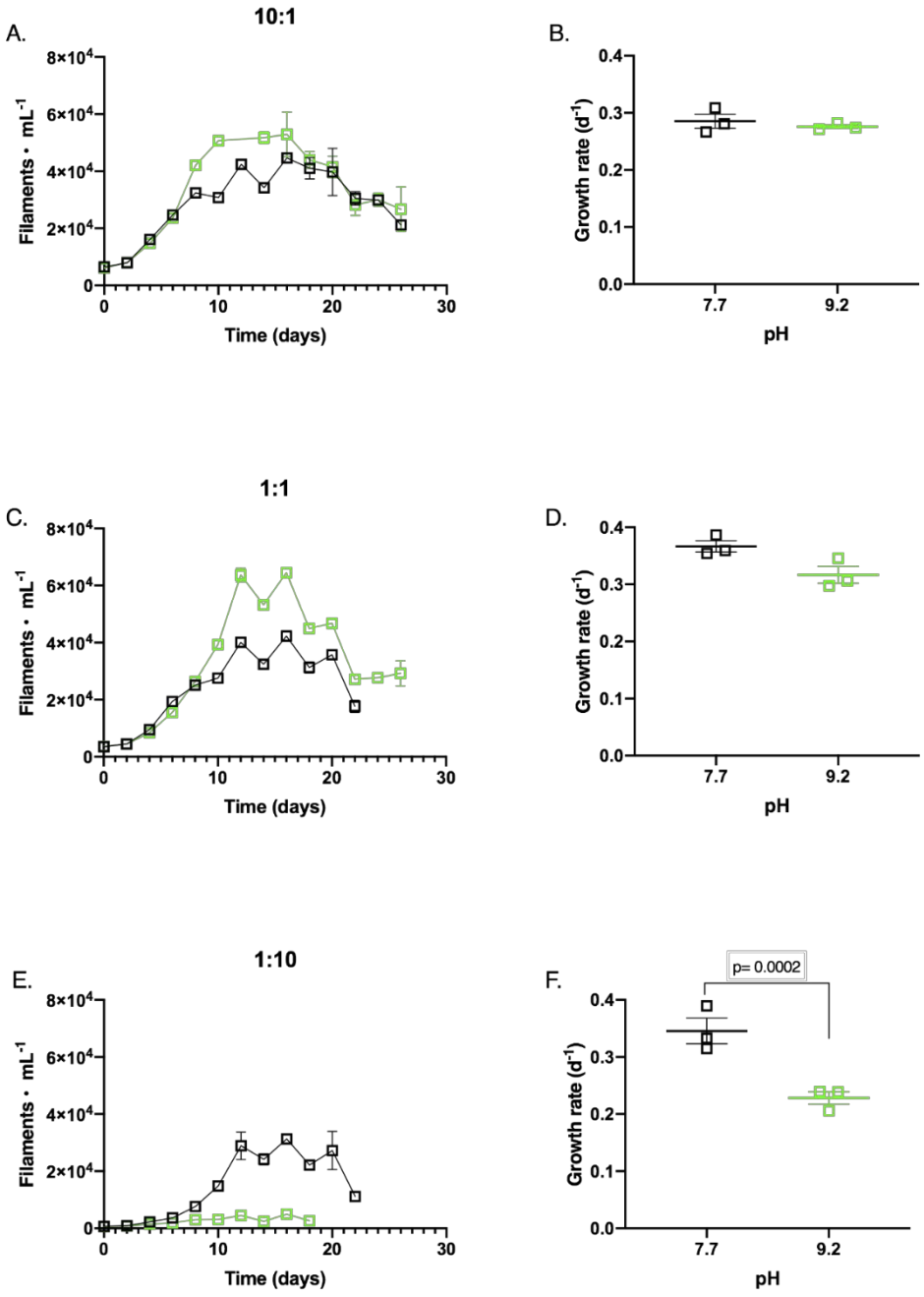


Figure 3.3 (A) *In vitro F. crotonensis* co-culture growth curves in a 10:1 ratio *(F. crotonensis: M. aeruginosa)* at pH 7.7 (black squares) and pH 9.2 (green squares). (B) *F. crotonensis* growth rate at 10:1 ratio (C) *F. crotonensis* growth curves in a 1:1 ratio (D) *F. crotonensis* growth rate in 1:1 ratio (E) *F. crotonensis* growth curves in a 1:10 ratio (F) *F. crotonensis* growth rate in a 1:10 ratio. Statistically significant differences between pH treatments are denoted by p values generated by Two-way ANOVAs. Standard error of the mean reported by error bars.

reached higher cell concentrations at pH 7.7 in all co- culture ratios compared to pH 9.2 equivalents (Appendix Figure 3.13a, c, e). Yet, *M. aeruginosa* culture ratios compared to pH 9.2 equivalents (Appendix Figure 3.13a, c, e). Yet, *M. aeruginosa* growth rates were unaffected by pH overall ($p > 0.503$) (Appendix Figure 13b, d, f).

M. aeruginosa concentrations correspond with pH increases

While *F. crotonensis* monocultures inoculated at pH 7.7 remained at this pH throughout the 30-d experiment (Appendix Figure 3.14), *M. aeruginosa* monocultures demonstrated a steady climb in pH, reaching ~8.0 by 30-d (Appendix Figure 3.15). Similarly, all 3 co-culture ratios inoculated at pH 7.7 demonstrated continual increases in pH throughout the 30-d experiment, reaching final pH levels of ~8.10 (Appendix Figure 3.16). In total, pH 7.7 inoculated *M. aeruginosa* monocultures and co-cultures all experienced increases in pH of ~0.30, coinciding with increases in *M. aeruginosa* concentrations throughout the 30-d experiment (Appendix Figure 3.13) (Appendix Figure 3.17a). Upon further analysis, *M. aeruginosa* concentrations demonstrated a strong linear relationship with culture pH increases observed in the mono and co-cultures (Simple linear regression $R^2 \geq 0.8460$) (Appendix Figure 3.18). Collectively, pH was maintained within a range of approximately +/- 0.40 pH units throughout the 30-d experiment (Appendix Figure 3.17).

Silica deposition decreases at alkaline pH in F. crotonensis monocultures

In vitro PDMPO incubations demonstrated a pronounced effect of alkaline pH on silica deposition. Epifluorescence microscopy revealed pH 7.7 acclimated cultures deposited more Si after 48-h PDMPO incubations (Figure 3.4a, c, e; Appendix Figure 3.19a, c) compared to pH 9.2 acclimated cultures (Figure 3.4b, d, f; Appendix Figure 3.19b, d). Quantitative counts of these

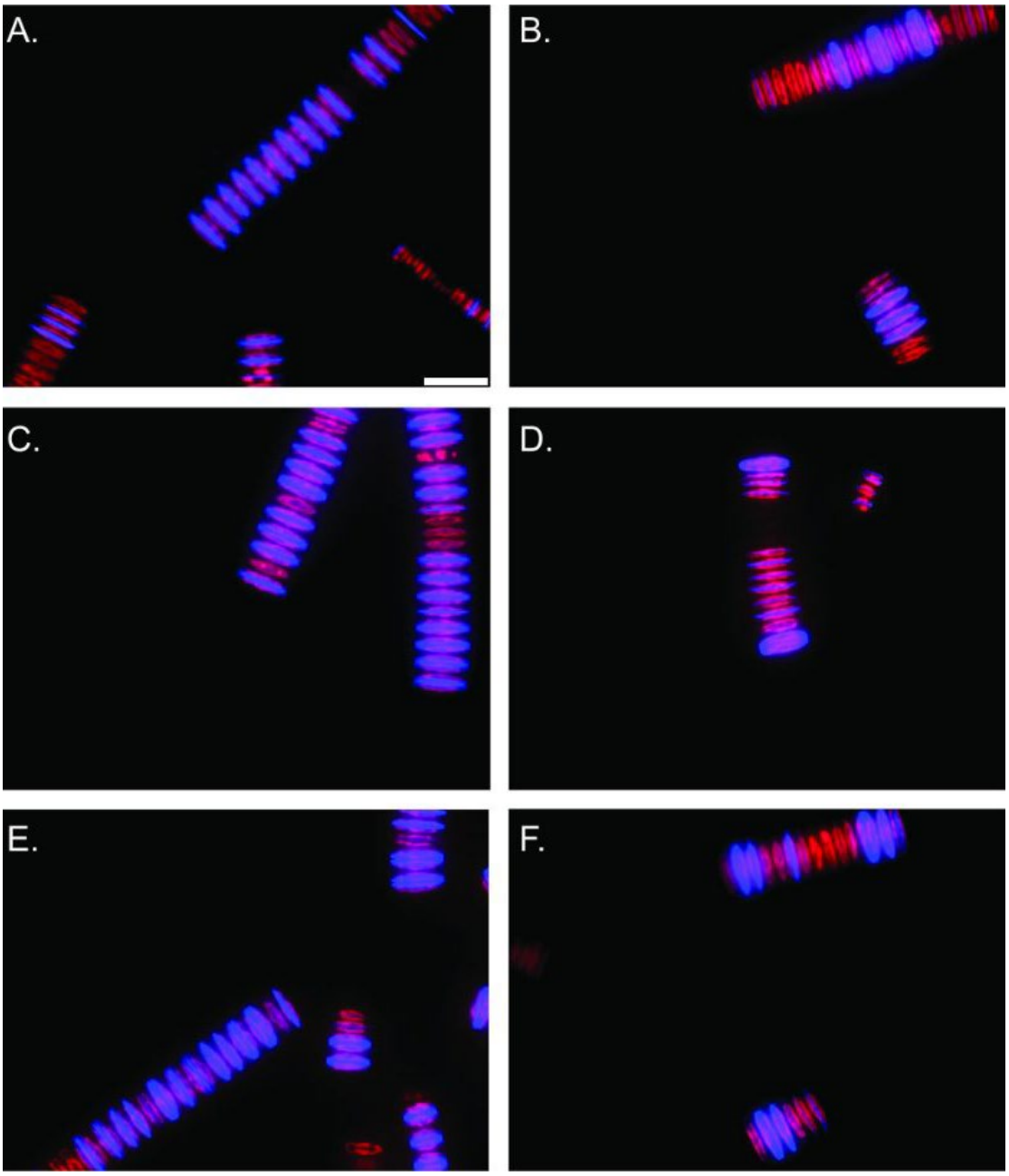


Figure 3.4 Epifluorescent microscopy images (40x magnification) of *F. crotonensis* filaments after 48 h PDMPO incubations. Scale bar represents 25 µm. Chlorophyll *a* autofluorescence is depicted in red, and PDMPO fluorescence is in blue. (A, C, E) *F. crotonensis* cultures acclimated to pH 7.7. (B, D, F) *F. crotonensis* cultures acclimated to pH 9.2.

images also demonstrated pH 9.2 acclimated cultures formed significantly smaller filaments than pH 7.7 acclimated cultures ($p<0.0001$; unpaired two-tailed t-test $t=4.057$, $df=197$, $n=100$) (Appendix Figure 3.20a). In total, ~66% of cells in each filament deposited silica after 48 h in the pH 7.7 treatments, while only ~30% of the cells in each filament had deposited Si at pH 9.2 ($p< 0.0001$; unpaired two-tailed t-test $t=9.457$, $df=197$, $n=100$) (Appendix Figure 3.20b). 100% of *F. crotonensis* filaments incubated at pH 7.7 exhibited at least one diatom cell depositing Si, while only 66% of pH 9.2 *F. crotonensis* filaments demonstrated at least one instance of Si deposition per filaments.

Fluorometric data revealed pH 7.7 acclimated cultures deposited a mean of 25.28 µmol Si total, while pH 9.2 acclimated cultures deposited a significantly lower mean of 15.81 µmol Si total ($p< 0.0001$; unpaired two-tailed t-test $t=8.544$, $df=8$, $n=5$) (Appendix Figure 3.21). Normalization of this data to abundance (final filament concentration) reflected a similar trend. *F. crotonensis* cultures acclimated to pH 7.7 deposited a mean of 1.17 nmol Si/filament, while cultures acclimated to pH 9.2 deposited a significantly lower mean of 0.59 nmol Si/filament ($p< 0.0001$; unpaired two-tailed t-test $t=9.446$, $df=8$, $n=5$) (Figure 3.5). Overall, diatoms acclimated to pH 9.2 deposited ~50% less silica in comparison to their pH 7.7 counterparts.

Silica deposition decreases at alkaline pH in Lake Erie diatom communities

Elevating the pH negatively influenced Si deposition in the Lake Erie diatom community (Figure 3.6). Samples incubated at pH 7.7, control pH (8.6), and pH 9.2 deposited a mean of 219.07 µmol Si total, 214.52 µmol Si total, and 194.36 µmol Si total, respectively (Appendix Figure 3.22). Total Si deposited in pH 9.2 treatments was less than pH 7.7 treatments, though not statistically significant ($p = 0.127$). Normalization of this data to chlorophyll *a* concentration

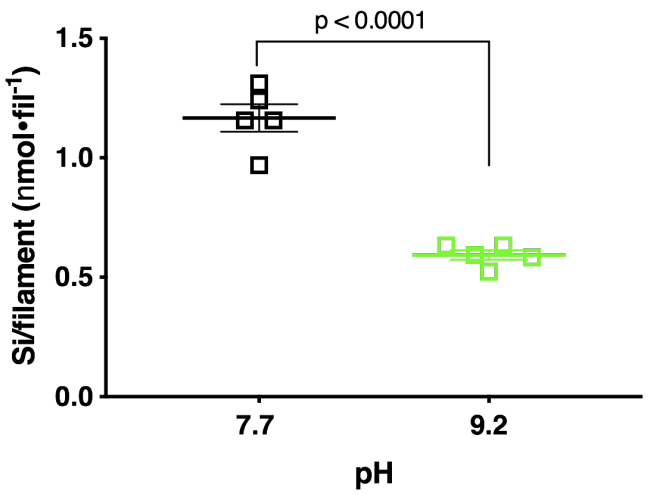


Figure 3.5 Si deposited per filament after 48 h PDMPO incubations in *F. crotonensis* cultures acclimated to pH 7.7 treatments (black squares) and pH 9.2 (green squares). Statistically significant differences are denoted by respective p values generated by unpaired two-tailed t-tests. Standard error of the mean reported by error bars.

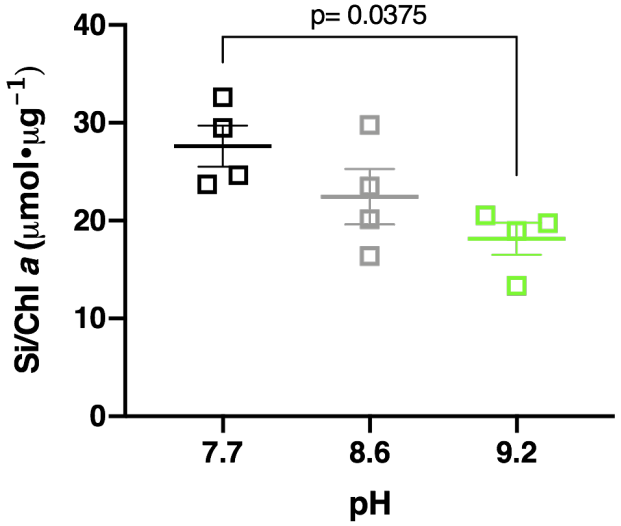


Figure 3.6 Si deposited per chl *a* concentration in pH 7.7 treatments (black squares), control pH 8.6 (grey squares), and pH 9.2 (green squares) after 48 h incubations. Statistically significant differences are denoted by respective p values generated by One-way ANOVAs. Standard error of the mean reported by error bars.

upheld this observation, with pH 7.7 treatments depositing a mean of 27.61 µmol Si/ Chl *a*, control treatments depositing 22.45 µmol Si/Chl *a*, and pH 9.2 treatments depositing 18.16 µmol Si/ Chl *a,* respectively (Figure 3.6). The pH 9.2 treated community deposited significantly less Si per chl *a* concentration after 48 h compared to the pH 7.7 treated community ($p = 0.037$). Overall, Lake Erie diatom communities incubated at pH 9.2 deposited ~1.5 times less Si per chl *a* concentration than their pH 7.7 counterparts.

Discussion

Seasonal succession drivers associated with *Microcystis* blooms are complicated. While it remains clear that nutrient-loading results in the planktonic biomass observed during toxic cyanobacterial blooms, the environmental conditions that allow specific organisms to outcompete others are more nuanced (Wilhelm et al., 2020). Here we build on the idea that pH serves as a contributing piece to this puzzle. Previous analyses have suggested a correlation between pH and diatom-*Microcystis* succession in Lake Taihu, China (Ke et al., 2008) and Lake Erie (Krausfeldt et al., 2019). In these and other cases, authors have suggested that the effects of pH on carbon acquisition and the superior carbon concentrating mechanisms of cyanobacteria were the major mechanistic drivers of these observations. Additionally, previous studies have indicated nutrient speciation at alkaline pH may favor *Microcystis*, such as the discovery that urea serves as both a carbon and nitrogen source to *M. aeruginosa* at alkaline pH levels (Krausfeldt et al., 2019). While the direct and indirect effects of pH on freshwater diatom carbon and nutrient acquisition cannot be discounted or ruled out, our data demonstrated a previously uncharacterized effect of pH on freshwater diatoms, which may serve to depress them beyond, or in addition to, their ability to acquire CO_2. We present this information as a factor that likely enhances the exclusion of Si depositing phytoplankton observed during heated summer

competition. These observations lead to a take-away message from this study: sometimes it is not the ability of *Microcystis* but the inability of its competitors that results in the taxa succession.

Effect of pH on freshwater diatom growth

We used pH manipulation in mono- and co-culture experiments to demonstrate that an elevated pH, consistent with *Microcystis*-bloom conditions, negatively affected the diatom *F. crotonensis*. *F. crotonensis* monocultures inoculated at pH 9.2 exhibited lower growth rates and failed to establish a substantial population, demonstrating alkaline pH alone decreases the viability of this model freshwater diatom. Likewise, when co-cultured with dominant concentrations of *M. aeruginosa* at the 1:10 ratio, these alkaline pH growth effects were exacerbated. This data is consistent with freshwater diatom decline at the alkaline pH levels observed during summer *Microcystis* blooms. Interestingly, when *F. crotonensis* was co-cultured in the 1:10 ratio at pH 7.7, it was able to maintain growth rates resembling those observed in the pH 7.7 monocultures, suggesting alkaline pH may have a larger role in diatom viability than previously thought. Surprisingly, when *F. crotonensis* was co-cultured with *M. aeruginosa* at 10:1 and 1:1 (*i.e.,* where the diatom biomass dominated) it did not exhibit significant declines in growth rate at pH 9.2. *F. crotonensis* cell abundances in the 10:1 and 1:1 co-culture were higher at pH 9.2 than their pH 7.7 counterparts, though statistical significance was lacking. While the underlying mechanisms of these results remain unelucidated, this data suggests that while pH is a factor, it alone is likely not the sole driver of diatom exclusion. Another important observation is that in all *M. aeruginosa* mono and co-cultures inoculated at pH 7.7, pH increases in tandem with *M. aeruginosa* cell concentration. This data demonstrates *M. aeruginosa* is indeed capable of driving the pH up substantially despite increased buffer use, and mimics environmental data

previously observed during a 2015 *Microcystis* bloom. Cumulatively, *in vitro* co-cultures suggest diatoms may be able to persist in the water column during the spring diatom blooms and onset *Microcystis* blooms regardless of water column pH. Yet, during peak *Microcystis* bloom conditions when the pH is driven to alkaline levels, diatoms are at a disadvantage. This data further suggests these persisting alkaline pH levels may prolong the *Microcystis* bloom period by preventing diatom fall resurgence as a result of decreased diatom growth and viability.

Effects of pH on diatom silica deposition

Though previous studies have investigated the effects of pH on marine diatom biosilicification (Vrieling et al., 1999; Martin-Jézéquel et al., 2000; Hansen, 2002), this study builds on these observations through an assessment of pH effects on freshwater diatoms. We used PDMPO assays to demonstrate that pH conditions consistent with *Microcystis* blooms significantly decrease silica deposition in both cultured and environmental freshwater diatoms. When interpreting this data it is important to note, flow cytometry analyses of filamentous microorganisms such as *F. crotonensis* count "filaments per volume" rather than "cells per volume". As a result, an estimate for average number of cells per chain is often used to calculate cells/mL (Bramburger et al., 2017). Our data demonstrate the average number of cells per filament differs significantly in response to culture pH (Appendix Figure 3.20), which has the potential to introduce additional error in estimates of cell/mL and biovolume. Indeed, epifluorescence microscopy revealed pH 9.2-acclimated *F. crotonensis* had ~ 1.5 times shorter filaments and ~2 times fewer silica depositing cells per filament. Fluorometric data from the Si deposition assays revealed a similar trend, with *F. crotonensis* cultures acclimated to pH 9.2 depositing ~50% less silica per filament in comparison to their pH 7.7 counterparts. This trend

was further observed in Lake Erie diatom communities, with communities incubated at pH 9.2 depositing ~1.5 times less Si per chl *a* concentration than their pH 7.7 counterparts. Cumulatively, this data suggests pH-induced decreases in silica deposition may serve as an important contributor to the freshwater diatom decline observed during *Microcystis* blooms. Furthermore, these results also bring to light a need to further optimize detection and normalization techniques in studies concerning filamentous phytoplankton.

While we have demonstrated a decrease in silica deposition at pH 9.2, the underlying mechanisms remain unclear. Part of our limitation comes from the lack of knowledge concerning functions in the organelle responsible for silica deposition, known as the silica deposition vesicle (SDV). Despite decades of research, the SDV has yet to be isolated or characterized (Martin-Jézéquel et al., 2000; Hildebrand et al., 2018). Additionally, intracellular proteins and pathways associated with diatom biosilicification remain elusive (Thamatrakoln and Hildebrand, 2008; Vardi et al., 2009; Otzen, 2012). External alkaline pH may negatively affect intracellular metabolism in the SDV, which relies on acidic conditions and an undisturbed pH gradient (Vrieling et al., 1999; Hervé et al., 2012). Previous studies have also demonstrated high pH levels may shape intra-cellular diatom silica storage pools (Werner, 1966; Azam et al., 1974; Sullivan, 1977; Martin-Jézéquel et al., 2000). Alkaline pH has previously been shown to limit silica deposition by altering the chemical species of silicic acid or decreasing diatom-uptake rates of dissolved silica (dSi) (Riedel and Nelson, 1985; Amo and Brzezinski, 1999). However, this is unlikely in our study due to the non-limiting concentration of silicic acid in our media (176 µM $Na_2SiO_3 \cdot 9H_2O$).

In this study, we observed both a decrease in growth rate and silica deposition in response to alkaline pH. Though evidence of a causal link between these two physiological processes is

lacking in this study, prior research has established that diatom silica uptake and deposition are tightly coupled with the cell cycle, thus exerting a dependency of silica metabolism on the growth rate (Martin-Jézéquel et al., 2000; Hildebrand et al., 2018). Yet, while silica deposition is essential to diatom viability and their ability to reproduce, diatoms can downregulate silica deposition (*i.e.*, form thinner frustules) to maintain optimal growth rates (Brzezinski et al., 1990; McNair et al., 2018). Alternatively, previous research has also demonstrated that as pH increases, growth rates decrease and intracellular silicic acid increases in marine diatoms, potentially indicating a decoupling to silica deposition (Hervé et al., 2012). Hence, pH-associated effects on alternate metabolic processes such as cellular respiration or photosynthesis (*i.e.,* disruptions in normal metabolic regulators) may also contribute to a decline in silica deposition. Furthermore, thinner-frustules have been shown to increase the potential for viral infection and mortality in marine diatoms, exacerbating population declines in the environment (Kranzler et al., 2019). Ultimately, several of these underlying mechanisms may contribute to the decreased silica deposition observed in this study, and further research is needed before any definitive relationship between growth rate, silica deposition, and alkaline pH can be established.

A growing influence of pH in future phytoplankton diversity

Climate change continues to pose a threat to freshwater and marine systems alike. As a result, there is a need to elucidate its effects on factors constraining the ecological success of phytoplankton, such as pH. A recent study has demonstrated ocean acidification has the potential to decrease marine diatom biosilicification rates (Petrou et al., 2019). Conversely, freshwater systems are experiencing a basification attributed to increases in the frequency and duration of HAB events (Wells et al., 2020), which has the potential to decrease freshwater diatom biosilicification. In this manner, the effects of projected pH shifts on phytoplankton succession

serve as a critical point of study for ensuring the integrity of global aquatic systems (Flynn et al., 2015; Wells et al., 2020). Our results build on these previous studies, demonstrating pH may play a pivotal role not only in cyanobacterium-driven diatom decline, but phytoplankton taxa diversity in general. While previous studies have demonstrated alkaline bloom-induced pH can serve as a positive feedback mechanism for *M. aeruginosa* (Krausfeldt et al., 2019), this work builds on these efforts by demonstrating these same conditions can facilitate the exclusion of siliceous algae (diatoms). Furthermore, while Lake Erie summer cyanobacterial blooms drive up the western basin pH to an average of ≥ 9.2, previous winter surveys demonstrate the diatom-dominated water column remains at an average of ~7.8-8.2 despite fluctuations in chlorophyll *a* and sampling location (Appendix Figure 3.23), though additional surveys are needed concerning winter diatom blooms. Cumulatively, this data suggests a role of pH on both the inter and intra-season shifts of phytoplankton taxa within Lake Erie and demonstrate the need to further assess the role of pH in phytoplankton succession.

We noted our pH co-cultures of 10:1 and 1:1 yield higher peak diatom abundance at pH 9.2 in comparison to pH 7.7, despite the diatom monoculture yielding markedly lower abundances at the same elevated pH. In this manner, there may be a window of opportunity for diatoms to persist, and even benefit at low densities of *M. aeruginosa* if the cyanobacterial populations do not become dominant. Many other biological / biogeochemical processes (*e.g.,* inorganic carbon cycling, nitrogen speciation, trace metal chemistry) are pH sensitive and likely play a role in shaping the outcomes of competition for niche space between phototrophs in fresh waters. Our observations serve as a salient reminder that competition in aquatic systems is condition dependent and often complicated by a mix of factors (Wilhelm et al., 2020).

In this study, we confirmed that pH levels of 9.2 decreased diatom growth rate in the filamentous diatom *F. crotonensis.* Our data further demonstrated that silica deposition in lab cultures and environmental diatom communities declined at alkaline pH levels. Cumulatively, these effects reduce diatom viability and fitness in the competition against *Microcystis* blooms. While the pH shift itself may not be sufficient to exclude the diatoms from this (or any) system, the resulting decrease in competitive ability for carbon and nutrients, in addition to pressure from other factors including top-down regulators such as predators and viruses (Kranzler et al., 2019; Pound et al., 2020) appear to tip the scale to favor the cyanobacteria. What remains to be determined beyond this study is how these pressures allow a specific genus of cyanobacteria to proliferate while in competition with many others.

Acknowledgements

We thank Dr. Gary LeCleir, Dr. Matthew Saxton, Dr. Robert McKay, Dr. George Bullerjahn, and Naomi Gilbert for comments and suggestions. We also thank Keara Stanislawczyk for facilitating field work at OSU Stone Lab.

References:

Allinger, L.E., and Reavie, E.D. (2013). The ecological history of Lake Erie as recorded by the phytoplankton community. *Journal of Great Lakes Research* 39**,** 365-382.

Amo, Y.D., and Brzezinski, M.A. (1999). The chemical form of dissolved Si taken up by marine diatoms. *Journal of Phycology* 35**,** 1162-1170.

Anderson, D.M. (2009). Approaches to monitoring, control and management of harmful algal blooms (HABs). *Ocean & Coastal Management* 52**,** 342-347.

Andersson, A., Haecky, P., and Hagström, Å. (1994). Effect of temperature and light on the growth of micro-nano-and pico-plankton: impact on algal succession. *Marine Biology* 120**,** 511-520.

Azam, F., Hemmingsen, B.B., and Volcani, B.E. (1974). Role of silicon in diatom metabolism. *Archives of Microbiology* 97**,** 103-114.

Beutler, M., Wiltshire, K.H., Meyer, B., Moldaenke, C., Lüring, C., Meyerhöfer, M., Hansen, U.-P., and Dau, H. (2002). A fluorometric method for the differentiation of algal populations i*n vivo* and *in situ*. *Photosynthesis Research* 72**,** 39-53.

Bramburger, A.J., Reavie, E.D., Sgro, G., Estepp, L., Chraïbi, V.S., and Pillsbury, R. (2017). Decreases in diatom cell size during the 20th century in the Laurentian Great Lakes: a response to warming waters? *Journal of Plankton Research* 39**,** 199-210.

Brzezinski, M.A., Olson, R.J., and Chisholm, S.W. (1990). Silicon availability and cell-cycle progression in marine diatoms. *Marine Ecology Progress Series***,** 83-96.

Bullerjahn, G.S., Mckay, R.M., Davis, T.W., Baker, D.B., Boyer, G.L., D'anglada, L.V., Doucette, G.J., Ho, J.C., Irwin, E.G., and Kling, C.L. (2016). Global solutions to regional problems: Collecting global expertise to address the problem of harmful cyanobacterial blooms. A Lake Erie case study. *Harmful Algae* 54**,** 223-238.

Chaffin, J.D., Kane, D.D., Stanislawczyk, K., and Parker, E.M. (2018). Accuracy of data buoys for measurement of cyanobacteria, chlorophyll, and turbidity in a large lake (Lake Erie, North America): implications for estimation of cyanobacterial bloom parameters from water quality sonde measurements. *Environmental Science and Pollution Research* 25**,** 25175-25189.

Clement, R., Jensen, E., Prioretti, L., Maberly, S.C., and Gontero, B. (2017). Diversity of CO2-concentrating mechanisms and responses to CO2 concentration in marine and freshwater diatoms. *Journal of Experimental Botany* 68**,** 3925-3935.

Davis, T.W., Stumpf, R., Bullerjahn, G.S., Mckay, R.M.L., Chaffin, J.D., Bridgeman, T.B., and Winslow, C. (2019). Science meets policy: a framework for determining impairment designation criteria for large waterbodies affected by cyanobacterial harmful algal blooms. *Harmful Algae* 81**,** 59-64.

Flynn, K.J., Clark, D.R., Mitra, A., Fabian, H., Hansen, P.J., Glibert, P.M., Wheeler, G.L., Stoecker, D.K., Blackford, J.C., and Brownlee, C. (2015). Ocean acidification with (de) eutrophication will alter future phytoplankton growth and succession. *Proceedings of the Royal Society B: Biological Sciences* 282**,** 20142604.

Guillard, R.R., and Lorenzen, C.J. (1972). Yellow-green algae with chlorophyllide C 1,2 *Journal of Phycology* 8**,** 10-14.

Hansen, P.J. (2002). Effect of high pH on the growth and survival of marine phytoplankton: implications for species succession. *Aquatic Microbial Ecology* 28**,** 279-288.

Hartig, J.H. (1987). Factors contributing to development of *Fragilaria crontonensis* Kitton Pulses in Pigeon Bay waters of western Lake Erie. *Journal of Great Lakes Research* 13**,** 65-77.

Hartig, J.H., and Wallen, D.G. (1986). The influence of light and temperature on growth and photosynthesis of *Fragilaria crotonensis* Kitton. *Journal of Freshwater Ecology* 3**,** 371-382.

Hervé, V., Derr, J., Douady, S., Quinet, M., Moisan, L., and Lopez, P.J. (2012). Multiparametric analyses reveal the pH-dependence of silicon biomineralization in diatoms. *PloS One* 7**,** e46722.

Hildebrand, M., Lerch, S.J., and Shrestha, R.P. (2018). Understanding diatom cell wall silicification—moving forward. *Frontiers in Marine Science* 5**,** 125.

Ke, Z., Xie, P., and Guo, L. (2008). Controlling factors of spring–summer phytoplankton succession in Lake Taihu (Meiliang Bay, China). *Hydrobiologia* 607**,** 41-49.

Kranzler, C.F., Krause, J.W., Brzezinski, M.A., Edwards, B.R., Biggs, W.P., Maniscalco, M., Mccrow, J.P., Van Mooy, B.A., Bidle, K.D., and Allen, A.E. (2019). Silicon limitation facilitates virus infection and mortality of marine diatoms. *Nature Microbiology* 4**,** 1790-1797.

Krausfeldt, L.E., Farmer, A.T., Castro Gonzalez, H., Zepernick, B.N., Campagna, S.R., and Wilhelm, S.W. (2019). Urea is both a carbon and nitrogen source for *Microcystis aeruginosa*: tracking 13C incorporation at bloom pH conditions. *Frontiers in Microbiology* 10**,** 1064.

Leblanc, K., and Hutchins, D.A. (2005). New applications of a biogenic silica deposition fluorophore in the study of oceanic diatoms. *Limnology and Oceanography: Methods* 3**,** 462-476.

Martin-Jézéquel, V., Hildebrand, M., and Brzezinski, M.A. (2000). Silicon metabolism in diatoms: implications for growth. *Journal of Phycology* 36**,** 821-840.

Mcnair, H.M., Brzezinski, M.A., and Krause, J.W. (2018). Diatom populations in an upwelling environment decrease silica content to avoid growth limitation. *Environmental Microbiology* 20**,** 4184-4193.

Michalak, A.M., Anderson, E.J., Beletsky, D., Boland, S., Bosch, N.S., Bridgeman, T.B., Chaffin, J.D., Cho, K., Confesor, R., and Daloğlu, I. (2013). Record-setting algal bloom in Lake Erie caused by agricultural and meteorological trends consistent with expected future conditions. *Proceedings of the National Academy of Sciences* 110**,** 6448-6452.

Otzen, D. (2012). The role of proteins in biosilicification. *Scientifica* 2012.

Paerl, H.W., Scott, J.T., Mccarthy, M.J., Newell, S.E., Gardner, W.S., Havens, K.E., Hoffman, D.K., Wilhelm, S.W., and Wurtsbaugh, W.A. (2016). It takes two to tango: When and where dual nutrient (N & P) reductions are needed to protect lakes and downstream ecosystems. *Environmental Science & Technology* 50**,** 10805-10813.

Peng, G., Martin, R.M., Dearth, S.P., Sun, X., Boyer, G.L., Campagna, S.R., Lin, S., and Wilhelm, S.W. (2018). Seasonally relevant cool temperatures interact with n chemistry to increase microcystins produced in lab cultures of *Microcystis aeruginosa* NIES-843. *Environmental Science & Technology* 52**,** 4127-4136.

Petrou, K., Baker, K.G., Nielsen, D.A., Hancock, A.M., Schulz, K.G., and Davidson, A.T. (2019). Acidification diminishes diatom silica production in the Southern Ocean. *Nature Climate Change* 9**,** 781-786.

Pound, H.L., Gann, E.R., Tang, X., Krausfeldt, L.E., Huff, M., Staton, M., Talmy, D., and Wilhelm, S. (2020). The “neglected viruses” of Taihu: Abundant transcripts for viruses infecting eukaryotes and their potenital role in phytoplankton succession *Frontiers in Microbiology* 11**,** 338.

Raven, J. (1981). "Nutrient transport in microalgae," in *Advances in microbial physiology*. Elsevier), 47-226.

Raven, J.A. (2010). Inorganic carbon acquisition by eukaryotic algae: four current questions. *Photosynthesis research* 106**,** 123-134.

Reavie, E.D., Barbiero, R.P., Allinger, L.E., and Warren, G.J. (2014). Phytoplankton trends in the Great Lakes, 2001–2011. *Journal of Great Lakes Research* 40**,** 618-639.

Reavie, E.D., Cai, M., Twiss, M.R., Carrick, H.J., Davis, T.W., Johengen, T.H., Gossiaux, D., Smith, D.E., Palladino, D., and Burtner, A. (2016). Winter–spring diatom production in Lake Erie is an important driver of summer hypoxia. *Journal of Great Lakes Research* 42**,** 608-618.

Riedel, G.F., and Nelson, D.M. (1985). Silicon uptake by algae with no kown Si requirement. II. Strong pH dependence of uptake kinetic parameters in *Phaeodactylum tricornutum (Bacillariophyceae)* 1. *Journal of Phycology* 21**,** 168-171.

Sandrini, G., Tann, R.P., Schuurmans, J.M., Van Beusekom, S.A., Matthijs, H.C., and Huisman, J. (2016). Diel variation in gene expression of the CO2-concentrating mechanism during a harmful cyanobacterial bloom. *Frontiers in Microbiology* 7**,** 551.

Saxton, M.A., D'souza, N.A., Bourbonniere, R.A., Mckay, R.M.L., and Wilhelm, S.W. (2012). Seasonal Si: C ratios in Lake Erie diatoms—evidence of an active winter diatom community. *Journal of Great Lakes Research* 38**,** 206-211.

Shapiro, J. (1990). Current beliefs regarding dominance by blue-greens: the case for the importance of CO2 and pH. *Internationale Vereinigung für theoretische und angewandte Limnologie: Verhandlungen* 24**,** 38-54.

Shruthi, M., and Rajashekhar, M. (2014). Effect of salinity and pH on the growth and biomass production in the four species of estuarine cyanobacteria. *J. Algal Biomass Utln* 5**,** 29-36.

Steffen, M.M., Belisle, B.S., Watson, S.B., Boyer, G.L., Bourbonniere, R.A., and Wilhelm, S.W. (2015). Metatranscriptomic evidence for co-occurring top-down and bottom-up controls on toxic cyanobacterial communities. *Appl. Environ. Microbiol.* 81**,** 3268-3276.

Steffen, M.M., Belisle, B.S., Watson, S.B., Boyer, G.L., and Wilhelm, S.W. (2014). Status, causes and controls of cyanobacterial blooms in Lake Erie. *Journal of Great Lakes Research* 40**,** 215-225.

Sullivan, C. (1977). Diatom mineralization of silicic acid. II. Regulation of Si (OH) 4 transport rates during the cell cycle of *Navicula pelliculosa* 1. *Journal of Phycology* 13**,** 86-91.

Suttle, C.A., and Fuhrman, J.A. (2010). Aquatic Viral Ecology. *Manual of Aquatic Viral Ecology***,** 145.

Taraldsvik, M., and Myklestad, S. (2000). The effect of pH on growth rate, biochemical composition and extracellular carbohydrate production of the marine diatom Skeletonema costatum. *European Journal of Phycology* 35**,** 189-194.

Thamatrakoln, K., and Hildebrand, M. (2008). Silicon uptake in diatoms revisited: a model for saturable and nonsaturable uptake kinetics and the role of silicon transporters. *Plant Physiology* 146**,** 1397-1407.

Twiss, M., Mckay, R., Bourbonniere, R., Bullerjahn, G., Carrick, H., Smith, R., Winter, J., D'souza, N., Furey, P., and Lashaway, A. (2012). Diatoms abound in ice-covered Lake

Erie: An investigation of offshore winter limnology in Lake Erie over the period 2007 to 2010. *Journal of Great Lakes Research* 38**,** 18-30.
Vanderploeg, H.A., Liebig, J.R., Carmichael, W.W., Agy, M.A., Johengen, T.H., Fahnenstiel, G.L., and Nalepa, T.F. (2001). Zebra mussel (*Dreissena polymorpha*) selective filtration promoted toxic *Microcystis* blooms in Saginaw Bay (Lake Huron) and Lake Erie. *Canadian Journal of Fisheries and Aquatic Sciences* 58**,** 1208-1221.
Vardi, A., Thamatrakoln, K., Bidle, K.D., and Falkowski, P.G. (2009). Diatom genomes come of age. *Genome Biology* 9**,** 245.
Verspagen, J.M., Van De Waal, D.B., Finke, J.F., Visser, P.M., Van Donk, E., and Huisman, J. (2014). Rising CO2 levels will intensify phytoplankton blooms in eutrophic and hypertrophic lakes. *PloS One* 9.
Vrieling, E.G., Gieskes, W., and Beelen, T.P. (1999). Silicon deposition in diatoms: control by the pH inside the silicon deposition vesicle. *Journal of Phycology* 35**,** 548-559.
Watanabe, M., Kawachi, M., Hiroki, M., and Kasai, F. (2000). NIES-Collection List of strains. Microalgae and protozoa. 159 pp. *National Institute for Environmental Studies, Environment Agency, Tsukuba*.
Wells, M.L., Karlson, B., Wulff, A., Kudela, R., Trick, C., Asnaghi, V., Berdalet, E., Cochlan, W., Davidson, K., and De Rijcke, M. (2020). Future HAB science: Directions and challenges in a changing climate. *Harmful algae* 91**,** 101632.
Welschmeyer, N.A. (1994). Fluorometric analysis of chlorophyll a in the presence of chlorophyll b and pheopigments. *Limnology and Oceanography* 39**,** 1985-1992.
Werner, D. (1966). Die kieselsäure im stoffwechsel von Cyclotella cryptica Reimann, Lewin und Guillard. *Archiv für Mikrobiologie* 55**,** 278-308.
Wilhelm, S., Bullerjahn, G., and Rlm, M. (2020). The complicated and confusing ecology of *Microcystis* blooms. *mBio*.
Wilhelm, S.W. (2017). CT media. *protocols.io*.
Wilson, A., Kinney, J.N., Zwart, P.H., Punginelli, C., D'haene, S., Perreau, F., Klein, M.G., Kirilovsky, D., and Kerfeld, C.A. (2010). Structural determinants underlying photoprotection in the photoactive orange carotenoid protein of cyanobacteria. *Journal of Biological Chemistry* 285**,** 18364-18375.
Zepernick, B.N., Krausfeldt, L.E., and Wilhelm, S.W. (2020). Flaming as part of aseptic technique increases CO2(g) and decreases pH in freshwater culture media. *Limnology and Oceanography: Methods*.
Zepernick, B.N., Saxton, M.A., and Wilhelm, S.W. (2019). "Quantifying biogenic silica (bSi) deposition rates adapted method", in: *Protocols.io*).

Appendix

Table 3.1: Statistical analysis of *F. crotonensis* growth rate in pH mono and co-culture assays. Statistical analyses: ordinary two-way ANOVA with Tukey's HSD multiple comparisons test.

Treatment comparison	Summary	P value
pH 7.7 10:1 vs. pH 7.7 1:1	**	0.0098
pH 7.7 10:1 vs. pH 7.7 1:10	ns	0.0815
pH 7.7 10:1 vs. pH 7.7. mc	ns	0.1696
pH 7.7 10:1 vs. pH 9.2 10:1	ns	0.9994
pH 7.7 10:1 vs. pH 9.2 1:1	ns	0.7142
pH 7.7 10:1 vs. pH 9.2 1:10	ns	0.1053
pH 7.7 10:1 vs. pH 9.2 mc	*	0.0378
pH 7.7 1:1 vs. pH 7.7 1:10	ns	0.9450
pH 7.7 1:1 vs. pH 7.7 mc	ns	0.7800
pH 7.7 1:1 vs. pH 9.2 10:1	**	0.0037
pH 7.7 vs. 1:1 vs. pH 9.2 1:1	ns	0.2063
pH 7.7 1:1 vs. pH 9.2 1:10	****	<0.0001
pH 7.7 1:1 vs. pH 9.2 mc	****	<0.0001
pH 7.7 1:10 vs. pH 7.7 mc	ns	0.9998
pH 7.7 1:10 vs. pH 9.2 10:1	*	0.0316
pH 7.7 1:10 vs. pH 9.2 1:1	ns	0.7745
pH 7.7 1:10 vs. pH 9.2 1:10	***	0.0002
pH 7.7 1:10 vs. pH 9.2 mc	****	<0.0001
pH 7.7 mc vs. pH 9.2 10:1	ns	0.0698
pH 7.7 mc vs. pH 9.2 1:1	ns	0.9423
pH 7.7 mc vs. pH 9.2 1:10	***	0.0005
pH 7.7 mc vs. pH 9.2 mc	***	0.0002
pH 9.2 10:1 vs. pH 9.2 1:1	ns	0.4212
pH 9.2 10:1 vs. pH 9.2 1:10	ns	0.2443
pH 9.2 10:1 vs. pH 9.2 mc	ns	0.0965
pH 9.2 1:1 vs. pH 9.2 1:10	**	0.0045
pH 9.2 1:1 vs. pH 9.2 mc	**	0.0015
pH 9.2 1:10 vs. pH 9.2 mc	ns	0.9990

Table 3.2: Statistical analysis of *M. aeruginosa* growth rate in pH mono and co-culture assays. Statistical analyses: ordinary two-way ANOVA with Tukey's HSD multiple comparisons test.

Treatment comparison	Summary	P value
pH 7.7 10:1 vs. pH 7.7 1:1	ns	0.8850
pH 7.7 10:1 vs. pH 7.7 1:10	ns	0.3390
pH 7.7 10:1 vs. pH 7.7 mc	*	0.0175
pH 7.7 10:1 vs. pH 9.2 10:1	ns	0.5031
pH 7.7 10:1 vs. pH 9.2 1:1	ns	0.1299
pH 7.7 10:1 vs. pH 9.2 1:10	ns	0.1243
pH 7.7 10:1 vs. pH 9.2 mc	**	0.0018
pH 7.7 1:1 vs. pH 7.7 1:10	ns	0.9643
pH 7.7 1:1 vs. pH 7.7 mc	ns	0.1893
pH 7.7 1:1 vs. pH 9.2 10:1	ns	0.9954
pH 7.7 1:1 vs. pH 9.2 1:1	ns	0.7273
pH 7.7 1:1 vs. pH 9.2 1:10	ns	0.7129
pH 7.7 1:1 vs. pH 9.2 mc	*	0.0231
pH 7.7 1:10 vs. pH 7.7 mc	ns	0.6945
pH 7.7 1:10 vs. pH 9.2 10:1	ns	>0.9999
pH 7.7 1:10 vs. pH 9.2 1:1	ns	0.9982
pH 7.7 1:10 vs. pH 9.2 1:10	ns	0.9977
pH 7.7 1:10 vs. pH 9.2 mc	ns	0.1504
pH 7.7 mc vs. pH 9.2 10:1	ns	0.5118
pH 7.7 mc vs. pH 9.2 1:1	ns	0.9527
pH 7.7 mc vs. pH 9.2 1:10	ns	0.9581
pH 7.7 mc vs. pH 9.2 mc	ns	0.9325
pH 9.2 10:1 vs. pH 9.2 1:1	ns	0.9794
pH 9.2 10:1 vs. pH 9.2 1:10	ns	0.9761
pH 9.2 10:1 vs. pH 9.2 mc	ns	0.0876
pH 9.2 1:1 vs. pH 9.2 1:10	ns	>0.9999
pH 9.2 1:1 vs. pH 9.2 mc	ns	0.3813
pH 9.2 1:10 vs. pH 9.2 mc	ns	0.3943

Table 3.3: Statistical analysis of *in vitro F. crotonensis* Si deposition assay. **(A)** Comparison of *F. crotonensis* cell concentration as a function of pH. Statistical analyses performed using unpaired two-tailed t-test (t=6.705, df=8, n=5). **(B)** Comparison of total Si deposited as a function of pH. Statistical analyses performed using unpaired two-tailed t-test (t=8.544, df=8, n=5). **(C)** Comparison of Si deposited per filament as a function of pH. Statistical analyses performed using unpaired two-tailed t-test (t=9.446, df=8, n=5). **(D)** Comparison of epifluorescence microscopy *F. crotonensis* cell number per filament and % of cells fluorescing PDMPO per filament as a function of pH. Statistical analyses performed using unpaired two-tailed t-test: #cells/filament: (t=4.057, df=197, n=100), %PDMPO cells/filament: (t=9.457, df=197, n=100).

Treatment comparison	Significance?	Summary	P value
pH 7.7 1:10 vs. pH 7.7 1:1	No	ns	0.9996
pH 7.7 1:10 vs. pH 7.7 10:1	No	ns	0.1853
pH 7.7 1:10 vs. pH 7.7. 0:1	Yes	*	0.0300
pH 7.7 1:10 vs. pH 9.2 1:10	No	ns	0.6941
pH 7.7 1:10 vs. pH 9.2 1:1	Yes	*	0.0160
pH 7.7 1:10 vs. pH 9.2 10:1	Yes	****	<0.0001
pH 7.7 1:10 vs. pH 9.2 0:1	No	ns	0.0819
pH 7.7 1:1 vs. pH 7.7 10:1	No	ns	0.3801
pH 7.7 1:1 vs. pH 7.7 0:1	Yes	*	0.0118
pH 7.7 1:1 vs. pH 9.2 1:10	No	ns	0.4156
pH 7.7 vs. 1:1 vs. pH 9.2 1:1	Yes	**	0.0063
pH 7.7 1:1 vs. pH 9.2 10:1	Yes	****	<0.0001
pH 7.7 1:1 vs. pH 9.2 0:1	No	ns	0.1881
pH 7.7 10:1 vs. pH 7.7 0:1	Yes	***	0.0002
pH 7.7 10:1 vs. pH 9.2 1:10	Yes	**	0.0080
pH 7.7 10:1 vs. pH 9.2 1:1	Yes	****	<0.0001
pH 7.7 10:1 vs. pH 9.2 10:1	Yes	**	0.0012
pH 7.7 10:1 vs. pH 9.2 0:1	No	ns	0.9996
pH 7.7 0:1 vs. pH 9.2 1:10	No	ns	0.4860
pH 7.7 0:1 vs. pH 9.2 1:1	No	ns	>0.9999
pH 7.7 0:1 vs. pH 9.2 10:1	Yes	****	<0.0001
pH 7.7 0:1 vs. pH 9.2 0:1	Yes	****	<0.0001
pH 9.2 1:10 vs. pH 9.2 1:1	No	ns	0.3180
pH 9.2 1:10 vs. pH 9.2 10:1	Yes	****	<0.0001
pH 9.2 1:10 vs. pH 9.2 0:1	Yes	**	0.0032
pH 9.2 1:1 vs. pH 9.2 10:1	Yes	****	<0.0001
pH 9.2 1:1 vs. pH 9.2 0:1	Yes	****	<0.0001
pH 9.2 10:1 vs. pH 9.2 0:1	Yes	**	0.0030

Table 3.4: Statistical analysis of *in situ* Lake Erie Si deposition assay**. (A)** Comparison of community chlorophyll *a* concentration as a function of pH. Statistical analyses performed using ordinary one-way ANOVA with Tukey's multiple comparisons test. **(B)** Comparison of total Si deposited as a function of pH. Statistical analyses performed using ordinary one-way ANOVA with Tukey's multiple comparisons test. **(C)** Comparison of Si deposited per chlorophyll *a* concentration as a function of pH. Statistical analyses performed using ordinary one-way ANOVA with Tukey's multiple comparisons test.

A.) Treatment comparison	**Summary**	**P value**
control 48 hr vs. pH 7.7 48 hr chlorophyll *a*	ns	0.7187
pH 7.7 48 hr vs. pH 9.2 48hr chlorophyll *a*	ns	0.4464
pH 9.2 48 hr vs. control 48hr chlorophyll *a*	ns	0.9614

B.) Treatment comparison	**Summary**	**P value**
Lake Erie diatom control vs. pH 7.7 Net Si	ns	0.916
Lake Erie diatom pH 7.7 vs. pH 9.2 Net Si	ns	0.127
Lake Erie diatom pH 9.2 vs. control Net Si	ns	0.229

C.) Treatment comparison	**Summary**	**P value**
Lake Erie diatom control vs. pH 7.7 Si/chl *a*	ns	0.285
Lake Erie diatom pH 7.7 vs. pH 9.2 Si/chl *a*	*	0.037
Lake Erie diatom 9.2 vs. control Si/chl *a*	ns	0.404

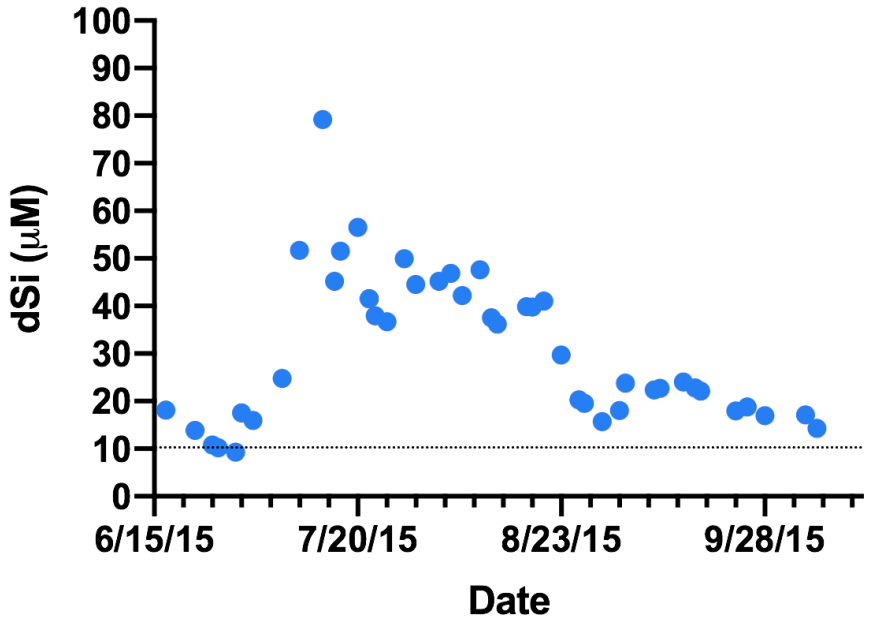


Figure 3.7 Dissolved silica profiles corresponding to a 2015 Lake Erie *M. aeruginosa* bloom in the western basin. Silica-limiting concentrations (defined in this study as 10μM) are indicated by the dotted black line. Complete details of this dataset can be found in (Chaffin et al., 2018).

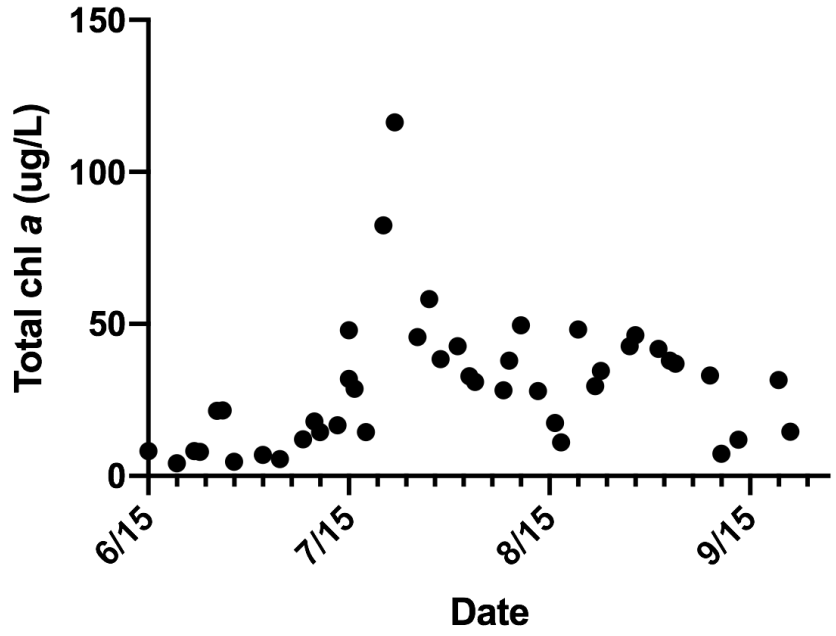


Figure 3.8 Total chlorophyll *a* concentration corresponding to a 2015 Lake Erie *M. aeruginosa* bloom in the western basin. Complete details of this dataset can be found in (Chaffin et al., 2018).

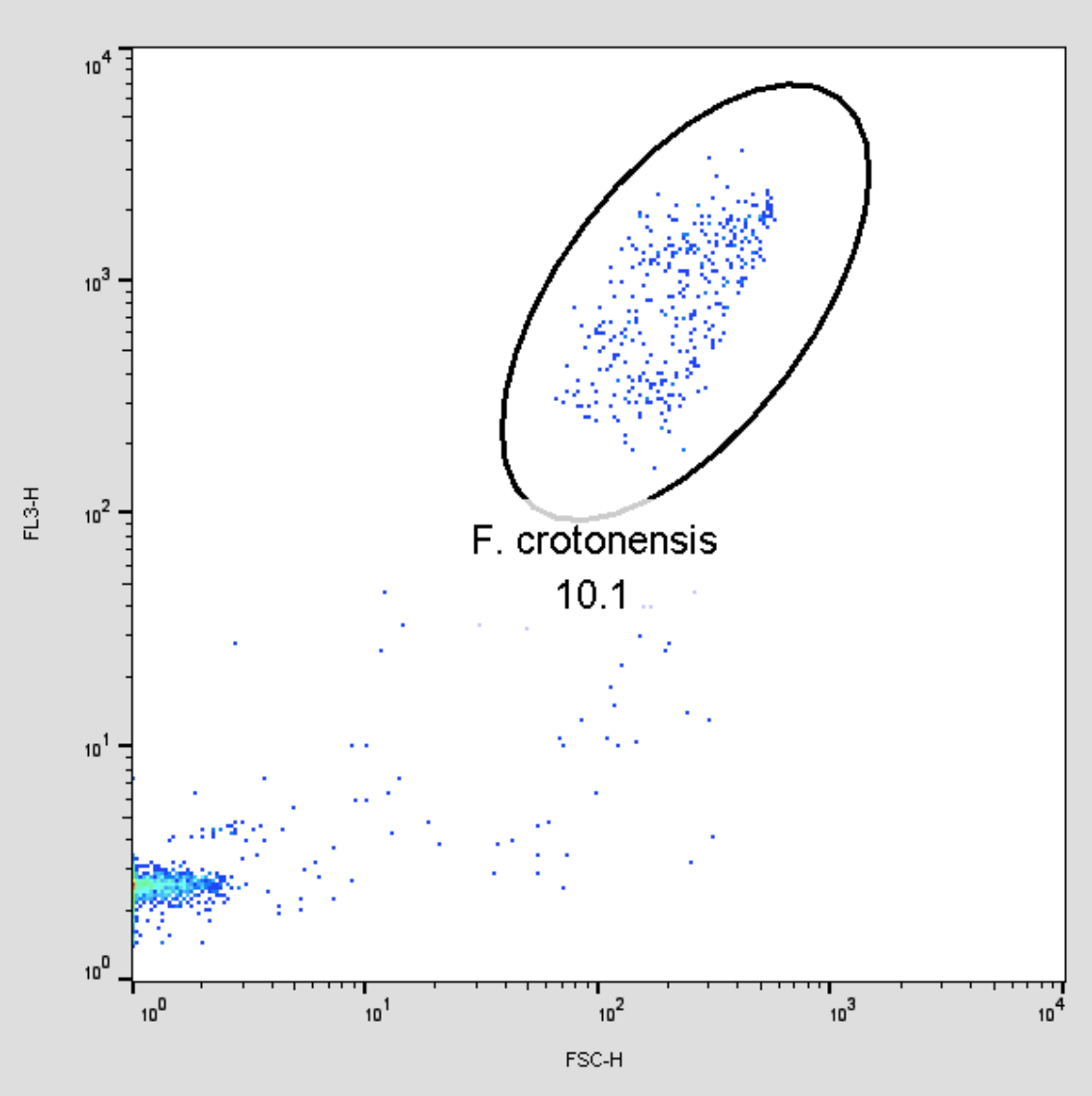


Figure 3.9 FlowJo graph depicting a gated population of *F. crotonensis* filaments run on the flow cytometer. Sample analyzed was a pH 7.7 *F. crotonensis* monoculture culture from 20-d. Background noise visible in lower graph quadrant results from CT media.

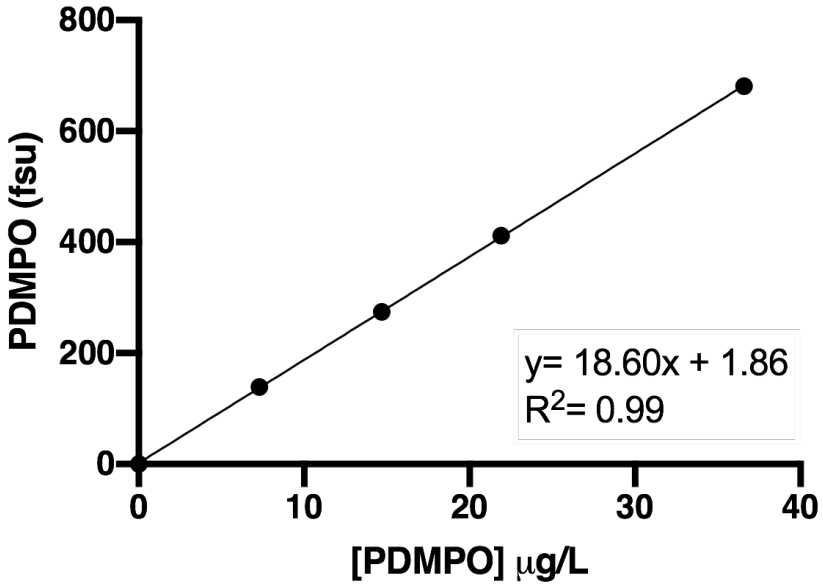


Figure 3.10 Standard curve for *in vitro F. crotonensis* Si deposition assay used to obtain silica deposited per cell reported in Figure 5. Simple linear regression (R^2=0.9999, F=53417, $p<0.0001$, n=5).

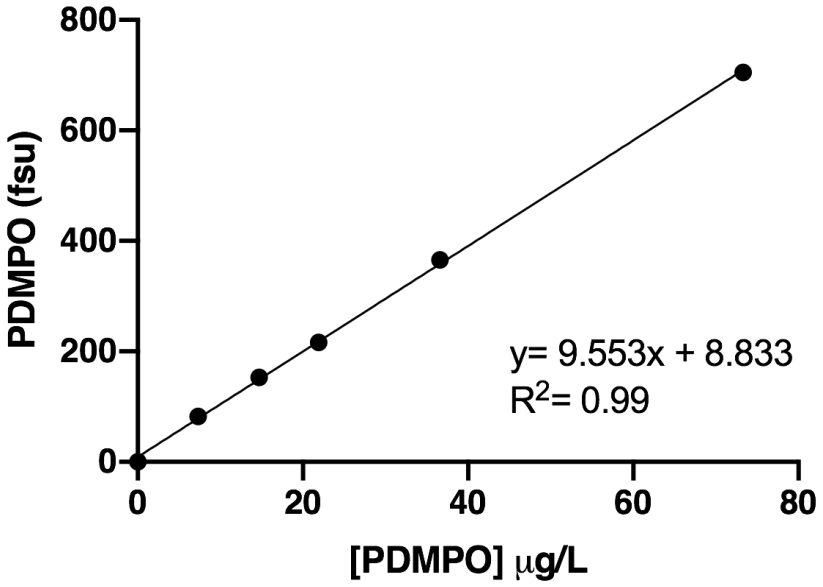


Figure 3.11 Standard curve for *in situ* Lake Erie Si deposition assay used to obtain silica deposited per chlorophyll *a* concentration reported in Figure 6. Simple linear regression (R^2=0.9995, F=7368, p<0.0001, n=6).

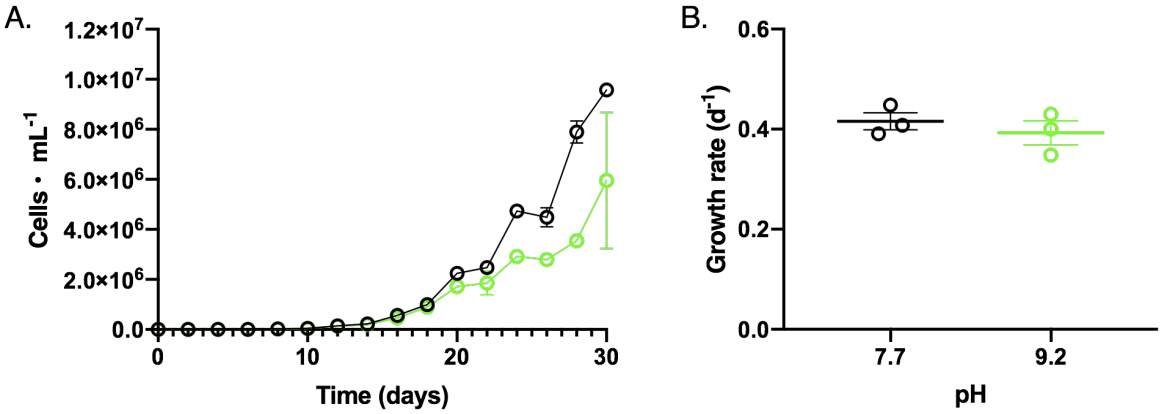


Figure 3.12 (A) *In vitro M. aeruginosa* monoculture growth curves at pH 7.7 (black circles) and pH 9.2 (green circles). (B) *M. aeruginosa* growth rate at pH 7.7 (black circles) and pH 9.2 (green circles). Statistically significant differences between pH treatments are denoted by p values generated by Two-way ANOVAs. Standard error of the mean reported by error bars.

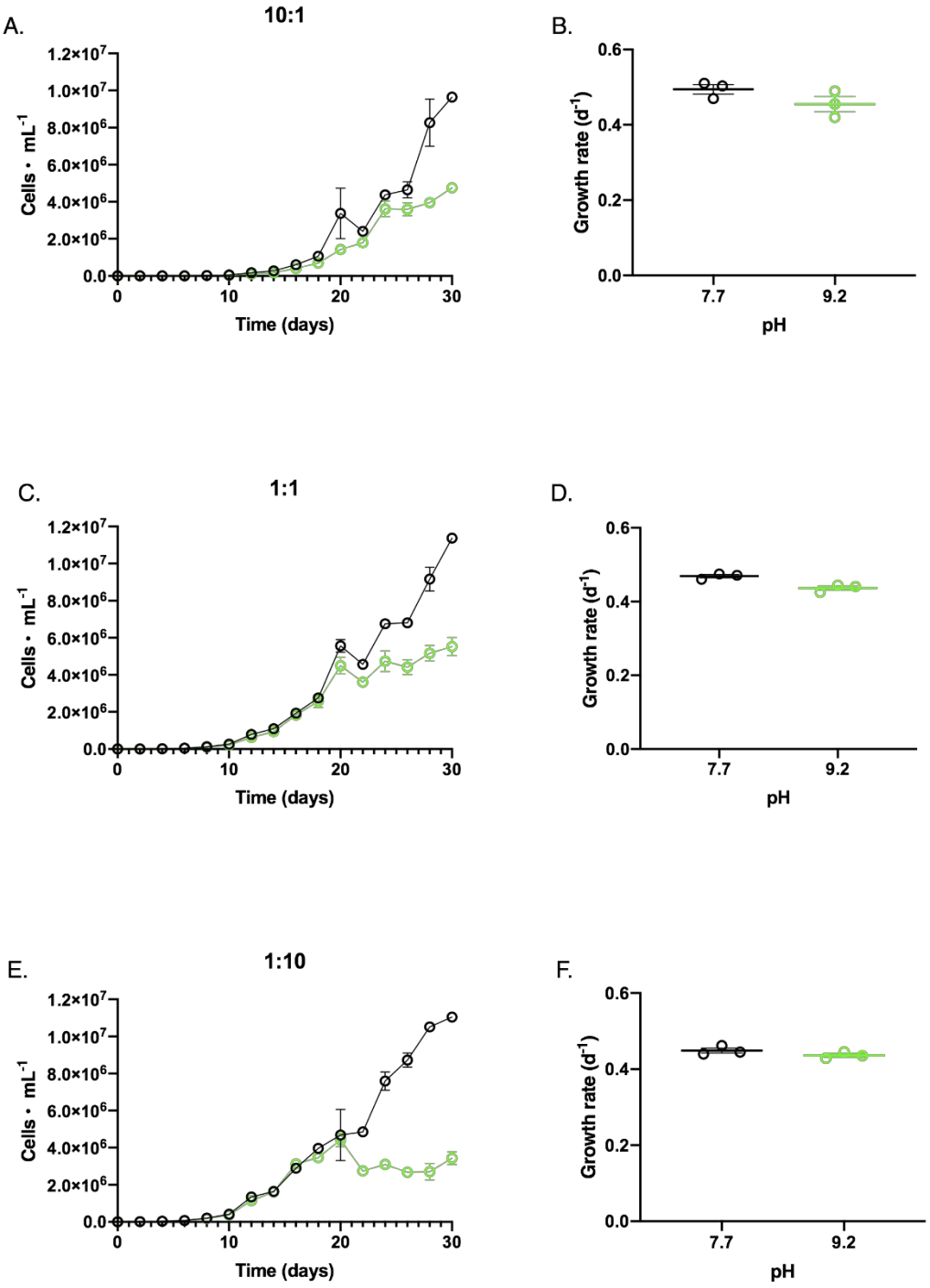


Figure 3.13 (A) *In vitro M. aeruginosa* growth curves in a 10:1 ratio *(F. crotonensis:M. aeruginosa)* at pH 7.7 (black circles) and pH 9.2 (green circles). (B) *M. aeruginosa* growth rate in a 10:1 ratio (C) *M. aeruginosa* growth curves in a 1:1 ratio (D) *M. aeruginosa* growth rate in a 1:1 ratio (E) *M. aeruginosa* growth curves in a 1:10 ratio (F) *M. aeruginosa* growth rate in a 1:10 ratio. Statistically significant differences between pH treatments are denoted by p values generated by Two-way ANOVAs. Standard error of the mean reported by error bars.

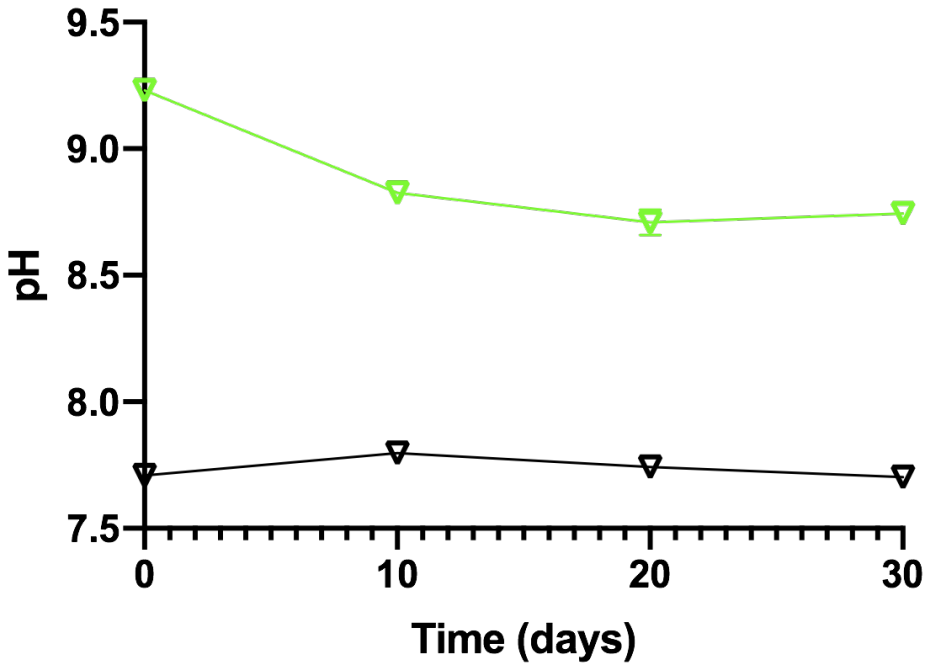


Figure 3.14 pH drift in F. *crotonensis* monocultures inoculated at pH 7.7 (black inverted triangles) and pH 9.2 (green inverted triangles). Standard error of the mean reported by error bars.

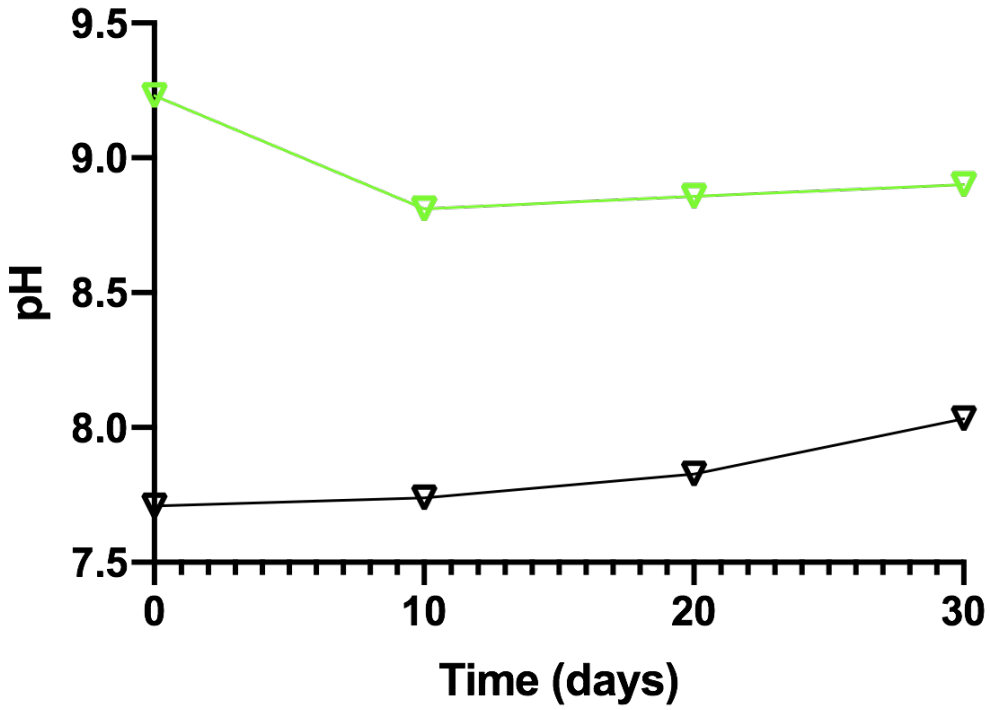


Figure 3.15 pH drift from initial pH in *M. aeruginosa* monocultures inoculated at pH 7.7 (black inverted triangles) and pH 9.2 (green inverted triangles). Standard error of the mean reported by error bars.

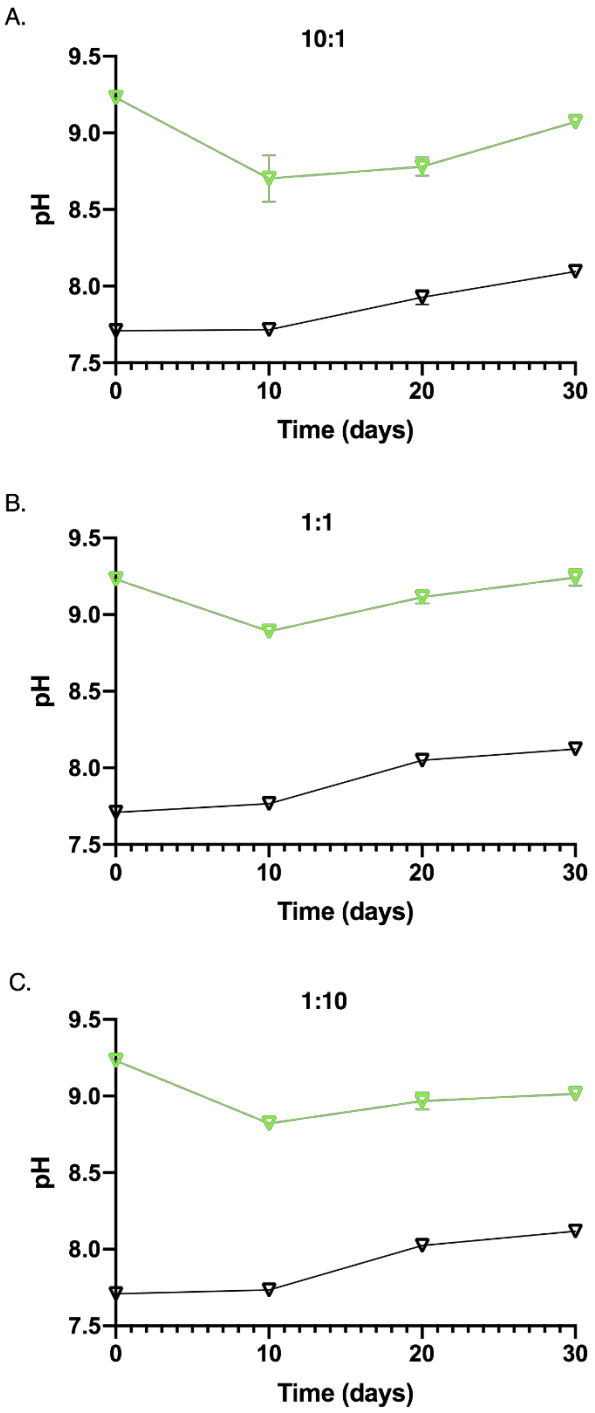


Figure 3.16 pH drift from initial pH in co-cultures inoculated at pH 7.7 (black inverted triangles) and pH 9.2 (green inverted triangles). Standard error of the mean reported by error bars.

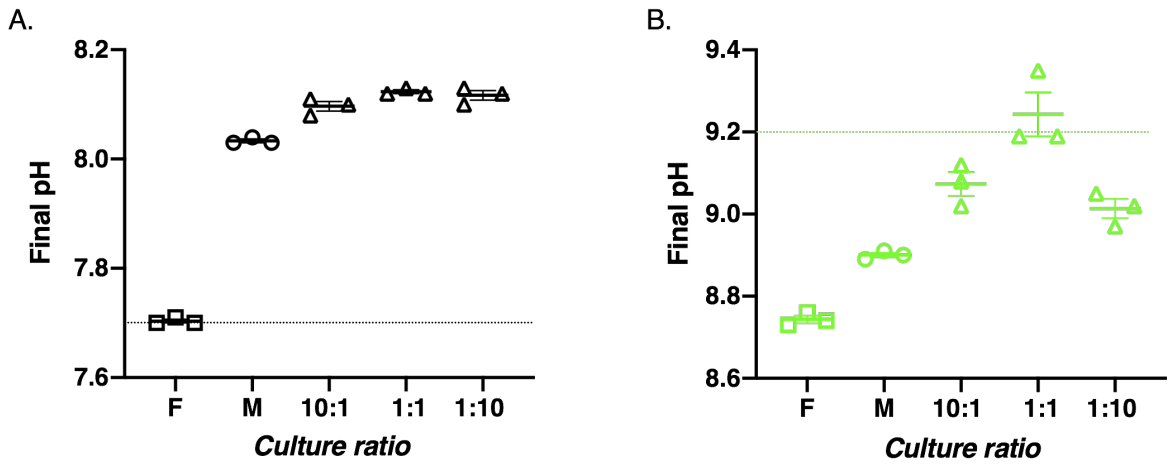


Figure 3.17 Final pH of all mono and co-cultures after 30-d. (A) Final pH of pH 7.7. treatment cultures (black) of *F. crotonensis* monocultures (squares), *M. aeruginosa* monocultures (circles) and co-cultures (triangles). (B) Final pH of pH 9.2 treatment cultures (green) of *F. crotonensis* monocultures (squares), *M. aeruginosa* monocultures (circles) and co-cultures (triangles). Initial pH levels at 0-d are indicated by dotted lines. Standard error of the mean reported by error bars.

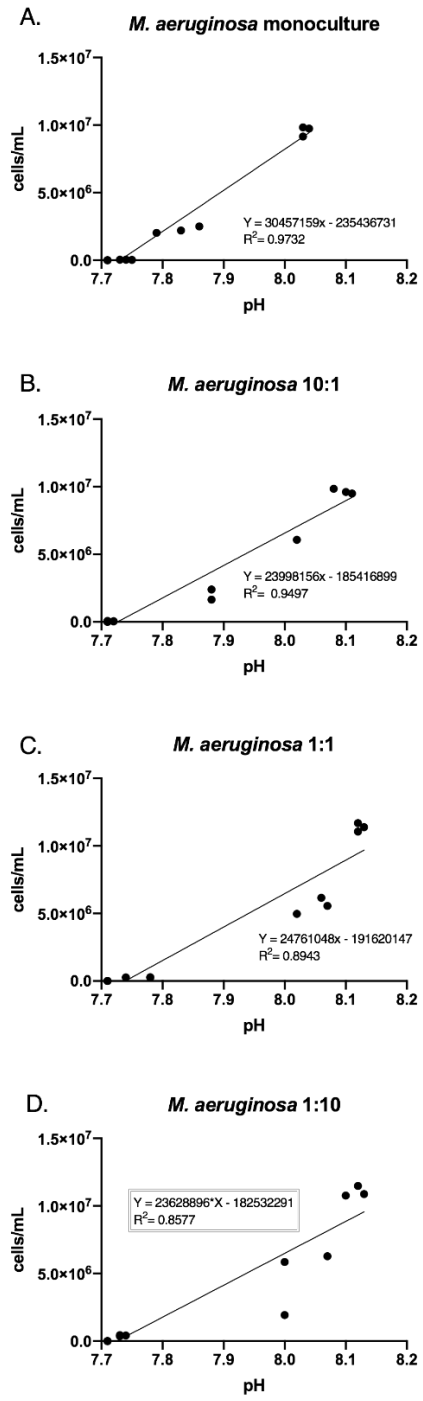


Figure 3.18 Simple linear regressions of *M. aeruginosa* concentration and pH drift of mono (A) and co-cultures (B, C, D) inoculated at pH 7.7. Cell concentrations and pH levels were sampled at 0, 10, 20, and 30 d. (A) Simple linear regression: R^2=0.9732, F=363.4,p<0.0001, n=12, (B) Simple linear regression: R^2=0.9497, F=188.9,p<0.0001,n=12, (C) Simple linear regression: R^2=0.8943, F=84.60, p<0.0001, n=12, (D) Simple linear regression: R^2=0.8577, F=60.29, p<0.0001, n=12).

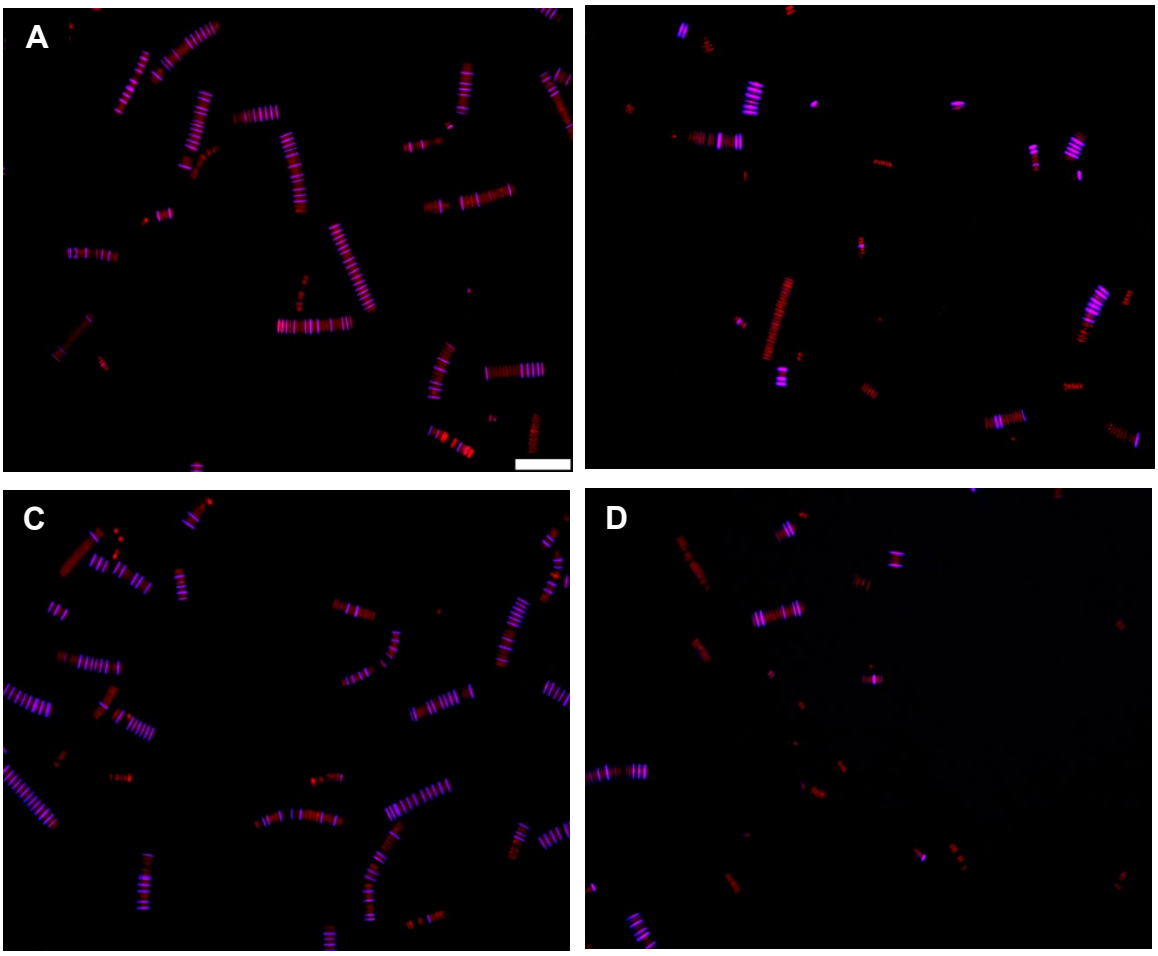


Figure 3.19 Epifluorescent microscopy images (10x magnification) of *in vitro F. crotonensis* filaments after 48 h PDMPO incubations. Scale bar represents 75 μm (depicted in panel A). Chlorophyll *a* autofluorescence is depicted in red, and PDMPO fluorescence is indicated in blue. (A, C) *F. crotonensis* chains acclimated to pH 7.7. (B, D) *F. crotonensis* filaments acclimated pH 9. 2.

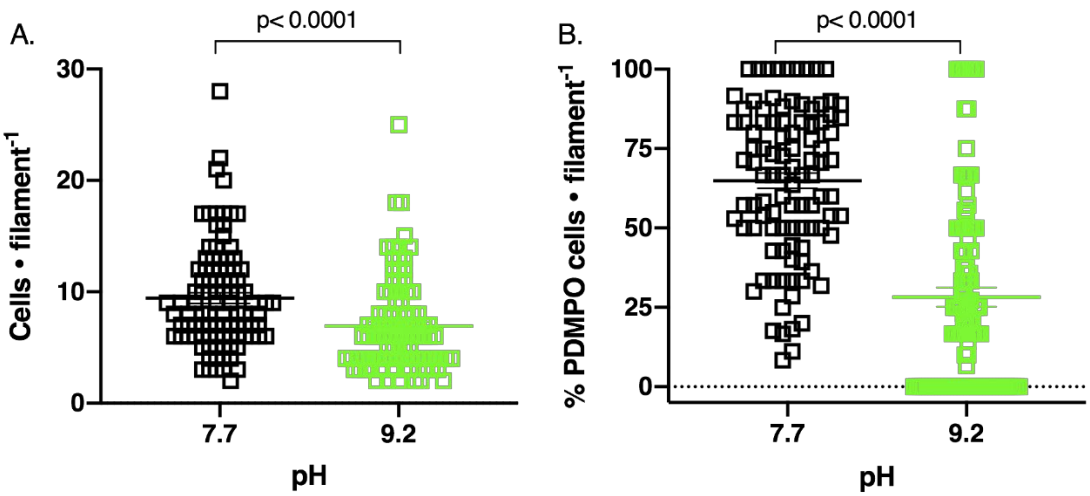


Figure 3.20 Epifluorescent microscopy data of *F. crotonensis* Si deposition assay after 48 h PDMPO incubations. **(A)** Number of cells per filament in pH 7.7 acclimated (black squares) and pH 9.2 acclimated (green squares) *F. crotonensis* cultures. **(B)** Percentage of cells fluorescing PDMPO per filament in pH 7.7 acclimated (black squares) and pH 9.2 acclimated (green squares) *F. crotonensis* cultures. Statistically significant differences are denoted by respective p values generated by unpaired two-tailed t-tests. Standard error of the mean reported by error bars.

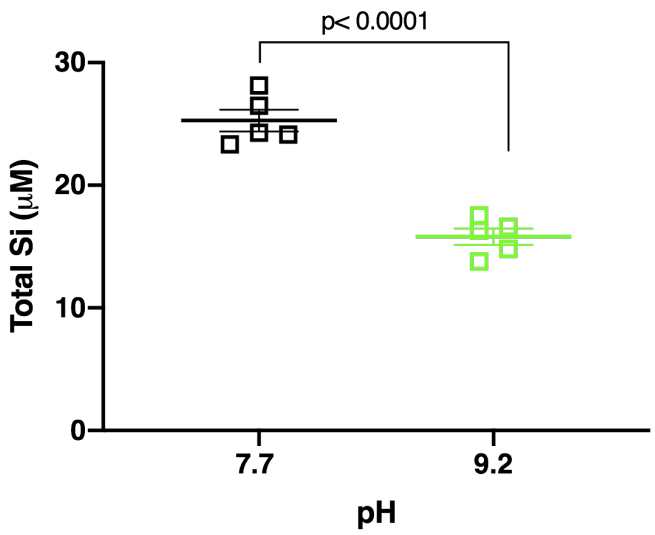


Figure 3.21 Total silica deposited per *F. crotonensis* culture after 48 h PDMPO incubations in pH 7.7 (black squares) and pH 9.2 (green squares) acclimated cultures. Data corresponds to *in vitro F. crotonensis* Si deposition assay. Statistically significant differences are denoted by respective p values generated by unpaired two-tailed t-tests. Standard error of the mean reported by error bars.

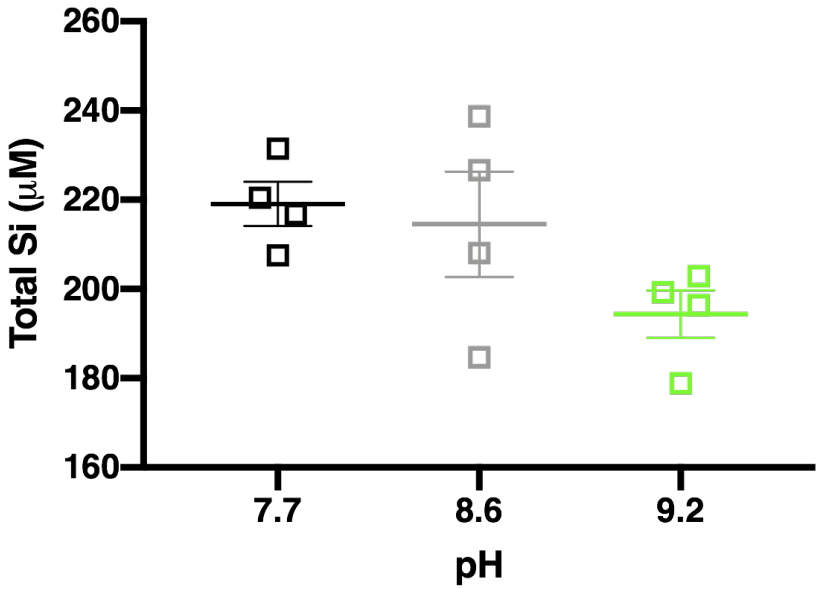


Figure 3.22 Total silica deposited per sample after 48 h PDMPO incubations in pH 7.7 (black squares), pH 8.6 (grey squares) and pH 9.2 (green squares) treatments. Data corresponds to *in situ* Lake Erie Si deposition assay. Statistically significant differences are denoted by respective p values generated by One-way ANOVAs. Standard error of the mean reported by error bars.

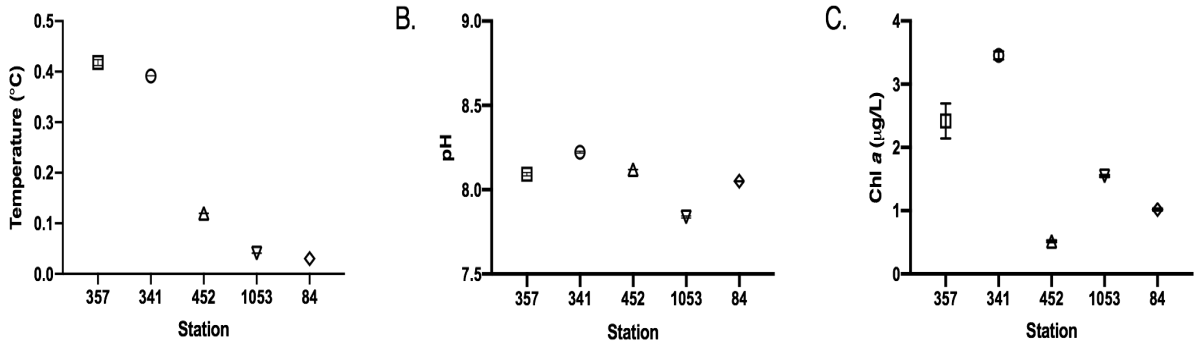


Figure 3.23: Water column profiles collected during a 2-day period (February 17-19) of a 2009 winter cruise in the western-central basins of Lake Erie. Sampling stations correspond to the following: Station 357, 341, 452 (western basin), station 1053, 84 (central basin). (A) Mean temperature per station. (B) Mean pH per station. (C) Mean chlorophyll *a* concentration per station. Standard error of the mean reported by error bars.

CHAPTER IV: INVESTIGATING ELEVATED PH EFFECTS ON FRESHWATER DIATOM TRANSCRIPTION, MORPHOLOGY AND PHYSIOLOGY

Publication Note

This chapter is a version of a peer-reviewed, published article in *Frontiers in Microbiology* 13(2022) by Brittany N. Zepernick, David J. Niknejad, Gwendolyn F. Stark, Alexander R. Truchon, Robbie M. Martin, Karen L. Rossignol, Hans W. Paerl, and Steven W. Wilhelm.

All culture work, pH assays, and sample collection performed by BZ and DN. FlowCAM analyses performed by BZ, DN. PhytoPAM measurements performed by GS. Photopigment extraction and HPLC analysis performed by KR, HP. RNA extractions and QC performed by BZ. Transcriptome analyses performed by BZ, AT, RM. PRIMER analyses performed by BZ.

Abstract

Harmful algal blooms (HABs) caused by the toxin-producing cyanobacteria *Microcystis* spp., can increase water column pH. While the effect(s) of these basified conditions on the bloom formers are of a high research priority, how these pH shifts affect other biota remains understudied. Recently, it was shown these high pH levels decrease growth and Si deposition rates in the freshwater diatom *Fragilaria crotonensis* and natural Lake Erie diatom populations. However, the physiological mechanisms and transcriptional responses of diatoms associated with these observations remain to be documented. Here, we examined *F. crotonensis* with a set of morphological, physiological, and transcriptomic tools to identify cellular responses to high pH. We suggest 2 potential mechanisms that may contribute to morphological and physiological pH effects observed in *F. crotonensis*. Moreover, we identified a significant upregulation of mobile genetic elements in the *F. crotonensis* genome which appears to be an extreme transcriptional response to this abiotic stress to enhance cellular evolution rates– a process we have termed "*genomic roulette*". We discuss the biological and biogeochemical effects high pH conditions impose on fresh waters and suggest a means by which freshwater diatoms such as *F. crotonensis* may evade high pH stress to survive in a "basified" future.

Introduction

Algal blooms are a symptom of an imbalanced ecosystem (Heisler et al., 2008; Watson et al., 2015), where both the biotic and abiotic characteristics of a lake's water column are altered (Anderson, 2009; Gobler and Sunda, 2012). In the case of freshwater *Microcystis* spp.-dominated harmful algal blooms (HABs), nutrient drawdown, oxygen depletion and increased light attenuation are well-documented consequences (Paerl et al., 2001; Verspagen et al., 2004; Lehman et al., 2013; Zepernick et al., 2022d). The effects of *Microcystis* blooms on water column pH serve as a recent addition to this growing list of consequences (Van Dam et al., 2018; Krausfeldt et al., 2019; Turner et al., 2021; Zepernick et al., 2021), raising the question how elevated pH levels associated with blooms influence other biota. Research has demonstrated *Microcystis* spp. blooms can increase lake pH to well above 9.0 via the photosynthetic depletion of CO_2 (Verspagen et al., 2014; Ji et al., 2020), a phenomenon recently termed "lake basification" (Zagarese et al., 2021; Zepernick et al., 2021). Basification events have been recorded in fresh waters including Lake Taihu, China and Lake Erie, U.S./Canada (Su et al., 2015; Wilhelm et al., 2020). In Lake Erie, the mean daily water column pH remained ≥ 9.2 for ~30 days during a record-breaking 2015 *Microcystis* spp. bloom (Zepernick et al., 2021). Further, these pH spikes oscillated on a diel cycle, with the highest pH levels (as much as 0.5 units above ambient) coinciding with peak photosynthetic periods in the late afternoon (Krausfeldt et al., 2019). While an increase in pH may benefit *Microcystis* spp. (Sandrini et al., 2016; Krausfeldt et al., 2019) and function as a positive feedback loop for late-stage bloom maintenance (Tang et al., 2018), it serves as a potential detriment to other organisms.

A recent study suggested elevated pH conditions have the potential to negatively affect algal communities beyond pH-induced carbon limitation (Zagarese et al., 2021). In a previous investigation, we demonstrated that the freshwater diatom *Fragilaria crotonensis*, which

historically bloomed during the summer in Lake Erie (Hartig, 1987), exhibited lower growth rates and silica (Si) deposition rates at pH 9.2 in both monoculture and co-culture with *M. aeruginosa* (Zepernick et al., 2021). That study identified factors which likely contributed to observed declines of diatom populations during HAB events, yet there remains a need for a comprehensive assessment of how these high pH conditions influence freshwater diatom morphology and physiology beyond growth and Si deposition rates.

In the present study, we used transcriptomics to generate hypotheses concerning the physiological response and mechanistic changes behind high-pH-induced effects in this freshwater diatom. We then performed morphological and physiological measurements to validate observed transcriptomic responses and quantitatively assess the effects of elevated pH conditions on *F. crotonensis.*

Methods

Culture conditions

To investigate the morphological and physiological effects high pH may impose on freshwater diatoms, non-axenic monocultures of *F. crotonensis* SAG 28.96 were acclimated for 6 d to either their optimal growth pH of 7.7 (Hervé et al., 2012) or the simulated Lake Erie *Microcystis* bloom-induced basification pH of 9.2 (Krausfeldt et al., 2019), as described previously (Zepernick et al., 2021). After a 6 d acclimation, samples were filter-concentrated and inoculated (T initial - T_i) into their respective pH treatments for the pH assay. All pH assays were inoculated at ~1,500 filaments mL^{-1} in this study except for the photopigment assay, as this method required higher biomass. These samples were incubated for an additional 2 d at conditions consistent with the Lake Erie summer water column (26° C; light intensity ~55-60 µmol photons m^{-2} s^{-1} on a 12:12 h light dark cycle) prior to sample collection on day 8 of pH

exposure (T final - T_f). In this study, the treatment pH of 9.2 will be referred to as "high pH" while the control treatment pH of 7.7 will be referred to as "low pH".

pH effects on F. crotonensis transcription

To assess how transcriptional activity was affected at high pH and generate preliminary hypotheses based on transcriptional findings, *F. crotonensis* cultures were inoculated at ~1,500 filaments mL^{-1} into the respective pH treatments (n = 3). At T_f, each replicate was collected on a 2.0-μm nominal pore-size 47-mm diameter polycarbonate filter to concentrate diatom biomass. Samples were flash frozen in liquid nitrogen and stored at -80° C until extraction. RNA extractions were performed using acid phenol-chloroform methods with ethanol precipitation (Martin and Wilhelm, 2020). Residual DNA in samples was digested using a modified version of the Turbo DNase protocol and the Turbo DNA-free kit (Ambion). Removal of genomic DNA was confirmed *via* the absence of an amplicon band in an agarose gel after 30 cycles of PCR amplification using 519F/785R 16s rRNA primers as reported previously (Zepernick et al., 2022a). Final RNA concentrations were determined using the HS Qubit RNA assay (Invitrogen). Sample library prep (Poly-A selection) and Illumina NovaSeq 6000 platform sequencing (~25 million reads, 100bp, paired end) were performed at Hudson Alpha (Discovery Life Sciences). Sequencing data was interleaved, filtered, and trimmed using CLC Genomics Workbench default settings (v.20) (Qiagen Digital Insights). The quality of trimmed reads was confirmed using FastQC (v.0.11.9) (Babraham Institute). BBMap.sh (default settings) was used to remove residual rRNA reads and BBMap.repair (default settings) was used to validate paired-end reads. (Bushnell, 2014a). Sorted reads were mapped to the annotated *F. crotonensis* reference genome (Zepernick et al., 2022c) in CLC (default settings: length fraction: 0.5,

similarity fraction 0.8) (Appendix Attachment 4.1a), and normalized to transcripts per million (TPM). To calculate similarity (Bray-Curtis) and identify contributors to gene-expression differences between samples, non-metric multi-dimensional scaling (nMDS) and Similarity Percentage (SIMPER) analyses were performed on normalized expression values (TPM) using PRIMER (v.7) (Clarke and Gorley, 2015). Differential Expression (DE) analyses were performed in CLC, and the results were stringently filtered by significance (FDR-corrected p-value ≤ 0.05, $\log_2$ |fold-change| > 2), with predicted genes of hypothetical or unknown functions omitted from downstream analyses. Heat maps were constructed *via* heatmapper.ca (Clustering method: Average linkage, Distance measurement method: Pearson) (Babicki et al., 2016) using standardized expression scores in which genes were grouped using gene descriptions based on EggNOG and COG categories pre-assigned by the EggNOG annotation database (Huerta-Cepas et al., 2019). Manual categorization of genes was further performed based on KEGG Mapper and the KEGG Orthology (KO) database (Kanehisa et al., 2016).

pH effects on F. crotonensis morphology

To directly test the morphological effects of high pH hinted at within our transcriptomes, *F. crotonensis* cultures were inoculated at ~1,500 filaments mL^{-1} into their respective pH treatments (n = 5). At T_f, filament morphology was assessed with a FlowCAM 8000 imaging system using the 10x objective with a particle per used image < 1.7 (PPUI) (FlowCAM 8000, Fluid Imaging Technologies, Yokogawa Electric Corporation). Briefly, ~1,000 *F. crotonensis* filaments per biological replicate were individually analyzed using the automated functions of the instrument with the following parameters measured: area (μm^2), biovolume (μm^3), length (μm), width (μm), roughness, and average green content.

pH effects on F. crotonensis photopigment composition

To test for photopigment changes hypothesized from the transcriptome, *F. crotonensis* cultures were inoculated at ~20,000 filaments mL^{-1} into their respective pH treatments (n = 5). At T_f, measurements were made for total filaments mL^{-1} by flow cytometry (Beckman Coulter CytoFLEX S, equipped with the blue laser (488nm, 50 mW), and red laser (638 nm, 50 mW) with populations gated on PerCP and FSC-H. Chlorophyll *a* (Chl *a*) autofluorescence was measured using a Turner Designs TD-700 fluorometer, equipped with a "blue" mercury bulb, a #10-050R excitation filter (λ = 340-500nm), and a #10-115 (λ = 680 nm) emission filter. A solid standard (Turner Designs #7000-994) was used to calibrate the fluorometer prior to each day's measurements. Subsequently, 20 mL of each culture was collected on 47-mm diameter GF/F (Whatman) filters for pigment extraction. Samples were stored at -20° C prior to pigment extraction and high-performance liquid chromatography (HPLC) analysis at *University of North Carolina Chapel Hill-Institute of Marine Sciences* as described previously (Paerl et al., 2014). Briefly, photopigment samples were extracted in 100% acetone, sonicated, and stored at -20° C for ~24 h. The extracts (200 µL) were next assessed *via* HPLC as described previously (Van Heukelem et al., 1994; Pinckney et al., 1996; Pinckney et al., 1998; Pinckney et al., 2001). Photopigments were identified based on absorption spectra, which were determined from commercially obtained pigment standards (DHI, Denmark). Net pigment concentrations (µg L^{-1}) were normalized to T_f filament counts (filaments L^{-1}) and mean filament length (µm).

pH effects on F. crotonensis photosynthetic physiology

To further evaluate the potential effects of pH on photosynthetic physiology derived from our transcriptomes, *F. crotonensis* cultures were inoculated at ~1,500 filaments mL^{-1} into the

respective pH treatments (n = 5). At T_f, photosynthetic efficiency metrics were assessed *via* Pulse-Amplitude-Modulation (PAM) fluorometry with the brown algae (diatom) taxa setting (Phyto-PAM-II Compact Version, WALZ). Samples were dark-acclimated for 20 min prior to Phyto-PAM readings as described previously (Ritchie, 2008; Torres et al., 2014; Gleich et al., 2020). After dark-acclimation, replicates were exposed to a white saturating light pulse (5,000 µmol m^{-2} s^{-1} PAR) prior to determination of the maximum theoretical photochemical quantum yield of photosystem II (PSII) ($F_v \bullet F_m{}^{-1}$). Subsequently, samples were exposed to rapid light curve measurements to determine the relative maximum rate of electron transport through PSII ($rETR_{max}$, µmol electrons/m^2 s^1). Rapid light curves were run in fourteen steps. For each step cultures were exposed to increasing actinic irradiances starting from 1 µmol m^{-2} s^{-1} PAR, until a maximum of 1,257 µmol m^{-2} s^{-1} PAR was reached. The steps were run in 20 second intervals and a saturating pulse of 5,000 µmol m^{-2} s^{-1} PAR was run after each step. The light intensity at which saturation of PSII occurs (I_K, µmol photons $m^{-2} \bullet s^{-1}$) was also determined.

Statistical analyses

Statistical analyses of data (Figures 4.2, 4.4, and 4.5) were performed in GraphPad Prism (v.9.3.1) using unpaired, two-tailed *t*-tests. For this study, we consider a *p*-value < 0.05 to be significant but report all values so the reader may decide their level of risk (Appendix Attachment 4.1-4.4). Statistical comparisons of gene expression (Figure 4.1, 4.3, and 4.6) were performed in CLC Genomics Workbench. All z-scores reported in heat maps were calculated by Heatmapper.ca. Variability in expression between replicates was assessed *via* PRIMER.

Results

In this study, we performed transcriptomics to generate preliminary hypotheses regarding how pH may affect the physiology and morphology of *F. crotonensis*. Our transcriptomes identified 3 COG categories of genes which formed most of the differentially expressed (DE) genes between pH treatments: 1.) Cell cycle control, cell division and chromosome partitioning, 2.) Energy production and conversion, 3.) Mobilome: transposons, prophages. Following, laboratory assays were used to test hypotheses regarding morphology and physiology for these main COG categories. Hence, our results are organized by COG category, with the transcriptome data presented first, followed by the physical laboratory assay used to test the transcriptome-derived hypotheses.

pH induced differential gene expression between treatments

nMDS revealed an 86% similarity among low pH replicates. In contrast, high pH replicates exhibited more variability, with replicates 2 and 3 sharing 76% similarity, but replicate 1 appearing more like low pH replicates (Appendix Figure 4.7). SIMPER analyses determined a mean dissimilarity of ~27% between low and high pH replicates and identified the contribution of each gene to this variation. Notably, ~60% of the top 50 genes driving dissimilarity were related to photosynthesis, including 17 copies of the chlorophyl a/b binding protein (LHCB3) and 8 copies of fucoxanthin-chlorophyll ac binding protein (FCP) (Appendix Attachment 1b) (Appendix Figure 4.8A). Of the ~26,000 predicted genes in the *F. crotonensis* genome, a total of 713 were differentially expressed (FDR-corrected p-value ≤ 0.05, $\log_2 |\text{fold-change}| > 2$) (Appendix Figure 4.9A). Of these, 435 genes are annotated as either hypothetical or of unknown function (Appendix Figure 4.9B). All downstream analyses focused on the 278 DE genes with

predicted function (Appendix Figure 4.9C) (Appendix Attachment 1c), of which 193 were increased in representation at pH 9.2 and 85 decreased in representation.

High pH decreased carbohydrate transport and metabolism gene expression

Overall, genes involved in the COG category "Carbohydrate transport and metabolism" decreased in representation at high pH relative to low pH (Appendix Figure 4.10). Genes involved in the Calvin-Benson-Basham (CBB) cycle decreased in expression, including glyceraldehyde 3-phosphate dehydrogenase (GAPDH), which catalyzes the single reductive step of the CBB cycle during photosynthetic carbon fixation. Carbon metabolism genes involved in cellular respiration also decreased in relative expression at high pH. Genes involved in the Krebs cycle, such as malate/L-lactate dehydrogenase (MLDH) and divalent anion/Na^+symporter (DASS)(Takahashi-Íñiguez et al., 2016; Lu, 2019), decreased in representation at high pH. Carbonic anhydrase (CA), which is responsible for the interconversion/acquisition of bicarbonate and CO_2 (Sültemeyer, 1998; Burkhardt et al., 2001), decreased in expression at high pH.

High pH increased expression of cell cycle control & cell wall biogenesis genes

The relative expression of genes categorized in "Cell cycle control, cell division and chromosome partitioning" increased at pH 9.2 (Figure 4.1A). Proportional transcript abundance increased in two copies of the ribosomal RNA processing protein (RRP15) at high pH, which has been found to activate the G_1 /S checkpoint in cancer cells and thus inducing cellular arrest in G_1

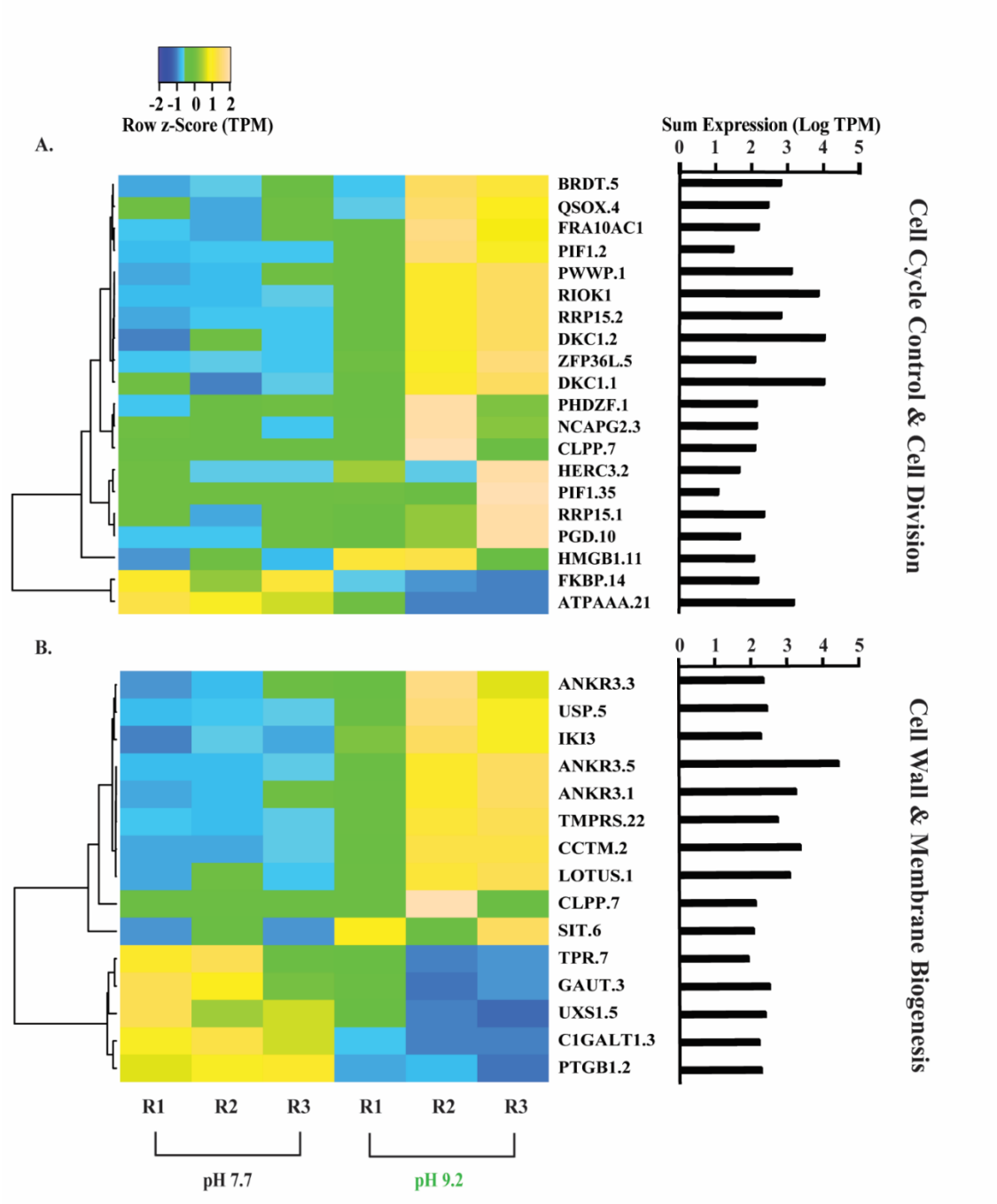


Figure 4.1 Heat maps depicting differentially expressed genes relating to *F. crotonensis* growth and cell wall morphology. (A) Genes in the COG category "Cell cycle control, cell division and chromosome partitioning". (B) Genes in the COG category "Cell wall, membrane, envelope biogenesis". Cladogram clustering is to demonstrate similarity in expression. All TPM values were row z-scored, with increases in proportional transcript abundance indicated in yellow, and decreases in proportional transcript abundance indicated in blue. The sum of transcripts across all treatments (LogTPM) is indicated for each gene.

stage of interphase (Dong et al., 2017). Expression levels of RI0 kinase 1 (RIOK1), which is required to enter S phase (LaRonde-LeBlanc and Wlodawer, 2005), also increased at pH 9.2. High pH increased the transcript abundance of butyrate response factor (ZFP36L), involved in cellular senescence and shown to induce cell cycle arrest at the G_1 phase (Saini et al., 2020).

Genes classified within the "Cell wall, membrane and envelope biogenesis" category also increased in overall expression (Figure 4.1B). A decrease in the representation of Tetratricopeptide repeat (TPR) was observed at high pH, a gene that has previously been shown to be positively correlated with silaffin expression (Frigeri et al., 2006). Further, we observed decreases in the relative expression of N-acetylgalactosamine 3-beta-galactosyltransferase (C1GALT1) and UDP glucuronate decarboxylase (UXS1) at high pH, both involved in glycosaminoglycan biosynthesis which has been implicated in diatom biosilicification processes (Alexander et al., 2015).

High pH shaped F. crotonensis filament morphology

FlowCAM analyses showed filaments grown at high pH had ~20% lower mean filament area ($p = 0.007$) (Figure 4.2A) and mean biovolume ($p = 0.031$) (Figure 4.2B) than those grown at low pH. These reductions in area and biovolume were likely due to decreased filament length at high pH. Specifically, pH 9.2 *F. crotonensis* filaments had a 25% lower mean filament length ($p = 0.002$) (Figure 4.2C), yet mean filament width was not significantly different ($p = 0.055$) (Figure 4.2D). Additionally, pH 9.2 filaments were significantly rougher on the surface ($p = 0.002$) (Figure 4.2E) and less green in color ($p < 0.0001$) (Figure 4.2F). The exact number of filaments assessed per biological replicate and. intra-variation of each replicate are reported in Appendix Attachment 4.2.

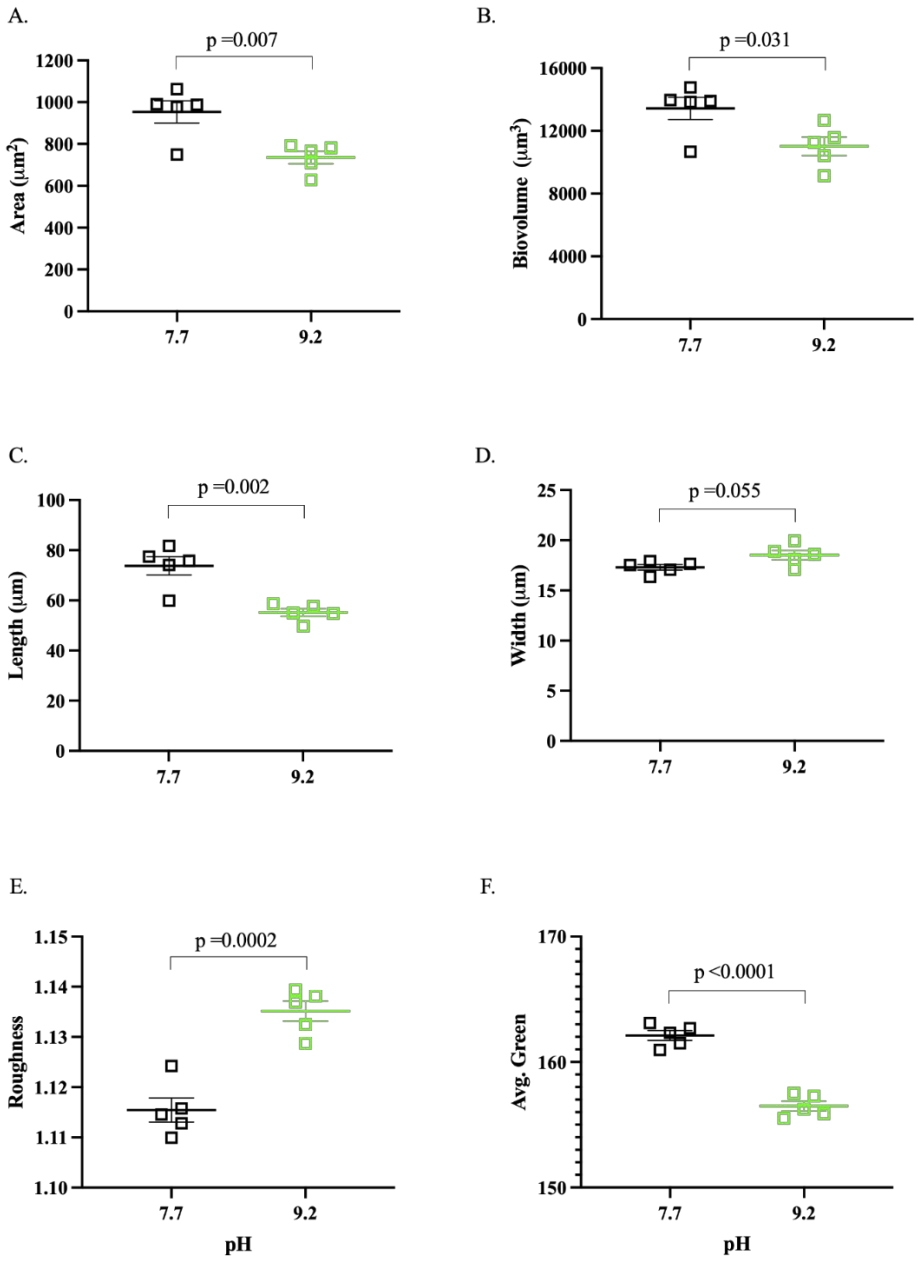


Figure 4.2 FlowCAM pH assay results collected at (T_f). pH 7.7 replicates denoted by open, black squares. pH 9.2 replicates denoted by open, green squares. Each data point represents the mean of ~1000 filaments per biological replicate, with the group mean of treatment replicates indicated by the central bar, and variability indicated by error bars representing the standard error of the mean (SEM). Variance for individual dots is reported is supplemental dataset 2. (A) Mean area (µm^2) of *F. crotonensis* filaments. (B) Mean biovolume (µm^3) of *F. crotonensis* filaments. (C) Mean length (µm) of *F. crotonensis* filaments. (D) Mean width (µm) of *F. crotonensis* filaments. (E) Mean roughness (dimensionless) of *F. crotonensis* filaments. (F) Mean green coloration of *F. crotonensis* filaments (dimensionless). P-values are for comparisons between treatments.

High pH decreased expression of energy production and conversion genes

Genes classified in the COG category "Energy production and conversion" were analyzed within the subcategories "Photosynthesis" and "Cellular respiration" that were created based on KEGG Mapper KO's (Figure 4.3). Photosynthesis-related genes decreased in representation at high pH (Figure 4.3A). All 5 copies of the PSII light harvesting complex III chlorophyll a/b binding genes (LHCB) and 3 copies of the fucoxanthin-Chl binding complex genes (FCP), both involved in light absorption and energy delivery during the first step of photosynthesis (Ballottari et al., 2012), decreased in relative expression at high pH. In the chlorophyll biosynthesis pathway, magnesium chelatase subunit D (*chl*D) and NADPH:protochlorophyllide oxidoreductase (POR) increased in relative expression at pH 9.2, while divinyl chlorophyllide *a* 8-vinyl-reductase (DVR) and bifunctional glutamyl/prolyl tRNA synthetase (EPRS) decreased. In contrast, genes within the carotenoid biosynthesis pathway such as Zeaxanthin epoxidase (ZEP) and violaxanthin de-epoxidase (VDE) decreased in representation at high pH. Regarding photosynthetic metabolism, ferredoxin NADP+ reductase (*pet*H) and photosystem I subunit VII (*psa*C), which are both involved in the final step of electron transfer from ferredoxin PSI to NADPH to fuel the Calvin cycle (Fischer et al., 1998; Nguyen et al., 2021), decreased in relative expression at pH 9.2. Genes involved in oxidative stress such as redoxin (PRDX5) (Hopkins and Neumann, 2019) and the catalase peroxidase gene (*kat*G.1), which quenches photosynthetically-produced ROS species (Nishiyama et al., 2001), appeared to decrease overall at high pH.

In contrast, genes classified within "cellular respiration" exhibited an overall increase in relative expression at pH 9.2 (Figure 4.3B). Representation of genes involved in oxidative phosphorylation increased at pH 9.2, including NADH quinone oxidoreductase chain 5 and 6

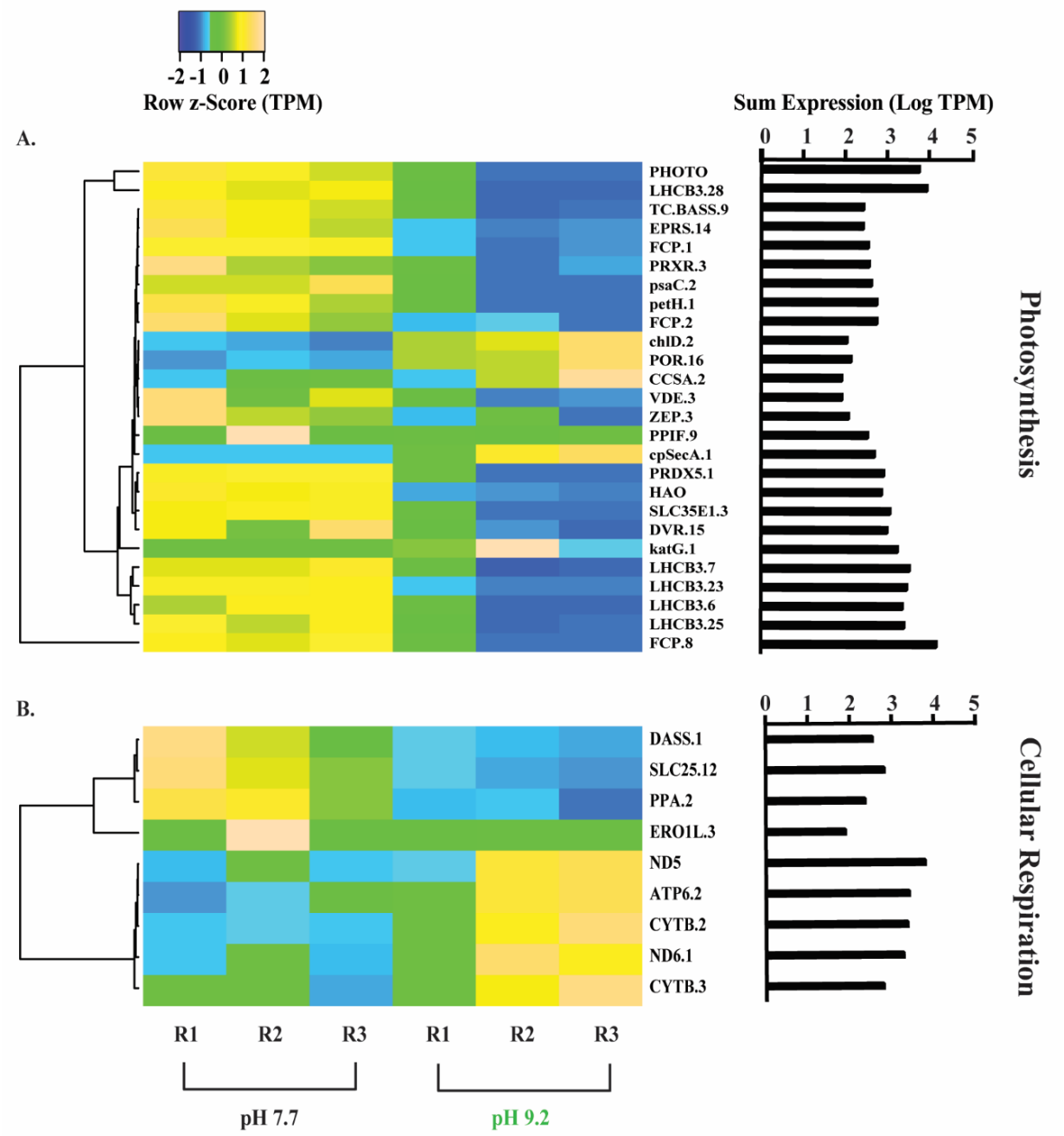


Figure 4.3 Heat map depicting differentially expressed genes relating to energy production and conversion. (A) Genes further sorted into photosynthesis and (B) cellular respiration categories. All TPM values were row z-scored, with increases in proportional transcript abundance indicated in yellow, and decreases in proportional transcript abundance indicated in blue. Cladogram clustering is to demonstrate similarity in expression. The sum of transcripts across all treatments (LogTPM) is indicated for each gene.

genes (ND5) (ND6) (Melo et al., 2004) and ATP synthase subunit α gene (ATP6) (Vázquez-Acevedo et al., 2016). In contrast, mitochondrial transport genes decreased in relative expression at high pH, including carrier gene (SLC25) (Ruprecht and Kunji, 2020).

High pH modified photopigment composition

After 8 d of pH exposure, there was no significant difference in filament concentration as a function of pH treatment ($p = 0.1745$) (Appendix Figure 4.11A). However, high pH replicates had significantly decreased in Chl *a* autofluorescence ($p < 0.0001$) (Appendix Figure 4.11B). Normalized photopigment concentrations of Chlorophyllide *a*, Chlorophyll *a,* Chlorophyll c^1c^2 (fg • μm fil^{-1}) ($p \geq 0.3263$) (Figure 4.4A, B, C), and Total Chl *a* (fg • μm fil^{-1}) ($p = 0.3503$) (Appendix Figure 4.12) were not significantly different as a function of pH. In contrast, high pH cultures had ~40% more β-carotene ($p = 0.0015$) (Figure 4.4D) and ~20% more Diadinoxanthin ($p = 0.0189$) (Figure 4.4F) per cell compared to low pH replicates. Further, high pH incubated cultures demonstrated ~30% less Violaxanthin (fg • μm fil^{-1}) compared to pH 7.7 counterparts ($p = 0.0090$) (Figure 4.4E), yet Fucoxanthin and Neoxanthin normalized pigments did not significantly vary per cell as a function of pH ($p \geq 0.337$) (Appendix Figure 4.13).

Ratios of total carotenoids:total Chl *a* were higher at pH 9.2 but fell short of significance ($p = 0.2207$) (Appendix Figure 4.14). However, β-carotene:total Chl *a* ($p = 0.0002$) and Diadinoxanthin:total Chl *a* ($p = 0.0008$) ratios were both significantly higher at pH 9.2 (Appendix Figure 4.15A, C). Mean Chl *a*/Chl c^1c^2 ratios, which serve as a proxy for the size of the light harvesting antenna complex (Lamote et al., 2003; Nguyen-Deroche et al., 2012; Heydarizadeh et al., 2019), demonstrated a consistent downward trend at high pH, though these results were not significant ($p = 0.4335$) (Appendix Figure 4.16).

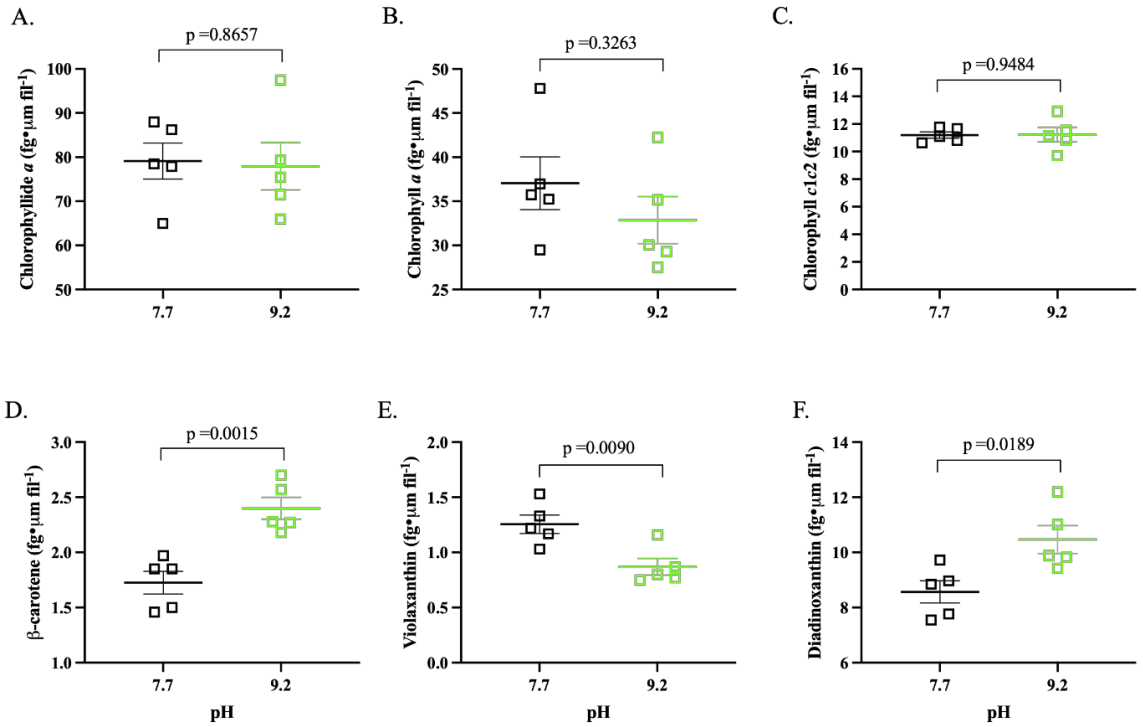


Figure 4.4 Photopigment pH assay results (n = 5) (fg • µm fil^{-1}) collected at (T_f). pH 7.7 replicates denoted by open, black squares. pH 9.2 replicates denoted by open, green squares. The group mean of treatment replicates indicated by the central bar and variability is indicated by error bars representing the standard error of the mean (SEM). (A) Chlorophyllida *a* of *F. crotonensis* filaments. (B) Chlorophyll *a*. (C) Chlorophyll *c*1*c*2. (D) β-Carotene. (E) Violaxanthin. (F) Diadinoxanthin. P-values are for comparisons between treatments.

In summary, pH did not significantly affect chlorophyll pigment concentration per cell, but a significant effect of pH 9.2 was observed on carotenoids (β-carotene and xanthophylls) in this study.

High pH altered F. crotonensis photophysiology

High pH of 9.2 did not significantly alter optimal photochemical quantum yields of photosystem II ($Fv \bullet Fm^{-1}$) ($p = 0.3089$) (Figure 4.5A). However, the relative mean maximum electron transport rate through photosystem II ($rETR_{max}$) was ~50% lower at pH 9.2 ($p < 0.0001$) (Figure 4.5B). Additionally, the photon flux at which light saturation of photosynthesis occurs (I_k) was ~50% lower at pH 9.2 ($p < 0.0001$) (Figure 4.5C).

High pH increased expression of transposon genes

Out of the 278 DE genes in the dataset, 193 were overrepresented at the high pH treatment. Further, of these 193 DE genes which increased in relative expression at pH 9.2, 25% belong to the "Mobilome: transposons, prophages" COG category (Figure 4.6). All 48 genes within the Mobilome COG category increased in representation at high pH. Notably, 9 copies of the plant transposon gene (PTRP) were overrepresented at high pH. No Mobilome categorized genes were decreased in relative expression at the high pH treatment within our DE dataset.

Discussion

HAB-induced increases in pH have been shown in the literature for decades (Talling, 1976; Jeppesen et al., 1990; Lopez-Archilla et al., 2004; Sandrini et al., 2016), yet these studies largely focus on carbon chemistry. Few assess the consequences on other members of the

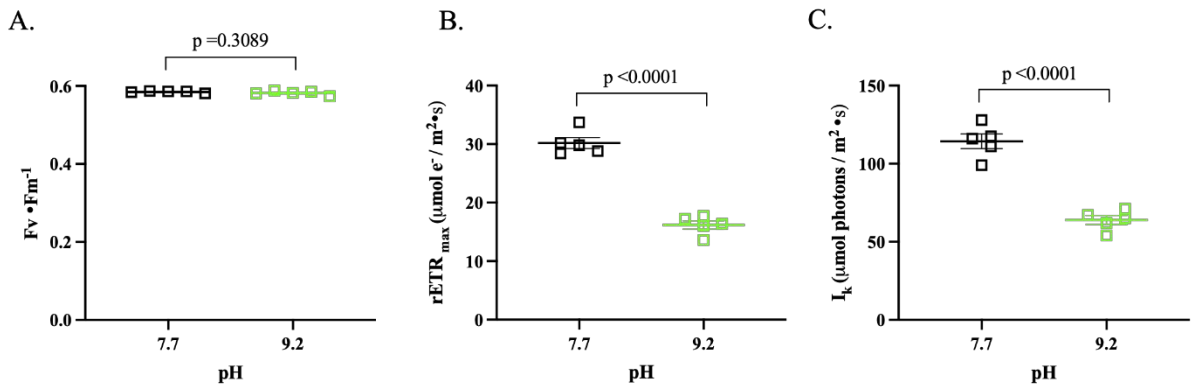


Figure 4.5 PhytoPAM pH assay results (n = 5) collected at (T_f). pH 7.7 replicates denoted by open, black squares. pH 9.2 replicates denoted by open, green squares. The group mean of treatment replicates indicated by the central bar and variability is indicated by error bars representing the standard error of the mean (SEM). (A) Fv • Fm^{-1} of *F. crotonensis* filaments. (B) $rETR_{max}$ (µmol electrons/m^2 • s^1). (C) Photon flux at which light saturation of photosynthesis occurs I_k (µmol photons m^{-2} • s^{-1}). P-values are for comparisons between treatments.

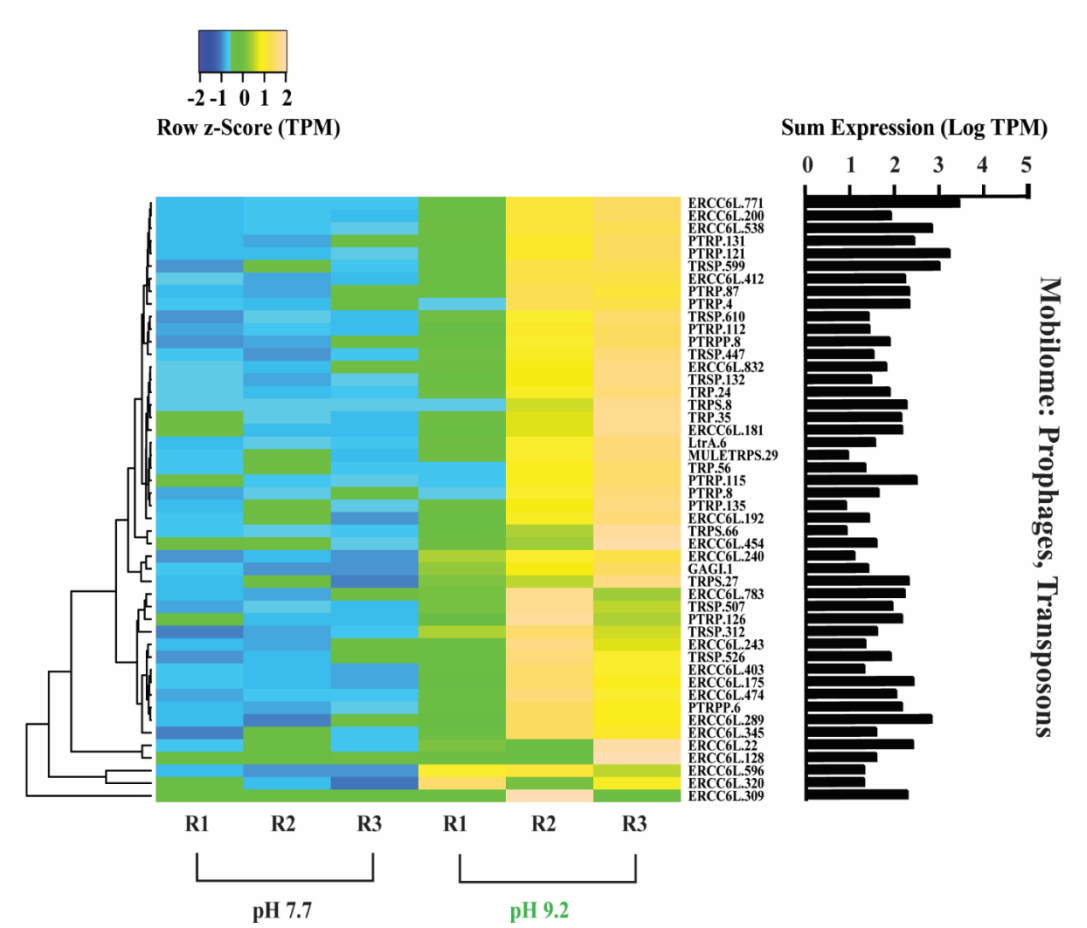


Figure 4.6 Heat map depicting differentially expressed genes relating to the "Mobilome: prophages and transposons. All TPM values were row z-scored, with increases in proportional transcript abundance indicated in yellow, and decreases in proportional transcript abundance indicated in blue. Cladogram clustering is to demonstrate similarity in expression. The sum of transcripts across all treatments (LogTPM) is indicated for each gene.

biotic community. Previously, we demonstrated that growth of *F. crotonensis* decreased at pH 9.2 and discovered Si deposition declined at high pH in diatom cultures as well as natural Lake Erie communities. Here, we built on this using transcriptomics to identify physiological processes and resulting morphological changes that may be altered by high pH. Then, we employed a variety of *in vitro* lab assays to better clarify and validate our transcriptomic results and identified potential mechanisms by which these changes may be occurring. Finally, we discuss these observations within the broader ecological scope of lake basification, and potential future implications on global freshwater diatom communities.

Evidence of carbon limitation is lacking in high pH transcriptomes

Declines in diatom viability during bloom-induced basification have historically been thought to be due to inorganic carbon-limitation. However, evidence of carbon limitation was lacking in our transcriptomes. Recent studies investigating carbon-limitation in the model diatom *Phaeodactylm tricorntum* observed increases in the expression of the CO_2 concentrating mechanism (CCM) genes (specifically CAs) in response to low CO_2 availability (Burkhardt et al., 2001; Heydarizadeh et al., 2019). However, there was an absence of biophysical CCM genes in our DE transcript list except for one CA, which was decreased at pH 9.2. Additionally, Heydarizadeh et al. (2019) concluded high light and carbon limitation increased the expression of genes associated with the biochemical CCM, yet we saw no evidence of this occurring within our transcriptomes. In addition, a prior study determined that environmental *F. crotonensis* bloom samples incubated at carbon-limited pH 9.4 did not recover photosynthetic rates after CO_2 enrichment compared to carbon-limited controls (Talling, 1976), suggesting *F. crotonensis* may not have been exclusively carbon limited. Further, the *F. crotonensis* photosynthesis rates at pH

9.4 in both carbon-limited and carbon-enriched samples were lower when compared to general phytoplankton photosynthetic rates (Talling, 1976). In contrast, when Talling (1976) replicated the experiment with natural *Microcystis* spp. bloom samples, a significant recovery of photosynthetic rate was observed after CO_2 enrichment. These results from (Talling, 1976) and others are consistent with our own; they suggest *F. crotonensis* is exhibiting decreased photosynthetic metabolism not due to pH-induced carbon-limitation alone, but due directly to alkaline pH. In summary, prior studies have induced C-limitation in diatoms and observed alterations in carbon-related genes within their transcriptomes. In our study, we did not observe these gene trends found to coincide with carbon-limitation, yet further research is needed concerning this phenomenon.

Photostress is a likely physiological consequence of high pH in F. crotonensis

Previously, we demonstrated that growth and Si deposition rates decline at high pH. Yet, the mechanisms driving these observations remained unclear. The present study indicated one of the primary processes driving these effects may be photostress. Surprisingly, ~60% of the top 50 genes contributing to pH transcriptome dissimilarity are involved in photosynthesis, with PSII and light antennae complex components forming the majority. Further, PhytoPAM data suggested a significant decrease in PSII electron flow and light saturation threshold at high pH, while pigment analysis indicated a significant increase in the photoprotective carotenoids β-carotene and diadinoxanthin. Cumulatively, this data suggests *F. crotonensis* experienced photostress at high pH.

Prior studies demonstrated that short-term photoacclimation strategies decrease photosynthetic processes *via* LHC modifications (Horton et al., 1996; Bassi and Caffarri, 2000),

reductions in the size of the LHC (Perry et al., 1981), and initiation of nonphotochemical quenching (NPQ) (Wilhelm et al., 2006a; Bertrand, 2010). In our study, *F. crotonensis* decreased electron flow through PSII at high pH as indicated by significantly lower PSII $rETR_{max}$ and decreased expression of genes encoding for the LHC of PSII (LHCBs and FCPS) (Ballottari et al., 2012). Additional transcriptomic data implied a corresponding decrease in PSI photosynthetic capacity at high pH, as evidenced by decreases in ferredoxin NADP+ oxidoreductase (FNR) enzyme gene expression (*pet*H and *psa*C). Cumulatively, these data suggest there are alterations to photosynthetic capacity at high pH. In addition, decreases in LHCB expression have been found to serve as a photoprotective response to excessive light intensities and light saturation to prevent damage to PSII and reduce ROS generation (Thomas, 2016). In our study, this strategy appeared to be successful, as PhytoPAM data demonstrated no significant differences in $(Fv \bullet Fm^{-1})$ as a function of pH. Regarding LHC modifications, significant increases in diadinoxanthin photopigment composition at high pH, decreases in carotenoid biosynthesis gene expression, and increases in expression of the key regulatory gene of the chlorophyll biosynthesis pathway (*chl*D), collectively suggest *F. crotonensis* may be restructuring the pigment composition of its LHCs in response to alkaline pH. Additionally, mean Chl a/Chl *c1c2* ratios, which serve as a size proxy for the LHC, exhibited a downward trend at pH 9.2, though this was not significant. This suggested that after 8 d of alkaline pH exposure, *F. crotonensis* may have begun reducing the size of its LHC as a photoacclimation strategy. However, this would likely result in an increase in $rETR_{max}$ as more light would then be required to drive rETR saturation, which we do not observe in this study. Hence, it is probable while *F. crotonensis* appears to be restructuring the photopigment constituents of its LHC, this does not appear to alter the LHC size overall. Moreover, we observed significant increases in

diadinoxanthin pigment at pH 9.2 and increased representative expression of thylakoid translocase subunit SecA gene (cpSecA.1), suggesting the activation of a NPQ energy dissipation pathway which is controlled by diadinoxanthin and a trans-thylakoid proton gradient (Muller et al., 2001; Bertrand, 2010). Indeed, the diadinoxanthin cycle has been described as the most important short-term photoprotective mechanism in diatoms (Bertrand, 2010). Cumulatively, these results indicate that *F. crotonensis* protects the photosynthetic membrane at high pH by employing short-term photoacclimation mechanisms such as modifying LHC composition and increasing the concentration of pigments involved in NPQ.

The photostress and photoresponse findings are supported by prior diatom studies. Park et al. (2010) determined that *Chaetoceros neogracile* alters diadinoxanthin levels and FCP expression in response to increased light intensity, and a recent study determined the diatom *P. tricornutum* alters the photopigment composition of its FCP binding complexes in response to varying light sources (Oka et al., 2020). Collectively, these prior studies suggest the high pH effects we observed in our study mirror diatom responses to high light intensity. Yet, the light intensity was held constant throughout the entirety of our experiments, implying that growth at pH 9.2 affects *F. crotonensis's* phototolerance. Indeed, in our study *F. crotonensis* filaments may be light saturated at pH 9.2 as evidenced by a 50% lower PSII saturation threshold (I_k), with saturation setting in at 60 μmol photons m^{-2} s^{-1}. This suggests that *F. crotonensis* is experiencing the light saturation of downstream metabolisms, with potential alterations to the light antennae serving as a secondary effect of this phenomenon. Further, photoprotective pigments increased at high pH while light harvesting pigments did not, implying filaments are prioritizing photoprotection over photon acquisition. Cumulatively, transcriptomic, morphological, and

physiological evidence in our study imply *F. crotonensis* may have a lower phototolerance of light at high pH, suggesting basification pH conditions alter diatom photophysiology.

Cell cycle arrest another physiological consequence of high pH?

High-pH-induced photostress explains altered photopigment composition and photosynthetic physiology but falls short of directly accounting for morphological changes observed in this study (*i.e.,* differences in filament length and frustule roughness) and prior observed physiological effects (*i.e.,* decreased growth and Si deposition rates). Our transcriptomic analyses indicate another factor may be driving these high pH effects: arrest of the cell cycle at the G_1/S checkpoint (Jang et al., 2005). Indeed, a prior study determined this checkpoint is typically regulated by light in photosynthetic eukaryotes (Moulager et al., 2010), thus photostress may be contributing to its arrest in the diatom *F. crotonensis*. In support of this, we observed an increase in the expression of multiple genes associated with the G_1/S checkpoint at high pH. Moreover, a recent study demonstrated cell cycle arrest in G_1 does not lead to changes in $Fv \bullet Fm^{-1}$, but does result in lower $rETR_{max}$, higher NPQ, and gene expression patterns consistent with LHC and ROS scavenging in the diatom *P. tricornutum* (Kim et al., 2017), all of which are observed in our study.

However, if photostress is inducing cell cycle arrest, how does this result in lower growth and Si deposition rates? With regard to growth, a prior diatom study indicated photosynthetic metabolism and the cell cycle are closely related, with photosynthetic capacity at its highest during the main growth phase of G_1 (Claquin et al., 2004). Biosilicification is also linked to the cell cycle and cell growth (Hildebrand et al., 2007; Shrestha et al., 2012), with the G_1 phase serving as the phase where diatoms reach their full size and where girdle band formation of the

frustules occurs (Javaheri et al., 2014). Additional studies suggest cell growth cannot occur without girdle band formation (Crawford, 1981; Volcani, 1981; Claquin et al., 2002). Hence, we may observe decreased growth and Si deposition rates, smaller filaments, and malformed frustules due in part to this arrest and disruption in the G_1 cell phase. It is well established that eukaryotic phototrophs use cell cycle arrest as a means to combat stress, with this mechanism induced by a variety of abiotic stressors (Eekhout and De Veylder, 2019; Takahashi et al., 2019). We suggest the photostress observed in pH 9.2 treatments may be responsible for this apparent cell cycle arrest hinted at in our transcriptomic data, and therefore contributing to morphological and physiological effects observed in *F. crotonensis*.

High pH results in smaller, rougher & browner F. crotonensis morphologies

In this study, growth at pH 9.2 resulted in significant morphological changes within our model freshwater diatom. Filaments maintained at high pH for 8 d exhibited significantly shorter lengths, resulting in lower biovolume and area. Despite this, individual diatom cells did not significantly differ in width. A prior study demonstrated warming temperatures results in smaller diatom cells across the Laurentian Great Lakes (Bramburger et al., 2017). Considering lake basification events will likely coincide with warming temperatures, future freshwater diatom communities may exhibit both smaller filaments and smaller individual cells.

FlowCAM analyses further indicated filaments had rougher exterior surfaces at high pH. We previously examined the pH dependence of Si deposition, demonstrating that it decreased at pH 9.2. Here, we build upon this with FlowCAM and transcriptomic data which suggest diatoms are struggling to deposit Si, and the diatoms that do successfully form frustules may have malformations which are evidenced by this “roughness”. We observed a decrease in the

expression of a gene (TPR) whose expression is positively correlated with silaffin expression (a gene directly involved in Si deposition) (Frigeri et al., 2006), suggesting *F. crotonensis* may be downregulating the biosilicification process (Shrestha et al., 2012). Genes suggested to encode for diatom cell wall components such as CLPP and ANKR3 (Frigeri et al., 2006), and C1GALT and UXS1 (Alexander et al., 2015), were also decreased in expression at high pH. Alterations in the expression of biosilicification genes, and/or those involved in forming the cell wall structures which the frustules sit upon, will produce morphological malformities (Round et al., 1990; Hildebrand et al., 2006). Cumulatively, these data suggest diatoms struggle to deposit Si frustules at pH 9.2, likely leading to cell walls with rougher and malformed phenotypes.

In addition to smaller and "rougher" filaments, high pH results in "browner" diatoms due to significantly increased concentrations of β-carotene and diadinoxanthin but ~constant chlorophyll concentrations. Prior studies demonstrate both fucoxanthin (involved in light harvesting) and diadinoxanthin (involved in photoprotection) are the main carotenoids of diatoms, serving as components of the LHCs (Ballottari et al., 2012). Indeed, total carotenoid:total Chl *a* ratios were higher at pH 9.2, though these findings fell short of significance due to ~constant fucoxanthin concentrations. Nonetheless, there were significant increases in the diadinoxanthin:total Chl *a* and β-carotene:total Chl *a* ratios observed in pH 9.2 filaments. This contradicts our transcriptomic data, as carotenoid biosynthesis genes (ZEP and VDE) were decreased in expression at pH 9.2. However, changes in pigment levels often occur without detectable changes in gene expression (Kuczynska et al., 2015). Regardless, significantly higher β-carotene and diadinoxanthin photopigment concentrations lead to "less green" filaments and significantly lower Chl *a* autofluorescence, all suggesting "browner" diatoms at pH 9.2.

Cumulatively, this data demonstrates lake basification induces significant changes to *F. crotonensis* morphology, resulting in smaller, rougher, and browner filaments.

Lake basification has ecological & biogeochemical implications

While acidification has been suggested to benefit the growth and ecological resilience of marine diatoms (Wu et al., 2014; Valenzuela et al., 2018), we suggest here that basification poses a detriment. Diatoms are responsible for ~20% of global primary production (Nelson et al., 1995), acting as an integral component of the aquatic primary producers. Hence, altering diatom populations will evoke significant biotic and biogeochemical implications within the aquatic ecosystem (Rühland et al., 2015). For example, here we demonstrate high pH results in smaller, browner, rougher diatoms. Based on prior research, we postulate these morphological alterations will modify grazing patterns of secondary consumers and selective filtration of higher trophic consumers (Vanderploeg et al., 2001; Baranowska et al., 2013; Vanderploeg et al., 2013). This decrease in size will also likely increase diatom predation by Dreissenids, as smaller diatoms seem to be selectively filtered (Reavie and Barbiero, 2013). Additionally, declines in Si deposition rates combined with rougher frustules suggests thinner and malformed cell walls which may reduce their effectiveness as a defense mechanism against zooplankton grazing (Pančić et al., 2019; Ryderheim et al., 2022) and viral infection (Kranzler et al., 2019).

Due in part to their heavy Si frustules, diatoms also play an instrumental role in global biogeochemical cycles and nutrient export to the benthos (Struyf et al., 2009; Benoiston et al., 2017), with studies demonstrating the Si cycle is more strongly inter-related with the carbon, nitrogen and phosphorus cycles than previously thought (Tréguer and De La Rocha, 2013; Tréguer et al., 2021). For example, Lake Erie undergoes such a high degree of diatom deposition

to the benthos in the winter-spring, that it serves as a substantial driver of summer hypoxia (Reavie et al., 2016). Another study demonstrated that even when an estuary water column was dominated by flagellates, the labile organic matter settling to the sediment was derived from diatoms (Haese et al., 2007). Thus, we postulate lake basification-induced changes to diatoms will have significant downstream effects within the lacustrine ecosystem and biogeochemical cycles, particularly with respect to the benthos which experience the highest diatom-nutrient deposition.

"Genomic roulette": the key to freshwater diatom success in a basified future?

Abundant transcripts from transposable elements within the *F. crotonensis* genome provide insight into a mechanism these diatoms may use to adapt and persist at high pH or other severe environmental stressors that could be otherwise detrimental. Approximately 25% of the DE genes that were increased in expression at high pH belonged within the "Mobilome: prophages, transposons" COG classification. Mobile elements like these change the architecture of an organism's genome by rearranging themselves to new locations or (in some cases) moving pieces of the genome itself. Such rearrangements can, for example, insert into a gene and disrupt it, or insert into a regulatory site and change how genes are expressed (Pennisi, 1998; Lisch, 2013; Schrader and Schmitz, 2019). Extensive genomic variation has been attributed to similar rearrangements in green alga like *Chlamydomonas reinhardtii* (Flowers et al., 2015).

It appears that a potential response to environmental conditions stressful enough to heavily damage an organism – like a shift to extreme pH conditions - is an attempt to make a significant, microevolutionary leap by re-arranging one's own genomic architecture at random. Diatoms have been described as "one of the most rapidly evolving eukaryotic taxa on Earth"

(Oliver et al., 2007; Vardi et al., 2009). This speed has been attributed to their high proportion of retrotransposons, long terminal repeats, and transposable elements (Bowler et al., 2008; Vardi et al., 2009; Rastogi et al., 2018). This type of win or lose strategy, which we have termed "genomic roulette", is perhaps an extreme interpretation of the role of "jumping genes" in organismal adaptation to ecological stress (McClintock, 1956; Capy et al., 2000; Horváth et al., 2017). We define genomic roulette as an upregulation of mobile elements in response to an environmental stressor to rapidly increase mutations within an organism, and thus the genetic diversity within a population, over a short period of time. While most random mutations of this nature can be hypothesized to prove disadvantageous, there remains the likelihood a small subset will confer fitness to the organism and facilitate survival.

Stress-induced alterations to genomic architecture have been suggested in other phototrophs ranging from single-celled cyanobacteria (Lin et al., 2010; Hu et al., 2018) to multicellular plants (Negi et al., 2016; Roquis et al., 2021). For example, *Microcystis aeruginosa* in lab cultures has been shown to massively upregulate transposases when shifted to urea as a nitrogen source for growth (Steffen et al., 2014b). Returning to diatoms, recent studies have suggested genome evolution was responsible for cold- climate adaptations in the polar marine diatom *Fragilariopsis cylindrus* (Mock et al., 2017) and warmer- climate adaptations in tropical marine diatoms in response to ocean warming (Jin and Agustí, 2018). Our observations provide a potential mechanism for how our freshwater diatom *F. crotonensis* may be gambling in the game of genomic roulette at high pH, with the potential to facilitate a rapid adaptation to these high pH conditions at the likely cost of many in the cohort. Going forward, there is a need to better elucidate this hypothesis within diatoms, determine if this strategy of genomic roulette

extrapolates to other organisms beyond photoautotrophs, and a necessity to develop an understanding of its rate of success.

Conclusion

In this study, transcriptomic analyses revealed genes associated with photosynthesis, not carbohydrate metabolism, were driving dissimilarity between high pH vs. low pH expression. We demonstrated that a pH of 9.2, which is routinely reached during lake basification events, significantly alters *F. crotonensis* filament morphology resulting in smaller, browner, and rougher diatoms after just 8 days of exposure. This pH further modifies F. *crotonensis* photophysiology by significantly decreasing both maximum electron transport rates through PSII and light saturation thresholds. Cumulatively, these transcriptomic, morphological, and physiological findings imply *F. crotonensis* experienced photostress in the high pH treatment, with evidence suggesting filaments invoke photoacclimative strategies in response. In turn, transcriptomic evidence suggests this photostress is inducing cell cycle arrest at the G_1 /S checkpoint, which would explain the decreased growth and Si deposition rates observed previously (Zepernick et al., 2021).

Increased sensitivity to light stress is likely exacerbated in the environment, as prior findings indicate the highest diel pH spikes coincide with peak photosynthesis rates and light levels during the afternoon (Krausfeldt et al., 2019), a phenomenon likely intensified by prolonged basification events of up to ~40 d in the environment (Zepernick et al., 2021). Yet, this stress may be partially alleviated by the thick *Microcystis* spp. scum associated with bloom events, as colonies regulate their own buoyancy and shade the water column. Thus, further research is needed to understand responses of freshwater diatoms to both diel variations in pH on a short-term scale, and the long-term effects basification will impose on freshwater diatom

communities. As climate change serves to increase cyanobacterial bloom distribution, duration and frequency (Wells et al., 2020), there is a need to elucidate how freshwater diatom communities will respond (and adapt) to these lake basification events.

Acknowledgements

We thank Dr. Gary LeCleir, Dr. R. Michael L. McKay, Dr. George Bullerjahn, Dr. Erik Zinser, Naomi Gilbert and Elizabeth Dennison for their comments and suggestions.

References:

Alexander, H., Jenkins, B.D., Rynearson, T.A., and Dyhrman, S.T. (2015). Metatranscriptome analyses indicate resource partitioning between diatoms in the field. *Proceedings of the National Academy of Sciences* 112**,** E2182-E2190.

Anderson, D.M. (2009). Approaches to monitoring, control and management of harmful algal blooms (HABs). *Ocean & Coastal Management* 52**,** 342-347.

Babicki, S., Arndt, D., Marcu, A., Liang, Y., Grant, J.R., Maciejewski, A., and Wishart, D.S. (2016). Heatmapper: web-enabled heat mapping for all. *Nucleic acids research* 44**,** W147-W153.

Ballottari, M., Girardon, J., Dall'osto, L., and Bassi, R. (2012). Evolution and functional properties of photosystem II light harvesting complexes in eukaryotes. *Biochimica et Biophysica Acta (BBA)-Bioenergetics* 1817**,** 143-157.

Baranowska, K., North, R.L., Winter, J., and Dillon, P. (2013). Long-term seasonal effects of dreissenid mussels on phytoplankton in Lake Simcoe, Ontario, Canada. *Inland Waters* 3**,** 285-295.

Bassi, R., and Caffarri, S. (2000). Lhc proteins and the regulation of photosynthetic light harvesting function by xanthophylls. *Photosynthesis Research* 64**,** 243-256.

Benoiston, A.-S., Ibarbalz, F.M., Bittner, L., Guidi, L., Jahn, O., Dutkiewicz, S., and Bowler, C. (2017). The evolution of diatoms and their biogeochemical functions. *Philosophical Transactions of the Royal Society B: Biological Sciences* 372**,** 20160397.

Bertrand, M. (2010). Carotenoid biosynthesis in diatoms. *Photosynthesis research* 106**,** 89-102.

Bowler, C., Allen, A.E., Badger, J.H., Grimwood, J., Jabbari, K., Kuo, A., Maheswari, U., Martens, C., Maumus, F., and Otillar, R.P. (2008). The *Phaeodactylum* genome reveals the evolutionary history of diatom genomes. *Nature* 456**,** 239.

Bramburger, A.J., Reavie, E.D., Sgro, G., Estepp, L., Chraïbi, V.S., and Pillsbury, R. (2017). Decreases in diatom cell size during the 20th century in the Laurentian Great Lakes: a response to warming waters? *Journal of Plankton Research* 39**,** 199-210.

Burkhardt, S., Amoroso, G., Riebesell, U., and Sültemeyer, D. (2001). CO_2 and HCO_3^- uptake in marine diatoms acclimated to different CO_2 concentrations. *Limnology and Oceanography* 46**,** 1378-1391.

Bushnell, B. (2014). "BBMap: a fast, accurate, splice-aware aligner". Lawrence Berkeley National Lab.(LBNL), Berkeley, CA (United States)).

Capy, P., Gasperi, G., Biémont, C., and Bazin, C. (2000). Stress and transposable elements: co-evolution or useful parasites? *Heredity* 85**,** 101-106.

Claquin, P., Kromkamp, J.C., and Martin-Jezequel, V. (2004). Relationship between photosynthetic metabolism and cell cycle in a synchronized culture of the marine alga *Cylindrotheca fusiformis* (Bacillariophyceae). *European Journal of Phycology* 39**,** 33-41.

Claquin, P., Martin-Jézéquel, V., Kromkamp, J.C., Veldhuis, M.J., and Kraay, G.W. (2002). Uncoupling of silicon compared with carbon and nitrogen metabolisms and the role of the cell cycle in continuous cultures of *Thalassiosira pseudonana* (Bacillariophyceae) under light, nitrogen, and phosphorus control1. *Journal of Phycology* 38**,** 922-930.

Clarke, K., and Gorley, R. (2015). Getting started with PRIMER v7. *PRIMER-E: Plymouth, Plymouth Marine Laboratory* 20.

Crawford, R. (1981). "The siliceous components of the diatom cell wall and their morphological variation," in *Silicon and siliceous structures in biological systems*. Springer), 129-156.

Dong, Z., Zhu, C., Zhan, Q., and Jiang, W. (2017). The roles of RRP15 in nucleolar formation, ribosome biogenesis and checkpoint control in human cells. *Oncotarget* 8**,** 13240.
Eekhout, T., and De Veylder, L. (2019). Plant stress: hitting pause on the cell cycle. *Elife* 8**,** e46781.
Fischer, N., Hippler, M., Sétif, P., Jacquot, J.-P., and Rochaix, J.-D. (1998). The *psa*C subunit of photosystem I provides an essential lysine residue for fast electron transfer to ferredoxin. *The EMBO Journal* 17**,** 849-858.
Flowers, J.M., Hazzouri, K.M., Pham, G.M., Rosas, U., Bahmani, T., Khraiwesh, B., Nelson, D.R., Jijakli, K., Abdrabu, R., and Harris, E.H. (2015). Whole-genome resequencing reveals extensive natural variation in the model green alga *Chlamydomonas reinhardtii*. *The Plant Cell* 27**,** 2353-2369.
Frigeri, L.G., Radabaugh, T.R., Haynes, P.A., and Hildebrand, M. (2006). Identification of Proteins from a Cell Wall Fraction of the Diatom *Thalassiosira pseudonana*: Insights into Silica Structure Formation. *Molecular & Cellular Proteomics* 5**,** 182-193.
Gleich, S.J., Plough, L.V., and Glibert, P.M. (2020). Photosynthetic efficiency and nutrient physiology of the diatom *Thalassiosira pseudonana* at three growth temperatures. *Marine Biology* 167**,** 1-13.
Gobler, C.J., and Sunda, W.G. (2012). Ecosystem disruptive algal blooms of the brown tide species, *Aureococcus anophagefferens* and *Aureoumbra lagunensis*. *Harmful Algae* 14**,** 36-45.
Haese, R.R., Murray, E.J., Smith, C.S., Smith, J., Clementson, L., and Heggie, D.T. (2007). Diatoms control nutrient cycles in a temperate, wave-dominated estuary (southeast Australia). *Limnology and Oceanography* 52**,** 2686-2700.
Hartig, J.H. (1987). Factors contributing to development of *Fragilaria crontonensis* Kitton Pulses in Pigeon Bay waters of western Lake Erie. *Journal of Great Lakes Research* 13**,** 65-77.
Heisler, J., Glibert, P.M., Burkholder, J.M., Anderson, D.M., Cochlan, W., Dennison, W.C., Dortch, Q., Gobler, C.J., Heil, C.A., and Humphries, E. (2008). Eutrophication and harmful algal blooms: a scientific consensus. *Harmful Algae* 8**,** 3-13.
Hervé, V., Derr, J., Douady, S., Quinet, M., Moisan, L., and Lopez, P.J. (2012). Multiparametric analyses reveal the pH-dependence of silicon biomineralization in diatoms. *PloS One* 7**,** e46722.
Heydarizadeh, P., Veidl, B., Huang, B., Lukomska, E., Wielgosz-Collin, G., Couzinet-Mossion, A., Bougaran, G., Marchand, J., and Schoefs, B. (2019). Carbon orientation in the diatom Phaeodactylum tricornutum: the effects of carbon limitation and photon flux density. *Frontiers in plant science* 10**,** 471.
Hildebrand, M., Frigeri, L.G., and Davis, A.K. (2007). Synchronized growth of *Thalassiosira psuedonana* (Bacillariophyceae) provides novel insights into cell-wall synthesis processes in relation to the cell cycle. *Journal of Phycology* 43**,** 730-740.
Hildebrand, M., York, E., Kelz, J.I., Davis, A.K., Frigeri, L.G., Allison, D.P., and Doktycz, M.J. (2006). Nanoscale control of silica morphology and three-dimensional structure during diatom cell wall formation. *Journal of Materials Research* 21**,** 2689-2698.
Hopkins, B.L., and Neumann, C.A. (2019). Redoxins as gatekeepers of the transcriptional oxidative stress response. *Redox Biology* 21**,** 101104.
Horton, P., Ruban, A., and Walters, R. (1996). Regulation of light harvesting in green plants. *Annual Review of Plant Biology* 47**,** 655-684.

Horváth, V., Merenciano, M., and González, J. (2017). Revisiting the relationship between transposable elements and the eukaryotic stress response. *Trends in Genetics* 33**,** 832-841.

Hu, L., Xiao, P., Jiang, Y., Dong, M., Chen, Z., Li, H., Hu, Z., Lei, A., and Wang, J. (2018). Transgenerational epigenetic inheritance under environmental stress by genome-wide DNA methylation profiling in cyanobacterium. *Frontiers in Microbiology* 9**,** 1479.

Huerta-Cepas, J., Szklarczyk, D., Heller, D., Hernández-Plaza, A., Forslund, S.K., Cook, H., Mende, D.R., Letunic, I., Rattei, T., and Jensen, L.J. (2019). eggNOG 5.0: a hierarchical, functionally and phylogenetically annotated orthology resource based on 5090 organisms and 2502 viruses. *Nucleic Acids Research* 47**,** D309-D314.

Jang, S.J., Shin, S.H., Yee, S.T., Hwang, B., Im, K.H., and Park, K.Y. (2005). Effects of abiotic stresses on cell cycle progression in tobacco BY-2 cells. *Molecules & Cells (Springer Science & Business Media BV)* 20.

Javaheri, N., Dries, R., and Kaandorp, J. (2014). Understanding the sub-cellular dynamics of silicon transportation and synthesis in diatoms using population-level data and computational optimization. *PLoS Computational Biology* 10**,** e1003687.

Jeppesen, E., Søndergaard, M., Sortkjær, O., Mortensen, E., and Kristensen, P. (1990). "Interactions between phytoplankton, zooplankton and fish in a shallow, hypertrophic lake: a study of phytoplankton collapses in Lake Søbygård, Denmark," in *Trophic Relationships in Inland Waters*. Springer), 149-164.

Ji, X., Verspagen, J.M., Van De Waal, D.B., Rost, B., and Huisman, J. (2020). Phenotypic plasticity of carbon fixation stimulates cyanobacterial blooms at elevated CO_2. *Science Advances* 6.

Jin, P., and Agustí, S. (2018). Fast adaptation of tropical diatoms to increased warming with trade-offs. *Scientific Reports* 8**,** 1-10.

Kanehisa, M., Sato, Y., Kawashima, M., Furumichi, M., and Tanabe, M. (2016). KEGG as a reference resource for gene and protein annotation. *Nucleic Acids Research* 44**,** D457-D462.

Kim, J., Brown, C.M., Kim, M.K., Burrows, E.H., Bach, S., Lun, D.S., and Falkowski, P.G. (2017). Effect of cell cycle arrest on intermediate metabolism in the marine diatom *Phaeodactylum tricornutum*. *Proceedings of the National Academy of Sciences* 114**,** E8007-E8016.

Kranzler, C.F., Krause, J.W., Brzezinski, M.A., Edwards, B.R., Biggs, W.P., Maniscalco, M., Mccrow, J.P., Van Mooy, B.A., Bidle, K.D., and Allen, A.E. (2019). Silicon limitation facilitates virus infection and mortality of marine diatoms. *Nature Microbiology* 4**,** 1790-1797.

Krausfeldt, L.E., Farmer, A.T., Castro Gonzalez, H., Zepernick, B.N., Campagna, S.R., and Wilhelm, S.W. (2019). Urea is both a carbon and nitrogen source for *Microcystis aeruginosa*: tracking ^{13}C incorporation at bloom pH conditions. *Frontiers in Microbiology* 10**,** 1064.

Kuczynska, P., Jemiola-Rzeminska, M., and Strzalka, K. (2015). Photosynthetic pigments in diatoms. *Marine Drugs* 13**,** 5847-5881.

Lamote, M., Darko, E., Schoefs, B., and Lemoine, Y. (2003). Assembly of the photosynthetic apparatus in embryos from *Fucus serratus*. *Photosynthesis Research* 77**,** 45-52.

Laronde-Leblanc, N., and Wlodawer, A. (2005). The RIO kinases: an atypical protein kinase family required for ribosome biogenesis and cell cycle progression. *Biochimica et Biophysica Acta (BBA)-Proteins and Proteomics* 1754**,** 14-24.

Lehman, P., Marr, K., Boyer, G., Acuna, S., and Teh, S.J. (2013). Long-term trends and causal factors associated with *Microcystis* abundance and toxicity in San Francisco Estuary and implications for climate change impacts. *Hydrobiologia* 718**,** 141-158.

Lin, S., Haas, S., Zemojtel, T., Xiao, P., Vingron, M., and Li, R. (2010). Genome-wide comparison of cyanobacterial transposable elements, potential genetic diversity indicators. *Nature Precedings***,** 1-1.

Lisch, D. (2013). How important are transposons for plant evolution? *Nature Reviews Genetics* 14**,** 49-61.

Lopez-Archilla, A.I., Moreira, D., López-García, P., and Guerrero, C. (2004). Phytoplankton diversity and cyanobacterial dominance in a hypereutrophic shallow lake with biologically produced alkaline pH. *Extremophiles* 8**,** 109-115.

Lu, M. (2019). Structure and mechanism of the divalent anion/Na^+ symporter. *International Journal of Molecular Sciences* 20**,** 440.

Martin, R.M., and Wilhelm, S.W. (2020). Phenol-based RNA Extraction from Polycarbonate Filters. *protocols.io*.

Mcclintock, B. (Year). "Controlling elements and the gene", in: *Cold Spring Harbor symposia on quantitative biology*: Cold Spring Harbor Laboratory Press), 197-216.

Melo, A.M., Bandeiras, T.M., and Teixeira, M. (2004). New insights into type II NAD (P) H: quinone oxidoreductases. *Microbiology and Molecular Biology Reviews* 68**,** 603-616.

Mock, T., Otillar, R.P., Strauss, J., Mcmullan, M., Paajanen, P., Schmutz, J., Salamov, A., Sanges, R., Toseland, A., and Ward, B.J. (2017). Evolutionary genomics of the cold-adapted diatom *Fragilariopsis cylindrus*. *Nature* 541**,** 536-540.

Moulager, M., Corellou, F., Vergé, V., Escande, M.-L., and Bouget, F.-Y. (2010). Integration of light signals by the retinoblastoma pathway in the control of S phase entry in the picophytoplanktonic cell *Ostreococcus*. *PLoS Genetics* 6**,** e1000957.

Muller, P., Li, X.-P., and Niyogi, K.K. (2001). Non-photochemical quenching. A response to excess light energy. *Plant Physiology* 125**,** 1558-1566.

Negi, P., Rai, A.N., and Suprasanna, P. (2016). Moving through the stressed genome: emerging regulatory roles for transposons in plant stress response. *Frontiers in Plant Science* 7**,** 1448.

Nelson, D.M., Tréguer, P., Brzezinski, M.A., Leynaert, A., and Quéguiner, B. (1995). Production and dissolution of biogenic silica in the ocean: revised global estimates, comparison with regional data and relationship to biogenic sedimentation. *Global Biogeochemical Cycles* 9**,** 359-372.

Nguyen, M.K., Shih, T.-H., Lin, S.-H., Lin, J.-W., Nguyen, H.C., Yang, Z.-W., and Yang, C.-M. (2021). Transcription profile analysis of chlorophyll biosynthesis in leaves of wild-type and chlorophyll *b*-deficient rice (Oryza sativa L.). *Agriculture* 11**,** 401.

Nguyen-Deroche, T.L.N., Caruso, A., Le, T.T., Bui, T.V., Schoefs, B., Tremblin, G., and Morant-Manceau, A. (2012). Zinc affects differently growth, photosynthesis, antioxidant enzyme activities and phytochelatin synthase expression of four marine diatoms. *The Scientific World Journal* 2012.

Nishiyama, Y., Yamamoto, H., Allakhverdiev, S.I., Inaba, M., Yokota, A., and Murata, N. (2001). Oxidative stress inhibits the repair of photodamage to the photosynthetic machinery. *The EMBO Journal* 20**,** 5587-5594.

Oka, K., Ueno, Y., Yokono, M., Shen, J.-R., Nagao, R., and Akimoto, S. (2020). Adaptation of light-harvesting and energy-transfer processes of a diatom *Phaeodactylum tricornutum* to different light qualities. *Photosynthesis Research* 146**,** 227-234.

Oliver, M.J., Petrov, D., Ackerly, D., Falkowski, P., and Schofield, O.M. (2007). The mode and tempo of genome size evolution in eukaryotes. *Genome Research* 17**,** 594-601.

Paerl, H.W., Fulton, R.S., Moisander, P.H., and Dyble, J. (2001). Harmful freshwater algal blooms, with an emphasis on cyanobacteria. *The Scientific World Journal* 1**,** 76-113.

Paerl, H.W., Hall, N.S., Peierls, B.L., Rossignol, K.L., and Joyner, A.R. (2014). Hydrologic variability and its control of phytoplankton community structure and function in two shallow, coastal, lagoonal ecosystems: the Neuse and New River Estuaries, North Carolina, USA. *Estuaries and Coasts* 37**,** 31-45.

Pančić, M., Torres, R.R., Almeda, R., and Kiørboe, T. (2019). Silicified cell walls as a defensive trait in diatoms. *Proceedings of the Royal Society B* 286**,** 20190184.

Park, S., Jung, G., Hwang, Y.-S., and Jin, E. (2010). Dynamic response of the transcriptome of a psychrophilic diatom, *Chaetoceros neogracile*, to high irradiance. *Planta* 231**,** 349-360.

Pennisi, E. (1998). "How the genome readies itself for evolution". American Association for the Advancement of Science).

Perry, M., Talbot, M., and Alberte, R. (1981). Photoadaption in marine phytoplankton: response of the photosynthetic unit. *Marine Biology* 62**,** 91-101.

Pinckney, J., Millie, D., Howe, K., Paerl, H., and Hurley, J. (1996). Flow scintillation counting of ^{14}C-labeled microalgal photosynthetic pigments. *Journal of Plankton Research* 18**,** 1867-1880.

Pinckney, J., Paerl, H., Harrington, M., and Howe, K. (1998). Annual cycles of phytoplankton community-structure and bloom dynamics in the Neuse River Estuary, North Carolina. *Marine Biology* 131**,** 371-381.

Pinckney, J.L., Richardson, T.L., Millie, D.F., and Paerl, H.W. (2001). Application of photopigment biomarkers for quantifying microalgal community composition and i*n situ* growth rates. *Organic Geochemistry* 32**,** 585-595.

Rastogi, A., Maheswari, U., Dorrell, R.G., Vieira, F.R.J., Maumus, F., Kustka, A., Mccarthy, J., Allen, A.E., Kersey, P., and Bowler, C. (2018). Integrative analysis of large scale transcriptome data draws a comprehensive landscape of *Phaeodactylum tricornutum* genome and evolutionary origin of diatoms. *Scientific Reports* 8**,** 1-14.

Reavie, E.D., and Barbiero, R.P. (2013). Recent changes in abundance and cell size of pelagic diatoms in the North American Great Lakes. *Phytotaxa* 127**,** 150-162.

Reavie, E.D., Cai, M., Twiss, M.R., Carrick, H.J., Davis, T.W., Johengen, T.H., Gossiaux, D., Smith, D.E., Palladino, D., and Burtner, A. (2016). Winter–spring diatom production in Lake Erie is an important driver of summer hypoxia. *Journal of Great Lakes Research* 42**,** 608-618.

Ritchie, R.J. (2008). Fitting light saturation curves measured using modulated fluorometry. *Photosynthesis Research* 96**,** 201-215.

Roquis, D., Robertson, M., Yu, L., Thieme, M., Julkowska, M., and Bucher, E. (2021). Genomic impact of stress-induced transposable element mobility in *Arabidopsis*. *Nucleic Acids Research* 49**,** 10431-10447.

Round, F.E., Crawford, R.M., and Mann, D.G. (1990). *Diatoms: biology and morphology of the genera.* Cambridge university press.
Rühland, K.M., Paterson, A.M., and Smol, J.P. (2015). Lake diatom responses to warming: reviewing the evidence. *Journal of Paleolimnology* 54**,** 1-35.
Ruprecht, J.J., and Kunji, E.R. (2020). The SLC25 mitochondrial carrier family: structure and mechanism. *Trends in Biochemical Sciences* 45**,** 244-258.
Ryderheim, F., Grønning, J., and Kiørboe, T. (2022). Thicker shells reduce copepod grazing on diatoms. *Limnology and Oceanography Letters*.
Saini, Y., Chen, J., and Patial, S. (2020). The tristetraprolin family of RNA-binding proteins in cancer: Progress and future prospects. *Cancers* 12**,** 1539.
Sandrini, G., Tann, R.P., Schuurmans, J.M., Van Beusekom, S.A., Matthijs, H.C., and Huisman, J. (2016). Diel variation in gene expression of the CO_2-concentrating mechanism during a harmful cyanobacterial bloom. *Frontiers in Microbiology* 7**,** 551.
Schrader, L., and Schmitz, J. (2019). The impact of transposable elements in adaptive evolution. *Molecular Ecology* 28**,** 1537-1549.
Shrestha, R.P., Tesson, B., Norden-Krichmar, T., Federowicz, S., Hildebrand, M., and Allen, A.E. (2012). Whole transcriptome analysis of the silicon response of the diatom *Thalassiosira pseudonana*. *BMC Genomics* 13**,** 499.
Steffen, M.M., Dearth, S.P., Dill, B.D., Li, Z., Larsen, K.M., Campagna, S.R., and Wilhelm, S.W. (2014). Nutrients drive transcriptional changes that maintain metabolic homeostasis but alter genome architecture in *Microcystis*. *The ISME Journal* 8**,** 2080-2092.
Struyf, E., Smis, A., Van Damme, S., Meire, P., and Conley, D.J. (2009). The global biogeochemical silicon cycle. *Silicon* 1**,** 207-213.
Su, X., Xue, Q., Steinman, A.D., Zhao, Y., and Xie, L. (2015). Spatiotemporal dynamics of microcystin variants and relationships with environmental parameters in Lake Taihu, China. *Toxins* 7**,** 3224-3244.
Sültemeyer, D. (1998). Carbonic anhydrase in eukaryotic algae: characterization, regulation, and possible function during photosynthesis. *Canadian Journal of Botany* 76**,** 962-972.
Takahashi, N., Ogita, N., Takahashi, T., Taniguchi, S., Tanaka, M., Seki, M., and Umeda, M. (2019). A regulatory module controlling stress-induced cell cycle arrest in *Arabidopsis*. *Elife* 8**,** e43944.
Takahashi-Íñiguez, T., Aburto-Rodríguez, N., Vilchis-González, A.L., and Flores, M.E. (2016). Function, kinetic properties, crystallization, and regulation of microbial malate dehydrogenase. *Journal of Zhejiang University-SCIENCE B* 17**,** 247-261.
Talling, J. (1976). The depletion of carbon dioxide from lake water by phytoplankton. *The Journal of Ecology***,** 79-121.
Tang, X., Krausfeldt, L.E., Shao, K., Lecleir, G.R., Stough, J.M., Gao, G., Boyer, G.L., Zhang, Y., Paerl, H.W., and Qin, B. (2018). Seasonal gene expression and the ecophysiological implications of toxic *Microcystis aeruginosa* blooms in Lake Taihu. *Environmental Science & Technology* 52**,** 11049-11059.
Thomas, B. (2016). *Encyclopedia of applied plant sciences.* Academic Press.
Torres, M., Ritchie, R., Lilley, R., Grillet, C., and Larkum, A. (2014). Measurement of photosynthesis and photosynthetic efficiency in two diatoms. *New Zealand Journal of Botany* 52**,** 6-27.
Tréguer, P.J., and De La Rocha, C.L. (2013). The world ocean silica cycle. *Annual Review of Marine Science* 5**,** 477-501.

Tréguer, P.J., Sutton, J.N., Brzezinski, M., Charette, M.A., Devries, T., Dutkiewicz, S., Ehlert, C., Hawkings, J., Leynaert, A., and Liu, S.M. (2021). Reviews and syntheses: The biogeochemical cycle of silicon in the modern ocean. *Biogeosciences* 18**,** 1269-1289.

Turner, E., Ombres, E., Bennett-Mintz, J., Dortch, Q., Broadwater, M., Berger, H., and Harris, M. (2021). "Ocean acidification program: Harmful algal blooms and ocean acidification workshop: Defining a research agenda". NOAA NCCOS, NOAA OAP).

Valenzuela, J.J., López García De Lomana, A., Lee, A., Armbrust, E., Orellana, M.V., and Baliga, N.S. (2018). Ocean acidification conditions increase resilience of marine diatoms. *Nature Communications* 9**,** 1-10.

Van Dam, B.R., Tobias, C., Holbach, A., Paerl, H.W., and Zhu, G. (2018). CO_2 limited conditions favor cyanobacteria in a hypereutrophic lake: an empirical and theoretical stable isotope study. *Limnology and Oceanography* 63**,** 1643-1659.

Van Heukelem, L., Lewitus, A.J., Kana, T.M., and Craft, N.E. (1994). Improved separations of phytoplankton pigments using temperature-controlled high performance liquid chromatography. *Marine Ecology Progress Series***,** 303-313.

Vanderploeg, H., Wilson, A., Johengen, T., Bressie, J.D., Sarnelle, O., Liebig, J., Robinson, S., and Horst, G. (2013). Role of selective grazing by dreissenid mussels in promoting toxic *Microcystis* blooms and other changes in phytoplankton composition in the Great Lakes. *Quagga and Zebra Mussels: Biology, Impacts, and Control***,** 509-523.

Vanderploeg, H.A., Liebig, J.R., Carmichael, W.W., Agy, M.A., Johengen, T.H., Fahnenstiel, G.L., and Nalepa, T.F. (2001). Zebra mussel (*Dreissena polymorpha*) selective filtration promoted toxic *Microcystis* blooms in Saginaw Bay (Lake Huron) and Lake Erie. *Canadian Journal of Fisheries and Aquatic Sciences* 58**,** 1208-1221.

Vardi, A., Thamatrakoln, K., Bidle, K.D., and Falkowski, P.G. (2009). Diatom genomes come of age. *Genome Biology* 9**,** 245.

Vázquez-Acevedo, M., Vega-Deluna, F., Sánchez-Vásquez, L., Colina-Tenorio, L., Remacle, C., Cardol, P., Miranda-Astudillo, H., and González-Halphen, D. (2016). Dissecting the peripheral stalk of the mitochondrial ATP synthase of chlorophycean algae. *Biochimica et Biophysica Acta (BBA)-Bioenergetics* 1857**,** 1183-1190.

Verspagen, J.M., Snelder, E.O., Visser, P.M., Huisman, J., Mur, L.R., and Ibelings, B.W. (2004). Recruitment of Benthic Microcystis (cyanophyceae) to the Water Column: Internal Buoyancy Changes or Resuspension? 1. *Journal of Phycology* 40**,** 260-270.

Verspagen, J.M., Van De Waal, D.B., Finke, J.F., Visser, P.M., Van Donk, E., and Huisman, J. (2014). Rising CO_2 levels will intensify phytoplankton blooms in eutrophic and hypertrophic lakes. *PloS One* 9.

Volcani, B. (1981). "Cell wall formation in diatoms: morphogenesis and biochemistry," in *Silicon and siliceous structures in biological systems*. Springer), 157-200.

Watson, S.B., Whitton, B.A., Higgins, S.N., Paerl, H.W., Brooks, B.W., and Wehr, J.D. (2015). "Harmful Algal Blooms," in *Aquatic Ecology, Freshwater Algae of North America,* eds. J.D. Wehr, R.G. Sheath & P.J. Kociolek. Second ed (Aquatic Ecology: Academic Press), 873-920.

Wells, M.L., Karlson, B., Wulff, A., Kudela, R., Trick, C., Asnaghi, V., Berdalet, E., Cochlan, W., Davidson, K., and De Rijcke, M. (2020). Future HAB science: Directions and challenges in a changing climate. *Harmful Algae* 91**,** 101632.

Wilhelm, C., Büchel, C., Fisahn, J., Goss, R., Jakob, T., Laroche, J., Lavaud, J., Lohr, M., Riebesell, U., and Stehfest, K. (2006). The regulation of carbon and nutrient assimilation in diatoms is significantly different from green algae. *Protist* 157**,** 91-124.

Wilhelm, S., Bullerjahn, G., and Rlm, M. (2020). The complicated and confusing ecology of *Microcystis* blooms. *mBio*.

Wu, Y., Campbell, D.A., Irwin, A.J., Suggett, D.J., and Finkel, Z.V. (2014). Ocean acidification enhances the growth rate of larger diatoms. *Limnology and Oceanography* 59**,** 1027-1034.

Zagarese, H.E., Sagrario, M.D.L.Á.G., Wolf-Gladrow, D., Nõges, P., Nõges, T., Kangur, K., Matsuzaki, S.-I.S., Kohzu, A., Vanni, M.J., and Özkundakci, D. (2021). Patterns of CO_2 concentration and inorganic carbon limitation of phytoplankton biomass in agriculturally eutrophic lakes. *Water Research* 190**,** 116715.

Zepernick, B.N., Denison, E.R., Chaffin, J.D., Bullerjahn, G.S., Pennacchio, C.P., Frenken, T., Peck, D.H., Anderson, J.T., Niles, D., and Zastepa, A. (2022a). Metatranscriptomic Sequencing of Winter and Spring Planktonic Communities from Lake Erie, a Laurentian Great Lake. *Microbiology Resource Announcements***,** e00351-00322.

Zepernick, B.N., Gann, E.R., Poiund, H.L., Martin, R.M., Krausfeldt, L.E., Chaffin, J.D., and Wilhelm, S.W. (2021). Elevated pH conditions associated with *Microcystis* spp. blooms decrease viability of the cultured diatom *Fragilaria crotonensis* and natural diatoms in Lake Erie. *Frontiers in Microbiology* 12**,** 598736.

Zepernick, B.N., Truchon, A.R., Gann, E.R., and Wilhelm, S.W. (2022b). Draft Genome Sequence of the Freshwater Diatom *Fragilaria crotonensis* SAG 28.96. *Microbiology Resource Announcements***,** e00289-00222.

Zepernick, B.N., Wilhelm, S.W., Bullerjahn, G.S., and Paerl, H.W. (2022c). Climate change and the aquatic continuum: A cyanobacterial comeback story. *Environmental Microbiology Reports*.

Appendix

Table 4.1 Statistical analysis of *F. crotonensis* morphological features (mean area, mean biovolume, mean length, mean width, mean roughness, and mean avg. green) collected at T_f of the morphology assay as a function of pH. Statistical analyses performed using unpaired two-tailed *t*-tests.

Treatment comparison	Summary	P value
pH 7.7 vs. pH 9.2 Area (μm^2)	**	p=0.0074
pH 7.7 vs. pH 9.2 Biovolume (μm^3)	*	p=0.0310
pH 7.7 vs. pH 9.2 Length (µm)	**	p=0.0017
pH 7.7 vs. pH 9.2 Width (µm)	ns	p=0.0553
pH 7.7 vs. pH 9.2 Roughness	***	p=0.0002
pH 7.7 vs. pH 9.2 Avg. Green Content	****	p<0.0001

Table 4.2 Statistical analysis of *F. crotonensis* filament concentrations and Chlorophyll *a* autofluorescence collected at T_f of the photopigment assay as a function of pH. Statistical analyses performed using unpaired two-tailed *t*-tests

Treatment comparison	Summary	P value
pH 7.7 vs. pH 9.2 filament conc. (filaments·mL^{-1})	ns	p=0.1745
pH 7.7 vs. pH 9.2 Chlorophyll *a* (fsu)	****	p<0.0001

Table 4.3 Statistical analysis of *F. crotonensis* normalized photopigment concentrations (Chlorophyllide *a*, Chlorophyll *a*, Chlorophyll *c*1*c*2, Total Chlorophyll *a*, β-carotene, Violaxanthin, Diadinoxanthin, Fucoxanthin, Neoxanthin) and photopigment ratios (Total Carotenoids/Total Chl *a*, β-car/ Total Chl *a*, Viola/ Total Chl *a*, Diadino/Total Chl *a*, Total Chl *a*/Chl *c*1*c*2) collected at T_f of the photopigment assay as a function of pH. Statistical analyses performed using unpaired two-tailed *t*-tests.

Treatment comparison	Summary	P value
pH 7.7 vs. pH 9.2 Chlorophyllide *a* (fg·µm fil^{-1})	ns	p=0.8657
pH 7.7 vs. pH 9.2 Chlorophyll *a* (fg·µm fil^{-1})	ns	p=0.3263
pH 7.7 vs. pH 9.2 Chlorophyll *c*1*c*2 (fg·µm fil^{-1})	ns	p=0.9484
pH 7.7 vs. pH 9.2 Total Chlorophyll *a* (fg·µm fil^{-1})	ns	p=0.3503
pH 7.7 vs. pH 9.2 β-carotene (fg·µm fil^{-1})	**	p=0.0015
pH 7.7 vs. pH 9.2 Violaxanthin (fg·µm fil^{-1})	**	p=0.0090
pH 7.7 vs. pH 9.2 Diadinoxanthin (fg·µm fil^{-1})	*	p=0.0189
pH 7.7 vs. pH 9.2 Fucoxanthin (fg·µm fil^{-1})	ns	p=0.4594
pH 7.7 vs. pH 9.2 Neoxanthin (fg·µm fil^{-1})	ns	p=0.3307
pH 7.7 vs. pH 9.2 Total Carotenoids/Total Chl *a*	ns	p=0.2207
pH 7.7 vs. pH 9.2 β-car/ Total Chl *a*	***	p=0.0002
pH 7.7 vs. pH 9.2 Viola/ Total Chl *a*	**	p=0.0093
pH 7.7 vs. pH 9.2 Diadino/Total Chl *a*	***	p=0.0008
pH 7.7 vs. pH 9.2 Total Chl *a*/Chl *c*1*c*2	ns	p=0.4335

Table 4.4 Statistical analysis of *F. crotonensis* PhytoPAM analyses ($Fv \cdot Fm^{-1}$, ETR_{max}, I_k) collected at T_f of the photo physiology assay as a function of pH. Statistical analyses performed using unpaired two-tailed *t*-tests.

Table 4.4 Statistical analysis of *F. crotonensis* PhytoPAM analyses ($Fv \cdot Fm^{-1}$, ETR_{max}, I_k) collected at T_f of the photo physiology assay as a function of pH. Statistical analyses performed using unpaired two-tailed *t*-tests.		
Treatment comparison	**Summary**	**P value**
pH 7.7 vs. pH 9.2 $Fv \cdot Fm^{-1}$	ns	p=0.3089
pH 7.7 vs. pH 9.2 ETR_{max} (µmol $e^-/m^2 \cdot s$)	****	p<0.0001
pH 7.7 vs. pH 9.2 I_k (µmol photons/ $m^2 \cdot s$)	****	p<0.0001

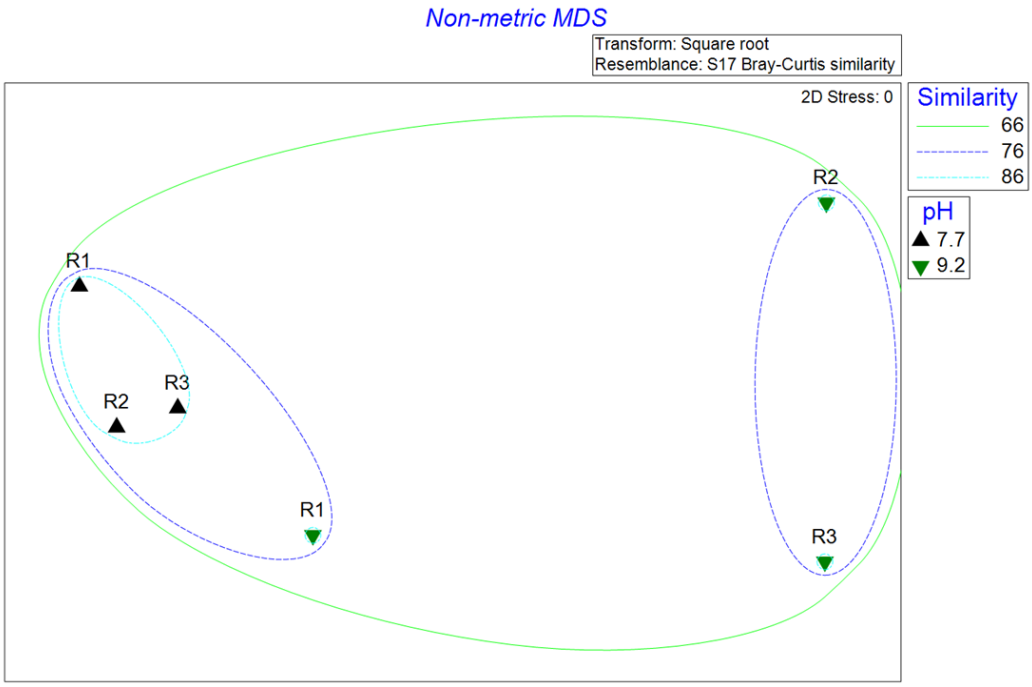


Figure 4.7 Non-metric Multidimensional analysis (nMDS) of similarity between pH 7.7 and pH 9.2 transcriptomes (TPM). pH 7.7 replicates are indicated by black triangles, pH 9.2 replicates are indicated by inverted green triangles.

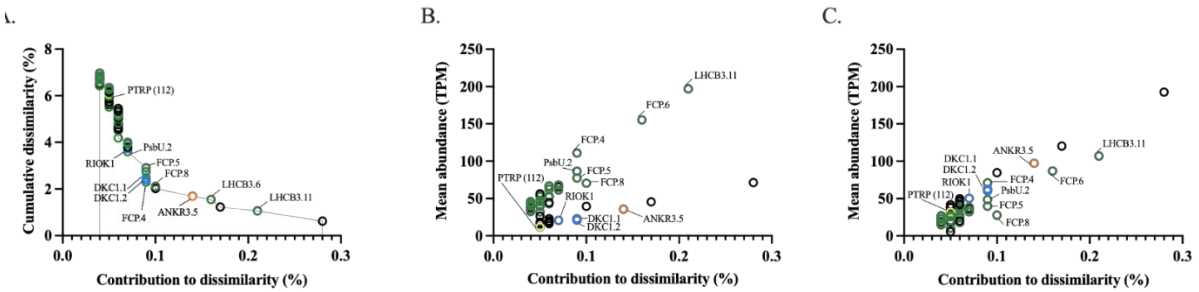


Figure 4.8 Top 50 genes contributing to mean pH treatment dissimilarity (~27%) determined by Similarity Percentages (SIMPER). Genes categorized in COG category photosynthesis depicted in green, genes categorized in cell cycle control, cell division, chromosome partitioning depicted in blue, genes categorized in cell wall, membrane, envelope biogenesis depicted in orange, and genes categorized in mobilome: transposons; prophages depicted in yellow. Only annotated genes were included in final reports (A) Contribution to dissimilarity (%) and cumulative dissimilarity (%) of the top 50 annotated genes driving mean dissimilarity between pH 7.7 and pH 9.2 normalized (TPM) expression values. (B) Mean abundance (TPM) of top 50 genes driving dissimilarity within the pH 7.7 replicates. (C) Mean abundance (TPM) of top 50 genes driving dissimilarity within pH 9.2 replicates.

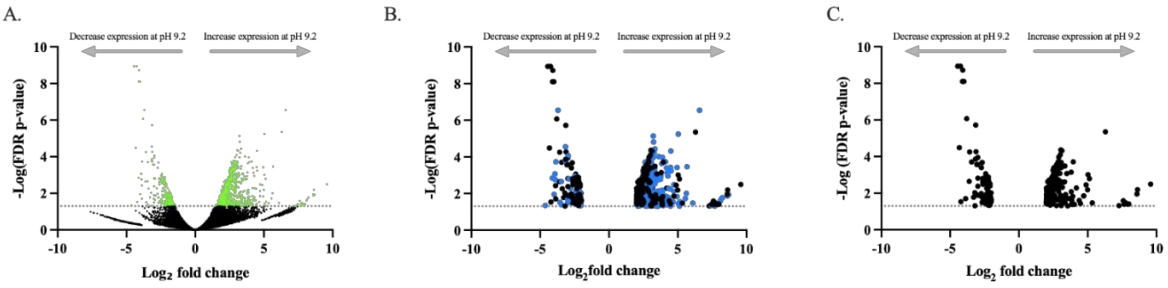


Figure 4.9 Volcano plots of differentially expressed genes at pH 9.2 compared to pH 7.7. (A) All genes within the pH transcriptome (B) All 713 DE genes according to the statistical cutoff (FDR-corrected p-value ≤ 0.05, $\log_2$ |fold-change| > 2) (C) All 435 DE and annotated genes with an assigned function used for all downstream analyses in this study.

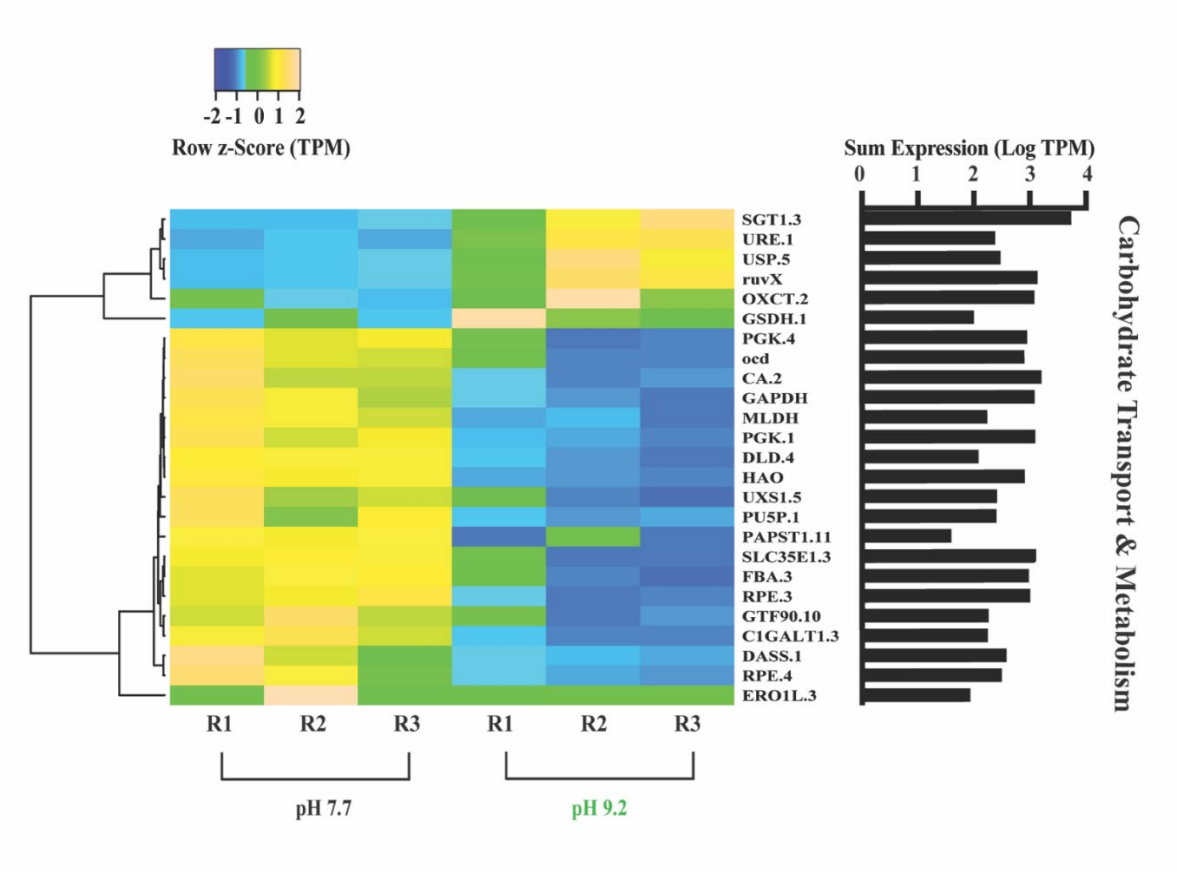


Figure 4.10 Heat map depicting differentially expressed genes relating to the "Carbohydrate transport and metabolism" COG category. All TPM values were row z-scored, with increases in proportional transcript abundance indicated in yellow, and decreases in proportional transcript abundance indicated in blue. The sum of transcripts across all treatments (LogTPM) is indicated for each gene.

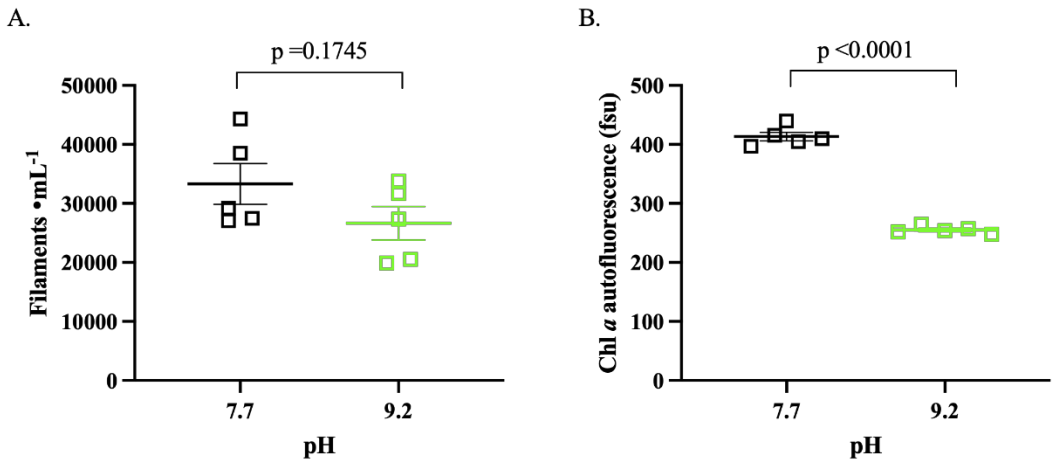


Figure 4.11 Flow cytometry and fluorometer analyses corresponding to the pigment pH assay. (A) *F. crotonensis* concentration (filaments • mL^{-1}) at the beginning (T_i) and end of the experiment (T_f). pH 7.7 replicates denoted by open, black squares. pH 9.2 replicates denoted by open, green squares. (B) *F. crotonensis* Chl *a* autofluorescence at (T_i) and (T_f). pH 7.7 replicates denoted by open, black squares. pH 9.2 replicates denoted by open, green squares. Mean values indicated by solid vertical bars, with variability (SEM) indicated.

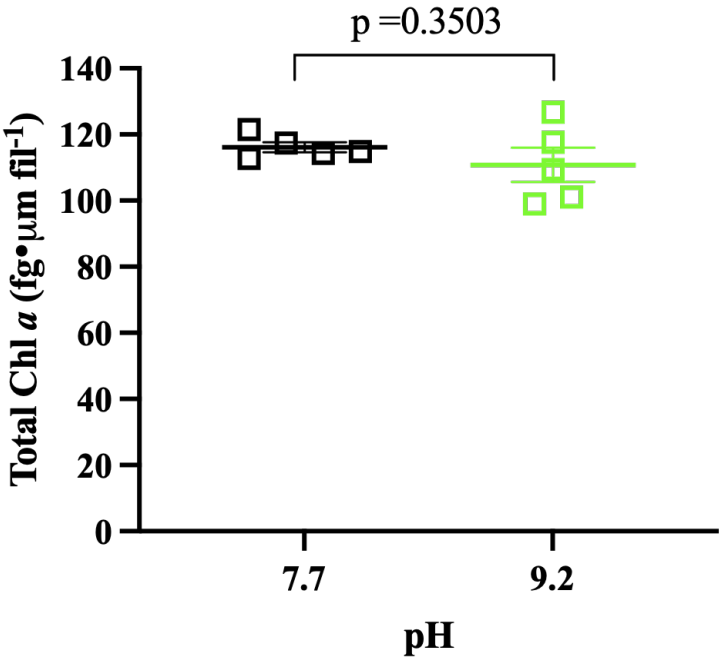


Figure 4.12 Total Chlorophyll *a* photopigment data concentrations collected at (T_f). pH 7.7 replicates denoted by open, black squares. pH 9.2 replicates denoted by open, green squares. (A) Net Chlorophyll *a* pigment concentration (µg • L^{-1}) of *F. crotonensi*s filaments. (B) Normalized Total Chlorophyll *a* pigment concentration (fg • µm fil^{-1}) of *F. crotonensi*s filaments.

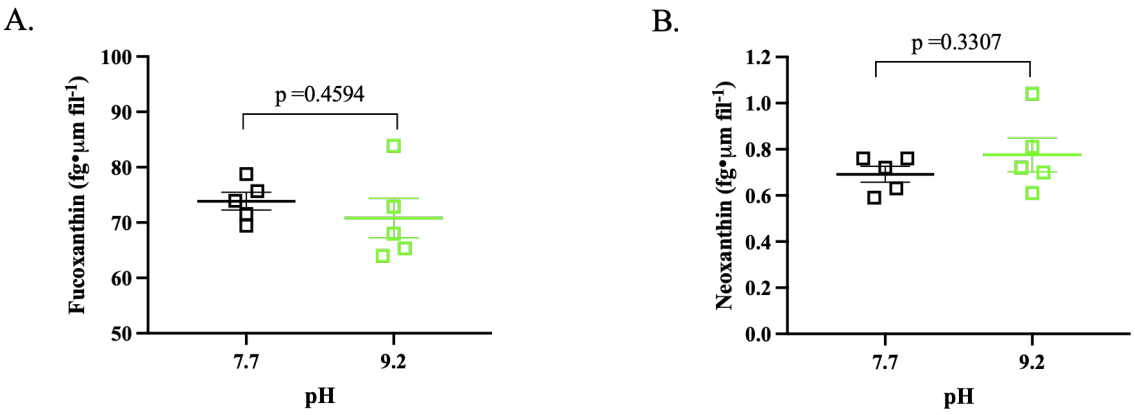


Figure 4.13 Fucoxanthin and Neoxanthin photopigment pH assay results collected at (T_f). pH 7.7 replicates denoted by open, black squares. pH 9.2 replicates denoted by open, green squares. (A) Fucoxanthin pigment concentration (fg • µm fil^{-1}) of *F. crotonensi*s filaments. (B) Neoxanthin pigment concentration (fg • µm fil^{-1}) of *F. crotonensi*s filaments.

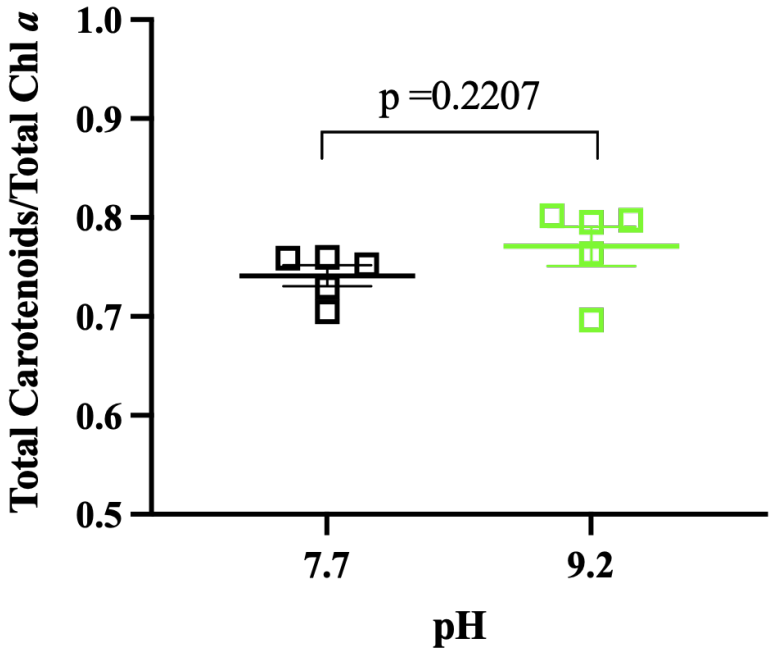


Figure 4.14 Ratio of total carotenoids:total Chlorophyll *a* pigment in *F. crotonensis* filaments. pH 7.7 replicates denoted by open, black squares. pH 9.2 replicates denoted by open, green squares.

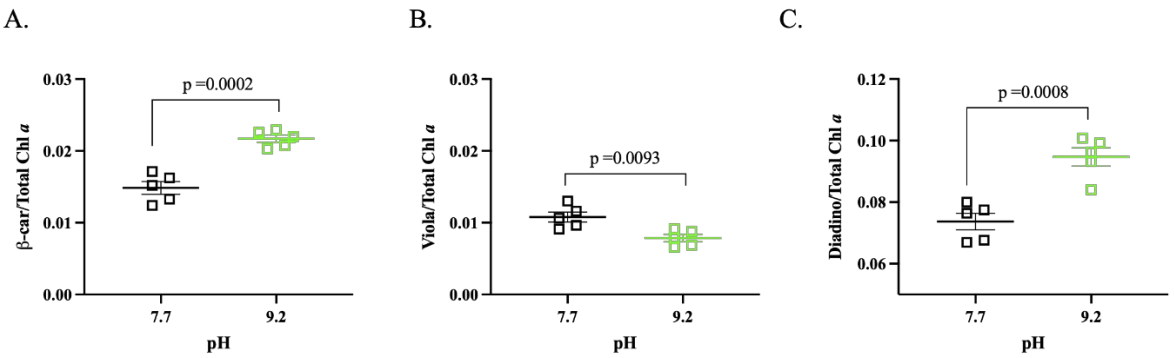


Figure 4.15 Ratios of significantly altered carotenoid pigments:total Chlorophyll *a* pigments in *F. crotonenis* filaments. pH 7.7 replicates denoted by open, black squares. pH 9.2 replicates denoted by open, green squares. (A) Ratio of β-carotene: total Chlorophyll *a* pigment concentration in filaments. (B) Ratio of Violaxanthin:total Chlorophyll *a* pigment concentration in filaments. (C) Ratio of Diadinoxanthin:total Chlorophyll *a* pigment concentration in filaments.

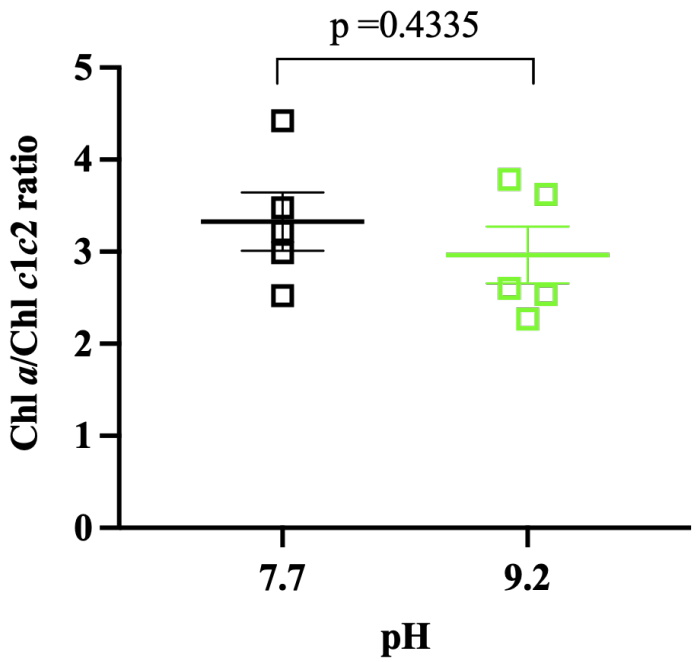


Figure 4.16 Ratio of Chlorophyll *a*:Chlorophyll c^1c^2 pigment concentration in *F. crotonensis* filaments.

CHAPTER V: DIATOM RESPONSES TO DECREASING ICE COVER IN LAKE ERIE

Publication Note

This chapter is a draft version of a manuscript to be submitted as a peer-reviewed, published article in *ISME Communications* by Brittany N. Zepernick, Elizabeth R. Dension, Naomi E. Gilbert, Emily E. Chase, Alexander R. Truchon, Robbie M. Martin, Thijs Frenken, William R. Cody, Justin D. Chaffin, George S. Bullerjahn, Robert Michael L. McKay, and Steven W. Wilhelm.

Samples were collected by RMLM, GB, TF and JC. RNA extractions and quality assessment performed by BZ. Metatranscriptomic processing performed by BZ, NG, EC and LD using a pipeline established by NG. Python scripts associated with metatranscriptomic pipeline were written by AT. Statistical analyses and figures were made by RM and BZ. The first draft was written by BZ. All authors contributed to the drafting of the current manuscript.

Abstract

The ecophysiology of phytoplankton communities beneath the ice has been a “black box” of limnology for decades. Winter surveys conducted throughout 2007-2012 discovered prolific winter diatom blooms embedded within and under the Lake Erie ice. These studies concluded ice plays a vital role in winter diatom dynamics, and concluded prolific winter-spring diatom blooms are a significant driver of summer hypoxia. Yet, due to logistical constraints the ecophysiology of winter diatom blooms and the role of ice in their bloom cycle remains widely unstudied. We opened this “black box” by using the first wide scale metatranscriptomic survey of the winter Lake Erie water column. We demonstrated ice cover alters diatom bloom magnitude and phylogeny. Further, we discovered polar centric diatoms significantly increased the expression of fasciclin genes, which we hypothesize is a means to “raft” together and optimize light acquisition during turbid conditions of the ice-free water column. The winter of 2023 was the lowest mean annual ice cover for Lake Erie on record, indicating large-scale climatic changes are already underway. Hence, it is necessary to investigate how diatoms respond to ice conditions of today to predict how they will fare in a climatically altered tomorrow.

Introduction

Winter has historically been considered "ecologically unimportant" with winter limnology only recently defined as a "New Frontier" (Powers and Hampton, 2016). Indeed, winter was often considered a period of planktonic death and persistence rather than growth (Sommer et al., 1986; Sommer et al., 2012). Yet, we now know this is far from the truth (Ozersky et al., 2021). Active planktonic growth under the ice was first reported in Lake Erie in the 1930's (Chandler, 1940; Chandler, 1942), but has since remained largely unexplored. A winter limnological survey conducted between 2007-2010 discovered dense blooms primarily comprised of the centric, filamentous diatom *Aulacoseira islandica* (Coscinodiscophyceae) distributed within and under the ice of Lake Erie (Twiss et al., 2012). This finding ignited interest in the Lake Erie winter water column, with subsequent studies demonstrating ice-associated communities were dominated by centric colonial diatoms such as *A. islandica* and *Stephanodiscus* spp. (Mediophyceae), while pennate diatoms often formed < 1% of the diatom community (D'souza, 2012; Twiss et al., 2012; Wilhelm et al., 2014; Beall et al., 2016; Edgar et al., 2016). In fact, chlorophyll *a* (Chl *a*) concentrations during winter surpassed those of spring (Twiss et al., 2012) and examinations of silica deposition in frustules demonstrated cells were metabolically active (Saxton et al., 2012). Additional studies determined winter-spring diatom biovolumes can surpass summer cyanobacterial biovolumes by 1.5- to 6-fold (Reavie et al., 2016), with diatom blooms driving recurrent summer hypoxia (*i.e.,* dead zones) within the central basin of Lake Erie (Wilhelm et al., 2014; Reavie et al., 2016; Ozersky et al., 2021).

One proposed physiological contributor to the ecologic success of winter diatoms is their ability to attach to ice cover *via* symbiotic interactions with ice-nucleating bacteria, which allows diatoms to co-locate themselves to the under-ice surface to maintain an optimal light climate for photosynthesis (D'souza, 2012; D'souza et al., 2013). Another contributor to success includes

psychrophilic adaptations that increase membrane fluidity and enhance light-harvesting under low-light conditions (Edgar et al., 2016). However, to date there is little known of winter diatom bloom ecophysiology. This critical gap is largely attributed to the inability to maintain these taxa (e.g. *A. islandica* and *Stephanodiscus binderanus*) in culture (D'souza, 2012). To circumvent this, recent studies have turned to molecular approaches to characterize *in situ* winter diatom communities (Beall et al., 2016; Edgar et al., 2016). These studies offer further support that ice cover plays a critical role in shaping winter diatom ecophysiology, with Beall et al., (Beall et al., 2016) noting diatom abundances of ice-associated *A. islandica* declined during the low-ice winter of 2012. While this study indicated centric, filamentous diatom taxa significantly decline during years of low ice cover due to wind-induced turbidity/mixing, it did not identify species-specific intracellular mechanisms behind this trend. Elucidating the ecophysiological response of the winter diatom community to ice coverage is of present-day importance, as Lake Erie is experiencing unprecedented declines in ice cover due to climate change (Mason et al., 2016; Wang et al., 2018; Ozersky et al., 2021). Indeed, projections suggest ice cover may disappear entirely by the end of the century (Filazzola et al., 2020). Given the keystone role of diatoms in freshwater food webs and global biogeochemical cycles (Nelson et al., 1995; Struyf et al., 2009; Rühland et al., 2015; Benoiston et al., 2017), there is a pressing need to elucidate current winter diatom ecophysiology in order to better project how they will respond to a climatically altered future.

In this study, we employed metatranscriptomics to investigate how Lake Erie winter diatom communities respond to ice cover vs. ice-free conditions. To our knowledge, this is the first large-scale bioinformatic assessment of the winter Lake Erie community. Driven by collaborative efforts with the U.S. and Canadian Coast Guards (McKay et al., 2011),

opportunistic samples were collected throughout 2019 and 2020 yielding winter samples collected from both the ice-covered (2019) and ice-free (2020) winter water column (Zepernick et al., 2022a). The survey included spring samples that serve as an outgroup. From this we offer new hypotheses on the dynamics of winter diatom communities and their physiological response to climate-induced variations in lake surface ice.

Methods

Lake Erie winter-spring water column sampling

Samples of opportunity (n = 77) from the Lake Erie planktonic community were collected across temporal, spatial, and climatic gradients throughout the winter of 2019 and 2020. This large-scale collaborative effort included multiple surveys conducted by USCGC *Neah Bay*, CCGS *Limnos* and M/V *Orange Apex,* resulting in a large metatranscriptomic dataset (Zepernick et al., 2022a). Prior to sample collection, water column physiochemical parameters were recorded along with meteorological conditions and ice cover observations. Briefly, water samples were collected from 0.5 m below the surface and processed for analyses of dissolved and particulate nutrients (mg L^{-1}), size-fractionated (<0.22-μm and <20 μm) Chl *a* biomass (μg L^{-1}), phytoplankton taxonomy and enumeration (Cells L^{-1}), and total community RNA. Class-level taxonomic assignments (i.e., Mediophyceae, Coscinodiscophyceae) of diatom microscopy results were performed according to the Barcode of Life Data System (BOLD) (Ratnasingham and Hebert, 2007). Metadata are available online at the Biological and Chemical Oceanography Data Management Office (BCO-DMO) (Bullerjahn et al., 2022). Refer to Appendix Methods/Results for further detail.

RNA extraction and sequencing

RNA extractions were performed using previously described acid phenol-chloroform methods with ethanol precipitation (Martin and Wilhelm, 2020). Residual DNA in samples was digested *via* a modified version of the Turbo DNase protocol using the Turbo DNA-free kit (Ambion, Austin, TX, USA). Samples were determined to be DNA-free *via* the absence of a band in the agarose gel after PCR amplification using 16S rRNA primers as previously reported (Zepernick et al., 2022a). Samples were quantified using the Qubit RNA HS Assay Kit (Invitrogen, Waltham, MA, USA) and sent to the Department of Energy Joint Genome Institute (DOE JGI) for ribosomal RNA reduction and sequencing using an Illumina NovaSeq S4 2 × 151-nucleotide indexed run protocol (15 million 150-bp paired-end reads per library) as reported previously (Zepernick et al., 2022a).

Metatranscriptomic analysis

Filtering and trimming of raw reads was performed by DOE JGI using BBDuk (v.38.92) and BBMap (v.38.86) (Bushnell, 2014a; Clum et al., 2021). Bioinformatic processing was conducted using a prior-established metatranscriptomic workflow (Gilbert et al., 2022). Trimmed and filtered libraries (n = 77) were concatenated and assembled (co-assembled) using MEGAHIT (v.1.2.9) (Li et al., 2016). Co-assembly statistics were determined *via* QUAST QC (v.5.0.2) (Gurevich et al., 2013). Trimmed reads were mapped to the co-assembly using BBMap (default settings) (v.38.90) (Bushnell, 2014a). Gene predictions within the co-assembly were called using MetaGeneMark (v.3.38) (Zhu et al., 2010) using the metagenome style model. Taxonomic annotations of predicted genes were determined using the MetaGeneMark protein file, EUKulele (v.1.0.6) (Krinos et al., 2020) and the PhyloDB database (v.1.076). Genes were functionally

annotated using eggNOG-mapper using a specified e-value of $1e^{-10}$ (v.2.1.7) (Cantalapiedra et al., 2021). Following, featureCounts (Liao et al., 2014) within the subread (v.2.0.1) package was used to tabulate read counts to predicted genes. Mapped reads were normalized to TPM (Transcripts Per Million), representing relative "expression" values.

To investigate transcriptional patterns of the winter diatom bloom community, we focused on a subset of libraries (n=20) selected for consistency in sample collection methods (whole water filtration) and diatom abundances (Appendix Table 5.1). Thus, all data reported hereafter pertains to these 20 libraries. Raw data for all 77 transcriptomic libraries are available at the JGI Data Portal (https://data.jgi.doe.gov) under Proposal ID 503851 (Zepernick et al., 2022a). Refer to Appendix Methods/Results and Appendix Attachments for further detail.

Phylogenetic analysis

A phylogenetic tree of fasciclin containing domains (proteins of interest) was produced using differentially expressed (DE) putative proteins of this study (n=18), domains recovered from the eggNOG orthology database and publicly available domains from NCBI (Wheeler et al., 2007). A custom database was curated using all NCBI diatom proteins. A DIAMOND (v.2.0.15) (Buchfink et al., 2015) blastp alignment was performed with putative fasciclin proteins and eggNOG domains against the diatom database to recover all putative diatom fasciclin domains. The recovered domains were then aligned (DIAMOND blastp) against the NCBI non-redundant database. These results were compiled and collapsed to 80% similarity using CD-HIT (v.4.7) (Fu et al., 2012) and a multiple sequence alignment was performed using MAFFT (v.7.310) (Katoh and Standley, 2013) with 500 iterations. Gaps were closed using trimAl with gappyout (v.1.4.rev15) (Capella-Gutiérrez et al., 2009) and examined using AliView (v.1.28)

(Larsson, 2014). A phylogenetic tree (1000 bootstraps) was constructed using a model test selecting for a general non-reversible Q matrix model estimated from Pfam database (v. 31) (El-Gebali et al., 2019) with a gamma rate heterogeneity. The consensus tree was visualized using iTOL (Letunic and Bork, 2019). Refer to Appendix Methods/Results and Appendix Attachments for further detail.

Statistical analyses

Comparisons of water column physiochemical features by ice cover were made in Prism (v. 9.3.1) *via* two-tailed unpaired *t*-tests. Variability in expression (TPM) between transcriptomic libraries was assessed *via* ANalysis Of Similarities (ANOSIM) and Similarity Percentage (SIMPER) analyses using PRIMER (v.7) (Clarke and Gorley, 2015). Bray-Curtis similarity and non-metric multi-dimensional scaling (nMDS) were performed in R. Differential expression (DE) of transcript abundance was performed using DESeq2 in R (v.1.28.1) (Love et al., 2014). Genes with an absolute $\log_2$ fold change (Log_2FC) >2 and adjusted p-value of < 0.05 were considered differentially expressed. Z-scores reported in heat maps were calculated by heatmapper.ca (Clustering method: Average linkage, Distance measurement method: Pearson) (Babicki et al., 2016)) using the DESeq2 variance stabilizing transformed values (VST) (Babicki et al., 2016). Refer to Appendix Methods/Results for further detail.

Results

Physiochemical profiles and winter community characterization

Samples were collected across 12 sites throughout the central basin of Lake Erie with true biological replication at a subset of stations (Figure 5.1A) (Appendix Table 5.1). Temporally,

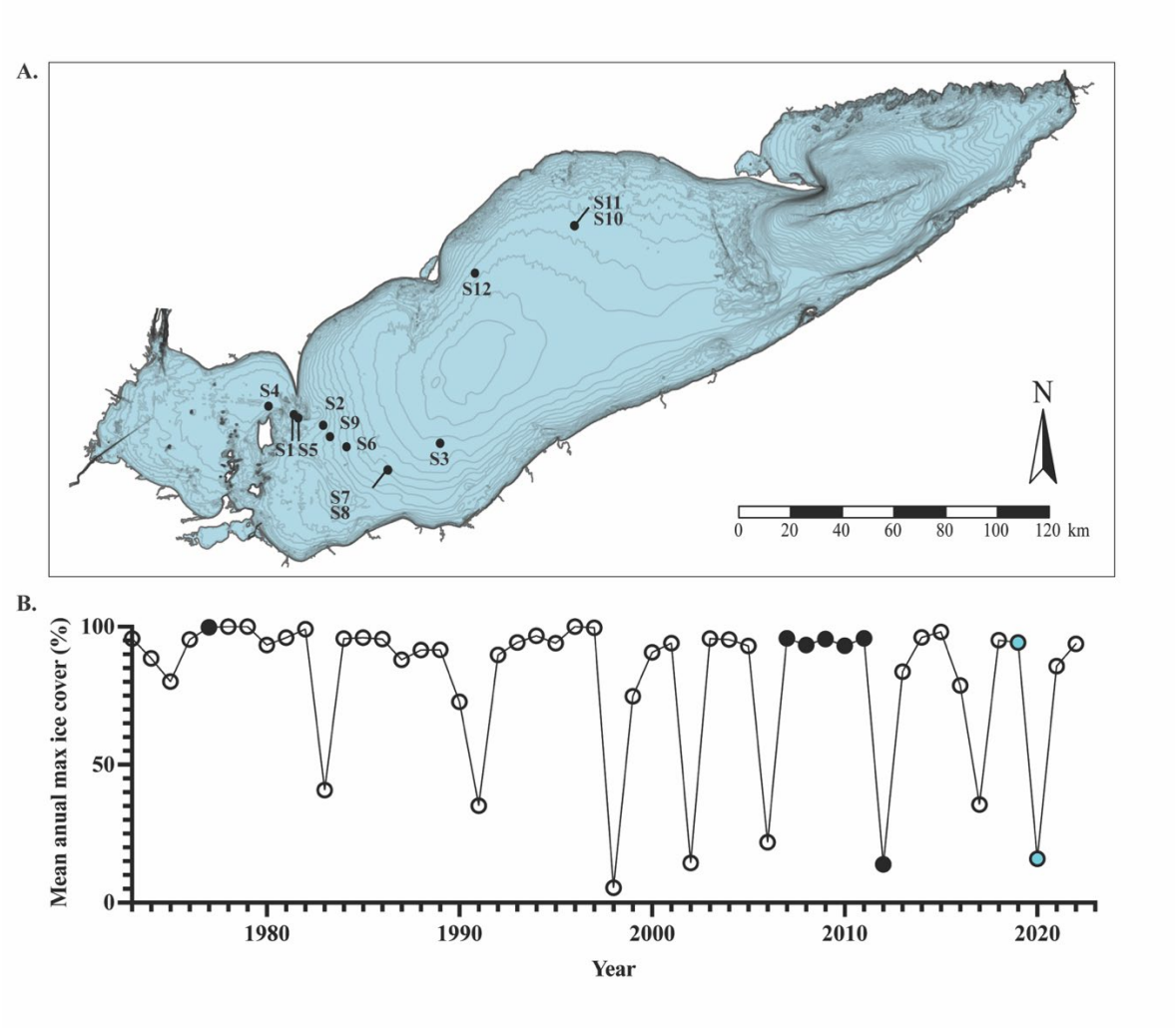


Figure 5.1: Spatial and climatic variability across samples. (A) Sample sites across Lake Erie visited throughout winter-spring 2019 and 2020. **(B)** Historical trends in Lake Erie mean annual maximum ice cover (%). Open circles are years that (to our knowledge) do not have peer-reviewed published survey data. Solid black circles are years that were previously surveyed in prior published studies. Solid blue circles are years sampled in this study. Figure adapted from data retrieved from NOAA GLERL database (NOAA-GLERL).

the samples span February-March 2019 and February-June 2020, yielding 14 winter and 6 spring libraries. Climatically, the winter of 2019 was a year of high ice cover (mean maximum ice cover of 80.9%), whereas winter 2020 was a year of negligible ice cover (mean maximum ice cover of 19.5%) (NOAA, 2021) (Figure 5.1B). Libraries 1-4 were collected during ice cover (ranging from 2.54 - 15.24 cm in thickness) while winter libraries 5-14 were collected during no ice cover conditions. Winter lake surface temperatures ranged from ~0-6 °C across sample sites (Appendix Figure 5.8A). Overall, nutrient concentrations at ice-covered sites were not significantly different from ice-free sites save for nitrate (Appendix Figure 5.8B-H). While not significant ($p \geq 0.13$), the highest total Chl *a* concentrations (> 0.22 μm) coincided with ice cover (Figure 5.2A, B). The larger sized-fraction of phytoplankton contributed an average of 70% (+/- 27%) to total Chl *a* during ice cover and 50% (+/- 13%) in ice-free winter sites (Appendix Figure 5.9), but the differences were not significant ($p = 0.22$). Cell concentrations of diatoms (Bacillariophyta) dominated the winter water column regardless of ice conditions, with other eukaryotic phytoplankton (*e.g.,* Chlorophyta, Cryptophyta, and Dinophyta) present at concentrations 1-2 orders of magnitude lower (Appendix Figure 5.10). While Bacillariophyta concentrations decreased slightly at ice-free sites ($p = 0.33$), Dinophyta concentrations significantly increased ($p = 0.03$), with Cryptophyta and Chlorophyta exhibiting similar trends ($p \geq 0.05$). Overall, centric diatoms dominated the winter diatom community while pennate diatoms were found at concentrations an order of magnitude lower (Figure 5.2C, D). Despite this dominance, centric diatoms demonstrated a decreasing trend in ice-free samples while pennate diatoms exhibited significant increases in ice-free samples ($p = 0.03$) albeit remaining at low abundances. Cell concentrations of the centric bloom formers *Stephanodiscus* spp. (Mediophyceae) and *A. islandica* (Coscinodiscophyceae) were generally highest during ice cover (Figure 5.2E, F).

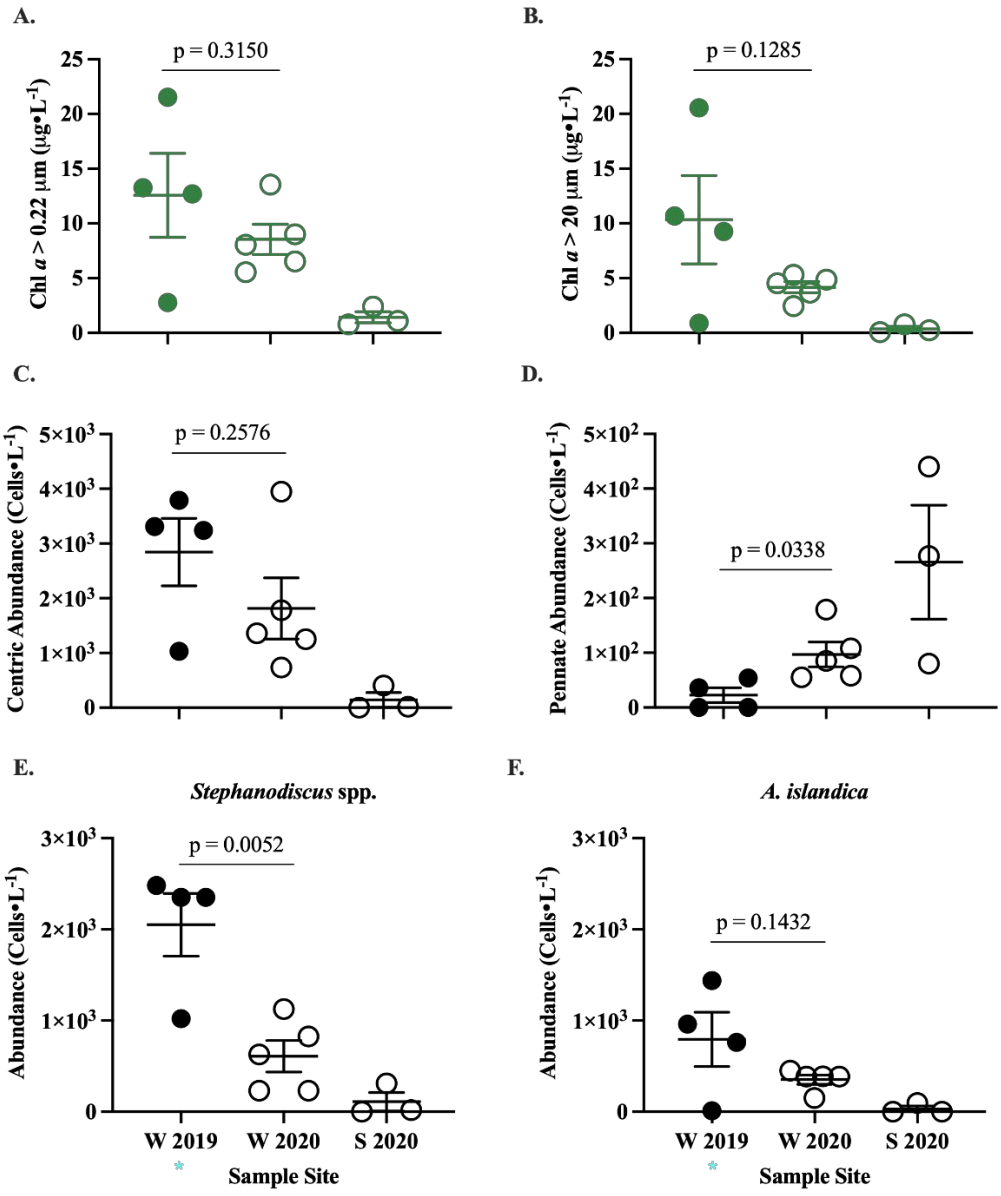


Figure 5.2: Characterization of the biotic community across the 12 Lake Erie sample sites. Samples are organied on the x-axis by season (W = winter, S = spring) and year. Solid shapes indicate the sample was collected during ice cover (2019) open shapes indicate the sample was collected during no ice cover (2020). Ice cover samples are indicated by a blue asterisk. **(A)** Total Chlorophyll *a* concentration of the whole water column community (i.e., >0.22 µm in size) (µg L^{-1}) **(B)** Chlorophyll *a* concentration of the large size fractioned community (i.e., >20 µm in size) (µg L^{-1}). **(C)** Cell abundances (Cells $\cdot L^{-1}$) of centric diatoms (*Stephanodiscus* spp. + *A. islandica* + Small centric diatoms of 5-20 µm). **(D)** Cell abundances of pennate diatoms (*Fragilaria* spp. + *Asterionella formosa* + *Nitzschia* spp). **(E)** Cell abundances (Cells $\cdot L^{-1}$) of *Stephanodiscus* spp., a common winter bloom-forming taxon (Mediophyceae class). **(F)** Cell abundances (Cells $\cdot L^{-1}$) of *A. islandica,* a common winter diatom bloom-forming taxon (Coscinodiscophyceae class).

Notably, *Stephanodiscus* spp. concentrations were significantly higher than *A. islandica* in ice-covered samples ($p = 0.03$), yet not significantly greater than *A. islandica* in ice-free samples ($p = 0.19$) (Appendix Figure 5.11). Concentrations of *Stephanodiscus* spp., were significantly reduced by ~50% in ice-free samples, ($p = 0.005$) (Figure 5.2E), while *A. islandica* abundances were not ($p = 0.14$) (Figure 5.2F). Further, while concentrations of small centric diatoms (5-20 μm size) were not detected in ice covered samples, they were found to range from ~300-3,000 cells L^{-1} in ice-free samples (Appendix Figure 5.12). While small centric diatom taxa accounted for ~83% of the winter diatom community at site 8, they otherwise contributed an average of 26% to the total diatom community in ice-free samples (Appendix Figure 5.13). Refer to the Appendix Material for further detail (Appendix Attachments 5.1D-G).

Transcriptomic response of winter diatom community to ice cover

While the number of raw reads mapping to Eukaryota decreased in ice-free samples, every other domain increased in proportional read abundance (Appendix Figure 5.17). Notably, the percentage of reads mapping to Eukaryota were higher than Prokaryotes within ice-cover but not ice-free samples. Diatoms dominated the winter transcriptional pool across major eukaryotic phytoplankton communities regardless of ice cover (Figure 5.3A). In turn, polar centric diatoms (Mediophyceae) dominated diatom community transcription regardless of ice cover (Figure 5.3B). Reference the Appendix Material (Appendix Methods/Results, Appendix Figures 5.15-5.20, Appendix Attachments 5.1G-O) for further detail on taxonomically resolved transcript distributions.

Normalized expression (TPM) profiles of the total water column community displayed clustering by ice cover (Figure 5.4A), with SIMPER analyses demonstrating an average

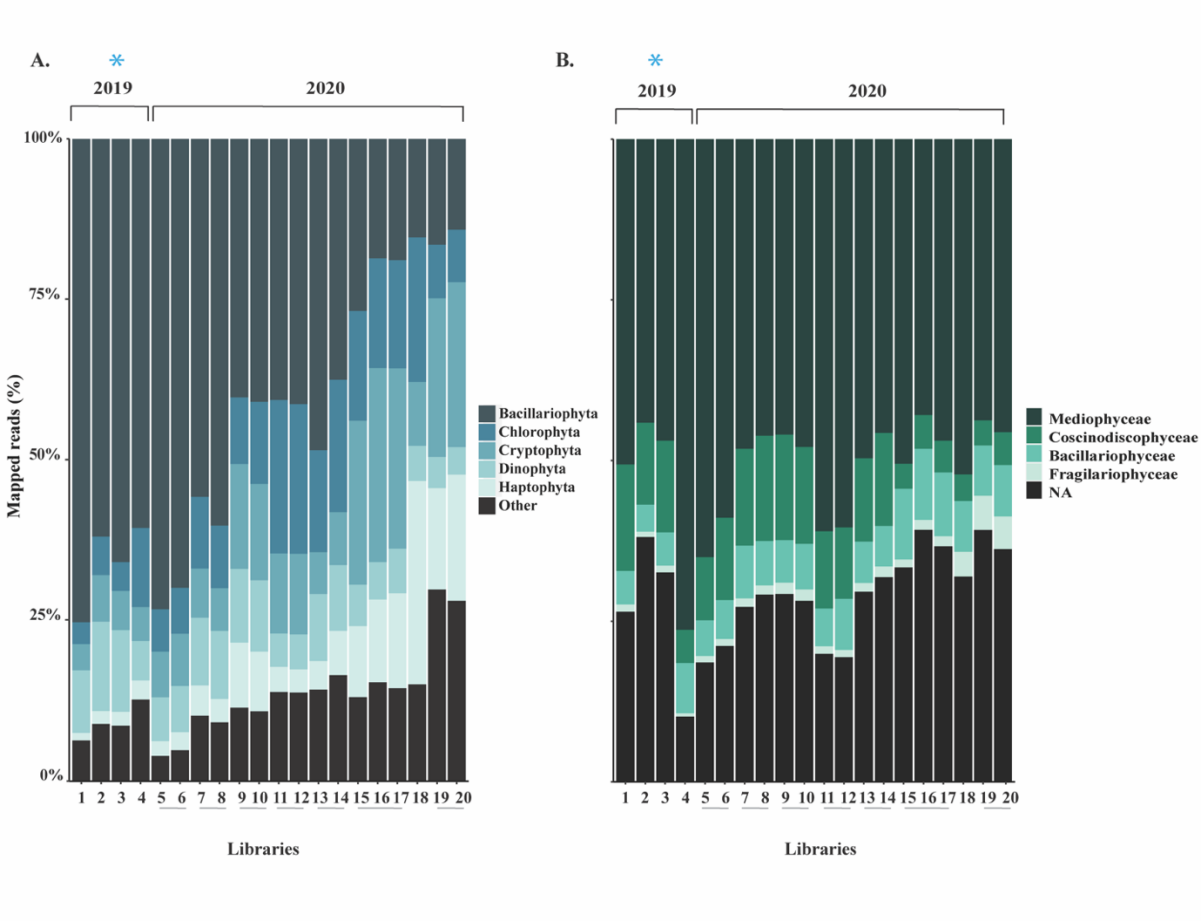


Figure 5.3: Relative transcript abundance of major eukaryotic phytoplankton taxa and diatom classes. Libraries/samples are listed in chronological order of sample date on x-axes, with biological replicates joined by grey horizontal bars. Ice cover samples are indicated by a blue asterisk. **(A)** Relative transcript abundance of MEPT. All groups which formed <5% of the total mapped reads are included within "Other" (Amoebozoa, Hilomonadea, Excavata, Rhizaria, NA). **(B)** Relative transcript abundance of Bacillariophyta classes Mediophyceae, Coscinodiscophyceae, Bacillariophyceae, Fragilariophyceae and those not annotated (NA).

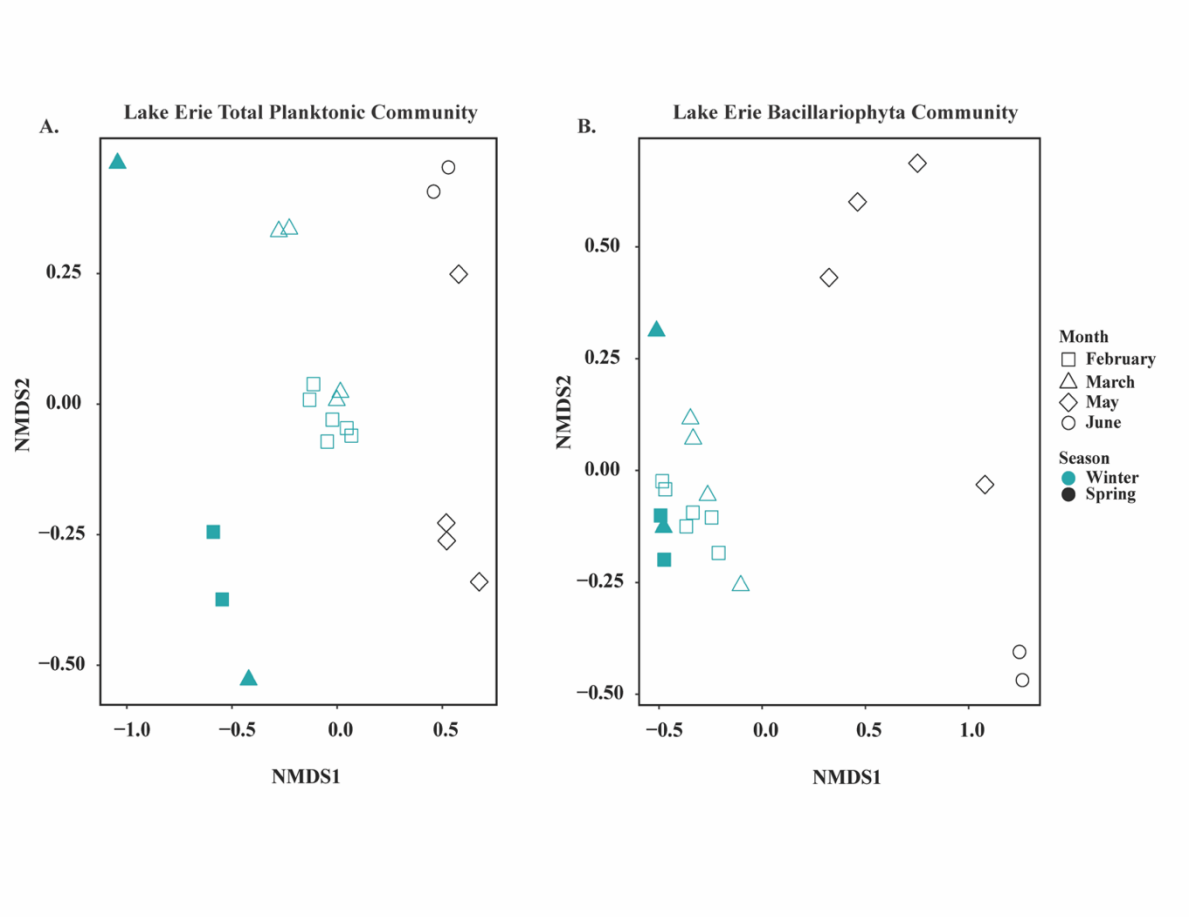


Figure 5.4: Dissimilarity (Bray-Curtis Matrix) clustering of the 20 metatranscriptomic libraries normalized expression values (TPM). **(A)** nMDS of the entire water column community expression, stress value = 0.0633. (**B)** nMDS of the Bacillariophyta community expression, stress value= 0.0497. Samples are presented as follows: February = squares, March = triangles. May = diamonds, June = circles. Blue indicates the sample was collected during the winter, black indicates the sample was collected during the spring. Solid shapes indicate the sample was collected during ice cover (2019) open shapes indicate the sample was collected during no ice cover (2020).

dissimilarity of 64% between ice cover and ice-free winter libraries (Appendix Attachment 5.1P). ANOSIM tests confirmed ice strongly affected winter community expression (R = 0.87, p = 0.002) (Appendix Figure 5.21A) (Appendix Attachment 5.1Q). Surprisingly, diatom community expression did not strongly cluster by ice cover (Figure 5.4B), with SIMPER analyses indicating an average dissimilarity of 47% between ice cover and ice-free libraries (Appendix Attachment 5.1T). ANOSIM tests confirmed ice cover exerts a lesser influence on winter diatom community expression overall compared to the full water column community (R = 0.282, p = 0.059) (Appendix Figure 5.21B). In contrast, season had a strong effect on diatom expression (SIMPER Average dissimilarity = 77%; ANOSIM R = 0.927, p = 0.001) (Appendix Attachments 1V, W).

To investigate how ice cover contributed to the ~50% dissimilarity in winter diatom expression, differential expression analyses were performed. These results indicated 354 genes belonging to putative Bacillariophyta were differentially expressed ($|Log_2FC| \geq 2$, $p_{adj} < 0.05$), with 311 of these genes increasing in relative expression in ice free samples and 43 decreasing (Appendix Attachment 5.1X). The Mediophyceae class had the highest representation within the DE genes, comprising ~50% of DE genes while other classes formed a net total of ~10% (NA~40%) (Appendix Figure 5.22A). Further analysis revealed 33% of the Mediophyceae DE genes were annotated as *Chaetoceros*-like (Appendix Figure 5.22B), despite *Chaetoceros*-like genes forming ≤ 10% of mapped reads throughout the winter libraries (Appendix Figure 5.16). Here, "*Chaetoceros*-like" indicates the transcriptomes were annotated with marine databases due to a lack of comprehensive freshwater taxonomic databases. Interestingly, genes categorized in the COG category C (Energy production and conversion) were the second highest represented COG category within the DE dataset, with most genes exhibiting increased transcript

representation within ice-free diatom communities (Figure 5.5). Of these genes, 64% belonged to Mediophyceae (Figure 5.5, Appendix Figure 5.23). Notably, the expression of genes encoding for iron-containing photosynthetic proteins such as cytochromes (CoxN, CtaC, Cob, NuoB, Cox1, Cox2) increased in relative expression in ice-free communities (Figure 5.5) along with other photosynthetic genes (ferrodoxin-*petF*, flavoprotein-*etfA*, ferritin-*ftnA*, and photosystem II-*psbA*). Likewise, relative expression of genes within COG category P (Inorganic ion transport and metabolism) increased in ice-free samples (Appendix Figure 5.24), with expression of 6 putative iron transporting genes (*tonB*_1-3 and OMFeT_1-3) increasing in ice-free communities. DE genes within COG category P largely belong to the Mediophyceae class, comprising ~40% of the annotated genes (Appendix Figure 5.24, 5.25). COG category G (Carbohydrate transport and metabolism) genes also increased in expression in ice-free communities (Appendix Figure 5.26). Notably, 4 genes encoding for pectinesterase (*pecT*, FBX011_1-3), which has a structural role in plant cell walls and has been implicated with intercellular communication (Shin et al., 2021), increased in expression. Further, two proton-pumping rhodopsin genes, which were recently found to be an alternative to classical phototrophy in a cold-adapted freshwater photosynthetic bacterium (Kopejtka et al., 2022), were increased in expression in ice-free diatom communities (Appendix Figure 5.27).

DE analyses in response to season were performed with diatom libraries to identify trends unique to the ice cover DE dataset. The top 10 COG categories represented in each dataset overlapped except for COG category M, which was the third most abundant in ice cover analyses compared to the twelfth most abundant in season analyses (Appendix Figure 5.28). Further analysis of these COG M (Cell wall, membrane, and envelope biogenesis) genes revealed 58% belonged to Mediophyceae (Figure 5.6A, Appendix Figure 5.29). Surprisingly, despite the large

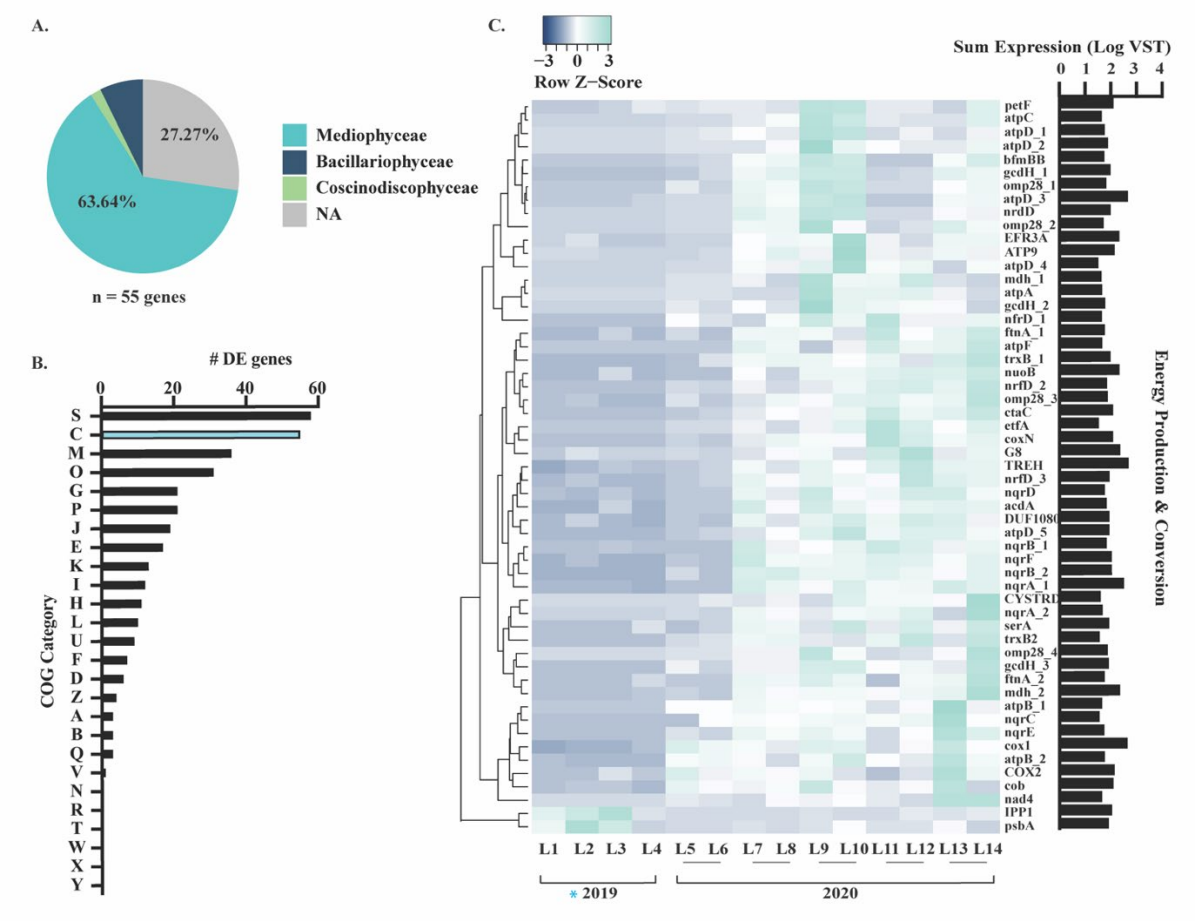


Figure 5.5: Bacillariophyta transcript abundance patterns in response to ice cover-COG C. **(A)** Taxonomic distribution of DE genes categorized within COG category C (Energy Production and Conversion). **(B)** COG assignments for all 354 DE genes in response to ice cover, with COG category C indicated in blue. **(C)** Heatmap depicting COG category C differentially expressed gene expression (VST) in response to ice cover across the 14 winter libraries.

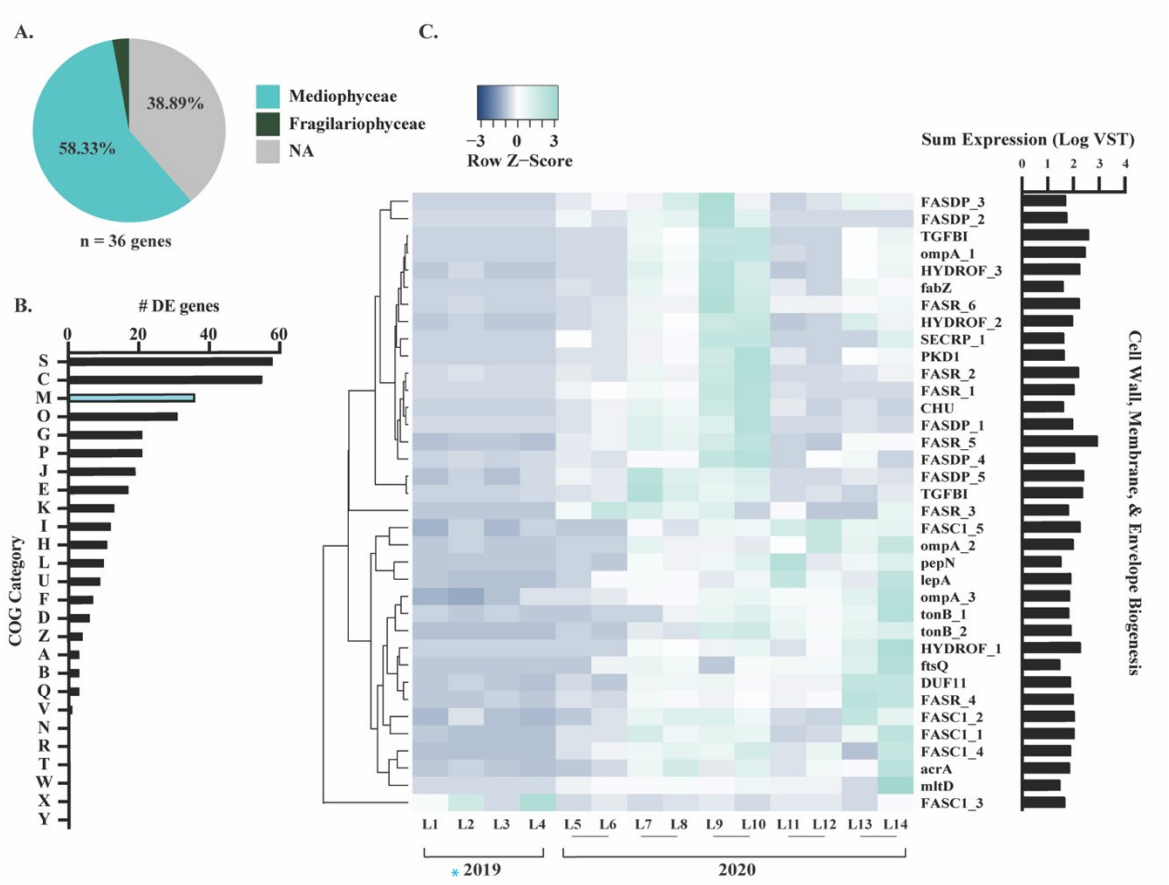


Figure 5.6: Bacillariophyta transcript abundance patterns in response to ice cover-COG M. **(A)** Taxonomic distribution of DE genes categorized within COG category M (Cell wall, membrane, envelope biogenesis). **(B)** COG assignments for all 354 DE genes in response to ice cover, with COG category M indicated in blue. **(C)** Heatmap depicting COG category M differentially expressed gene expression (VST) in response to ice cover across the 14 winter libraries.

abundance of *A. islandica* (Cosinodiscophyceae) according to cell counts, transcripts belonging to the Coscinodiscophyceae class were not represented within DE COG M genes. Intriguingly, 50% of the DE COG M genes encode for fasciclins (FASDP, TGFBI, FASR, FASC) (Figure 5.6B, C) also called the FAS1 domain. Fasciclins are secreted glycoproteins involved in diatom cell-cell adhesion and cell-extracellular matrix adhesion (Willis et al., 2014; Lachnit et al., 2019). Expression of fasciclins increased during ice-free periods and decreased during ice cover, with all 18 DE fasciclin genes taxonomically assigned to Mediophyceae or unresolved. Phylogenetic analyses indicated diatoms horizontally acquired FAS1 from bacteria, as there is evidence for at least 6 instances of horizontal gene transfer within our analysis (Figure 5.7). Broadly, the FAS1 domain is widely distributed in diatoms, with ~140 marine and freshwater diatoms found to contain this protein domain including cold-adapted diatom such as *Fragilariopsis cylindrus* and *Thalassiosira antarctica.* Refer to Appendix Methods/Results and Appendix Attachments for further details.

Discussion

The winter period in lakes remains a limnological "blind spot" due to a lack of research (Ozersky et al., 2021). Our investigations into this Lake Erie "black box" revealed another gap: Lake Erie winter surveys conducted since the turn of the millennium were during (or directly following) consecutive periods of high ice cover (mean maximum ice cover >80%) (Saxton et al., 2012a; Twiss et al., 2012; Twiss et al., 2014; Wilhelm et al., 2014; Beall et al., 2016; Edgar et al., 2016) (Figure 5.1B). Thus, foundations established by these studies do not necessarily represent current or future communities or conditions. Historically, Lake Erie experienced 4-5

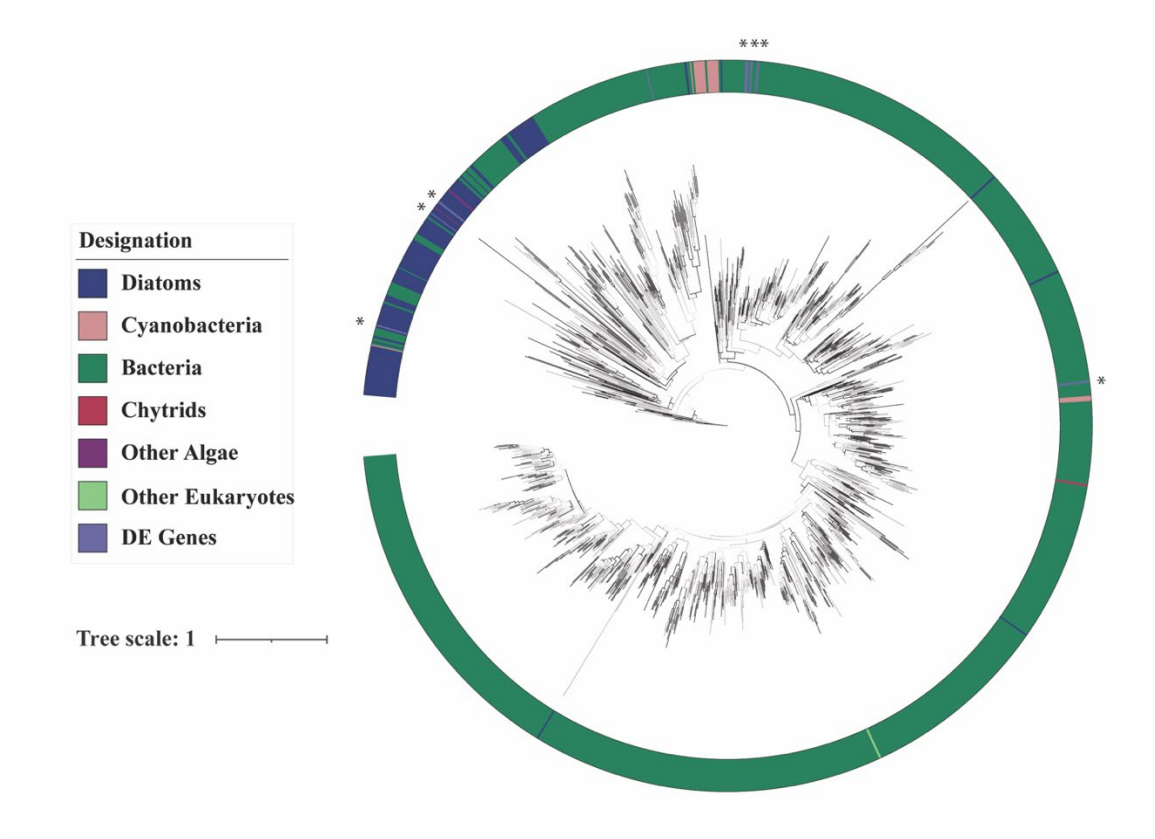


Figure 5.7: Phylogenetic tree of fasciclin distribution within diatoms. Bootstrap values above 70 are indicated with black lines. The FAS1 domain was found in 141 marine and freshwater diatoms of diverse ecological habitats (indicated in blue). The 18 DE diatom fasciclins noted in this studies metatranscriptomes are indicated in purple with asterisks. Fasciclins are most widely distributed in bacteria (indicated in dark green). Notably, they were also found within cyanobacteria (indicated in pink), chytrids (indicated in red), other algae (indicated in purple), and other eukaryotes (indicated in light green), but at a much lesser extent.

consecutive years of high ice cover followed by one year of low ice cover (Figure 5.1B). Thus, foundations established by these studies do not necessarily represent current or future communities or conditions. Historically, Lake Erie experienced 4-5 consecutive years of high ice cover followed by one year of low ice cover (Figure 5.1B). Yet since 2012, there has been a lack of consecutive periods of ice cover. Notably, the winter of 2023 has unprecedented low ice coverage (mean maximum ice cover 5% as of March 7th 2023), indicating large scale climatic changes are underway (NOAA, 2023). In light of this, the present study investigated how winter diatoms respond to ice cover. We demonstrate the winter diatom community has shifted from observations made during the period 2007-2011. Comparisons between ice-cover and ice-free samples demonstrate shifts in winter diatom abundance and phylogeny. Transcriptional trends suggest key diatom genera elicit a physiological response to ice cover, primarily within the diatom class Mediophyceae (polar centric). Notably, diatoms exhibited increased relative expression of photosynthetic and fasciclin genes during ice-free conditions. These observations lead to a new hypothesis regarding the ecophysiological role of fasciclins within ice-free winter diatom communities. We provide this information couched within the context of the ecological implications within a climatically altered future.

Declining ice cover alters winter diatom bloom magnitude and phylogeny

Our findings are in juxtaposition to prior Lake Erie winter studies (2007-2011) which reported winter diatom communities overwhelmingly dominated by *A. islandica,* with *Stephanodiscus spp.* present in lesser concentrations (Saxton et al., 2012a; Twiss et al., 2012; Twiss et al., 2014; Wilhelm et al., 2014; Edgar et al., 2016). Our study demonstrated the inverse, with cell abundances of *Stephanodiscus* spp. significantly higher than *A. islandica* in the ice-

covered community. We hypothesize a decrease in consecutive years of high ice cover may drive this decline of *A. islandica* dominance. The breakdown of this historical trend appears to favor a shift to *Stephanodiscus* spp. dominance within the larger, centric filamentous diatom community. Broadly, abundances of these taxa were 1-2 magnitudes lower than previously reported by Twiss et al., (Twiss et al., 2012), with Chl *a* concentrations supporting this trend. Hence, we suggest the collective seasonal decline of ice cover may have contributed to this decrease in winter diatom bloom magnitude. Yet, an alternative explanation exists for this decline in diatom abundance observed in our study. We acknowledge our surface-sample grabs of the winter water column do not reflect the full depth of the water column. Thus, we speculate our study may underestimate the abundances of centric diatom taxa within the winter water column, noting the well-mixed, isothermal conditions which come with ice-free winters would evenly distribute algae throughout (Appendix Figure 5.30). In support of this, a 2007 survey noted concentrated diatom communities were found ten meters below the surface of an ice-free area, while very dilute seston was found at a nearby ice-covered area at six meters depth with the diatoms concentrated within the ice cover (Appendix Figure 5.31). Cumulatively, this suggests ice cover may not alter winter diatom abundance as previously suggested but alter diatom distribution within the water column.

Surprisingly, Chl *a* concentrations did not significantly decrease relative to ice cover in our study, though they exhibited a declining trend. Cell counts confirmed centric diatoms were the primary eukaryotic phototrophs within winter samples regardless of ice cover, though abundances were lower in ice-free samples. Indeed, a prior study reported significant declines in *A. islandica* abundance during a low-ice winter in Lake Erie and suggested this niche would be filled by cryptophytes and dinoflagellates better suited for the turbid water column (Beall et al.,

2016; Ozersky et al., 2021). While we observed higher abundances of these groups in ice-free samples within our study, their cellular and transcriptional abundances remained below centric diatoms by an order of magnitude. Hence, our results demonstrated that low ice cover during this season did not induce significant large-scale phyla-level shifts in major eukaryotic phytoplankton community composition. This suggests that future ice-free winter communities may remain dominated by centric diatoms as observed in this study, but at a lesser magnitude.

While centric diatom abundances did not significantly differ by ice conditions, diatom community composition exhibited significant changes. Cell abundances of *Stephanodiscus* spp., were ~50% lower in ice-free samples, resulting in ~equal abundances of *Stephanodiscus* spp. and *A. islandica* within the ice-free water column. Further, small centric diatom taxa (5-20 μm size) were absent in samples from ice-covered sites yet formed 10-82% of total diatom counts in ice-free sites, with a bloom of these taxa noted at site 8. This suggests ice-free conditions may increase populations of smaller, centric diatoms in future warmer and ice-free winters. The trend is supported by prior studies which demonstrate warming temperatures decrease phytoplankton cell size (Bramburger et al., 2017) and select for smaller taxa (Daufresne et al., 2009; Winder et al., 2009). If these observations represent longer-term trends, future ice-free diatom communities will be more diverse with lesser biomass. In addition, significant increases in pennate diatoms in ice-free samples suggest lake warming/ice-free conditions will likely increase pennate diatoms throughout the winter and further drive winter diatom community heterogeneity.

Key diatom genera transcriptionally respond to declining ice cover

Despite the effect of ice cover on winter diatom phylogeny, the transcriptionally active diatom community did not exhibit substantial trends. Transcript abundances of diatoms were

lower in ice-free libraries yet reads mapping to diatom classes and the genera within did not definitively change. Diatoms of the class Mediophyceae (polar centric) dominated transcript abundances regardless of ice cover and formed ~50% of genes differentially expressed by ice cover. In contrast, only ~10% of differential represented transcripts belonged to the other 3 diatom classes combined (NA = ~40%). Cumulatively, this suggests diatoms within Mediophyceae elicit a strong physiological response to changes in ice cover. In contrast, though *A. islandica* (Coscinodiscophyceae) was strongly present in cell counts, Coscinodiscophyceae transcripts formed only ~10% of reads across winter diatom libraries and was nearly absent from DE genes, suggesting this species did not respond to ice conditions.

One cautionary note arising from this study is the lack of sequenced freshwater diatom taxa and an absence of freshwater taxonomic annotation databases. Edgar et al., (Edgar et al., 2016) noted only 23% of the taxonomic diatom annotations within their Lake Erie metatranscriptome could be tied to genera present within the Great Lakes. Hence, there may be transcriptional changes within the winter diatom community which have gone undetected within this study. Many of the annotations we generated were best aligned to marine counterparts (*i.e.,* where reads are annotated as belonging to a genus "-*like*" genome). Further, sequence data is often not coincident with classic taxonomy. We note numerous different taxonomic databases conflict regarding diatom taxonomy, especially concerning which genera belong to Mediophyceae (polar centric) vs. Coscinodiscophyceae (centric) classes. More broadly, Reavie (2023) discussed the lack of studies regarding Great Lakes diatoms in general, citing there are various undescribed and unclassified diatoms to date. This lack of clarity and consensus within freshwater taxonomy is a knowledge gap which requires further attention. Beyond the taxonomic gap, we observed a disconnect between *A. islandica* cell counts and transcript abundance in our

study. This suggests *A. islandica* cells were not transcriptionally active, and is in accordance with other studies which report a stark juxtaposition between "who is there" vs. "who is metabolically active" (Xie et al., 2020).

The most definitive trend to emerge from differential expression analyses by ice cover was the increase in expression of putative fasciclins (COG M) within ice-free diatom communities. Though these genes remain widely uncharacterized in diatoms, prior studies have described fasciclins within the Bacillariophyceae genera *Amphora coffeaeformis* (Lachnit et al., 2019) and *Phaeodactylum tricornutum* (Willis et al., 2014). Notably, both studies identified fasciclin proteins within diatom-secreted exopolymer substance adhesion trails and concluded these molecules facilitate diatom motility, adhesion, and aggregation. These studies built upon a prior publication which first described algal fasciclins and referred to them as "cell adhesion molecules" (Huber and Sumper, 1994). In this study, 58% of the DE diatom fasciclins belonged to the class Mediophyceae (27% to the NA group). We also observed increased transcripts for outer membrane proteins involved in cell adhesion and pectinesterases involved in cell signaling. These observations have led us to hypothesize that diatoms within Mediophyceae increased expression of cell adhesion and signaling genes to form large colonial "mats" that facilitate buoyancy. Indeed, a similar "rafting" strategy has been well-documented in centric marine diatoms *Rhizosolenia* spp. (Villareal et al., 1993; Villareal and Lipschultz, 1995; Villareal et al., 1996; Villareal et al., 1999b) and *Ethmodiscus* spp. (Villareal and Carpenter, 1994; Villareal et al., 1999a). These studies demonstrated rafts can be positively and negatively buoyant in response to physiological stressors (Villareal et al., 1996; McKay et al., 2000; Villareal, unpublished). Here, we propose Mediophyceae diatoms form colonial mats to optimize their location within the ice-free water column and maintain photosynthetic quotas.

The rafting hypothesis: A role of fasciclins in the ice-free turbid water column

Ice cover has been suggested to create a niche that promotes diatom photosynthetic processes *via* its high light transmittance, especially through snow-free ice which is common to Lake Erie (Bolsenga and Vanderploeg, 1992; Twiss et al., 2012; D'souza et al., 2013). Indeed, prior research has demonstrated diatom and bacterial communities promote the formation of frazil ice, which "rafts" them throughout the water column to partition to the surface ice cover where the light climate is enhanced (D'souza et al., 2013). In the absence of ice cover, winter storms resuspend sediment (Chandler, 1944; Valipour et al., 2017) (Supplemental Figure 23), with increased turbidity and deep-mixing posed to negatively affecting diatom light harvesting (Vanderploeg et al., 1992; Vanderploeg et al., 2007; Beall et al., 2016; Ozersky et al., 2021). We observed increased relative expression of photosynthetic genes and iron transporters within ice-free diatom communities, suggesting efforts to optimize photosynthesis within the turbid water column. Of these transcripts, 64% phylogenetically belonged to Mediophyceae (with NA = 27%). Phylogenetic analyses demonstrated diatoms acquired fasciclins from horizontal gene transfer events with bacteria, and fasciclins were identified in ~140 marine and freshwater diatoms including the model polar marine diatom *Fragilariopsis cylindrus* (Otte et al., 2023). Hence, this further suggests a physiological role for these proteins in the frigid water column. As a result, we hypothesize Mediophyceae diatoms were rafting *via* cell-adhesion fasciclins to optimize their location within the turbid Lake Erie water column.

In a supporting twist to this theory, we also observed increases in the expression of genes encoding proton-pumping rhodopsins within the ice-free diatom community. Proton-pumping rhodoposins were recently found to be an alternative to classical phototrophy in a freshwater photosynthetic bacterium (Kopejtka et al., 2022), and they have been characterized within

marine diatoms (Marchetti et al., 2015) and dinoflagellates (Slamovits et al., 2011). Globally, it is thought rhodopsin driven, retinal-based phototrophy is a major marine light harvesting process (Gomez-Consarnau et al., 2019). Our observations suggest that the role of these proton-pumping rhodopsins within fresh waters demands more attention (Sharma et al., 2009), as it is possible that in future scenarios (less ice cover, more turbidity) they may serve as important evolutionary selectors.

Implications of an ice-free future for the Lake Erie winter community

Our results suggest declining ice cover will have ecological and biogeochemical consequences for future winter communities. Using relative transcript abundance as a proxy for activity, our results suggest eukaryotes were more active than bacteria in ice covered samples but not ice-free samples. This confirms observations made by Beall et al. (2016), which suggested the Lake Erie winter water column directly contradicts the well-established paradigm that bacteria dominate eukaryotes in terms of sheer cell abundance (Oh et al., 2011; Eiler et al., 2013; Mou et al., 2013; Eiler et al., 2014). We build upon this central finding by demonstrating bacteria appear to be less transcriptionally active *in summa* in the ice-covered winter water column: observations in concurrence with reduced bacterial production rates that have been previously measured in winter-collected samples (Wilhelm et al., 2014). Indeed, a decline in eukaryotic phototrophic winter dominance could induce substantial biogeochemical and physiochemical alterations within the water column (*i.e.*, higher CO_2 and lower O_2 concentrations, *etc.*).

Beyond the effect of ice cover on community structure, we observed alterations to winter diatom bloom magnitude and phylogeny. We noted consistently lower Chl *a* concentration, total diatom cell abundance, and total diatom transcript abundance within the ice-free water column

(albeit at $p \geq 0.1285$). Considering summer hypoxia is in large part fueled by winter-spring diatom blooms (Wilhelm et al., 2014; Reavie et al., 2016), the lower diatom abundance of ice-free winters could be favorable by decreasing oxygen depletion. Moreover, the associated change in diatom community composition has ecological implications as grazers and filter-feeders preferentially select for smaller and less silicified diatom taxa (Reavie and Barbiero, 2013; Pančić et al., 2019). Thus, if ice decline in the future leads to a shift to small centric and pennate diatoms, we may observe food web alterations at its base.

During periods of ice cover, large filamentous winter diatoms embed themselves within this ice cover and rely on frazil ice to optimize their location in the water column (Twiss et al., 2012; D'souza et al., 2013). Currently, we hypothesize diatoms are increasing the expression of fasciclin-encoding genes to raft and evade light limitation in response to declining ice cover. Ozersky et al. (2021) suggested warmer winters serve to induce a change in the Great Lakes mixing regime, shifting from dimictic mixing patterns to a warm monomictic mixing pattern characterized by continuous isothermal conditions throughout winter. Hence, this fasciclin-induced rafting would be of increasing importance in future winter diatom survival within the warming and ice-free water column. Nevertheless, with diatoms previously described as "one of the most rapidly evolving eukaryotic taxa on Earth" (Oliver et al., 2007; Vardi et al., 2009) and prone to promiscuous horizontal gene transfer events (Dorrell et al., 2021), it would be surprising if they failed to adapt to an ice-free future.

Ultimately, we cannot place the consequences of the observations we describe in a quantitative framework. As noted, diatoms are a key component of the food web and lake biogeochemical function, and thus it is anticipated that changes to this group will reshape the entire ecosystem. To this end, our observations, which demonstrate variability associated with

conditions consistent with projected future climate scenarios, carve out a critical path forward and provide cautionary insight of what may be yet to come in lakes such as Lake Erie.

Acknowledgements

We are grateful to the command and members of the U.S. Coast Guard Cutter Neah Bay, Canadian Coast Guard Ship *Limnos* and M/V *Orange Apex* for their help with sample collection and the generation of hydrochemistry data. We thank Daniel H. Peck, James T. Anderson, Derek Niles and Arthur Zastepa for their help with sample collection and pre-processing. We thank Christa Pennacchio with the JGI for her coordination and sequencing expertise. We thank Dr. Gary LeCleir, Katelyn Houghton, Dr. Erik Zinser, and Dr. Jill Mikucki for their comments and suggestions. This work was funded by the National Institutes of Health, NIEHS grant 1P01ES023-28939-01, National Science Foundation grant OCE-1840715 (GB, RMLM, JC, SW), NSERC grant RGPN-2019-03943 (RMLM), and JGI project 503851 (SW and RMLM). The work conducted by the U.S. DOE JGI is under contract DE-AC02-05CH11231.

References:

Babicki, S., Arndt, D., Marcu, A., Liang, Y., Grant, J.R., Maciejewski, A., and Wishart, D.S. (2016). Heatmapper: web-enabled heat mapping for all. *Nucleic acids research* 44**,** W147-W153.

Beall, B., Twiss, M., Smith, D., Oyserman, B., Rozmarynowycz, M., Binding, C., Bourbonniere, R., Bullerjahn, G., Palmer, M., and Reavie, E. (2016). Ice cover extent drives phytoplankton and bacterial community structure in a large north-temperate lake: implications for a warming climate. *Environmental microbiology* 18**,** 1704-1719.

Benoiston, A.-S., Ibarbalz, F.M., Bittner, L., Guidi, L., Jahn, O., Dutkiewicz, S., and Bowler, C. (2017). The evolution of diatoms and their biogeochemical functions. *Philosophical Transactions of the Royal Society B: Biological Sciences* 372**,** 20160397.

Bolsenga, S., and Vanderploeg, H. (1992). Estimating photosynthetically available radiation into open and ice-covered freshwater lakes from surface characteristics; a high transmittance case study. *Hydrobiologia* 243**,** 95-104.

Bramburger, A.J., Reavie, E.D., Sgro, G., Estepp, L., Chraïbi, V.S., and Pillsbury, R. (2017). Decreases in diatom cell size during the 20th century in the Laurentian Great Lakes: a response to warming waters? *Journal of Plankton Research* 39**,** 199-210.

Buchfink, B., Xie, C., and Huson, D.H. (2015). Fast and sensitive protein alignment using DIAMOND. *Nature methods* 12**,** 59-60.

Bullerjahn, G.S., Anderson, J.T., and Mckay, R.M. (2022). "Winter survey data from Lake Erie from 2018-2020". 3 ed. (Biological and Chemical Oceanography Data Management Office (BCO-DMO)).

Bushnell, B. (2014). "BBMap: a fast, accurate, splice-aware aligner". Lawrence Berkeley National Lab.(LBNL), Berkeley, CA (United States)).

Cantalapiedra, C.P., Hernández-Plaza, A., Letunic, I., Bork, P., and Huerta-Cepas, J. (2021). eggNOG-mapper v2: functional annotation, orthology assignments, and domain prediction at the metagenomic scale. *Molecular biology and evolution* 38**,** 5825-5829.

Capella-Gutiérrez, S., Silla-Martínez, J.M., and Gabaldón, T. (2009). trimAl: a tool for automated alignment trimming in large-scale phylogenetic analyses. *Bioinformatics* 25**,** 1972-1973.

Chandler, D.C. (1940). Limnological studies of western Lake Erie: I. Plankton and certain physical-chemical data of the Bass Islands region, from Septbember 1938, to November, 1939. *Ohio Journal of Science* 40**,** 291-336.

Chandler, D.C. (1942). Limnological Studies of Western Lake Erie. III, Phytoplankton and Physical-Chemical Data from November, 1939, to November 1940.

Chandler, D.C. (1944). Limnological studies of western Lake Erie IV. Relation of limnological and climatic factors to the phytoplankton of 1941. *Transactions of the American Microscopical Society* 63**,** 203-236.

Clarke, K., and Gorley, R. (2015). Getting started with PRIMER v7. *PRIMER-E: Plymouth, Plymouth Marine Laboratory* 20.

Clum, A., Huntemann, M., Bushnell, B., Foster, B., Foster, B., Roux, S., Hajek, P.P., Varghese, N., Mukherjee, S., and Reddy, T. (2021). DOE JGI metagenome workflow. *Msystems* 6**,** e00804-00820.

Confer, A.W., and Ayalew, S. (2013). The OmpA family of proteins: roles in bacterial pathogenesis and immunity. *Veterinary Microbiology* 163**,** 207-222.

D'souza, N., Kawarasaki, Y., Gantz, J., Lee, R., Beall, B., Shtarkman, Y., Koçer, Z., Rogers, S., Wildschutte, H., and Bullerjahn, G. (2013). Diatom assemblages promote ice formation in large lakes. *The ISME journal* 7**,** 1632-1640.

D'souza, N.A. (2012). *Psychrophilic diatoms in ice-covered Lake Erie.* Bowling Green State University.

Daufresne, M., Lengfellner, K., and Sommer, U. (2009). Global warming benefits the small in aquatic ecosystems. *Proceedings of the National Academy of Sciences* 106**,** 12788-12793.

Dorrell, R.G., Villain, A., Perez-Lamarque, B., Audren De Kerdrel, G., Mccallum, G., Watson, A.K., Ait-Mohamed, O., Alberti, A., Corre, E., and Frischkorn, K.R. (2021). Phylogenomic fingerprinting of tempo and functions of horizontal gene transfer within ochrophytes. *Proceedings of the National Academy of Sciences* 118**,** e2009974118.

Edgar, R., Morris, P., Rozmarynowycz, M., D'souza, N., Moniruzzaman, M., Bourbonniere, R., Bullerjahn, G., Phuntumart, V., Wilhelm, S., and Mckay, R. (2016). Adaptations to photoautotrophy associated with seasonal ice cover in a large lake revealed by metatranscriptome analysis of a winter diatom bloom. *Journal of Great Lakes Research* 42**,** 1007-1015.

Eiler, A., Drakare, S., Bertilsson, S., Pernthaler, J., Peura, S., Rofner, C., Simek, K., Yang, Y., Znachor, P., and Lindström, E.S. (2013). Unveiling distribution patterns of freshwater phytoplankton by a next generation sequencing based approach. *PLoS One* 8**,** e53516.

Eiler, A., Zaremba-Niedzwiedzka, K., Martínez-García, M., Mcmahon, K.D., Stepanauskas, R., Andersson, S.G., and Bertilsson, S. (2014). Productivity and salinity structuring of the microplankton revealed by comparative freshwater metagenomics. *Environmental Microbiology* 16**,** 2682-2698.

El-Gebali, S., Mistry, J., Bateman, A., Eddy, S.R., Luciani, A., Potter, S.C., Qureshi, M., Richardson, L.J., Salazar, G.A., and Smart, A. (2019). The Pfam protein families database in 2019. *Nucleic acids research* 47**,** D427-D432.

Filazzola, A., Blagrave, K., Imrit, M.A., and Sharma, S. (2020). Climate change drives increases in extreme events for lake ice in the Northern Hemisphere. *Geophysical Research Letters* 47**,** e2020GL089608.

Fu, L., Niu, B., Zhu, Z., Wu, S., and Li, W. (2012). CD-HIT: accelerated for clustering the next-generation sequencing data. *Bioinformatics* 28**,** 3150-3152.

Gilbert, N.E., Lecleir, G.R., Strzepek, R.F., Ellwood, M.J., Twining, B.S., Roux, S., Pennacchio, C., Boyd, P.W., and Wilhelm, S.W. (2022). Bioavailable iron titrations reveal oceanic Synechococcus ecotypes optimized for different iron availabilities. *ISME Communications* 2**,** 1-12.

Gomez-Consarnau, L., Raven, J.A., Levine, N.M., Cutter, L.S., Wang, D., Seegers, B., Aristegui, J., Fuhrman, J.A., Gasol, J.M., and A., S.-W.-S. (2019). Microbial rhodopsins are major contributors to the solar energy captured in the sea. *Sciecne Advances* 5**,** eaaw8855.

Gurevich, A., Saveliev, V., Vyahhi, N., and Tesler, G. (2013). QUAST: quality assessment tool for genome assemblies. *Bioinformatics* 29**,** 1072-1075.

Huber, O., and Sumper, M. (1994). Algal-CAMs: isoforms of a cell adhesion molecule in embryos of the alga Volvox with homology to Drosophila fasciclin I. *The EMBO journal* 13**,** 4212-4222.

Katoh, K., and Standley, D.M. (2013). MAFFT multiple sequence alignment software version 7: improvements in performance and usability. *Molecular biology and evolution* 30**,** 772-780.

Kopejtka, K., Tomasch, J., Kaftan, D., Gardiner, A.T., Bína, D., Gardian, Z., Bellas, C., Dröge, A., Geffers, R., and Sommaruga, R. (2022). A bacterium from a mountain lake harvests light using both proton-pumping xanthorhodopsins and bacteriochlorophyll-based photosystems. *Proceedings of the National Academy of Sciences* 119**,** e2211018119.
Krinos, A.I., Hu, S.K., Cohen, N.R., and Alexander, H. (2020). EUKulele: Taxonomic annotation of the unsung eukaryotic microbes. *arXiv preprint arXiv:2011.00089*.
Lachnit, M., Buhmann, M.T., Klemm, J., Kröger, N., and Poulsen, N. (2019). Identification of proteins in the adhesive trails of the diatom Amphora coffeaeformis. *Philosophical Transactions of the Royal Society B* 374**,** 20190196.
Larsson, A. (2014). AliView: a fast and lightweight alignment viewer and editor for large datasets. *Bioinformatics* 30**,** 3276-3278.
Letunic, I., and Bork, P. (2019). Interactive Tree Of Life (iTOL) v4: recent updates and new developments. *Nucleic acids research* 47**,** W256-W259.
Li, D., Luo, R., Liu, C.-M., Leung, C.-M., Ting, H.-F., Sadakane, K., Yamashita, H., and Lam, T.-W. (2016). MEGAHIT v1. 0: a fast and scalable metagenome assembler driven by advanced methodologies and community practices. *Methods* 102**,** 3-11.
Liao, Y., Smyth, G.K., and Shi, W. (2014). featureCounts: an efficient general purpose program for assigning sequence reads to genomic features. *Bioinformatics* 30**,** 923-930.
Love, M.I., Huber, W., and Anders, S. (2014). Moderated estimation of fold change and dispersion for RNA-seq data with DESeq2. *Genome Biology* 15**,** 1-21.
Marchetti, A., Catlett, D., Hopkinson, B.M., Ellis, K., and Cassar, N. (2015). Marine diatom proteorhodopsins and their potential role in coping with low iron availability. *The ISME Journal* 9**,** 2745-2748.
Martin, R.M., and Wilhelm, S.W. (2020). Phenol-based RNA Extraction from Polycarbonate Filters. *protocols.io*.
Mason, L.A., Riseng, C.M., Gronewold, A.D., Rutherford, E.S., Wang, J., Clites, A., Smith, S.D., and Mcintyre, P.B. (2016). Fine-scale spatial variation in ice cover and surface temperature trends across the surface of the Laurentian Great Lakes. *Climatic Change* 138**,** 71-83.
Mckay, R.M.L., Beall, B.F., Bullerjahn, G.S., and Woityra, L.W.C. (2011). Winter limnology on the Great Lakes: The role of the US Coast Guard. *Journal of Great Lakes Research* 37**,** 207-210.
Mckay, R.M.L., Villareal, T.A., and La Roche, J. (2000). Vertical migration by Rhizosolenia spp.(Bacillariophyceae): Implications for Fe acquisition. *Journal of Phycology* 36**,** 669-674.
Mou, X., Jacob, J., Lu, X., Robbins, S., Sun, S., and Ortiz, J.D. (2013). Diversity and distribution of free-living and particle-associated bacterioplankton in Sandusky Bay and adjacent waters of Lake Erie Western Basin. *Journal of Great Lakes Research* 39**,** 352-357.
Nelson, D.M., Tréguer, P., Brzezinski, M.A., Leynaert, A., and Quéguiner, B. (1995). Production and dissolution of biogenic silica in the ocean: revised global estimates, comparison with regional data and relationship to biogenic sedimentation. *Global Biogeochemical Cycles* 9**,** 359-372.
Noaa. 2021. NOAA projects 30% maximum Great Lakes ice cover for winter. Available: https://www.workboat.com/government/noaa-projects-30-maximum-great-lakes-ice-cover-for-winter [Accessed Febraury 8m 2023].
Noaa (2023). Low ice on the Great Lakes this winter. *NOAA Research News*.

Noaa-Glerl *Historical Ice Cover* [Online]. NOAA-GLERL. Available: https://www.glerl.noaa.gov/data/ice/#historical [Accessed 2-12-2023 2023].
Oh, S., Caro-Quintero, A., Tsementzi, D., Deleon-Rodriguez, N., Luo, C., Poretsky, R., and Konstantinidis, K.T. (2011). Metagenomic insights into the evolution, function, and complexity of the planktonic microbial community of Lake Lanier, a temperate freshwater ecosystem. *Applied and environmental microbiology* 77**,** 6000-6011.
Oliver, M.J., Petrov, D., Ackerly, D., Falkowski, P., and Schofield, O.M. (2007). The mode and tempo of genome size evolution in eukaryotes. *Genome Research* 17**,** 594-601.
Otte, A., Winder, J.C., Deng, L., Schmutz, J., Jenkins, J., Grigoriev, I.V., Hopes, A., and Mock, T. (2023). The diatom Fragilariopsis cylindrus: A model alga to understand cold-adapted life. *Journal of Phycology*.
Ozersky, T., Bramburger, A.J., Elgin, A.K., Vanderploeg, H.A., Wang, J., Austin, J.A., Carrick, H.J., Chavarie, L., Depew, D.C., and Fisk, A.T. (2021). "The changing face of winter: lessons and questions from the Laurentian Great Lakes". (Journal of Geophysical Research: Biogeosciences: Wiley Online Library).
Pančić, M., Torres, R.R., Almeda, R., and Kiørboe, T. (2019). Silicified cell walls as a defensive trait in diatoms. *Proceedings of the Royal Society B* 286**,** 20190184.
Powers, S.M., and Hampton, S.E. (2016). Winter limnology as a new frontier. *Limnology and Oceanography Bulletin* 25**,** 103-108.
Ratnasingham, S., and Hebert, P.D. (2007). BOLD: The Barcode of Life Data System (http://www. barcodinglife. org). *Molecular ecology notes* 7**,** 355-364.
Reavie, E. (2023). Asymmetric, biraphid diatoms from the Laurentian Great Lakes. *PeerJ Aquatic Biology*.
Reavie, E.D., and Barbiero, R.P. (2013). Recent changes in abundance and cell size of pelagic diatoms in the North American Great Lakes. *Phytotaxa* 127**,** 150-162.
Reavie, E.D., Cai, M., Twiss, M.R., Carrick, H.J., Davis, T.W., Johengen, T.H., Gossiaux, D., Smith, D.E., Palladino, D., and Burtner, A. (2016). Winter–spring diatom production in Lake Erie is an important driver of summer hypoxia. *Journal of Great Lakes Research* 42**,** 608-618.
Rühland, K.M., Paterson, A.M., and Smol, J.P. (2015). Lake diatom responses to warming: reviewing the evidence. *Journal of Paleolimnology* 54**,** 1-35.
Saxton, M.A., D'souza, N.A., Bourbonniere, R.A., Mckay, R.M.L., and Wilhelm, S.W. (2012). Seasonal Si: C ratios in Lake Erie diatoms—evidence of an active winter diatom community. *Journal of Great Lakes Research* 38**,** 206-211.
Sharma, A.K., Sommerfeld, K., Bullerjahn, G.S., Matteson, A.R., Wilhelm, S.W., Jezbera, J., Brandt, U., Doolittle, W.F., and Hahn, M.W. (2009). Actinorhodopsin genes discovered in diverse freshwater habitats and among cultivated freshwater Actinobacteria. *The ISME journal* 3**,** 726-737.
Shin, Y., Chane, A., Jung, M., and Lee, Y. (2021). Recent advances in understanding the roles of pectin as an active participant in plant signaling networks. *Plants* 10**,** 1712.
Slamovits, C.H., Okamato, N., Burri, L., James, E.R., and J., K.P. (2011). A bacterial proteorhodopsin proton pump in marine eukaryotes. *Nature Communications* 2**,** 183.
Sommer, U., Adrian, R., De Senerpont Domis, L., Elser, J.J., Gaedke, U., Ibelings, B., Jeppesen, E., Lürling, M., Molinero, J.C., and Mooij, W.M. (2012). Beyond the Plankton Ecology Group (PEG) model: mechanisms driving plankton succession. *Annual review of ecology, evolution, and systematics* 43**,** 429-448.

Sommer, U., Gliwicz, Z.M., Lampert, W., and Duncan, A. (1986). The PEG-model of seasonal succession of planktonic events in fresh waters. *Archiv für Hydrobiologie* 106**,** 433-471.
Struyf, E., Smis, A., Van Damme, S., Meire, P., and Conley, D.J. (2009). The global biogeochemical silicon cycle. *Silicon* 1**,** 207-213.
Twiss, M., Mckay, R., Bourbonniere, R., Bullerjahn, G., Carrick, H., Smith, R., Winter, J., D'souza, N., Furey, P., and Lashaway, A. (2012). Diatoms abound in ice-covered Lake Erie: An investigation of offshore winter limnology in Lake Erie over the period 2007 to 2010. *Journal of Great Lakes Research* 38**,** 18-30.
Twiss, M.R., Smith, D.E., Cafferty, E.M., and Carrick, H.J. (2014). Phytoplankton growth dynamics in offshore Lake Erie during mid-winter. *Journal of Great Lakes Research* 40**,** 449-454.
Valipour, R., Boegman, L., Bouffard, D., and Rao, Y.R. (2017). Sediment resuspension mechanisms and their contributions to high-turbidity events in a large lake. *Limnology and Oceanography* 62**,** 1045-1065.
Vanderploeg, H., Johengen, T., Lavrentyev, P.J., Chen, C., Lang, G., Agy, M., Bundy, M., Cavaletto, J., Eadie, B., and Liebig, J. (2007). Anatomy of the recurrent coastal sediment plume in Lake Michigan and its impacts on light climate, nutrients, and plankton. *Journal of Geophysical Research: Oceans* 112.
Vanderploeg, H.A., Bolsenga, S.J., Fahnenstiel, G.L., Liebig, J.R., and Gardner, W.S. (1992). Plankton ecology in an ice-covered bay of Lake Michigan: Utilization of a winter phytoplankton bloom by reproducing copepods. *Hydrobiologia* 243**,** 175-183.
Vardi, A., Thamatrakoln, K., Bidle, K.D., and Falkowski, P.G. (2009). Diatom genomes come of age. *Genome Biology* 9**,** 245.
Villareal, T.A. (unpublished).
Villareal, T.A., Altabet, M.A., and Culver-Rymsza, K. (1993). Nitrogen transport by vertically migrating diatom mats in the North Pacific Ocean. *Nature* 363**,** 709-712.
Villareal, T.A., and Carpenter, E.J. (1994). CHEMICAL COMPOSITION AND PHOTOSYNTHETIC CHARACTERISTICS OF ETHMODISCUS REX (BACILLARIOPHYCEAE): EVIDENCE FOR VERTICAL MIGRATION 1. *Journal of Phycology* 30**,** 1-8.
Villareal, T.A., Joseph, L., Brzezinski, M.A., Shipe, R.F., Lipschultz, F., and Altabet, M.A. (1999a). Biological and chemical characteristics of the giant diatom Ethmodiscus (Bacillariophyceae) in the central North Pacific gyre. *Journal of Phycology* 35**,** 896-902.
Villareal, T.A., and Lipschultz, F. (1995). Internal nitrate concentrations in single cells of large phytoplankton from the sargasso sea 1. *Journal of Phycology* 31**,** 689-696.
Villareal, T.A., Pilskaln, C., Brzezinski, M., Lipschultz, F., Dennett, M., and Gardner, G.B. (1999b). Upward transport of oceanic nitrate by migrating diatom mats. *Nature* 397**,** 423-425.
Villareal, T.A., Woods, S., Moore, J.K., and Culverrymsza, K. (1996). Vertical migration of Rhizosolenia mats and their significance to NO3− fluxes in the central North Pacific gyre. *Journal of Plankton Research* 18**,** 1103-1121.
Wang, J., Kessler, J., Bai, X., Clites, A., Lofgren, B., Assuncao, A., Bratton, J., Chu, P., and Leshkevich, G. (2018). Decadal variability of Great Lakes ice cover in response to AMO and PDO, 1963–2017. *Journal of Climate* 31**,** 7249-7268.

Wheeler, D.L., Barrett, T., Benson, D.A., Bryant, S.H., Canese, K., Chetvernin, V., Church, D.M., Dicuccio, M., Edgar, R., and Federhen, S. (2007). Database resources of the national center for biotechnology information. *Nucleic acids research* 35**,** D5-D12.

Wilhelm, S.W., Lecleir, G.R., Bullerjahn, G.S., Mckay, R.M., Saxton, M.A., Twiss, M.R., and Bourbonniere, R.A. (2014). Seasonal changes in microbial community structure and activity imply winter production is linked to summer hypoxia in a large lake. *FEMS microbiology ecology* 87**,** 475-485.

Willis, A., Eason-Hubbard, M., Hodson, O., Maheswari, U., Bowler, C., and Wetherbee, R. (2014). Adhesion molecules from the diatom Phaeodactylum tricornutum (Bacillariophyceae): genomic identification by amino-acid profiling and in vivo analysis. *Journal of Phycology* 50**,** 837-849.

Winder, M., Reuter, J.E., and Schladow, S.G. (2009). Lake warming favours small-sized planktonic diatom species. *Proceedings of the Royal Society B: Biological Sciences* 276**,** 427-435.

Xie, G., Tang, X., Shao, K., Hu, Y., Liu, H., Martin, R.M., and Gao, G. (2020). Spatiotemporal patterns and environmental drivers of total and active bacterial abundances in Lake Taihu, China. *Ecological Indicators* 114**,** 106335.

Zepernick, B.N., Denison, E.R., Chaffin, J.D., Bullerjahn, G.S., Pennacchio, C.P., Frenken, T., Peck, D.H., Anderson, J.T., Niles, D., and Zastepa, A. (2022). Metatranscriptomic Sequencing of Winter and Spring Planktonic Communities from Lake Erie, a Laurentian Great Lake. *Microbiology Resource Announcements***,** e00351-00322.

Zhu, W., Lomsadze, A., and Borodovsky, M. (2010). Ab initio gene identification in metagenomic sequences. *Nucleic acids research* 38**,** e132-e132.

Appendix

Appendix Methods

Lake Erie winter-spring water column sampling

To assess Chl *a* concentration, 50 mL volumes of sample water were collected on 0.22-μm nominal pore-size polycarbonate filters and stored at -20°C until Chl *a* extraction at *Bowling Green State University*. In addition, 200 mL volumes of sample water were collected on 20 μm nominal pore-size polycarbonate filters and stored at -20°C. Subsequently, samples were subject to a 24-hour extraction in 90% acetone at 4°C and quantified on a fluorometer (Turner Designs TD-700) equipped with a blue mercury bulb, a #10-050R excitation filter (340–500 nm) and a #10–115 (680 nm) emission filter (Welschmeyer, 1994). Samples for RNA isolation were filtered through 0.22-μm nominal pore-size filters until the filter was saturated, flash frozen, and stored at -80 °C until extraction at *The University of Tennessee Knoxville.* For dissolved nutrients (SiO_2, NO_3, NO_2, NH_3, SRP, SO_4, Cl), 50 mL volumes of filtrate from the sterivex were collected and stored at -20°C until processing. Whole water samples for particulate nutrients (TN, TP) were also stored at -20°C until processing at *The Ohio State University Stone Laboratory.* There, samples were subsequently processed on a SEAL Analytical QuAAtro 5-Chaneel continuous segments flow auto-analyzer (Chaffin et al., 2019). Fifty milliliter samples of whole water were preserved with Lugol's iodine and stored at room temperature until phytoplankton identification and enumeration at *Aquatic Taxonomy Specialists*, (Malinta OH). Briefly, samples were analyzed by counting phytoplankton in a measured aliquot using a modified inverted microscope for the Utermöhl method plus a small magnification modification of the stratified counting technique of Munawar and Munawar (Munawar and Munawar, 1976). A measured aliquot of mixed sample was placed into an inverted microscope counting chamber

and allowed to settle a minimum of 4 h per centimeter of overlying water depth. Larger and recognizable rare cells were counted at 400× along a minimum of one transect across the entire counting chamber. Smaller algae were counted at 1000× along a measured transect until a minimum of 300 cells were enumerated. Phytoplankton were counted as individual cells. All water column data was plotted in prism (v.9.3.1) by Julian Day to account for the interannual variability (2019-2020). Visualization of the 12 sample sites was performed in R using tmap (Tennekes, 2018) and open source shapefiles of Lake Erie shoreline (https://gis-michighan.opendata.arcgis.com/datasets) and bathymetry (https://www.ngdc.noaa.gov/mgg/fliers).

Metatranscriptomic analysis

The bioinformatic workflow used to process the libraries within this manuscript was initially compiled and published by Gilbert et al. (2022). Trimming and filtering of raw reads to remove adaptors, contaminants, and sequence spike in-ins was performed by JGI *via* BBDuk (v.38.92) within the BBtools package (Bushnell, 2014b). Following, ribosomal RNA was removed using BBMap (default settings) (v.38.86) in line with the DOE JGI pipeline (Clum et al., 2021). Filtered, trimmed reads from all 77 metatranscriptomic libraries were concatenated and assembled with MEGAHIT (v.1.2.9) (Li et al., 2016), with the concatenated file serving as the input as performed previously (Gilbert et al., 2022). Quality assessment of the coassembly was performed using QUAST (v.5.0.2) (Mikheenko et al., 2018) with all statistics included in (Supplemental Dataset 1). Trimmed, filtered reads from each library (n=20) were mapped to the coassembly *via* BBMap (default settings) (v.38.86) with mapping statistics included in (Supplemental Dataset 2). Following, calling of the open reading frames (ORFs) within the

coassembly was performed *via* MetaGeneMark (v.3.38) (Besemer and Borodovsky, 1999; Zhu et al., 2010) using the gene finding algorithm. Taxonomic annotation of the coassembly genes was performed using EUKulele (Krinos et al., 2020) to perform a blast against the PhyloDB (v.1.076) database. Functional annotation of coassembly genes was conducted *via* eggNOG-mapper using orthology data and a specified e-value of $1e^{-10}$ (v.2.1.7) (Cantalapiedra et al., 2021). In this study, genes that were not assigned a "Preferred Name" by eggNOG were given one which we made based on the gene description provided by eggNOG-mapper. A list of the genes and their eggNOG preferred name (or the name we assigned in this study) is provided in the Appendix Materials (Appendix Attachments 5.1Z-5.2C). Trimmed, mapped reads were then tabulated according to ORF coordinates using featureCounts (Liao et al., 2014) within the subread (v.2.0.1) package. . After, the tabulated read counts, EUKulele annotations, and eggNOG-mapper annotations were merged into a single file in R (v.4.0.0). Read mappings were normalized to transcripts-per-million (TPM) prior to statistical analyses (ANOSIM, SIMPER, nMDS etc.). Raw reads were used for DESeq2 analysis as required by the program.

Relative transcript abundance and taxonomy

To investigate taxonomic trends inferred from proportional raw transcript abundance, coassembly genes were sorted according to the 7 classification levels of taxonomy assigned by EUKulele (domain-genus/species). To focus on diatoms specifically, analysis of raw reads mapped to domains (classification level 1), eukaryota supergroups (classification level 2), major eukaryotic phytoplankton phyla (classification level 3 and 4), bacillariophyta classes (classification level 6), and genus (classification level 7) were performed to determine relative proportions of the transcriptionally active community as performed previously (Kranzler et al.,

2021). Major eukaryotic phytoplankton taxa common to Lake Erie were selected based on prior long-term environmental surveys and manual sorting (Reavie et al., 2014). In the analysis of the relative transcript abundance, groups that were <5% of the total mapped reads were classified as "Other" as performed previously (Kranzler et al., 2021). Due to the low resolution of taxonomic annotation at the genus level, "not annotated" reads were not included in the calculations at the genus level (Appendix Figures 5.16-5.19). Rather, the NA reads were included within the "Other" group to allow for the visualization of taxonomic trends of annotated taxa. Relative abundances were graphically visualized in R using ggplot2 (Wickham, 2016) and further modified in Adobe Illustrator (Adobe Inc., 2022).

In this study, we used a marine taxonomic annotation database (EUKulele and PhyloDB) due to their unmatched depth and diversity. Hence, at the genus level all genera are reported as "genus-like" to reflect that these are annotations made based on marine taxonomy which we have extrapolated to our freshwater system. For example, *Aulacoseira*-like annotated genes within our dataset can be confidently suggested to be *Aulacosiera* based on freshwater cell abundances and taxonomy, yet we report it as *Aulacoseira*-like for consistency. Unfortunately, freshwater systems have not been as comprehensively sequenced/studied as marine systems. Indeed, TARA Oceans propelled the marine sequencing and taxonomic curation far beyond freshwater capacities (Sunagawa et al., 2015). Further, there is a lack of eukaryotic representatives within available freshwater sequencing datasets, which further exacerbates taxonomic annotation difficulties associated with freshwater communities such as Lake Erie diatom blooms. In turn, this study illuminates a critical gap and limitation to freshwater meta-omics work; comprehensive taxonomic databases are required for more direct and fine-scale community identification. Diatom classes (Coscinodiscophyceae, Mediophyceae, Bacillariophyceae,

Fragilariophyceae) for diatom genera including *A. islandica* and *Stephanodiscus* spp. were assigned based on the BOLD taxonomic database (Ratnasingham and Hebert, 2007).

Phylogenetic analysis

The phylogenetic tree was made using fasciclin containing domains recovered from this study (Appendix Attachment 5.2D), domains recovered from the eggNOG orthology database (Appendix Attachment 5.2E), and publicly available domains downloaded from NCBI. The resulting diatoms found to contain fasciclins (n=141) are provided in the Appendix Attachment 5.2F.

Appendix Results

Taxonomically resolved winter diatom community transcriptional response to ice cover

While the number of reads mapping to Eukaryota did not vary as a function of ice-cover, every other domain demonstrated an increasing trend in read abundance in ice-free samples (Appendix Figure 5.14). Eukaryota contributed an average of 66.99% (+/- 6.48) of transcripts in ice cover samples and 47.99% (+/- 9.06) of reads in ice-free winter samples. Notably, the number of reads mapping to Eukaryota were higher than bacteria within ice-cover samples but not ice-free samples. Stramenopiles contributed an average of 56.79% (+/-8.04) of the Eukaryota transcripts during ice cover and 44.72% (+/- 12.33) during ice-free conditions (Appendix Figure 5.15). Bacillariophyta reads were dominated by the class Mediophyceae (polar centric diatoms), which remained the most abundant of the transcriptionally active winter diatom community regardless of ice cover (Figure 5.3B). Coscinodiscophyceae (centric) was the second most abundant, while pennate classes Bacillariophyceae and Fragilariophyceae remained at very low

transcriptional abundances. Approximately 25% of the winter Mediophyceae community were classified as *Thalassiosir*a-like (Appendix Figure 5.16), while 50% of the Coscinodiscophyceae winter community was annotated as *Aulacoseira*-like (Appendix Figure 5.17). In contrast, pennate diatom classes Bacillariophyceae and Fragilariophyceae exhibited small trends in genera transcript abundance as a function of ice cover (Appendix Figures 5.18-5.19). Overall, diatom transcriptional abundance did not correlate with diatom cell abundances ($R^2 = 0.02$) (Appendix Figure 5.20).

Phylogenetic analysis

The FAS1 domain appears to primarily originate from bacteria and is widely distributed throughout the bacterial domain. The FAS1 domain was found in 141 diatoms which span freshwater and marine distributions. Notably, the FAS1 domain was found in various strains of the polar, cold-adapted marine diatom *Fragilariopsis cylindrus*, which has been recently designated as a "model for understanding cold-adapted alga" (Otte et al., 2023). Further, phylogenetic analysis demonstrates multiple instances of horizontal gene transfer (HGT), thus the FAS1 domain within diatoms appears to have been horizontally acquired from bacteria. Two of the putative HGT branches are quite long. This is likely due to lack of available genomes/sequencing for the respective diatom species. One long HGT branch corresponds to the diatom *Mayamaea pseudoterrestris,* the only member of genus *Mayamaea* with a genome sequenced (many of the individuals in this group are newly defined–*e.g.,* 2020, 2021, 2022). The second is from a transcriptomic dataset, and labeled as an unculturered *Nitzschia*, four genomes are sequenced for this group, however given that it is an environmental sample it could likely be considered as *Nitzschia* because that is the closest relative/hit to current databases. Therefore, it

could be a group not defined or not well defined to date. Generally, the branch lengths are long for the “diatom section”, also likely related to incomplete taxonomy. Notably, the FAS1 domain is well represented in diatoms compared to other alga and cyanobacteria, yet most of the FAS1 diatom domains were annotated as “hypothetical, unnamed, or predicted protein” (Appendix Attachment 5.2F). Hence, the FAS1 domain is not well-annotated or characterized within diatoms. Cumulatively, this data suggests the FAS1 domain distribution within diatoms is a result of HGT events with bacteria. Further, this data suggests the FAS1 domain is well-distributed across at least 141 diatom taxa as found in this study yet remains unannotated and undefined in most publicly available diatom sequencing data.

Appendix References:

Besemer, J., and Borodovsky, M. (1999). Heuristic approach to deriving models for gene finding. *Nucleic acids research* 27**,** 3911-3920.

Bushnell, B. (2014). BBTools software package. *URL http://sourceforge. net/projects/bbmap* 578**,** 579.

Cantalapiedra, C.P., Hernández-Plaza, A., Letunic, I., Bork, P., and Huerta-Cepas, J. (2021). eggNOG-mapper v2: functional annotation, orthology assignments, and domain prediction at the metagenomic scale. *Molecular biology and evolution* 38**,** 5825-5829.

Chaffin, J.D., Mishra, S., Kane, D.D., Bade, D.L., Stanislawczyk, K., Slodysko, K.N., Jones, K.W., Parker, E.M., and Fox, E.L. (2019). Cyanobacterial blooms in the central basin of Lake Erie: Potentials for cyanotoxins and environmental drivers. *Journal of Great Lakes Research* 45**,** 277-289.

Clum, A., Huntemann, M., Bushnell, B., Foster, B., Foster, B., Roux, S., Hajek, P.P., Varghese, N., Mukherjee, S., and Reddy, T. (2021). DOE JGI metagenome workflow. *Msystems* 6**,** e00804-00820.

Gilbert, N.E., Lecleir, G.R., Strzepek, R.F., Ellwood, M.J., Twining, B.S., Roux, S., Pennacchio, C., Boyd, P.W., and Wilhelm, S.W. (2022). Bioavailable iron titrations reveal oceanic Synechococcus ecotypes optimized for different iron availabilities. *ISME Communications* 2**,** 1-12.

Kranzler, C.F., Brzezinski, M.A., Cohen, N.R., Lampe, R.H., Maniscalco, M., Till, C.P., Mack, J., Latham, J.R., Bruland, K.W., and Twining, B.S. (2021). Impaired viral infection and reduced mortality of diatoms in iron-limited oceanic regions. *Nature Geoscience* 14**,** 231-237.

Krinos, A.I., Hu, S.K., Cohen, N.R., and Alexander, H. (2020). EUKulele: Taxonomic annotation of the unsung eukaryotic microbes. *arXiv preprint arXiv:2011.00089*.

Li, D., Luo, R., Liu, C.-M., Leung, C.-M., Ting, H.-F., Sadakane, K., Yamashita, H., and Lam, T.-W. (2016). MEGAHIT v1. 0: a fast and scalable metagenome assembler driven by advanced methodologies and community practices. *Methods* 102**,** 3-11.

Liao, Y., Smyth, G.K., and Shi, W. (2014). featureCounts: an efficient general purpose program for assigning sequence reads to genomic features. *Bioinformatics* 30**,** 923-930.

Mikheenko, A., Prjibelski, A., Saveliev, V., Antipov, D., and Gurevich, A. (2018). Versatile genome assembly evaluation with QUAST-LG. *Bioinformatics* 34**,** i142-i150.

Munawar, M., and Munawar, I.F. (1976). A lakewide study of phytoplankton biomass and its species composition in Lake Erie, April–December 1970. *Journal of the Fisheries Board of Canada* 33**,** 581-600.

Otte, A., Winder, J.C., Deng, L., Schmutz, J., Jenkins, J., Grigoriev, I.V., Hopes, A., and Mock, T. (2023). The diatom Fragilariopsis cylindrus: A model alga to understand cold-adapted life. *Journal of Phycology*.

Ratnasingham, S., and Hebert, P.D. (2007). BOLD: The Barcode of Life Data System (http://www. barcodinglife. org). *Molecular ecology notes* 7**,** 355-364.

Reavie, E.D., Barbiero, R.P., Allinger, L.E., and Warren, G.J. (2014). Phytoplankton trends in the Great Lakes, 2001–2011. *Journal of Great Lakes Research* 40**,** 618-639.

Sunagawa, S., Coelho, L.P., Chaffron, S., Kultima, J.R., Labadie, K., Salazar, G., Djahanschiri, B., Zeller, G., Mende, D.R., and Alberti, A. (2015). Structure and function of the global ocean microbiome. *Science* 348**,** 1261359.

Tennekes, M. (2018). tmap: Thematic Maps in R. *Journal of Statistical Software* 84**,** 1-39.

Welschmeyer, N.A. (1994). Fluorometric analysis of chlorophyll a in the presence of chlorophyll b and pheopigments. *Limnology and Oceanography* 39**,** 1985-1992.
Wickham, H. (2016). ggplot2: Elegant Graphics for Data Analysis. Springer-Verlag, New York. ISBN 978-3-319-24277-4.
Zhu, W., Lomsadze, A., and Borodovsky, M. (2010). Ab initio gene identification in metagenomic sequences. *Nucleic acids research* 38**,** e132-e132.

Appendix Tables/Figures

Table 5.1. Metatranscriptomic libraries with respect to spatial, temporal, and climatic variables. Libraries listed within the same row are biological replicates. Sample sites are listed in chronological order of sampling (S1-12). Samples that were collected from under the ice are denoted with "Yes" and samples collected during a no ice cover are denoted with "No". Season is listed as either "Winter" or "Spring". Sample day is presented in Julian day, to account for interannual variability. Samples collected during 2019, a year of high ice cover overall throughout Lake Erie, are indicated with an asterisk. Samples collected during 2020, a year of low ice cover throughout Lake Erie, do not have an asterisk.

Library	Site	Ice cover	Season	Julian day	Month	Year
L1	S1	Yes	Winter	57	February	2019*
L2	S2	Yes	Winter	57	February	2019*
L3	S3	Yes	Winter	70	March	2019*
L4	S4	Yes	Winter	70	March	2019*
L5, L6	S5	No	Winter	45	February	2020
L7, L8	S6	No	Winter	45	February	2020
L9, L10	S7	No	Winter	45	February	2020
L11, L12	S8	No	Winter	62	March	2020
L13, L14	S9	No	Winter	62	March	2020
L15, L16, L17	S10	No	Spring	122	May	2020
L18	S11	No	Spring	143	May	2020
L19, L20	S12	No	Spring	160	June	2020

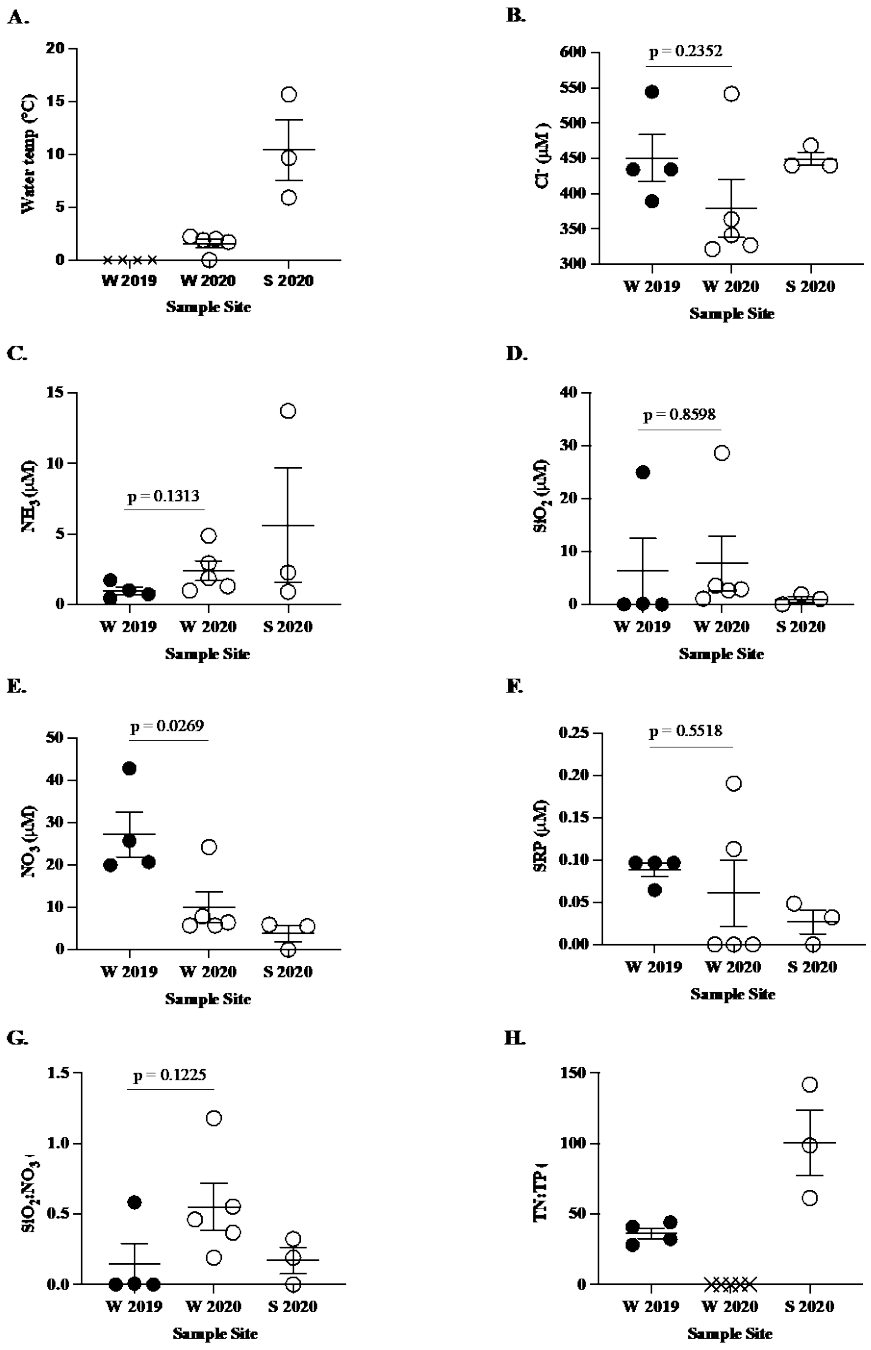


Figure 5.8: Temperature and nutrient profiles (µM) across the 12 sample sites organized by season. W = winter (February-March), S = spring (May-June). Solid shapes indicate the sample was collected during ice cover (2019), open shapes indicate the sample was collected during no ice cover (2020**).** X's indicate there was no data reported. **(A)** Water temperature. **(B)** Dissolved Chlorine. **(C)** Dissolved Ammonia. **(D)** Dissolved Silicate. **(E)** Dissolved Nitrate. **(F)** Dissolved Soluble Reactive Phosphorus **(G)** Silica: Nitrate ratios. **(H)** Total Particulate Nitrogen: Total Particulate Phosphorus. Statistical comparisons as a function of ice cover were made using unpaired, two-tailed t-tests.

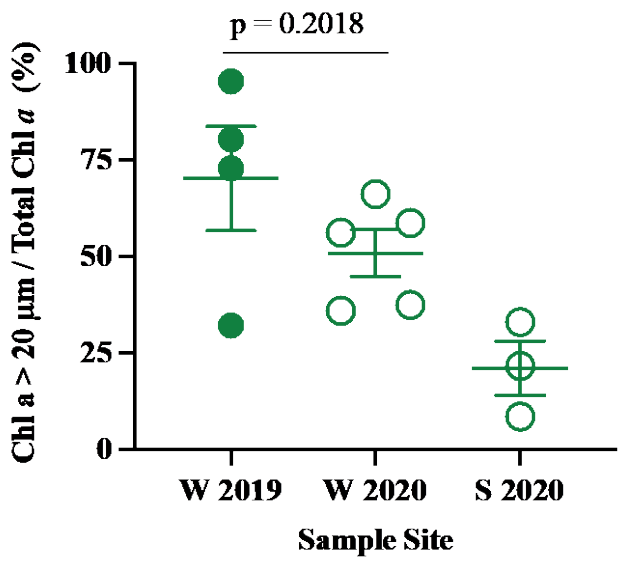


Figure 5.9: Mean percent contribution of Chl *a* >20 µm to total Chl *a* across sample sites organized by season. W = winter (February-March), S = spring (May-June). Solid shapes indicate the sample was collected during ice cover (2019) open shapes indicate the sample was collected during no ice cover (2020). Statistical comparisons as a function of ice cover were made using unpaired, two-tailed t-tests.

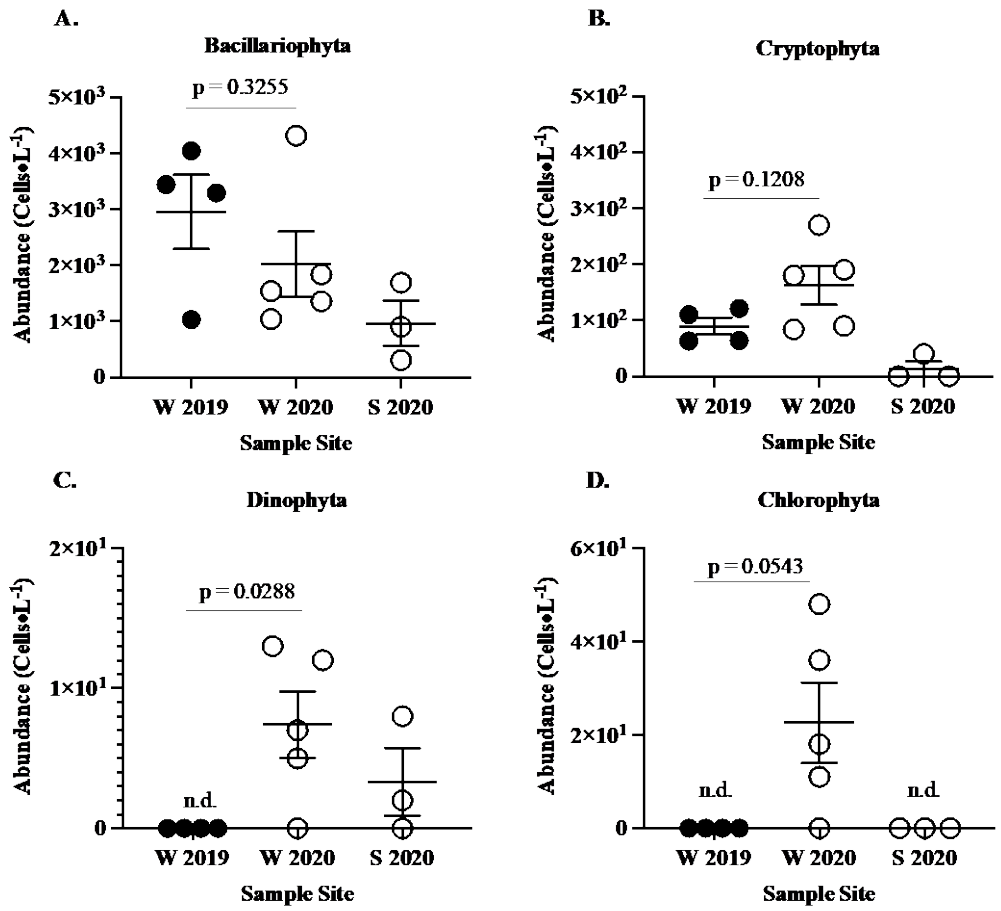
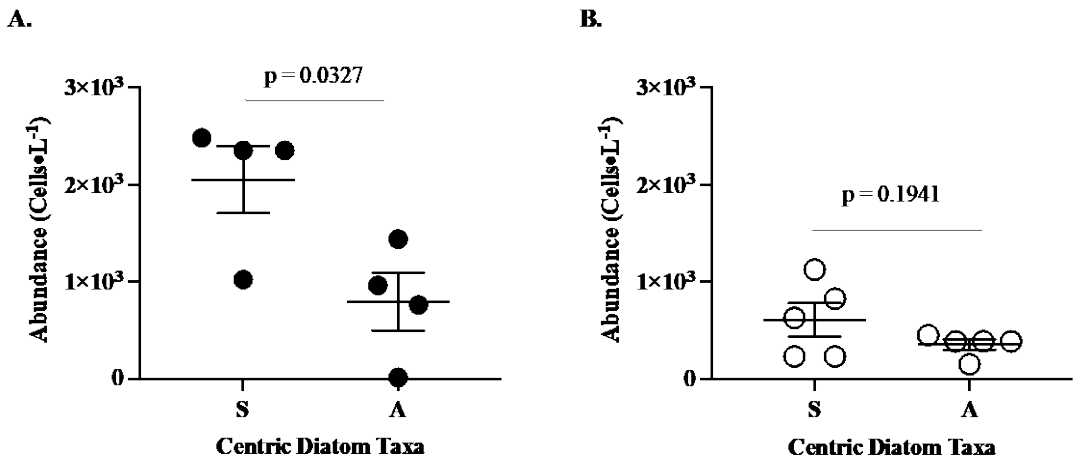


Figure 5.10: Abundance (Cells•L^{-1}) of major eukaryotic phytoplankton taxa across sample sites organized by season. W = winter (February-March), S = spring (May-June). Solid shapes indicate the sample was collected during ice cover (2019) open shapes indicate the sample was collected during no ice cover (2020**).** Sites were the taxa was not detected are indicated with "n.d.". **(A)** Sum diatom counts (*A. islandica* + *Stephanodiscus* spp. + centric diatoms of 5-20 μm + *Fragilaria* spp. + *Asterionella formosa*. + *Nitzschia* spp.). **(B)** Abundance of cryptophytes across sample sites. **(C)** Abundance of dinoflagellates across sample sites. **(D)** Abundance of chlorophytes. Statistical comparisons as a function of ice cover were made using unpaired, two-tailed t-tests. The y-axis scales are different between panels.



Supplemental Figure 5.11: Abundance (Cells•L^{-1}) of major centric, filamentous bloom-forming diatom taxa (S = *Stephanodiscus* spp., A = *A. islandica*) across winter sample sites organized by ice cover. Solid shapes indicate the sample was collected during ice cover (2019) open shapes indicate the sample was collected during no ice cover (2020)**. (A)** Abundances of *Stephanodiscus* spp and *A. islandica* in winter ice-cover samples. **(B)** Abundances of *Stephanodiscus* spp and *A. islandica* in winter ice-free samples. Statistical comparisons as a function of ice cover were made using unpaired, two-tailed t-tests.

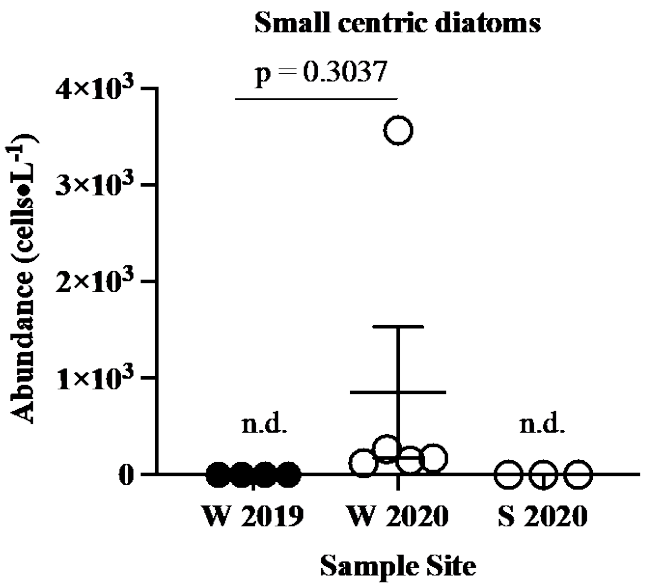


Figure 5.12: Abundance (Cells•L^{-1}) small centric diatom taxa (5-20 μm size) across sample sites organized by season. W = winter (February-March), S = spring (May-June). Solid shapes indicate the sample was collected during ice cover (2019) open shapes indicate the sample was collected during no ice cover (2020). Sites were the taxa was not detected are indicated with "n.d.". Statistical comparisons as a function of ice cover were made using unpaired, two-tailed t-tests.

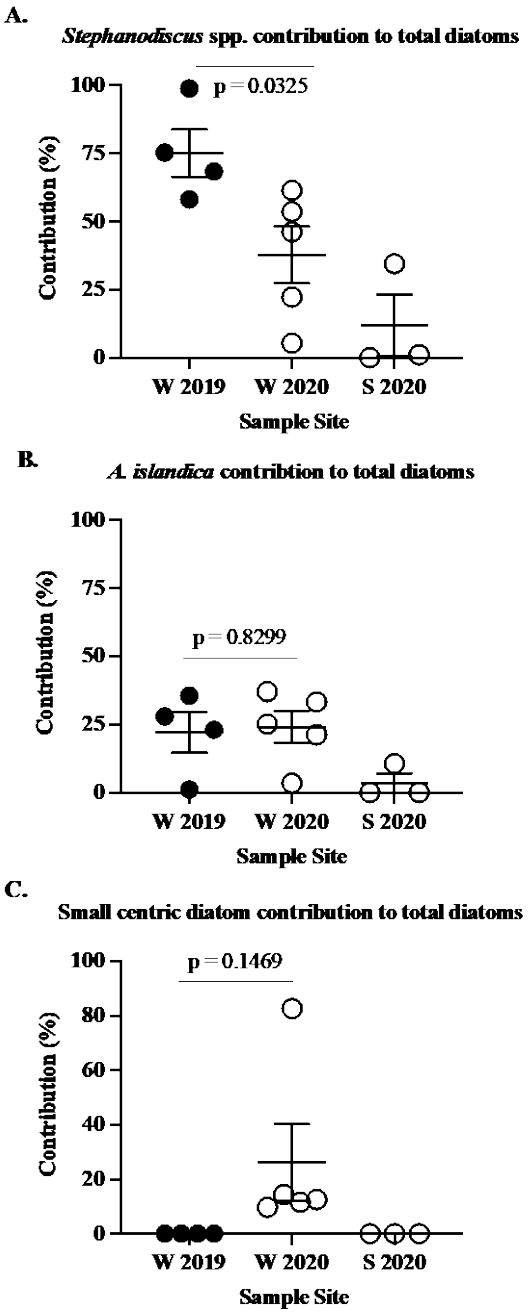


Figure 5.13: Mean percent contribution of three centric diatom abundance to total diatom abundance across sample sites organized by season. W = winter (February-March), S = spring (May-June). Solid shapes indicate the sample was collected during ice cover (2019) open shapes indicate the sample was collected during no ice cover (2020). **(A)** Percent contribution of *Stephanodiscus* spp. genera abundance to total diatom abundance**. (B)** Percent contribution of *A. Islandica* abundance to total diatom abundance. **(C)** Percent contribution of small centric diatom taxa (5-20 μm size) to total diatom abundance. Statistical comparisons as a function of ice cover were made using unpaired, two-tailed t-tests.

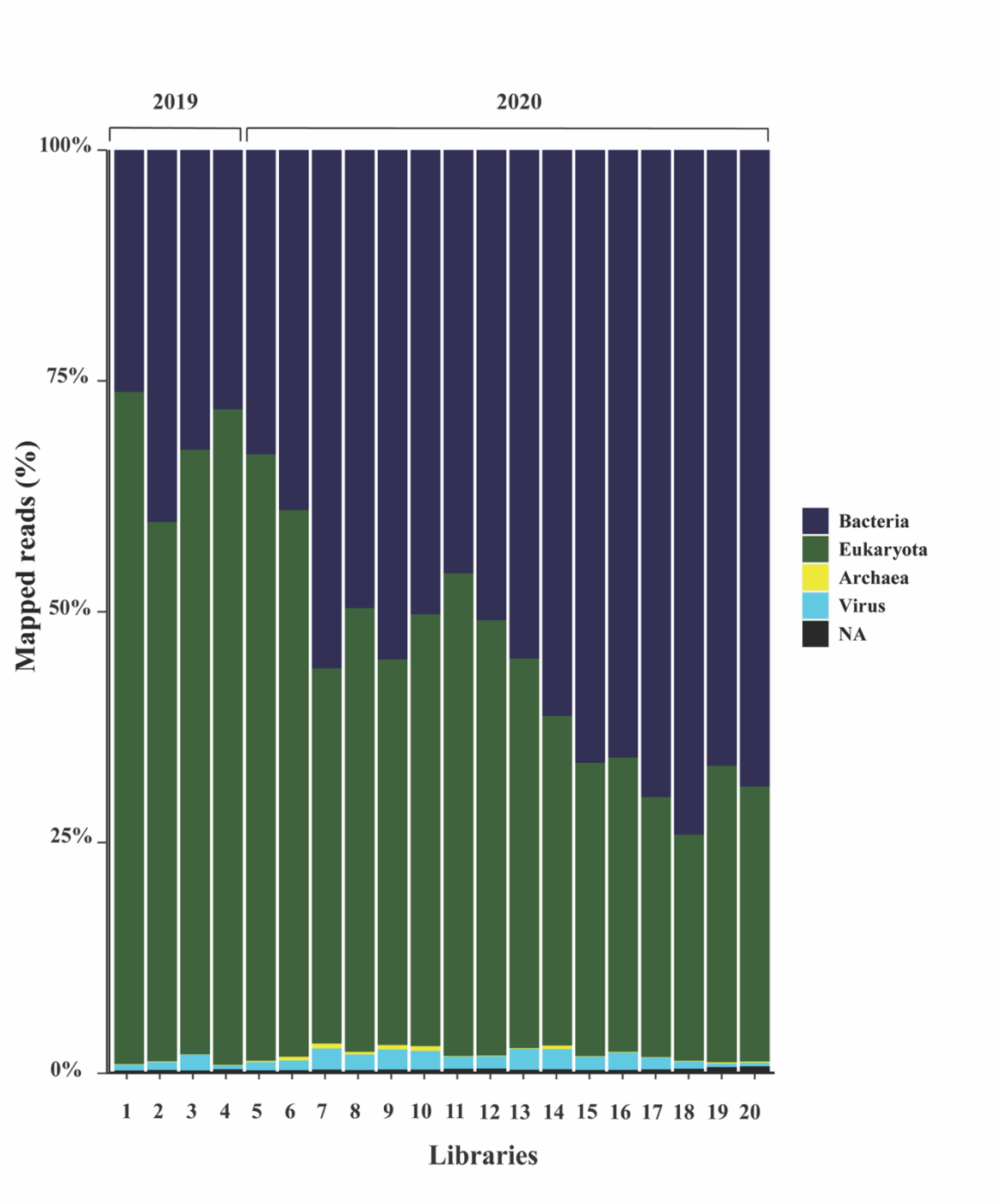


Figure 5.14: Relative transcript abundance of domains across the 20 libraries (listed in chronological order of sample date on the x-axis). NA = not annotated.

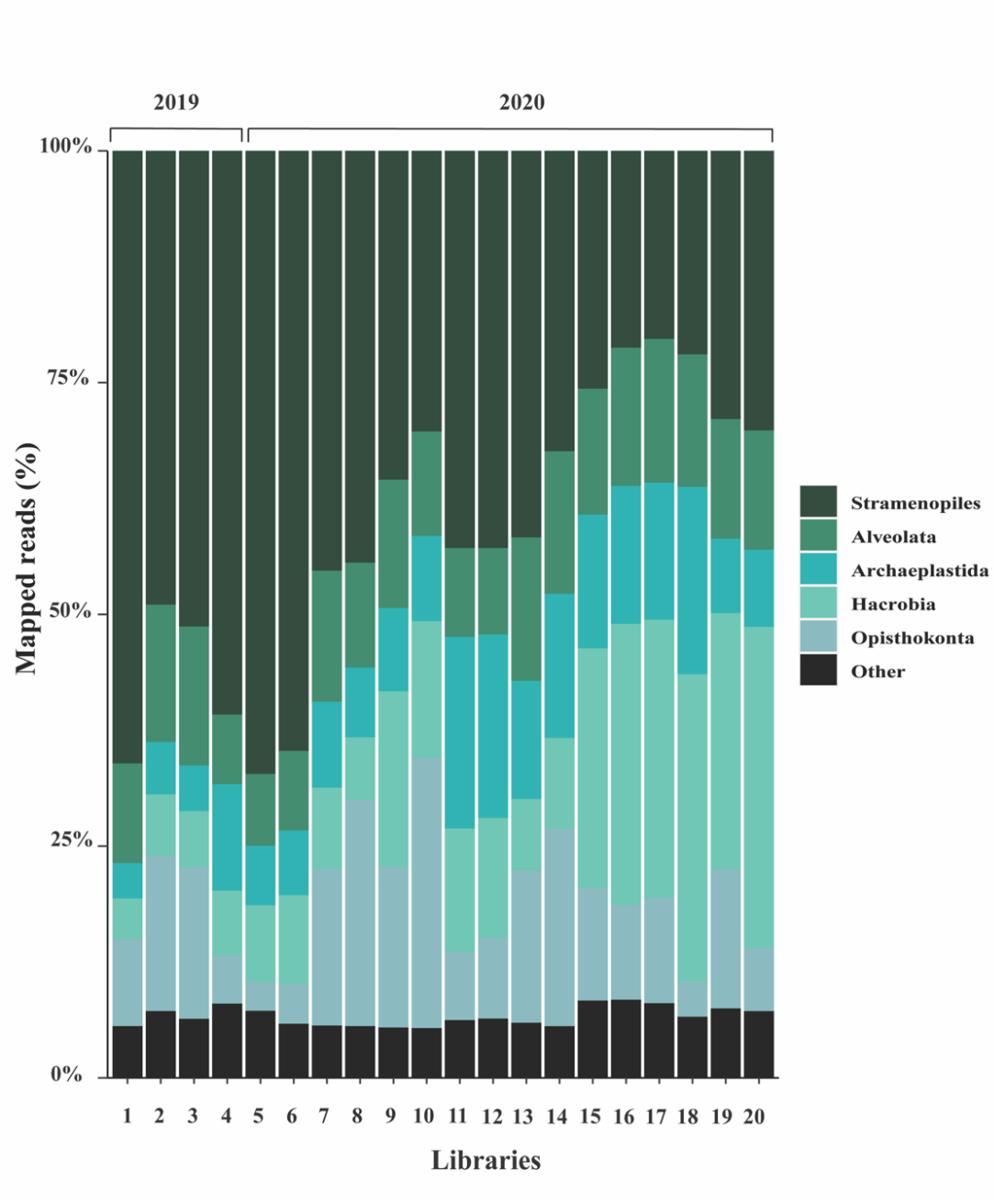
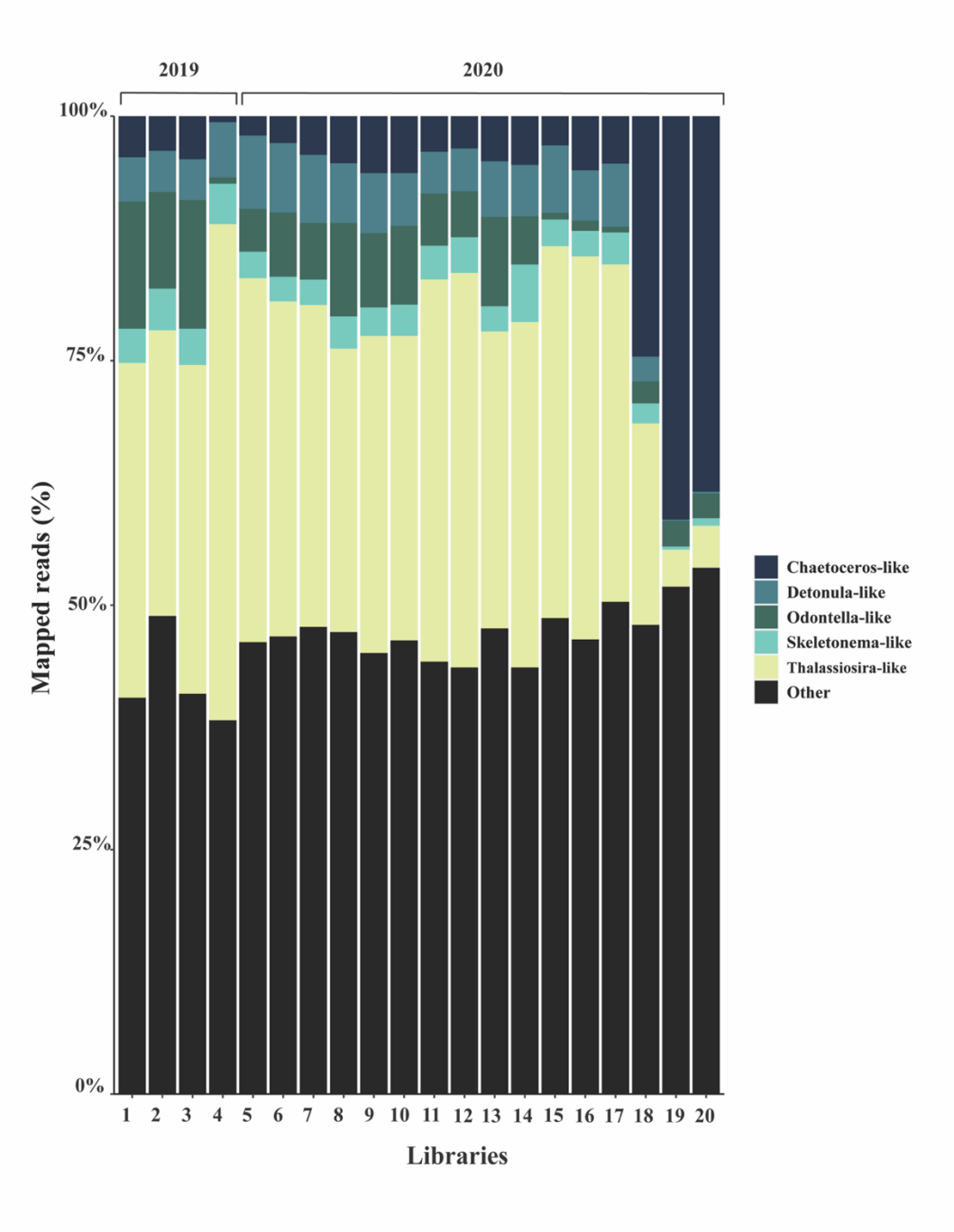


Figure 5.15: Relative transcript abundance of major eukaryota across the 20 libraries (listed in chronological order of sample date on the x-axis). All groups which formed <5% of the total mapped reads are included within "Other" (Amoebozoa, Hilomonadea, Excavata, Rhizaria, NA).



5.16: Relative transcript abundance of Mediophyceae genera across the 20 libraries (listed in chronological order of sample date on the x-axis). All groups which formed <5% of the total mapped reads are included within "Other" (*Attheya* spp., *Cyclotella* spp., *Ditylum* spp., *Eucampia* spp., *Extubocellulus* spp., *Helicotheca* spp., *Minutocellus* spp., *Triceratium* spp). At the genus level, NA counts were not included within total % read mapping calculations due to low-resolution at the genus level. They have been included within "Other" despite accounting for 59.04% of the total mapped reads to emphasize trends within annotated genera.

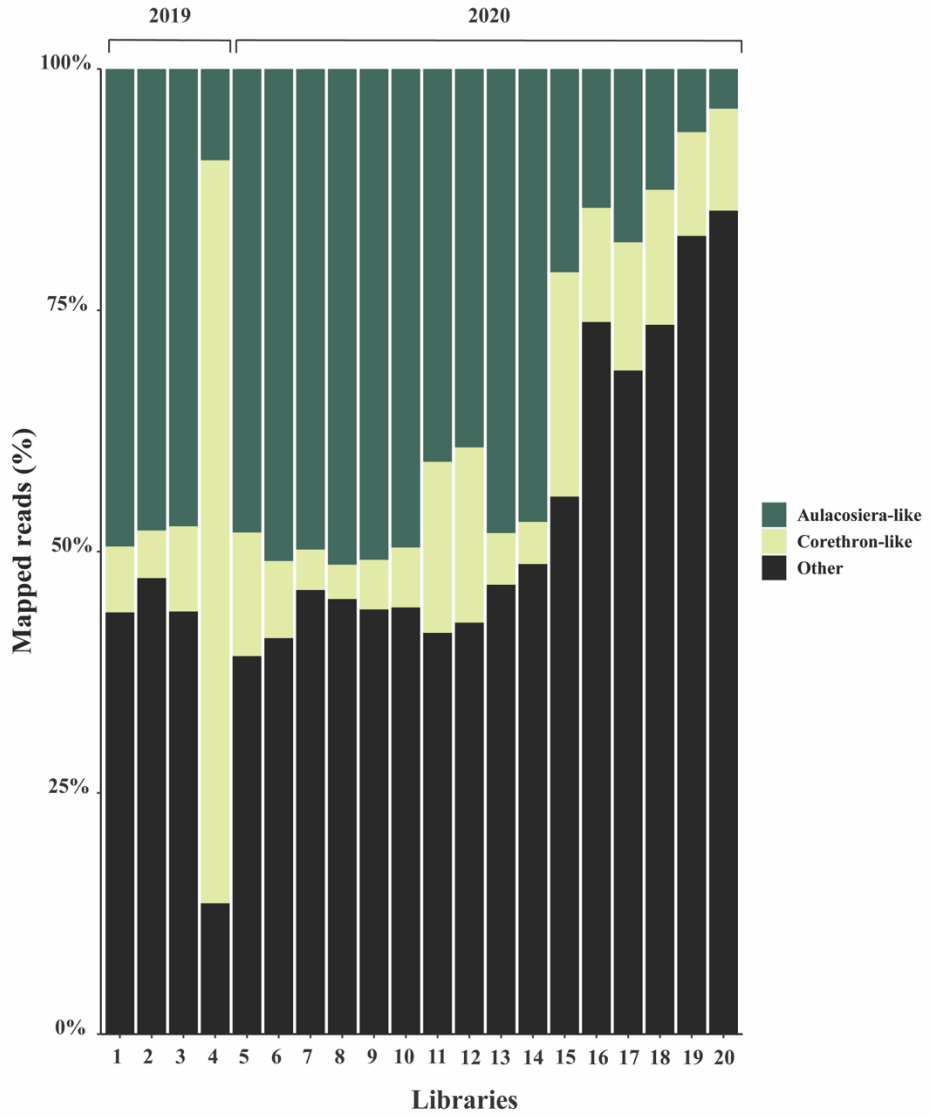


Figure 5.17: Relative transcript abundance of Coscinodiscophyceae genera across the 20 libraries (listed in chronological order of sample date on the x-axis). All groups which formed <5% of the total mapped reads are included within "Other" (*Coscinodiscus* spp., *Dactyliosolen* spp., *Lepticylindrus* spp., *Proboscia* spp., *Rhizosolenia* spp., *Stephanopyxis* spp). At the genus level, NA counts were not included within total % read mapping calculations due to low-resolution at the genus level. They have been included within "Other" despite accounting for 40.98% of the total mapped reads to emphasize trends within annotated genera.

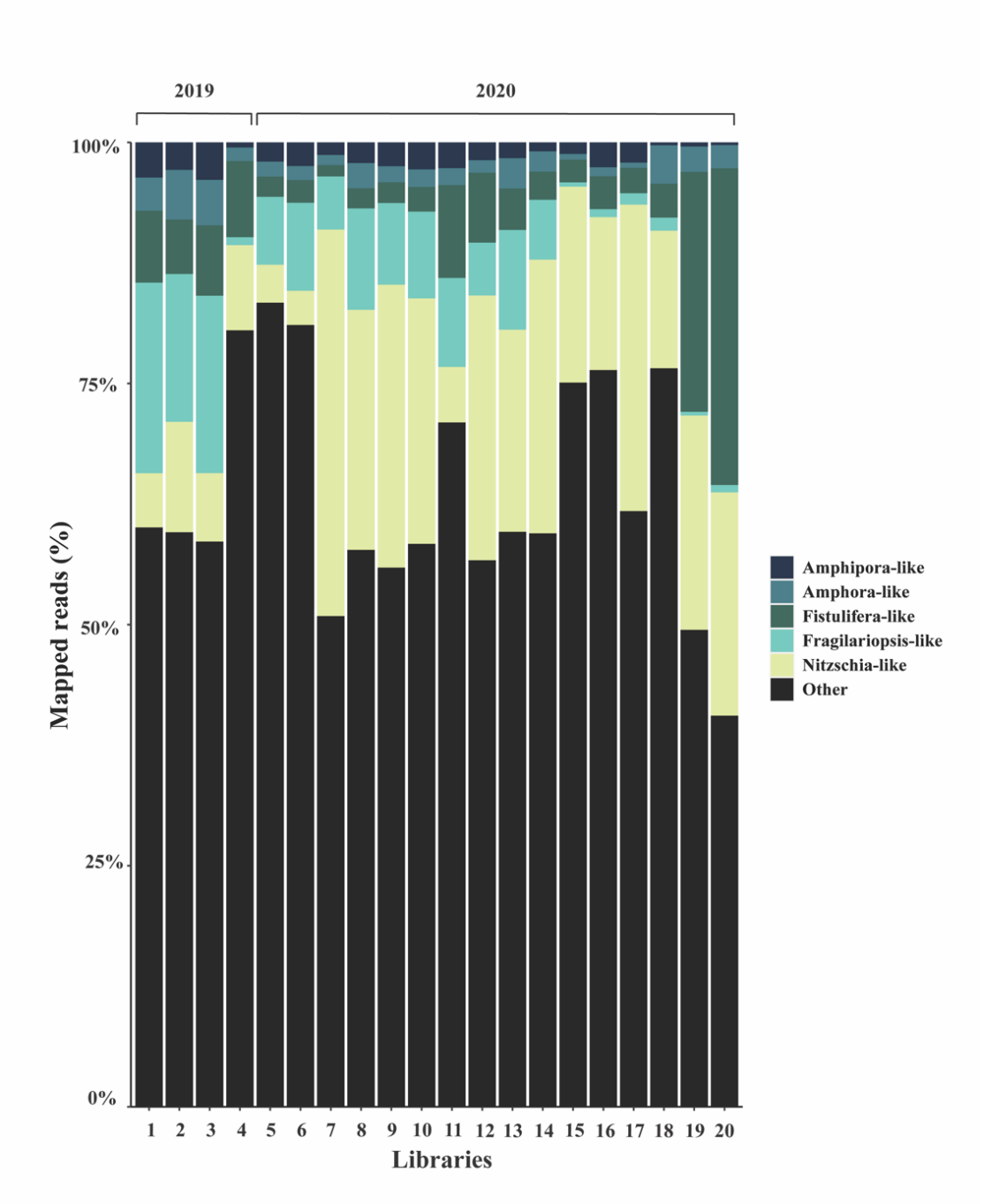


Figure 5.18: Relative transcript abundance of Bacillariophyceae genera across the 20 libraries (listed in chronological order of sample date on the x-axis). All groups which formed <5% of the total mapped reads are included within "Other" (*Craspedostauris* spp., *Cylindrotheca* spp., *Entomoneis* spp., *Phaeodactylum* spp., *Psuedo-nitzschia* spp., *Stauroneis* spp). At the genus level, NA counts were not included within total % read mapping calculations due to low-resolution at the genus level. They have been included within "Other" despite accounting for 66.00% of the total mapped reads to emphasize trends within annotated genera.

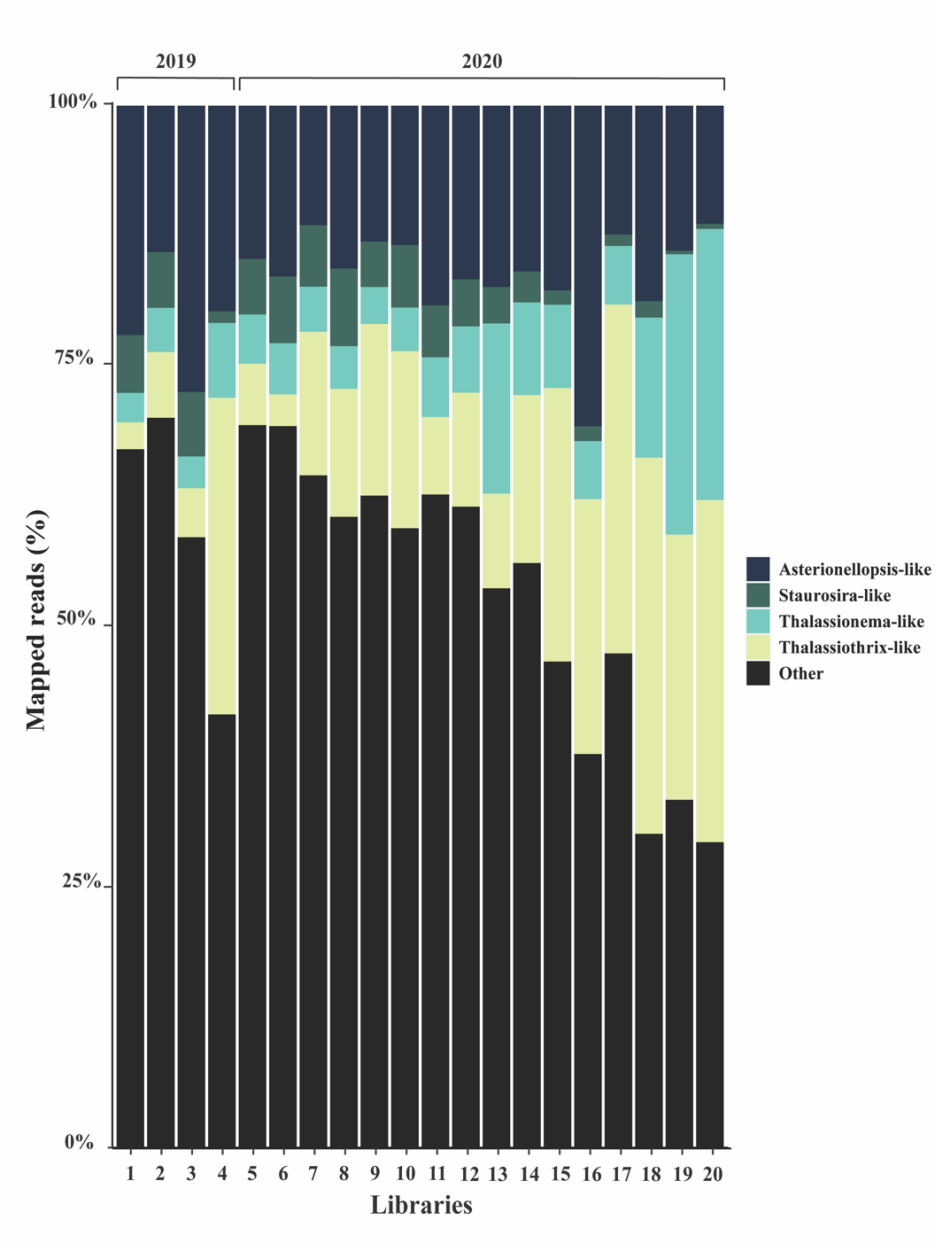


Figure 5.19: Relative transcript abundance of Fragilariophyceae genera across the 20 libraries (listed in chronological order of sample date on the x-axis). All groups which formed <5% of the total mapped reads are included within "Other" (*Astrosyne* spp., *Cyclophora* spp., *Grammatophora* spp., *Licmophora* spp., *Striatella* spp., and *Syndropsis* spp.). At the genus level, NA counts were not included within total % read mapping calculations due to low-resolution at the genus level. They have been included within "Other" despite accounting for 50.27% of the total mapped reads to emphasize trends within annotated genera.

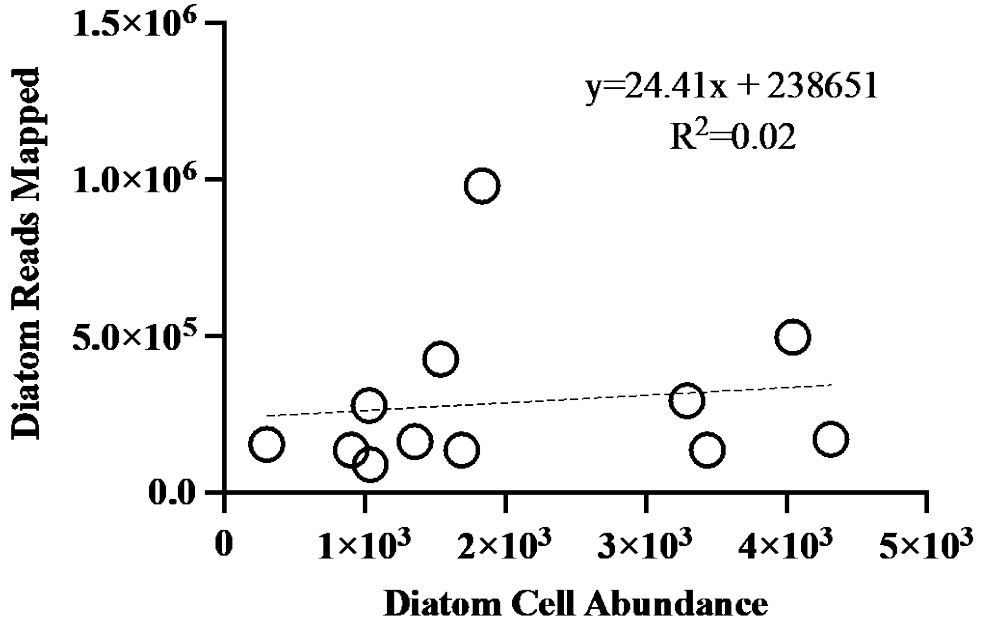


Figure 5.20: Simple linear regression of diatom transcriptional abundances and diatom cell abundances.

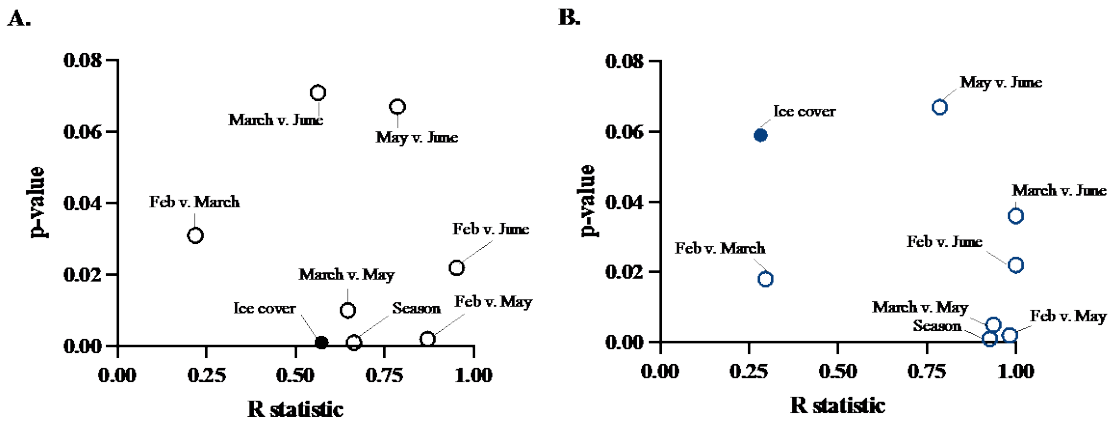


Figure 5.21: ANOSIM tests plotted by R statistic and p-value. An R statistic close to 1.00 and a p-value < 0.05 indicates there is a significant difference between the 2 variables. Ice cover is indicated by a filled circle. (**A)** ANOSIM tests on the relative expression profiles (TPM) of the whole winter community comparing months, season (winter vs. spring), and ice cover (ice cover vs. no ice cover). (**B)** ANOSIM tests on the relative expression profiles (TPM) of the Bacillariophyta community comparing months, season (winter vs. spring), and ice cover (ice cover vs. no ice cover).

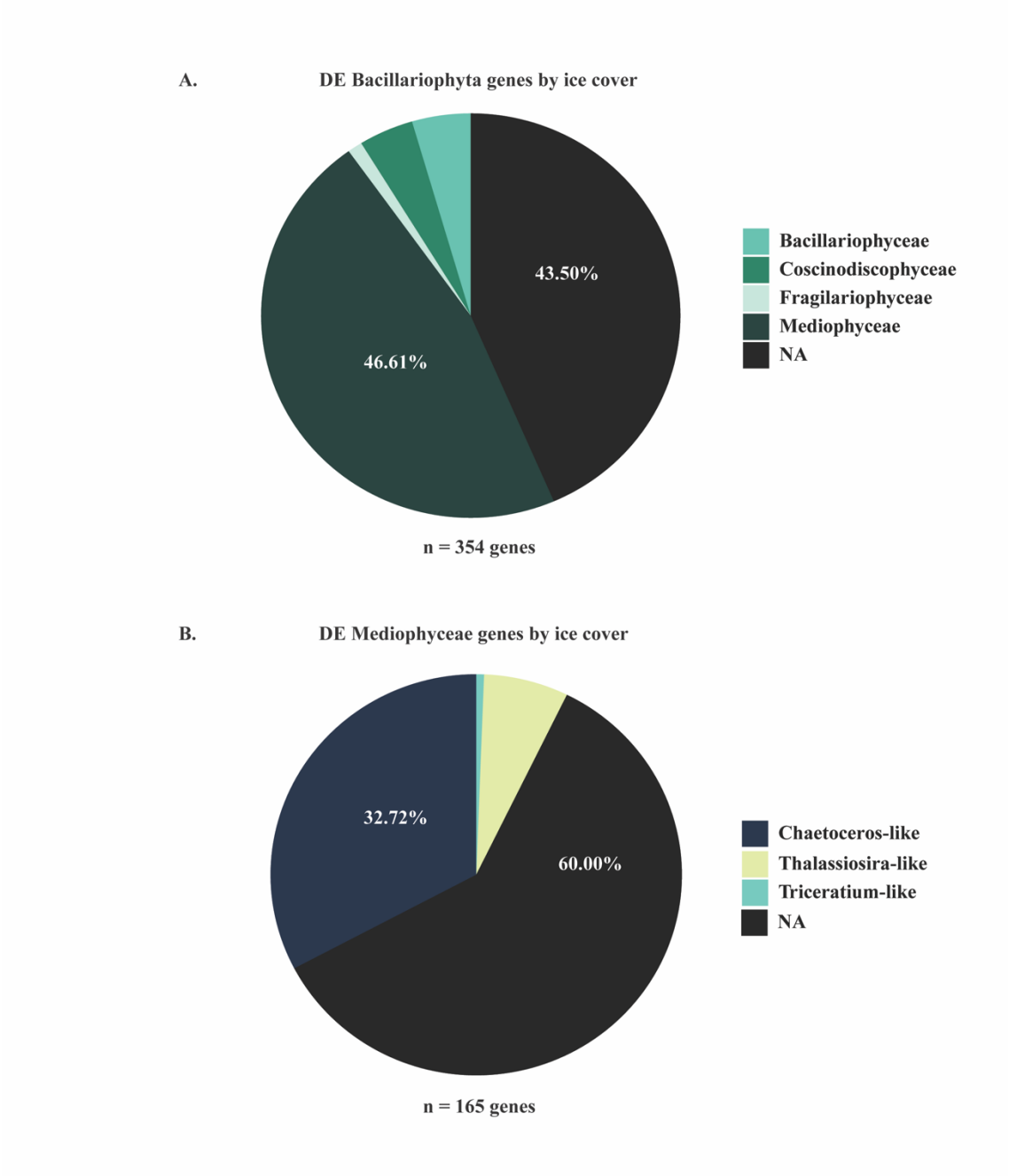


Figure 5.22: Taxonomic distributions of diatom genes that were differentially expressed by ice cover. **(A)** Taxonomic distribution of all 354 DE genes by diatom class. **(B)** Taxonomic distribution of DE genes belonging to the Mediophyceae class.

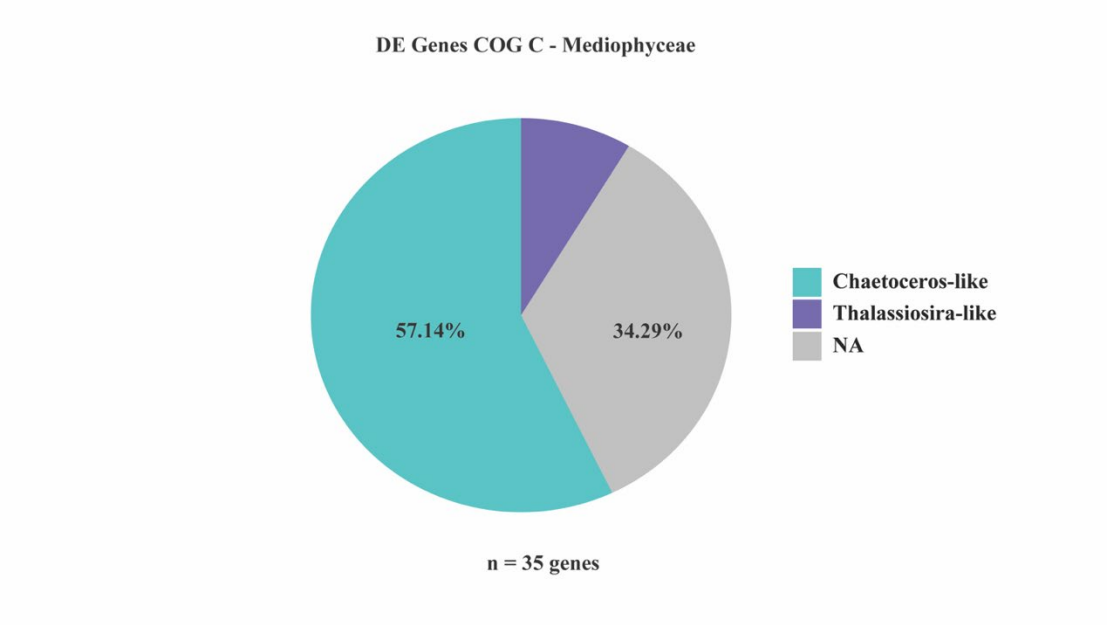


Figure 5.23: Taxonomic distributions of Mediophyceae diatom genes that were differentially expressed by ice cover within COG Category C.

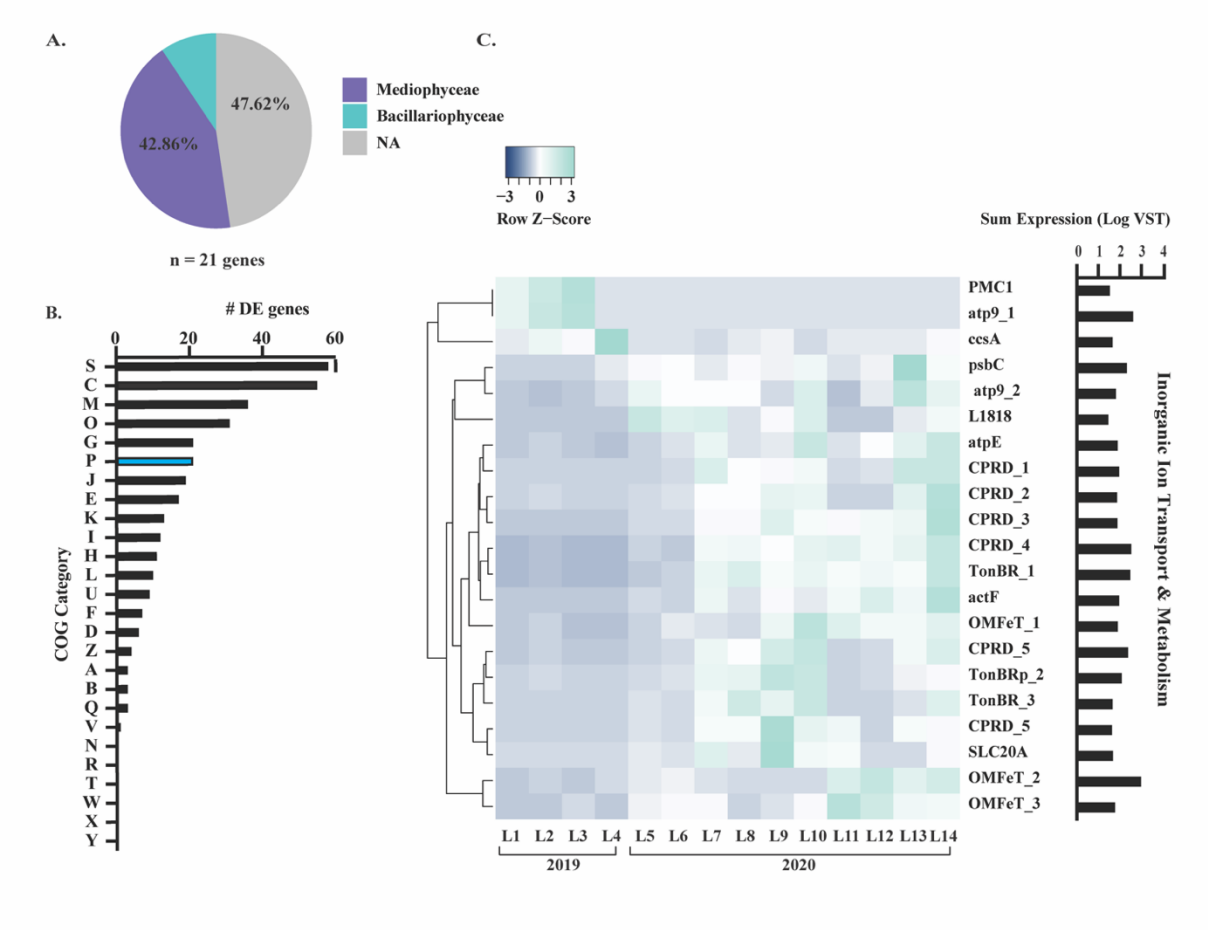


Figure 5.24: Bacillariophyta transcript abundance patterns in response to ice cover-COG P (Inorganic ion transport and metabolism). **(A)** Taxonomic distribution of DE genes categorized within COG category P. **(B)** COG assignments for all 354 DE genes in response to ice cover, with COG category P indicated in blue. **(C)** Heatmap depicting COG category P differentially expressed gene expression (VST) in response to ice cover across the 14 winter libraries.

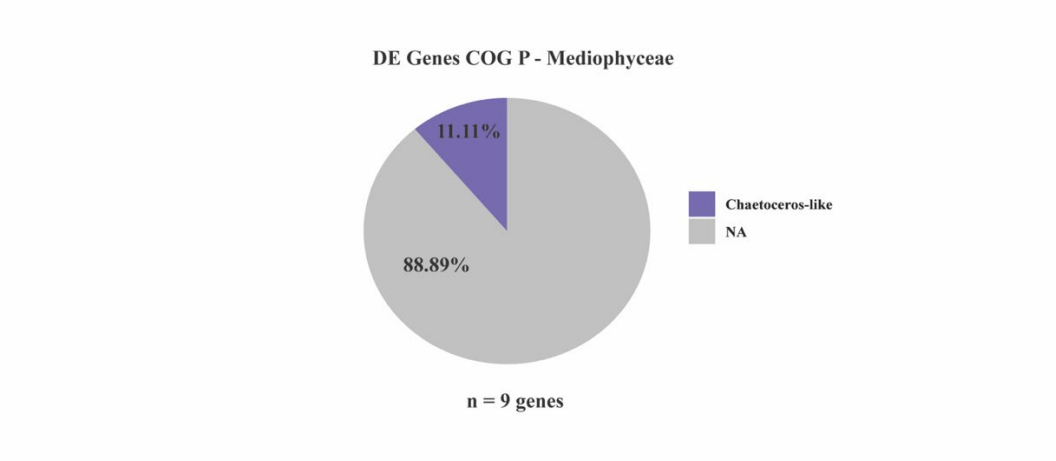


Figure 5.25: Taxonomic distributions of Mediophyceae diatom genes that were differentially expressed by ice cover within COG Category P.

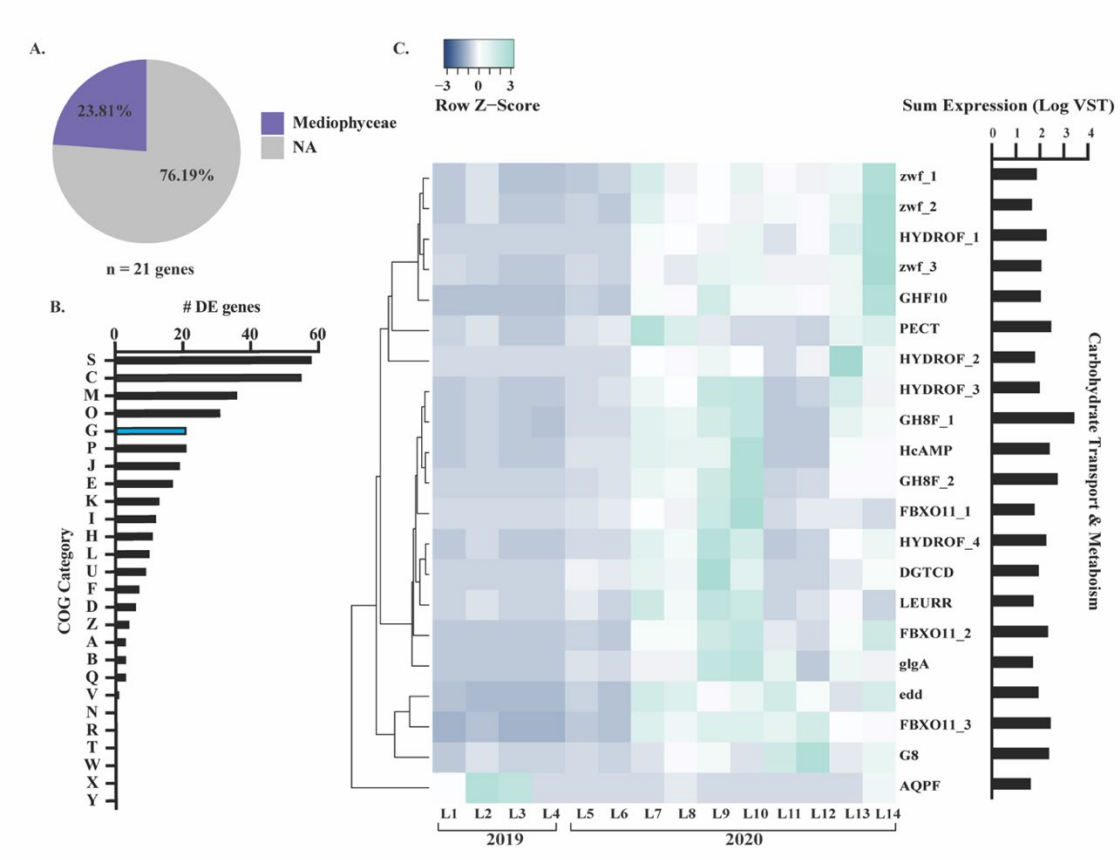


Figure 5.26: Bacillariophyta transcript abundance patterns in response to ice cover-COG G (Carbohydrate transport and metabolism). **(A)** Taxonomic distribution of DE genes categorized within COG category G. All Mediophyceae genes were not annotated at the genus level. **(B)** COG assignments for all 354 DE genes in response to ice cover, with COG category G indicated in blue. **(C)** Heatmap depicting COG category G differentially expressed gene expression (VST) in response to ice cover across the 14 winter libraries.

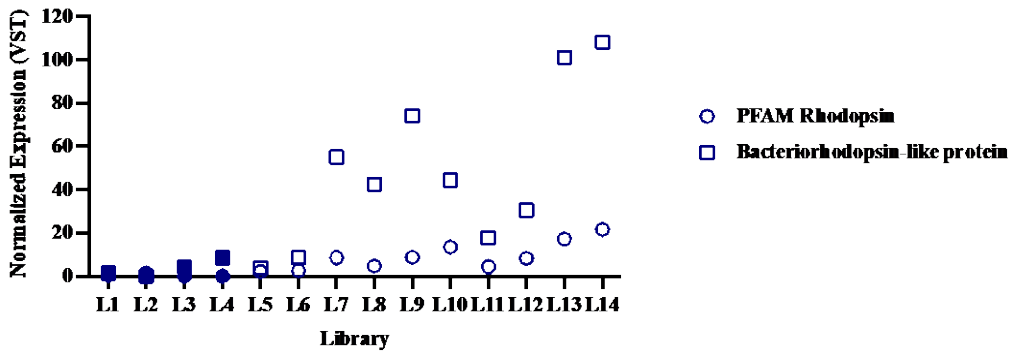


Figure 5.27: Normalized expression (VST) of two genes functionally annotated as rhodopsins (PFAM Rhodopsin indicated by circles, Bacteriorhodopsin-like protein indicated by squares). Solid shapes indicate the sample was collected during ice cover (2019) open shapes indicate the sample was collected during no ice cover (2020**).**

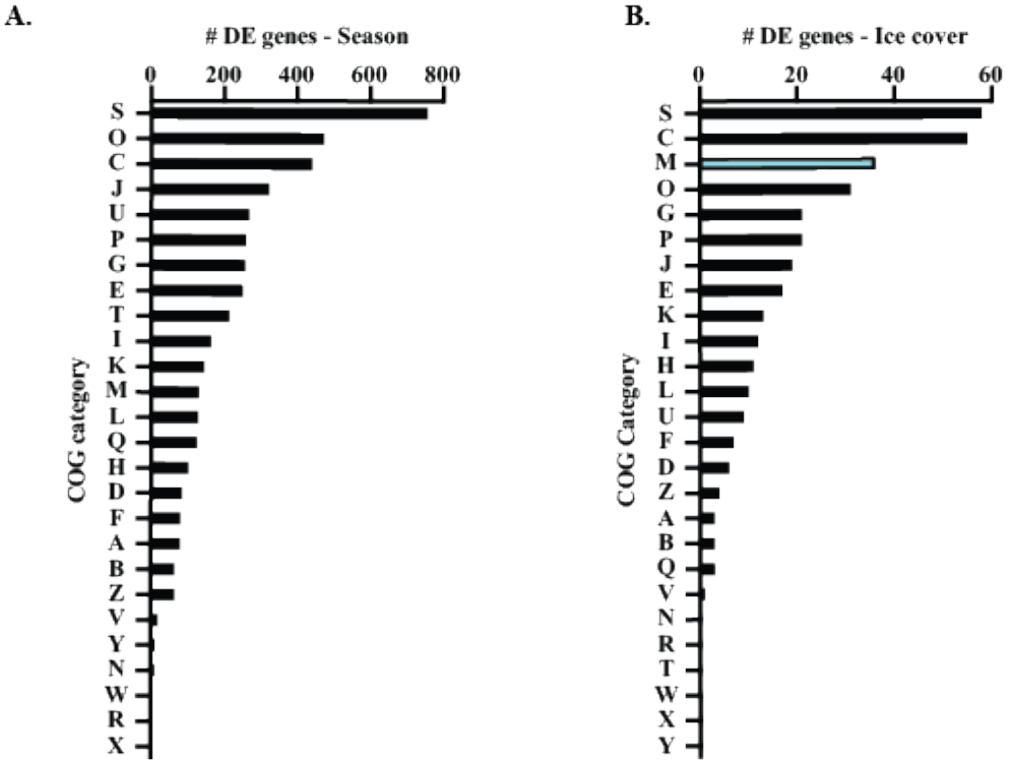


Figure 5.28: Distribution of DE genes by COG category. **(A)** COG assignments for all DE genes (n = 4,854) in response to season (winter vs. spring). **(B)** COG assignments for all DE genes (n = 354) in response to ice cover, with COG category M indicated in blue.

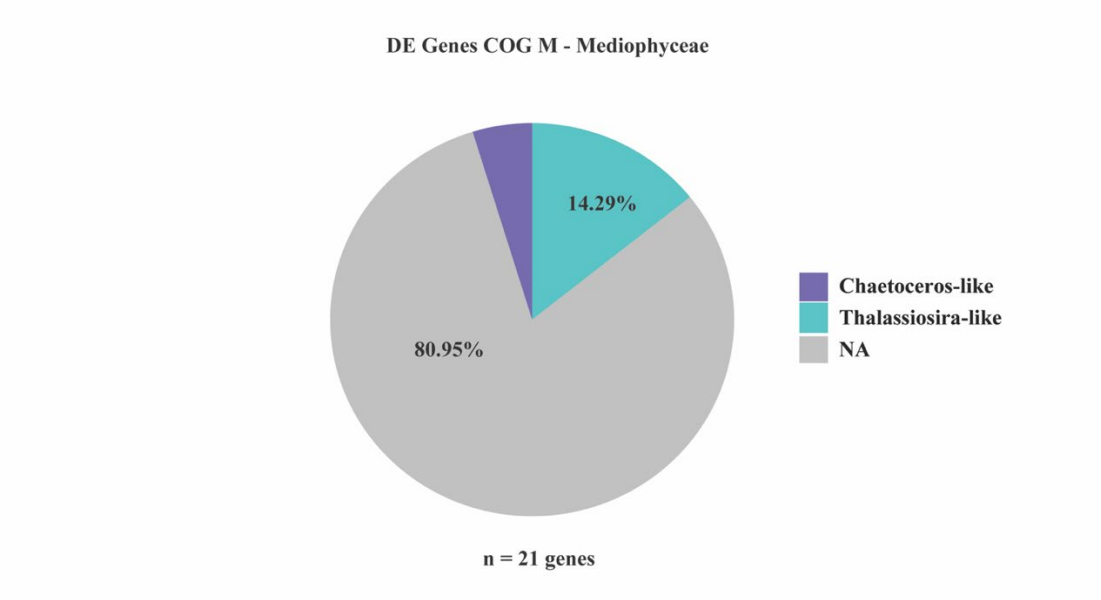


Figure 5.29: Taxonomic distributions of Mediophyceae diatom genes that were differentially expressed by ice cover within COG Category M.



Figure 5.30: MODIS satellite image (photo takes February 12th, 2023) demonstrating a lack of ice cover across the Great Lakes. Sediment plumes can be observed throughout Lake Erie, the shallowest of the Great Lakes. Photo Credit: NOAA GLERL/NOAA Great Lakes CoastWatchNode.

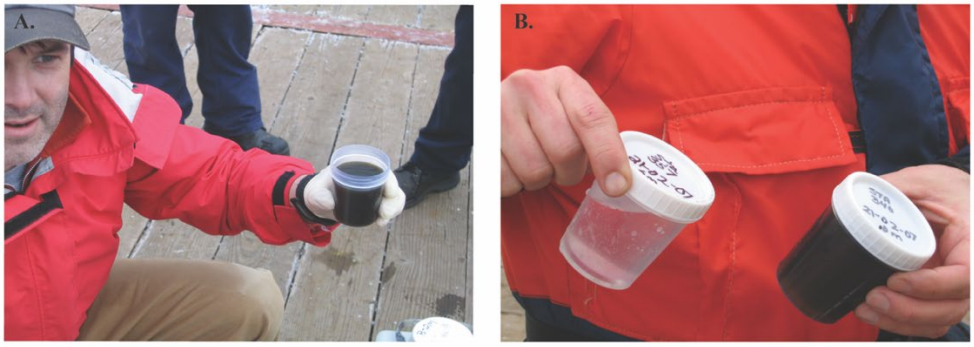


Figure 5.31: Plankton net tows from a 2007 Lake Erie winter survey. (A) Concentrated diatom seston from a net-tow conducted in ice free waters at station 340 at 10 meters depth. (B) Dilute seston from a net-tow conducted in ice-covered waters at station 357 at 6 meters depth. Both samples were collected on February 2, 2007. Dr. R. Michael M. McKay is holding the samples, Dr. Steven W. Wilhelm took the photographs.

CHAPTER VI: CONCLUSIONS

Lakes are sentinels of climate change, serving as a window into how anthropogenically driven influences alter ecological and biogeochemical phenomena. The body of this work investigates the ecological success and succession of algal bloom communities within Lake Erie: a Great Laurentian Lake which is undergoing rapid large-scale climatic changes. In turn, a myriad of recent advancements coupled with climatic alterations suggest a need to re-assess many of the classic paradigms which are thought to constrain algal bloom success and succession. Here, we address these paradigms by investigating the role of bloom-induced pH levels and alterations in winter ice cover on the ecological success and succession of algal bloom taxa common to Lake Erie. Notably, this works focuses primarily on the widely unstudied diatom bloom forms of Lake Erie such as the summer bloom-forming *F. crotonensis* and winter diatom bloom formers *A. islandica* and *Stephanodiscus* spp. By employing a combination of *in vitro, in situ,* and *in silico* approaches we demonstrate the ecological importance of bloom-induced pH, ice cover, and diatom communities at the intersection of limnology, climate change, and harmful algal blooms.

The first contribution of this work (Chapter II) serves as a cautionary tale of the unintended consequences of classical laboratory techniques. Preliminary optimizations of the pH assays revealed aseptic flaming of algal cultures introduced $CO_{2(g)}$ into the cultures which significantly decreased the pH. In turn, fluctuations in culture pH differentially altered growth dynamics of *Microcystis aeruginosa* cultures, with the $CO_{2(g)}$ serving as a carbon source. In total, this project has widescale implications for climate change work (*i.e.,* ocean acidification and lake basification studies) which require precise pH/CO_2 levels. As a result of this work, the buffer capacity of our freshwater media was increased and aseptic flaming was markedly reduced, facilitating the establishment of the in vitro pH assay used in Chapters III and IV.

The next contribution of this work (Chapter III) demonstrates *Microcystis* induced pH levels significantly decrease growth and silica deposition in the model diatom *F. crotonensis* and *in situ* Lake Erie diatom communities. We discovered *Microcystis* increases the water column pH during photosynthetic CO_2 drawdown, driving pH levels up to an average daily of 9.2 for ~30 days during a 2015 *Microcystis* bloom in Lake Erie. While this elevated pH did not significantly affect *Microcystis* growth, it invoked detrimental consequences for *in vitro F. crotonensis* and *in situ* diatom viability. Cumulatively, this suggests pH plays a role in *Microcystis*'s suppression and out competition of summer diatom communities. Further, considering elevated pH levels were found to persist well into September, we hypothesize pH likely plays a role in delaying fall diatom succession. While this work is foundational in establishing the emerging field of lake basification, it falls short of identifying the intracellular mechanisms responsible for the observed declines in diatom growth and silica deposition at high pH levels. Hence, Chapter III sought to investigate this knowledge gap using *in vitro* pH assays and transcriptomics.

Transcriptomic analyses conducted in Chapter IV generated hypotheses concerning how the elevated pH level of 9.2 alters *F. crotonensis* intracellular physiology. Notably, the expression of genes involved in cell cycle control and cell wall biogenesis increased at pH 9.2, and follow-up FlowCAM analyses demonstrated alkaline pH levels cause smaller, browner, and rougher *F. crotonensis* filaments. In contrast, at pH 9.2 genes involved in photosynthesis decreased in expression, with follow-up PhytoPAM and photopigment analyses indicating declines in maximum electron transport rates of PSII and light saturation thresholds of PSII while photopigments of diadinoxanthin and B-carotene significantly increased. Further, 25% of DE genes which increased in expression at pH 9.2 belonged to the "Mobilome" COG category, suggesting *F. crotonensis* filaments were increasing instances for potential mutations.

Cumulatively, these results suggested *F. crotonensis* filaments were undergoing photostress and potentially cell cycle arrest at elevated pH levels. Further, this work led to the "genomic roulette hypothesis" that *F. crotonensis* filaments are upregulating mobile elements in response to an environmental stressor to rapidly increase mutations within an organism over a short period of time. Hence, despite the various physiological consequences high pH imposes on diatoms, there exists the opportunity for diatoms to adapt to a "basified future". Nonetheless, Chapter II and III provide contextual explanations for the ecological "lack of success" of summer diatoms in the Lake Erie water column.

In juxtaposition to Chapters III and IV which focus on the ecologically "unsuccessful" summer diatom community, Chapter V pivots to the ecologically "successful" winter diatom blooms. Despite reports of winter diatom blooms under the Lake Erie ice dating back to the 1930's, they remained widely unstudied save for a large-scale winter survey conducted from 2007-2012. Our study addressed this gap by serving as the first wide scale bioinformatic survey of the winter Lake Erie water column. Notably, our 2 year survey spanned a year of high ice cover (2019) and a year of low ice cover (2020), thus serving as a window into the "ice-free" future of Lake Erie. Indeed, Lake Erie is observing a rapid decline in ice cover, with the winter of 2023 demonstrating unprecedentedly negligible ice cover. Our study demonstrates the winter diatom community has shifted from prior observations made in 2007-2012. Diatom abundances and Chl *a* concentrations were significantly lower, and *Stephandiscus* (rather than *A. islandica*) dominated the centric diatom assemblage. Despite these contrasting findings, diatoms still dominated the ice-free water column, contradicting prior speculations that a phyla-level regime shift would be observed in the ice-free water column to favor cryptophytes and dinoflagellates. Most surprising, the metatranscriptomes from this dataset led to the formation of the "fasciclin

rafting hypothesis" which suggests polar centric diatoms are employing fasciclins to raft together and co-locate in the turbid ice-free Lake Erie water column. Hence, further physiological observations are required to investigate this potentially critical phenomenon, which may prove pivotal in the future ice-free and climatically altered Lake Erie water column.

In summary, these collective works aim to tease apart the complicated and confusing story of algal bloom success and succession. Here, we re-assess classical paradigms of ecological succession and propose novel paradigms such as a role of pH in algal niche competition. We identify mechanisms which facilitate the ecological successes (or failures) of diatoms within the basified summer water column and ice-free winter water column. Further, we offer hypotheses which serve to facilitate freshwater diatom adaptations to the climatically altered water column including the "genomic roulette" and "fasciclin rafting" hypotheses. While algal bloom succession remains a complicated and confusing phenomenon, this work serves to identify a few novel pieces of the puzzle.

While this cumulative work has made contributions to the limnological field at large, it has also revealed there are many questions which remain to be answered. For example, the role of pH in algal bloom success and succession remains widely unexplored to date. While this work made advancements regarding how freshwater diatoms are affected by *Microcystis* bloom-induced pH levels, it has yet to be ascertained how *Microcystis* itself responds to elevated pH levels. Hence, elucidating the intracellular and ecophysiological response of *Microcystis* to high pH remains a research priority. Yet more generally, this work provides a foundation for which the emerging field of "Lake Basification" can build upon. Another future direction of this work is a comprehensive bioinformatic characterization of the winter diatom bloom community. Indeed, our metatranscriptomic work presented in Chapter V illuminated the need for freshwater

diatom sequencing efforts and further taxonomic resolution. In contrast to the large-scale sequencing efforts concerning the marine environment such as Tara Oceans, the limnological field lacks sequencing depth and comprehensive annotation databases. Hence, obtaining taxonomic resolution within freshwater diatom bioinformatic datasets is greatly hindered. More broadly, diatoms within Lake Erie are widely overlooked within the literature at large. Indeed, novel diatom taxa are continuously reported within the Great Lakes in as recent as the past few months. Hence, further attention is required not just pertaining to freshwater diatom sequencing efforts or the winter diatom community, but diatoms across the Great Lakes in general. Beyond the gap in freshwater diatom sequencing, this study reported that fasciclins remain widely unstudied within diatoms. Indeed, at the time of this dissertation only two studies were found mentioning fasciclins and diatoms. Yet, we located fasciclins within ~140 different freshwater and marine diatom genera. Hence, there is a need to elucidate the functional role these proteins play within diverse diatom genera and the ecophysiological role they may have as a function of environment. Another future direction which stems from this work is the need to functionally and taxonomically characterize proton pumping rhodopsins within freshwater diatoms. To our knowledge, the work presented in Chapter V is the first report of proton pumping rhodopsins in freshwater diatoms. While proton pumping rhodopsins have been identified across the marine diatom lineage, the distribution of these proteins within freshwater diatoms remains largely unstudied. This serves as a significant gap in the freshwater field, especially considering proton pumping rhodopsins have been suggested to generate as much energy as classical photosynthesis. Hence, while the chapters within this dissertation present a few novel pieces of the puzzle of algal bloom success and succession, many more remain to be discovered.

VITA

Brittany Noel Zepernick was born in Cleveland, Ohio and raised in Aurora, Ohio. She attended Aurora High School and graduated in 2014. Here, she was broadly interested in Biology, Chemistry, and English literature. She received her Honors Bachelor of Science Degree in Biology with a Specialization in Marine and Aquatic Science from Bowling Green State University in 2017. Here, she discovered her passion for Limnology and freshwater Harmful Algal Blooms (HABs). She worked with Dr. George S. Bullerjahn and Dr. R. Michael L. McKay researching the freshwater cyanobacteria *Microcystis aeruginosa.* This work included 2 field courses abroad focused on assessing anthropogenic influences on HABs in the Baltic Sea (Zingst, Germany) and Lake Balaton (Balaton, Hungary). During the summer of 2016, she conducted a National Science Foundation Research Experience for Undergraduates at Dauphin Island Sea Laboratory in the lab of Dr. Jeffrey Krause and Dr. Behzad Mortazavi, where she worked on a marine ecology project investigating how dissolved organic matter influences coastal phytoplankton communities. In 2018, she joined the lab of Dr. Steven Wilhelm at the University of Tennessee Knoxville Department of Microbiology. Here, she worked on a multitude of topics within freshwater systems and HABs, developed a model freshwater diatom system in the lab, and partook in national (Lake Erie, United States) and international (Lake Victoria, Kenya) research expeditions concerning aquatic ecosystem health and HABs. She defended her PhD at the University of Tennessee Knoxville in April 2023 and was honored to receive the Jimmy and Ileen Graduate Student Medal of Excellence.